NUREG/CR-0948

NONLINEAR STRUCTURAL DYNAMIC ANALYSIS PROCEDURES FOR CATEGORY I STRUCTURES

URS/John A. Blume & Associates, Engineers

520 001

7908070709

Prepared for
U. S. Nuclear Regulatory Commission

NOTICE

This report was prepared as an account of work sponsored by an agency of the United States Government. Neither the United States Government nor any agency thereof, or any of their employees, makes any warranty, expressed or implied, or assumes any legal liability or responsibility for any third party's use, or the results of such use, of any information, apparatus product or process disclosed in this report, or represents that its use by such third party would not infringe privately owned rights.

523 001

528 002

Available from
National Technical Information Service
Springfield, Virginia 22161

NUREG/CR-0948
RD

NONLINEAR STRUCTURAL DYNAMIC ANALYSIS PROCEDURES FOR CATEGORY I STRUCTURES

URS/John A. Blume & Associates, Engineers
130 Jessie Street
San Francisco, CA 94105

Manuscript Completed: September 1978
Date Published: July 1979

Prepared for
Division of Reactor Safety Research
Office of Nuclear Regulatory Research
U. S. Nuclear Regulatory Commission
Washington, D.C. 20555
Under Contract No. NRC-03-77-173

528 003

CONTENTS

528 004

CONTENTS (Continued)

TABLES

528 005

TABLES (Continued)

528 006

TABLES (Continued)

528 007

TABLES (Continued)

033

FIGURES

528 009

FIGURES (Continued)

528 010

528 011

APPENDICES

528 012

ACKNOWLEDGEMENTS

Many individuals were instrumental in the preparation of this report. D. C. Jeng and S. P. Chan of U.S. Nuclear Regulatory Commission provided excellent technical guidance in the course of the project. R. M. Czarnecki, A. F. Kabir and R. E. Scholl of URS/Blume were responsible for the technical aspects of the work, and their efforts were greatly aided by consultation with Dr. John A. Blume. C. L. Perry and J. P. Harkins provided technical support, and M. T. Stauduhar provided technical editing and supervised report production.

528 013

1. INTRODUCTION

1.1 Purpose

This report presents the results of studies conducted to identify and recommend a simplified dynamic analysis procedure applicable for performing nonlinear analyses of Category I nuclear power plant structures. For the recommended simplified analysis procedure, the theoretical background, mathematical formulation, analytical solution, verification of reliability, and interpretation of results were to be established. In addition, studies were conducted to compare the results of conventional linear analysis with nonlinear analyses to establish the relative merits of the two approaches.

This is a generic study dealing with the subject of nonlinear structural response. Various aspects of this study, including the structures considered, the analysis criteria, the dynamic loadings, and the material properties, are purely hypothetical. These aspects are intended to model Category I conditions, and any resemblance to specific nuclear power plant structures is purely coincidental.

1.2 Scope of Study

The process used to identify and evaluate the applicability of a simplified nonlinear analysis procedure consisted of three main tasks, as follows:

Task I: A literature search for both rigorous and simplified nonlinear dynamic analysis procedures applicable for Category I nuclear power plant structures.

Task II: An evalutaion of various simplified nonlinear analysis methods to identify the most pertinent yet practical procedure for Category I structures. This task also included studies and evaluations aimed at establishing analysis guidelines, reliability of the analysis, and guidelines for interpreting the results for the recommended simplified method.

528 014

Task III: An analysis of specific benchmark problems for the purpose of comparing the rigorous and simplified analysis methods and for evaluating the relative merits of conventional elastic analysis vis-a-vis nonlinear analysis. The analysis procedures studied are general and can be applied to most types of dynamic loadings. Budget limitations for this study dictated that verification of these procedures be limited to the base-input-motion earthquake problem.

1.3 Report Organization and Summary

The various phases of work and the conclusions of the study are all presented in this report in seven chapters and three appendices. In addition to scope and purpose, this chapter includes a background section, which presents general information on the types of structures, types of nonlinearities, and approaches to nonlinear response analysis.

1.3.1 Literature Search. The literature survey included identification of all available simplified and rigorous nonlinear analysis procedures specifically applicable to the earthquake problem. The procedures identified are discussed in Appendix A.

On the basis of judgment evaluations of the applicability of these procedures, four candidate simplified methods were considered for more detailed evaluation:

- the Reserve Energy Technique (RET)
- the Substitute Structure Method
- the Elasto-Plastic Spectrum Method (EPSM)
- the Approximate Inelastic Response Method (AIRM)

In addition, two rigorous nonlinear response analysis methods (computer programs) were recommended for use in making the comparative evaluation analysis:

523 015

- DRAIN-2D
- DRAIN-TABS

The survey also revealed that there is currently no computer program available for performing rigorous nonlinear analysis of shell structures for nonaxisymmetric loading.

These simplified and rigorous methods are described in detail in Chapter 2.

1.3.2 Simplified Method Selection. Each of the four candidate simplified methods was studied in detail to establish its merits, limitations, and accuracy in connection with predicting nonlinear response. Rigorous and simplified nonlinear response analyses were performed for each of four hypothetical structures:

- a 1-story plane frame
- a 4-story plane frame
- a 2-story shear wall
- a 4-story torsion building

The nonlinear analyses of these structures were conducted using each of the four candidate simplified methods. The results are given in Chapter 3. The rigorous nonlinear analyses of the same structures are described in Chapter 4. Conventional mathemetical modeling procedures were used in the analyses. A comparison of the rigorous and simplified analysis results for the four structures, given in Chapter 5, shows that both the EPSM and the RET predict inelastic response ductilities that compare well with those predicted from the rigorous analysis. The RET is recommended as the better simplified nonlinear analysis procedure because its methodology is suitable for analysis and design whereas the EPSM is intended for design application. Details of the reasons for this selection as well as the detailed theoretical background, mathematical formulation, basic assumptions, method of solution, and guidelines for interpreting the results for RET analyses are also given in Chapter 5.

528 916

1.3.3 Verification. Verification of the applicability of the RET for specific Category I nuclear power plant structures was done by performing rigorous and simplified analyses for two benchmark problems. These benchmark problems were selected to be representative of the auxiliary and turbine buildings of nuclear power plants. An example RET analysis was also done for a containment building. These analyses are presented in Chapter 6.

Chapter 6 also shows the results of studies conducted to evaluate the relative merits of conventional elastic analyses and nonlinear analyses. As compared to a rigorous nonlinear seismic analysis, a rigorous elastic seismic analysis is generally not sufficiently accurate although it may be adequate in cases involving very limited inelastic response. A rigorous elastic analysis generally establishes a lower bound of inelastic response.

1.3.4 Conclusions and Recommendations. Conclusions and recommendations of the study are presented in detail in Chapter 7. The principal conclusion of the study is that the simplified RET can be used effectively to predict the nonlinear response behavior of Category I nuclear power plant structures.

Additional recommendations concern the need for further study of nonlinear seismic structural response. Specific topics that need additional investigation are: nonlinear modeling techniques; verification of nonlinear response calculations with experimental data, parameter, and sensitivity studies; and the development of a quasi-rigorous nonlinear analysis method. Also included as a recommendation for future work is the improvement of the RET to allow a redistribution of shear forces based on the character of the inelastic response.

1.4 Background

The following discussion concerns the types of structures, the types of nonlinearities, and the basis approaches involved in this study.

1.4.1 Types of Structures. The three most important groupings of Category I building structures are the containment structure, the auxiliary buildings,

528 017

and the turbine building. (The turbine building is not always Category I.) In combination with Category I equipment supports and piping, these structures encompass many distinct classes of structural behavior. Each of the structural classes is subjected to different operating conditions: safety limitations may require some of them to remain elastic while others can be permitted to undergo significant inelastic deformation under the safe shutdown earthquake (SSE) level. Consequently, this study does not address the implications of ductility on safety; rather, it reviews the ranges of structural types and structural behavior over which the simplified nonlinear analysis techniques apply.

The containment structure is a continuous shell-type structure that is distinct from the shear wall and frame structures. Continuous shell-type structures contain significant reserve strength after the onset of yield (or cracking), but the combined design requirements of a simultaneous loss-of-coolant accident (LOCA) and a safe shutdown earthquake may prevent this reserve capacity from being used fully. Because continuous structures have significant load-redistribution capability, the nature of the failure mode can also be difficult to assess without a full-scale and extensive analysis.

Auxiliary buildings are generally heavy, reinforced concrete shear wall structures, with the shear walls interconnected by concrete floor diaphragms. The combination of shear walls and diaphragms can either be determinate, having a single effective load path, or redundant, having several effective load paths. The individual walls and diaphragms often possess little ductility, but the structural system may have a reserve strength due to the combination of elements.

The turbine building complex is typically a series of transverse ductile frames that are connected longitudinally by bracing or by shear walls. The behavior of such a turbine building will typically be governed by bending in the transverse direction and by shear in the longitudinal direction. In addition, it is not uncommon to encounter combinations of shear wall and braced-frame structural systems.

528 018

Equipment is often supported by bracing or moment-resisting connections that can be made ducti'e. The pipe portions of piping systems represent a distinctly ductile structural system characterized by a high degree of redundancy and a large number of branching paths. Failure of the piping system, however, is the result of a combination of temperature, pressure, and ground motion effects. Piping supports, on the other hand, can be either ductile or nonductile. Because of the substantial influence of temperature and pressure and because of the lack of available simplified methods of earthquake analysis, equipment and piping are considered to be beyond the scope of this study.

The complete range of Category I structures pertinent to this study can be categorized as follows:

- shell structures
- shear wall structures
- braced-frame structures
- ductile, moment-resisting frame structures
- combinations of the above

1.4.2 Nonlinearities and Nonlinear Response Behavior of Structures. Simplified forms of nonlinear analysis are feasible only when the structure contains a predictable mode of deformation or failure. The type of nonlinearity, or the combination of nonlinearities, therefore has a strong influence on the selection of an appropriate technique. It is essential to be able to characterize nonlinearities according to their influence on structural behavior because this is the controlling influence on the success or failure of most of the approximate methods. Nonlinearities important in connection with establishing useful simplified analysis procedures are material force-deformation relationships and geometric deformation magnitude (P-Δ effects). The structure configuration (i.e., the degree of redundancy in the assemblage of structural components) and variations in energy-absorption characteristics are also important factors for assessing the nonlinear-response capacity of a structure.

528 019

The most important factor governing the behavior of a structure is its transition from the elastic state to the collapse state. Brittle structures make the transition rapidly, and the modes of deformation associated with each state are distinctly different. Statically determinate structures also tend to make the transition rapidly, irrespective of the component material properties. Ductile structures, on the other hand, make the transition from elastic behavior to collapse slowly, and highly redundant structures tend to do the same. The modes of failure for ductile and redundant structures do not differ as drastically from elastic behavior as do the modes of failure for brittle or determinate structures. These characteristics of structural behavior imply important generalizations about the nature of successful analytic techniques:

- Approximate techniques appropriate to the analysis of brittle or determinate structures require assumptions of two distinct structural states, with instantaneous transition from one state to the other.
- Suitable approximations of the structural behavior for brittle structures can assume mutually exclusive deformation patterns, i.e., the structure is either elastic or at failure.
- Ductile structures require a mechanism of transfer from the elastic to the inelastic state that is more complex than the corresponding mechanism for brittle structures.
- Approximate techniques appropriate to the analysis of ductile or redundant structures require more elaborate representations of the elastic, prefailure condition. Because ductile structures are less likely to reach structural collapse before component limitations have been exceeded, approximations of their failure state can be less accurate than approximations for brittle structures.

The inclusion of nondissipative nonlinearities is rarely treated in the literature, although these nonlinearities can have pronounced effects on structural behavior. Nondissipative nonlinearities, notably buckling, influence structural behavior by producing a frequency shift in the response spectrum with an accompanying change in the structural behavior. Because there is no appreciable energy dissipation, there is no change in the

528 020

response spectrum amplitude. The net effect is to require a nontrivial transition in the structural behavior between the elastic state and collapse. Any structure with elastic nonlinear behavior must be treated in the same fashion as a structure in the ductile or redundant category because the transition has a significant influence on the response.

Summarizing the range of structures typical for a Category I facility, the following behavioral combinations should logically be considered for developing reliable simplified analysis methods:

Structure Assemblage	Material	Energy Absorption	Magnitude of Deformation
Highly Redundant	Brittle	Dissipative	No P-Δ
Nearly Determinate	Ductile	Nondissipative	P-Δ

1.4.3 Approaches to Nonlinear Analysis. For convenience, all nonlinear analysis methods can be grouped under four basic headings: Refined Analysis/Refined Model (RA/RM), Refined Analysis/Simplified Model (RA/SM), Simplified Analysis/Refined Model (SA/RM), and Simplified Analysis/Simplified Model (SA/SM). The basic characteristics of each analysis are noted below:

RA/RM: The solution class contains all major nonlinear software packages and represents a refined finite-element idealization that employs a time integration numerical procedure. RA/RM analysis is expensive, but it eliminates the uncertainty associated with approximation techniques.

RA/SM: The solution class contains the same major software packages to analyze simplified models of the complete structure. RA/SM analysis is commonly used to reduce three dimensions to two dimensions and is often used to reduce the cost associated with a complex analysis.

SA/RM: The solution class is similar to normal mode analysis because it is based on approximate solutions to refined models. In the SA/RM analysis, modeling assumptions are minimized at the expense of truncating the solution accuracy.

528 021

SA/RM solutions also include pseudoelastic formulations.

SA/SM: The solution class is commonly associated with hand calculation methods, notably response spectrum analysis. Analyses are formulated from equivalent damping models or from failure mechanism models.

528 022

2. SIMPLIFIED AND RIGOROUS NONLINEAR ANALYSIS METHODS CONSIDERED

2.1 Introduction

Phase I of this project consisted of a literature survey to identify available simplified and rigorous nonlinear analysis procedures that could potentially be used for the analysis of Category I nuclear power plant structures, systems, and components.

A review of the literature revealed that simplified methods available for performing nonlinear analyses of structures can be separated into two categories: time-history analyses and response spectrum analyses. The former methods generally involve the use of sophisticated models, with simplification introduced only with respect to the analytical solution of the nonlinear equations of motion. The latter methods generally involve simplification of the model to that of an equivalent linear system. Thus, analysis is simplified as well because only linear equations of motion need be solved.

At the conclusion of the literature survey phase of this study, four simplified nonlinear analysis techniques were recommended for further study: the Substitute Structure Method, the Elasto-Plastic Spectrum Method (EPSM), the Approximate Inelastic Response Method (AIRM), and the Reserve Energy Technique (RET). Each of these is described in detail in Appendix A. Additional information concerning the application of these methods is summarized in this chapter.

Refined (rigorous) nonlinear computational procedures for the dynamic analysis of various structures subjected to dynamic excitation generally involve the step-by-step integration of the equations of motion, dividing the response history into short time increments and assuming the properties of the structure to remain constant during each increment but to change in accordance with the deformation state existing at the end of the increment. Thus, the nonlinear analysis procedure is actually a sequence of linear analyses of a successively changing structure. The structures are usually discretized with a group of finite elements.

528 023

There are several rigorous nonlinear analysis programs available to industry. These may be classified broadly into two categories. The first type includes programs developed at universities under grants from various government organizations and private foundations. Such programs are generally available to the public. The second type of computer program is developed and maintained by private companies. Well-known programs, both public and private, are described below. In Phase I, each of these programs was categorized on the basis of underlying assumptions, limitations, and applicability to the nonlinear dynamic analyses of nuclear power plant structures subjected to dynamic excitations.

On the basis of this survey, DRAIN-2D[2.1] and DRAIN-TABS[2.2] were selected for use in this study. The general characteristics of these programs were outlined in the literature survey and are described in Appendix A; additional information concerning the formulation and solution techniques of these programs is summarized here.

2.2 Simplified Methods

2.2.1 Features Common to All Methods. Certain fundamental principles are common to all the simplified nonlinear analysis methods considered in this study. These principles include the concept of structural capacity, the concept of demand, and the reconciliation of demand and capacity as a means of predicting the inelastic dynamic response. The following paragraphs discuss these common principles.

The term capacity, as used in this study, refers to the total seismic input required to bring a structure to particular milestones of behavior. Capacity is not a single value but rather a set of values reflecting various structural milestones such as the development of working stress levels, the development of yield stress levels, the cracking and spalling of concrete, the initiation of significant nonlinear response, and ultimate failure. Various seismic lateral-force characterizations, such as base shear, base overturning moment, or maximum acceleration, could be used to quantify the capacity at these milestones. For this study, a plot of load versus deflection is a convenient way of expressing capacity. A simple example, consisting of a 1-story steel frame with a rigid beam and flexible columns, is illustrated in Figure 2.1. In this case, the capacity is represented by a plot of base

528 024

shear versus roof deflection. The plot consists of two parts: in the elastic region, the base shear is proportional to the roof displacement, and the constant of proportionality is the stiffness of the columns; in the plastic region, unbounded displacements can occur without an increase in base shear. Often the plastic region is given a small stiffness to account for strain hardening and the fact that the columns cannot instantaneously form perfect plastic hinges.

For seismic loads, it is frequently useful to express capacity in terms of spectral response parameters. This is possible because base shear is proportional to spectral acceleration, S_a, and roof displacement is proportional to spectral displacement, S_d. Hence, application of the appropriate factors to a load-deflection diagram (such as shown in Figure 2.1) can convert it into a capacity diagram in terms of S_a and S_d. The latter representation has the same shape as the curve shown in Figure 2.1.

A major step in all simplified nonlinear analysis methods is determination of the structural capacity corresponding to the initiation of inelastic response. This is defined as the point on a load-deflection curve at which there is a drastic change in structural stiffness. Structural response beyond this point is often expressed in terms of a ductility factor, μ, which is the ratio of the maximum displacement to yield displacement. A ductility factor equal to 1.0 is assigned to the initiation of inelastic response.

Determining the initiation of inelastic response may be straightforward or extremely complicated, depending on structural redundancy and on stress-strain characteristics of the material of construction. A simple case is illustrated in Figure 2.1. The column moment of inertia and yield moment, M_y, can be determined from conventional analysis. The base shear, V_y, and roof deflection, Δ_y, that cause M_y in the columns may be computed as shown. In this case, it is clear that the initiation of inelastic response is coincident with the development of yield moment in the column; thus, the calculation of the displacement associated with $\mu = 1$ is straightforward.

Because of the redistribution of load to redundant elements, the yielding of a single beam or column may not be as significant for a complex structure as for a simple structure. The load deflection characteristics for a complex struc-

528 025

ture may be similar to those shown in Figure 2.2. Note the gradual reduction in stiffness in Figure 2.2 as compared with Figure 2.1. For this type of nonlinearity, it is necessary to arbitrarily select a point on the load deflection diagram as the initiation of inelastic response. The arbitrary selection of $\mu = 1$ should be made on a rational basis. For example, $\mu = 1$ may be assigned to the point on the load deflection curve at which the tangent stiffness is 30% to 50% of the initial tangent stiffness.

Another common feature of the various simplified methods is the concept of demand. This is simply a convenient way of quantifying the input load or disturbance that causes nonlinear structural response. For all the simplified nonlinear methods, demand is expressed in terms of a response spectrum. The spectrum alone is a sufficient representation of demand for some of the methods; however, the RET requires additional demand calculations.

All the simplified nonlinear analysis methods require that load demand and structural capacity be expressed in similar units. Several methods require demand and capacity to be calculated in terms of spectral response acceleration; the RET requires calculations in terms of kinetic and strain energy.

One aspect of nonlinear dynamic analysis that sets it apart from linear and static analyses is the fact that both demand and capacity are a function of peak response. Hence, several of the simplified methods involve an iterative procedure to reconcile demand and capacity. Initial demand and capacity calculations are based on an assumed response (i.e., displacement, velocity, or acceleration). Demand and capacity are compared, and the assumed response is varied until the demand equals the capacity.

The following paragraphs summarize the simplified nonlinear analysis methods considered in this study.

2.2.2 Modified Substitute Structure Method. The Substitute Structure Method is basically a design method that has been modified to perform the analysis tasks required by this study. Both demand and capacity can be expressed in terms of spectral acceleration for this method. Substitute structure analysis requires a mathematical model of the structure for calculation of the elastic period of vibration and other structural dynamic properties. The

528 026

model may also be used to determine the base shear that, when resolved into lateral forces, causes the initiation of inelastic response. The corresponding spectral acceleration is computed as follows:

$$S_{ay} = \frac{V_{by}}{W}\left(\frac{1}{\alpha}\right) \qquad (2.1)$$

where:

V_{by} = base shear causing initiation of inelastic response ($\mu = 1$)

W = weight

α = ratio of base shear to spectral acceleration

S_{ay} = spectral acceleration causing initiation of inelastic response

S_{ay} in Equation (2.1) is referred to as the capacity of the structure. The demand is the spectral acceleration taken from a response spectrum the period, T_s, and damping, λ_s, of the substitute structures. T_s and λ_s are functions of ductility:

$$T_s = T\sqrt{\mu} \qquad (2.2)$$

$$\lambda_s = 0.2\left\{1-\left[\frac{1}{(M)^{\frac{1}{2}}}\right]\right\} + 0.02 \qquad (2.3)$$

where:

T = elastic period

μ = an assumed ductility factor equal to the ratio of total displacement to yield displacement

The ductility factor, μ, is varied until the demand spectral acceleration equals S_{ay}.

Appendix A provides a more detailed description of the Substitute Structure Method.

528 027

2.2.3 Elasto-Plastic Spectrum Method (EPSM). The EPSM is similar to the Substitute Structure Method in that it was originally developed as a design method. The EPSM also requires the computation of the elastic period, T, and yield spectral acceleration. As in the Substitute Structure Method, the comparison of demand and capacity is made by means of a response spectrum.

For the EPSM, an elastic response spectrum is reduced by a function of μ to obtain an inelastic response spectrum. The demand spectral acceleration is obtained from the inelastic spectrum at the elastic period of the structure. The ductility is varied until the demand spectral acceleration is equal to S_{ay}.

Construction of the inelastic response spectrum, detailed elsewhere,[2.3,2.4] is provided in Appendix A.

2.2.4 The Approximate Inelastic Response Method (AIRM). Structural capacity is expressed as a diagram of spectral acceleration versus period of vibration for the AIRM. When this plot is superimposed on a response spectrum, the intersection of the capacity curve and the demand response spectrum gives the period and acceleration of the predicted response. The corresponding ductility factor is computed as follows:

$$\mu = S'_d / S_{dy} \tag{2.4}$$

$$S'_d = S'_a \left(\frac{T'}{2\pi}\right)^2 \tag{2.5}$$

$$S_{dy} = S_{ay} \left(\frac{T}{2\pi}\right)^2 \tag{2.6}$$

528 028

where:

μ = ductility factor

S'_d = spectral displacement corresponding to S'_a and T'

S'_a = the spectral acceleration obtained from the intersection of the demand and capacity curves

T' = period obtained from the intersection of the demand and capacity curves

S_{ay} = yield spectral acceleration

T = elastic period of vibration

The calculation of structural capacity in terms of spectral acceleration and period of vibration is described in Appendix A.

2.2.5 The Reserve Energy Technique (RET). The RET was originally developed for use in both the design and the analysis of structures. The basic principle of the method is the conservation of energy. The RET assumes that the energy dissipated by a structure during its peak response is equal to the energy demand created by a dynamic disturbance.

Both demand and capacity calculations are based on the force-deformation characteristics of the building or of the part of the building under consideration. The demand is calculated using the assumption of linear elastic behavior. The capacity is based on the area under the force-derormation curve including both the elastic and the nonlinear range of response.

One important feature of the RET is that it may be applied to a building as a whole, to a portion of a building (such as a story), or to an individual element (such as a beam, column, or wall). In each case, the demand, capacity, and calculated ductility refer to the item being considered. This feature provides the RET with flexibility not found in the other methods.

The RET has been presented in several formats.[2.5-2.8] Any of these may be used for simplified nonlinear analysis; however, the form of RET presented in Appendix B is especially useful because many of the details of demand and capacity calculation have been greatly simplified. This version of the RET has been used in this study. For a multistory structure, the required capacity information consists of the elastic period of vibration and the shears that cause first yielding in each story. The demand shears are calculated from a response spectrum using linear elastic structural dynamics methods, and story ductility factors are based on the ratios of the demand to the yield story shears. This calculation of ductility is based on an elasto-plastic force-deformation relationship, with a factor applied to account for other types of nonlinear behavior.

528 029

2.3 Rigorous Methods

The following criteria were applied in the selection of the computer programs for rigorous nonlinear analyses of the structures: program availability, dimensions of structures, input ground motion capability, and finite-element library. Elaboration of these criteria follows.

As stated in the introduction to this chapter, there are several nonlinear analysis programs available to industry. Those developed and maintained by private companies can be used by anyone after payment of a fee, but program listings are not available to the public. It was felt that, for a research-oriented project such as this, a program in the public domain would be preferable because complete information is available.

Programs with the capability to analyze both two- and three-dimensional structures were needed for this study. For seismic analysis, it is always convenient to have acceleration time histories input as ground motion. Some programs have only a nodal load history input option, and seismic analyses with such programs require prior processing of the input data.

A finite-element library with relevant material-behavior models was necessary. The following elements and material models were required in this study:

- A truss element, to represent the steel brace behavior, with axial load-deformation behavior that is bilinear elasto-plastic in tension and buckling in compression.
- A beam-column element, to model steel beams and columns, that represents the elasto-plastic behavior of steel and incorporates bending moment-axial force interaction curves as yield surfaces.
- A beam element, to model the degrading-stiffness hysteretic behavior of reinforced concrete frames, that is capable of representing the formation of plastic hinges as well as the load-reversal characteristics observed in reinforced concrete frames.
- A shear panel element to represent the reinforced concrete shear walls of the structures of this type that are under investigation.

528 030

Various programs were studied with the above criteria in mind (a detailed discussion is presented in Appendix A). A checklist of the capabilities of these programs is presented in Table 2.1. On the basis of the criteria discussed above, it was decided that DRAIN-2D[2.1] and DRAIN-TABS[2.2] would be most appropriate for the rigorous nonlinear analysis of the two- and three-dimensional structures of the current study. These two programs are discussed in the following sections.

2.4 DRAIN-2D

The computer program DRAIN-2D, developed at the University of California, Berkeley, was used for the rigorous nonlinear analyses of two-dimensional structures. The elements used in modeling the various structures are: truss, beam with degrading stiffness, shear (infill) panel, and beam-column. A brief description of each element follows.

2.4.1 Truss Element. Truss elements may be arbitrarily oriented in the two-dimensional plane but can transmit axial load only. Two alternative modes of inelastic behavior may be specified: yielding in both tension and compression (Figure 2.3a) and yielding in tension but elastic buckling in compression (Figure 2.3b). Strain-hardening effects are included by considering an element to consist of two parallel components, one elastic and one inelastic (Figure 2.4).

Large displacement effects may be approximated by including, for the dynamic phase of the analysis, a geometric stiffness based on the element axial force under static load.

2.4.2 Beam Element with Degrading Stiffness. The beam element with degrading stiffness is formulated to model reinforced concrete beams, which characteristically exhibit degrading flexural stiffness properties when subjected to cyclic loads. The degrading-stiffness beam may be oriented arbitrarily in the two-dimensional plane. The element possesses flexural and axial stiffness, and elements of variab[illegible]ss section can be considered by specifying appropriate flexural stiffness coefficients. Flexural shear deformations and the effects of eccentric end connections can be taken into account.

528 031

Yielding may take place only in concentrated plastic hinges at the element ends. Strain-hardening and degrading flexural stiffness are approximated by assuming that the element consists of a linear elastic beam element with nonlinear rotational springs at each end, as shown in Figure 2.5. All plastic deformation effects, including the effects of degrading stiffness, are introduced by means of the moment-rotation relationships for the hinge springs.

The moment-rotation relationship for each hinge is an extended version of Takeda's model,[2.9] which has the behavior illustrated in Figure 2.5. The basic relationship is in the form of a bilinear curve, with an initial stiffness and a subsequent strain-hardening stiffness characteristic of monotonic loading conditions. The degrading stiffness of the hinges is introduced when reversed loading is applied. Figure 2.5 also indicates rules that are followed for small-amplitude oscillations. The numbers on the legs of the relationship are yield codes printed by the computer program.

The extensions that have been made to the Takeda model are shown in Figure 2.6. These include (1) a reduction of the unloading stiffness by an amount that depends on the largest previous hinge rotation and (2) incorporation of a variable reloading stiffness that is larger than that of the Takeda model and also depends on the past rotation history. To a large degree, these extensions reflect behavior observed in practice. However, some of the features assumed for the extended model, particularly those associated with small-amplitude oscillations, were selected on the basis of engineering judgment and because of the need to avoid illogical or inconsistent patterns of hinge behavior. Such assumed features are necessary because no test data appear to be available for the case of small-amplitude loading cycles that follow large-amplitude cycles.

The unloading stiffness, K_u, depends on the maximum hinge rotation and is controlled by the input parameter α. This parameter controls the unloading stiffness by locating the recovery point, R_{rec}, as shown in Figure 2.6a. It must be nonnegative and might typically lie between zero and 0.4. Regardless of the value of α, the unloading slope is never permitted to be less than the reloading slope; otherwise, a hysteresis loop with a negative area could be produced.

528 032

The reloading stiffness, K_ℓ, also depends on the maximum hinge rotation and is governed by the input parameter β, as shown in Figure 2.6b. The parameter β must be nonnegative and might typically lie between zero and 0.6.

The yield moments may be specified to be different at the two element ends and for positive and negative bending. There is no interaction between axial force and bending moment in producing yield.

Static loads applied within any element length may be taken into account by specifying fixed-end force values. The results of separate static load analyses can be incorporated by specifying initial force values.

Large displacement effects may be approximated in the dynamic analysis by including simple geometric stiffnesses based on the element axial forces under static load.

In the analysis of reinforced concrete frame structures, difficulties inevitably arise in assigning cross-sectional and material properties. The nonlinear material behavior of the concrete, the nonhomogeneous composition of the cross section, and the presence of a varying cross section that is the result of cracking and steel-area changes all combine to make it difficult to assign accurate stiffness values. Considerable experience and experimentation are needed before the element properties can be specified with confidence.

An effective flexural stiffness, EI, which might typically be the EI value for the cracked section, must be specified for the linear elastic line element. An axial stiffness, EA, and an effective shear stiffness, GA', must also be specified.

2.4.3 Infill Panel Element. Infill panel elements are included to permit approximate consideration of infill panels of masonry and similar materials. They may also be used to construct inelastic shear beams.

The element is assumed to have only shear stiffness in the two-dimensional plane. Hence, it provides resistance, through shear deformation, to relative horizontal and/or vertical displacement of the nodes it connects. The

528 033

relationship between shear stress and shear strain may be inelastic, as shown in Figure 2.7. If sudden failure takes place, the forces being resisted by the element immediately prior to failure will suddenly be transferred to the remaining structure, essentially as a shock loading.

Infill panel elements most commonly are rectangular. However, provisions are included to permit variations from a rectangular shape without violating equilibrium. Any variations from a rectangular shape should normally be small; otherwise, the assumption that the element has only shear stiffness may be grossly incorrect.

The shear strain in XY coordinates at the element center is the only deformation considered. The element is treated as an isoparametric finite element, and the increment in shear strain, γ_{xy}, is related to the increments of horizontal and vertical displacement at the nodal points by a displacement transformation. The inelastic deformation is the amount of shear strain beyond yield in the elasto-plastic component of the element.

It is important to note that infill panel elements have shear stiffness only. If these elements are used without a surrounding frame (for example, to represent a shear beam), it is essential that the displacement degrees of freedom permitted not allow modes of deformation for which there is no shear strain at the element center; otherwise, the structure stiffness matrix will be singular.

2.4.4 Beam-Column Element. Beam-column elements may be arbitrarily oriented in the two-dimensional plane. The elements possess flexural and axial stiffness, and elements of variable cross section can be considered by specifying appropriate flexural stiffness coefficients. Flexural shear deformations and the effects of eccentric end connections can be taken into account.

Yielding may take place only in concentrated plastic hinges at the element ends. Strain hardening is approximated by assuming that the element consists of elastic and elasto-plastic components in parallel, as for the truss element. The hinges in the elasto-plastic component yield under constant moment, but the moment in the elastic component may continue to increase. The yield moments may be specified to be different at the two ele-

528 034

ment ends and for positive and negative bending. The interaction between axial force and moment in producing yield may be taken into account approximately.

Static loads applied along any element length may be taken into account by specifying fixed-end force values. The results of separate static load analyses can be incorporated by specifying initial force values.

Large displacement effects may be approximated in the dynamic analysis by including simple geometric stiffnesses based on the element axial forces under static load.

Yield interaction surfaces of three types may be specified, as follows:

- Beam type (shape code = 1, Figure 2.9a), specified where axial forces are small or are ignored. Yielding is affected by bending moment only.
- Steel column type (shape code = 2, Figure 2.9b), intended for use with steel columns.
- Concrete column type (shape code = 3, Figure 2.9c), intended for use with concrete columns.

For any combination of axial force and bending moment within a yield surface, the cross section is assumed to be elastic. If the force-moment combination lies on or outside the surface, a plastic hinge is introduced. Combinations outside the yield surface are permitted only temporarily, being compensated for by applying corrective loads in the succeeding time step.

This procedure is not strictly correct because the axial and flexural deformations interact after yield, and it is therefore wrong to assume that only the flexural stiffness changes and that the axial stiffness remains unchanged. However, this procedure is believed to be reasonable for practical analyses of buildings.

2.5 DRAIN-TABS

528 035

The three-dimensional structures in this study were analyzed with DRAIN-TABS, an extension of the DRAIN-2D program. The element library is the same

as for DRAIN-2D; however, discussion of the three-dimensional idealization of these structures is appropriate.

The building is idealized as a series of independent plane substructures interconnected by rigid horizontal diaphragms. Each substructure can be of arbitrary geometry and may include elements of various types. The elements of each substructure (beams, columns, braces, shear panels, etc.) are thus assumed to be under two-dimensional stress and two-dimensional yielding and failure criteria are applied to beams, columns, etc. This is only an approximation of the general three-dimensional case, but in the case of the structures studied here it is quite adequate.

528 036

REFERENCES

2.1 Kanaan, A. E., and G. H. Powell, *DRAIN-2D, a General-Purpose Computer Program for Dynamic Analysis of Inelastic Plane Structures,* EERC 73-6, Earthquake Engineering Research Center, University of California, Berkeley, 1973.

2.2 Israel, G. R., and G. H. Powell, *DRAIN-TABS, A Computer Program for Inelastic Eqrthquake Response of Three-Dimensional Buildings,* UCB-EERC-77/08, Earthquake Engineering Research Center, University of California, Berkeley, 1977.

2.3 Newmark, N.M., "Current Trends in the Seismic Analysis and Design of High Rise Structures," Chapter 16 in *Earthquake Engineering,* R. L. Wiegel, Ed., Prentice-Hall, Englewood Cliffs (New Jersey), 1970.

2.4 Newmark, N. M., and W. J. Hall, "Procedures and Criteria for Earthquake Resistant Design," *Building Practices for Disaster Mitigation, Building Science Series 46,* National Bureau of Standards, Washington, D.C., February 1973.

2.5 Blume, J. A., "A Reserve Energy Technique for the Earthquake Design and Rating of Structures in the Inelastic Range," *Proceedings, Second World Conference on Earthquake Engineering,* Tokyo, 1960.

2.6 Blume, J. A., N. M. Newmark, and L. H. Corning, Appendix B of *Design of Multistory Reinforced Concrete Buildings for Earthquake Motions,* Portland Cement Association, Skokie (Illinois), 1961.

2.7 Blume, J. A., "Elements of a Dynamic-Inelastic Design Code," *Proceedings, Fifth World Conference on Earthquake Engineering,* Rome, 1973.

2.8 Blume, J. A., "Analysis of Dynamic Earthquake Response," State of Art Report No. 3, Technical Committee 6, Earthquake Loading and Response, *Proceedings, ASCE-IABSE International Conference on the Planning and Design of Tall Buildings,* August 1972.

528 037

2.9 Takeuchi, T., "Study of the Load-Deflection Characteristics of Reinforced Concrete Beams Subjected to Alternating Loads," *Transactions, Architectural Institute of Japan*, Volume 76, September 1962.

523 038

TABLE 2.1

CHECKLIST OF VARIOUS NONLINEAR PROGRAM CAPABILITIES

Program	Availability	Dimension	Input Ground Motion	Steel Brace Element	Steel Beam-Column Element	Reinforced Concrete Beam-Column Element	Reinforced Concrete Shear Panel Element
DRAIN-2D	Public	2-D	Yes	Yes	Yes	Yes	Yes
DRAIN-TABS	Public	3-D	Yes	Yes	Yes	Yes	Yes
NONSAP	Public	3-D	No	No	No	No	Yes
ADINA	Private	3-D	No	No	Yes	No	Yes
ANSR	Public	3-D	Yes	Yes	No	No	No
SAKE	Public	2-D	Yes	No	No	Yes	Yes
MARC-CDC	Private	3-D	Yes	Yes	Yes	No	No
ANSYS	Private	3-D	Yes	Yes	Yes	No	No

528 039

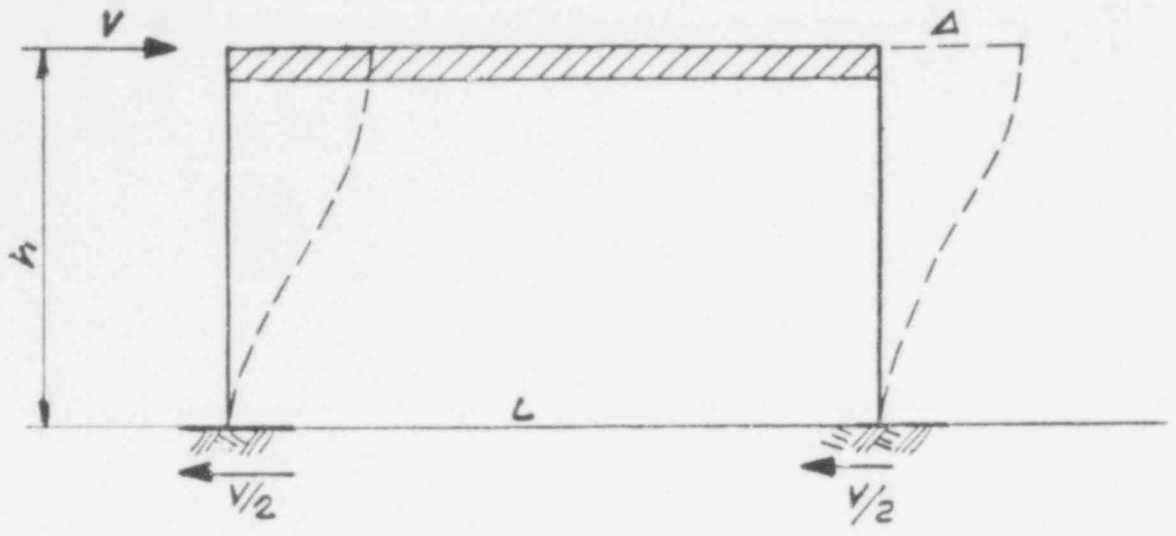

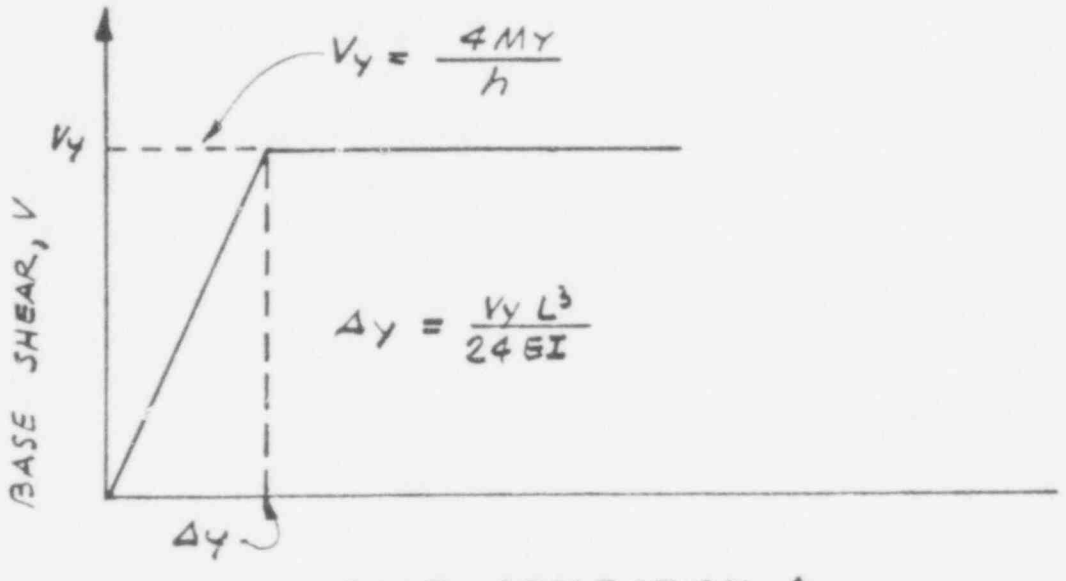

V_y = YIELD SHEAR
Δ_y = YIELD DEFLECTION
M_y = COLUMN YIELD MOMENT

LOAD DEFLECTION
RESPONSE OF A SIMPLE STRUCTURE

NRC/NONLIN FIGURE 2.1

528 040

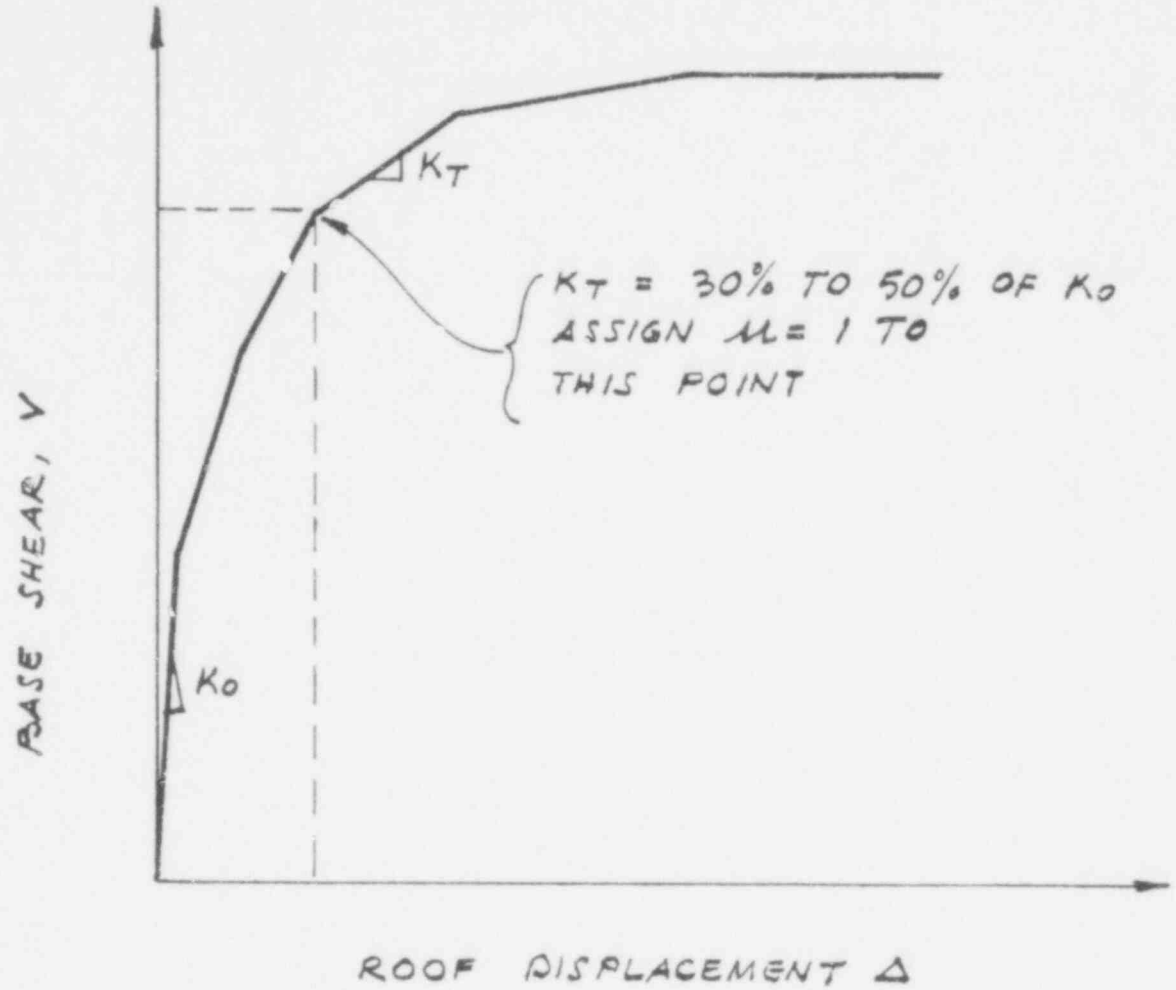

LOAD DEFLECTION

RESPONSE OF A COMPLEX STRUCTURE

NRC/NONLIN FIGURE 2.2

528 041

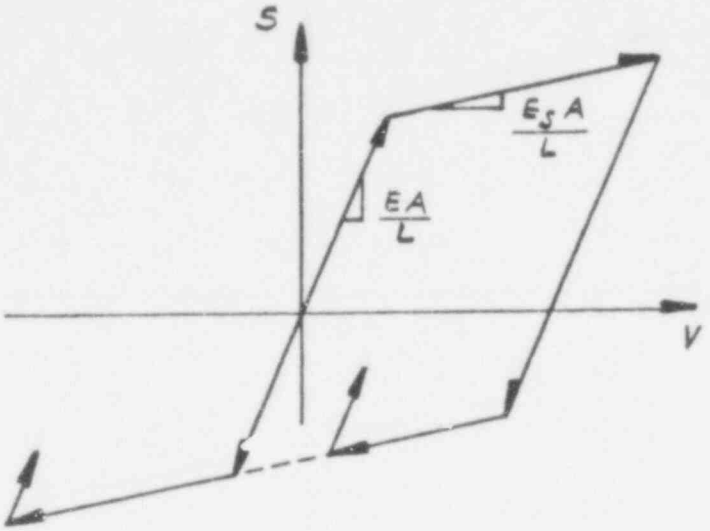

a. YIELD IN TENSION AND COMPRESSION

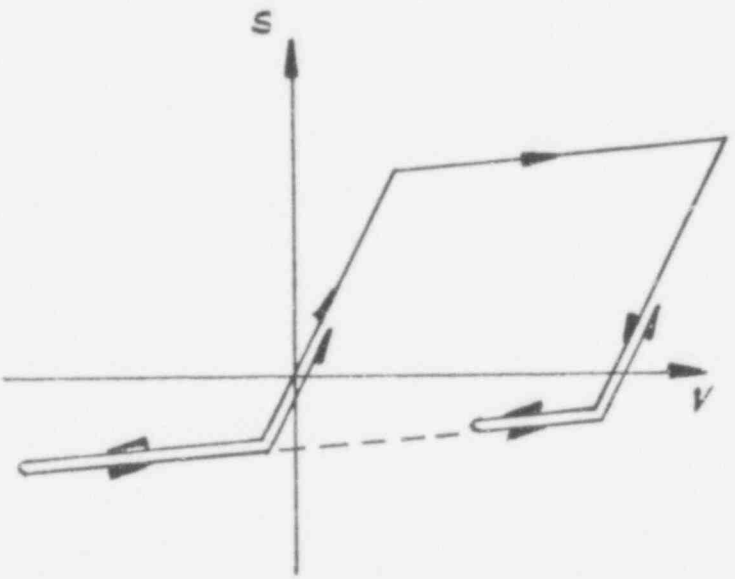

b. YIELD IN TENSION, BUCKLING IN COMPRESSION

TRUSS ELEMENT BEHAVIOR UNDER LOAD REVERSAL

NRC/NONLIN FIGURE 2.3

528 042

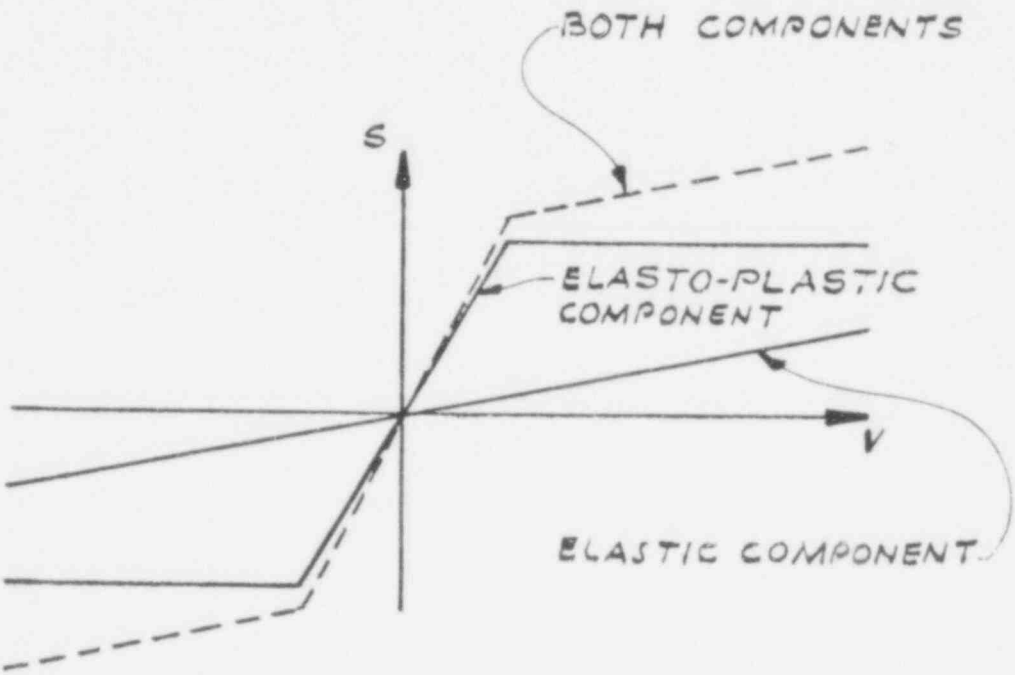

TRUSS ELEMENT BILINEAR BEHAVIOR
INCLUDING STRAIN HARDENING

528

NRC/ NONLIN

FIGURE 2.4

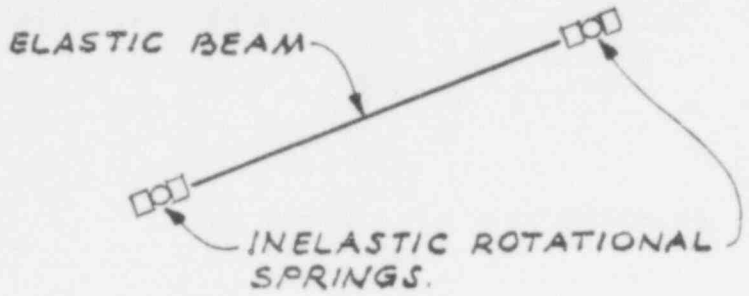

a. ELEMENT IDEALIZATION

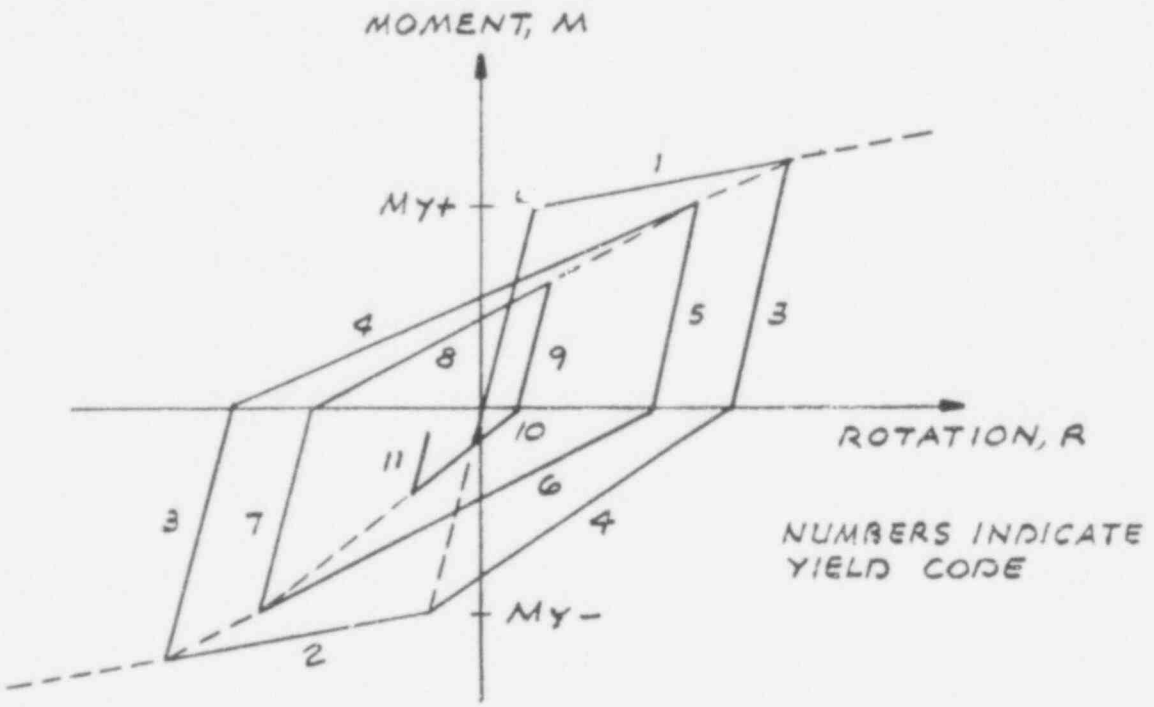

b. HINGE MOMENT - ROTATION RELATIONSHIP FOR TAKEDA MODEL OF REINF. CONC. COLS.

REINFORCED CONCRETE BEAM ELEMENT WITH DEGRADING STIFFNESS

NRC/NONLIN FIGURE 2.5

528 044

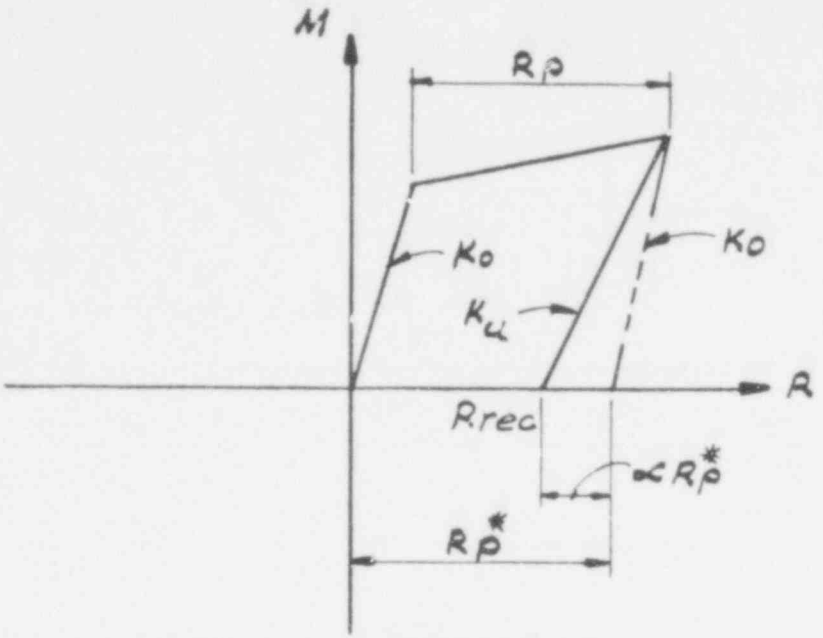

a. UNLOADING STIFFNESS

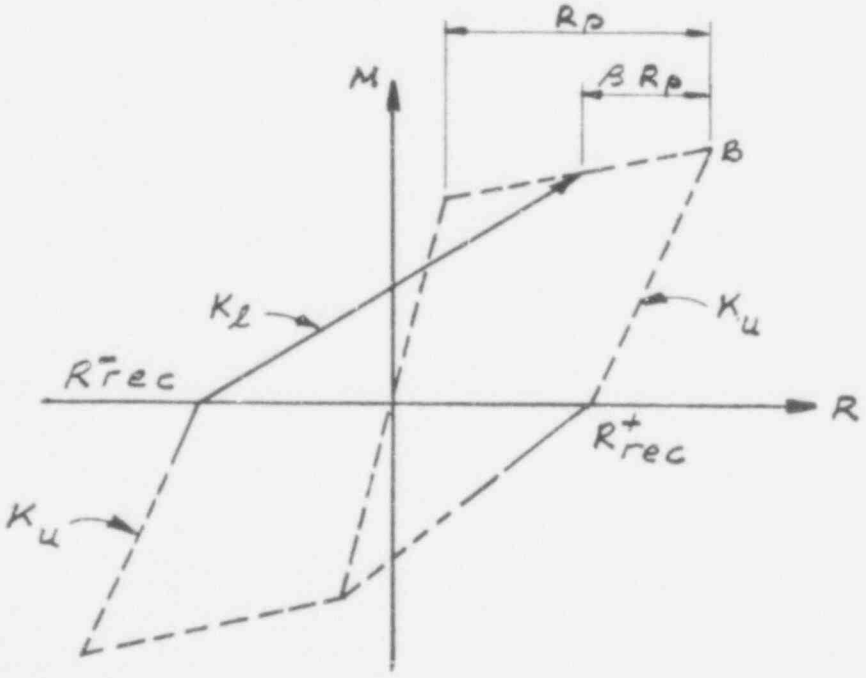

b. RELOADING STIFFNESS

HINGE MOMENT-ROTATION RELATIONSHIP FOR EXTENDED TAKEDA MODEL OF REINFORCED CONCRETE BEAM-COLUMNS

NRC/NONLIN FIGURE 2.6

528 045

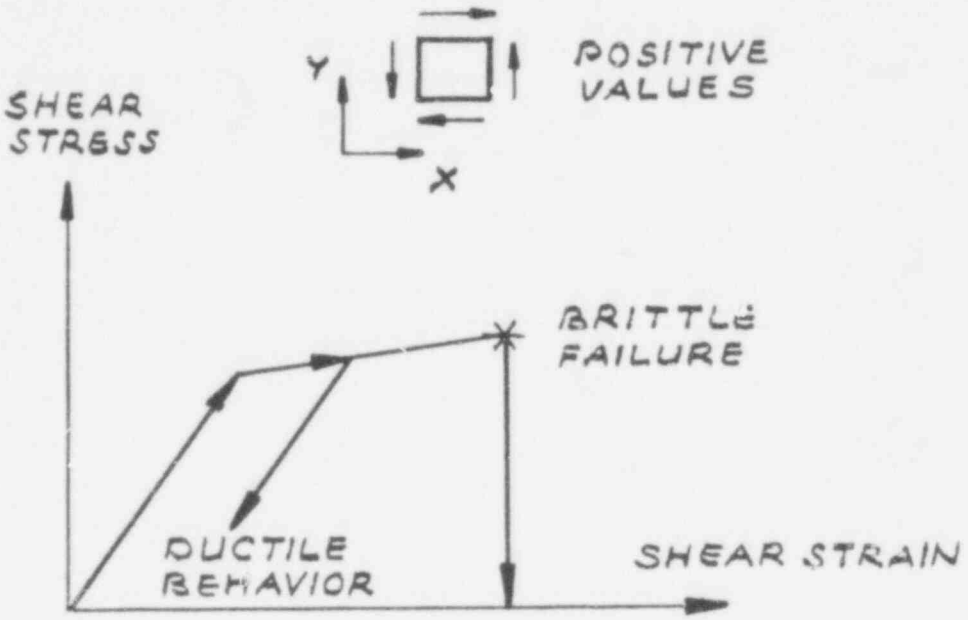

STRESS - STRAIN RELATIONSHIP FOR INFILL PANEL

528 046

NRC/NONLIN FIGURE 2.7

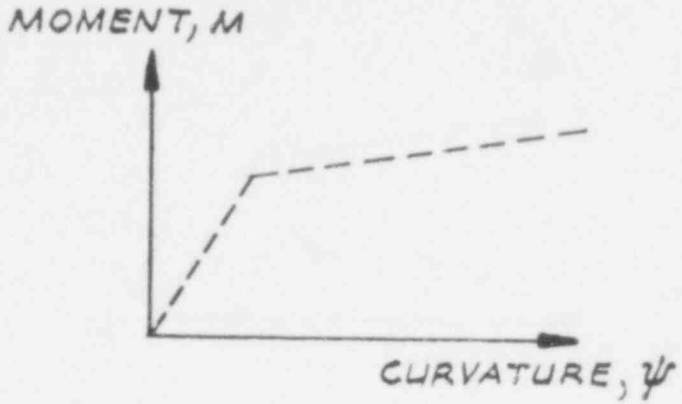

(a)

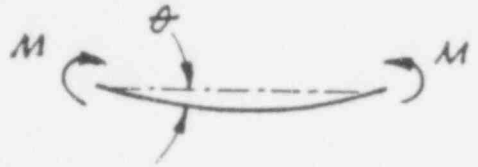

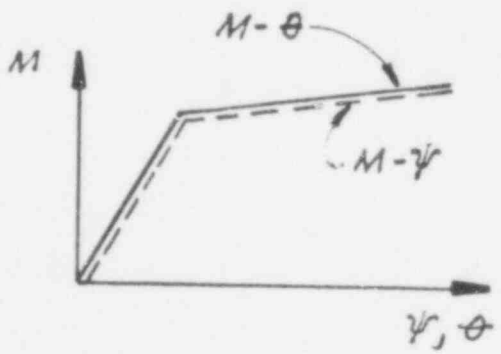

(b)

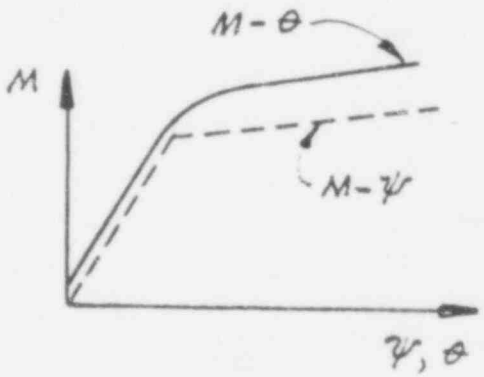

(c)

MOMENT-CURVATURE AND
MOMENT-ROTATION RELATIONSHIPS

NRC/NONLIN

FIGURE 2.8

523 047

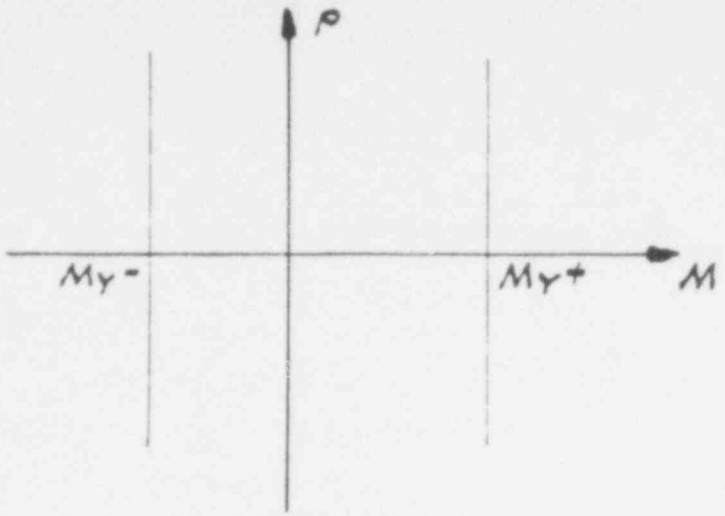

a. SHAPE CODE = 1

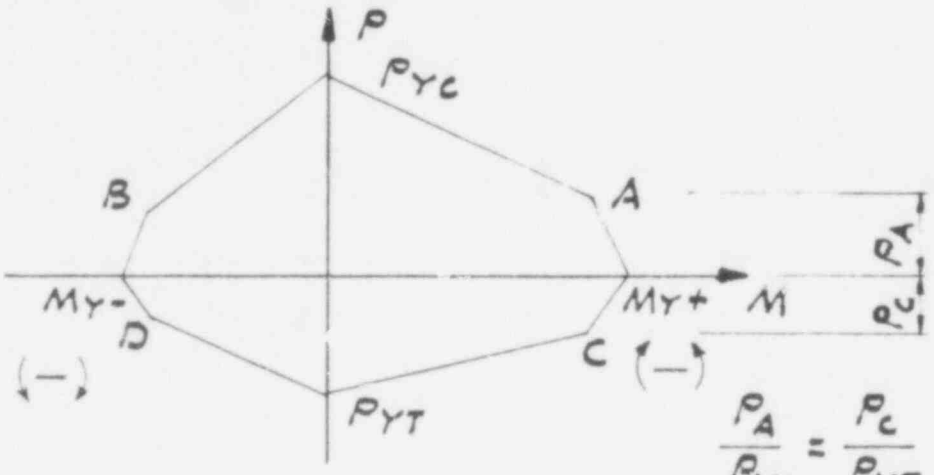

$$\frac{P_A}{P_{YC}} = \frac{P_C}{P_{YT}}$$

b. SHAPE CODE = 2

SIMILARLY FOR B & D

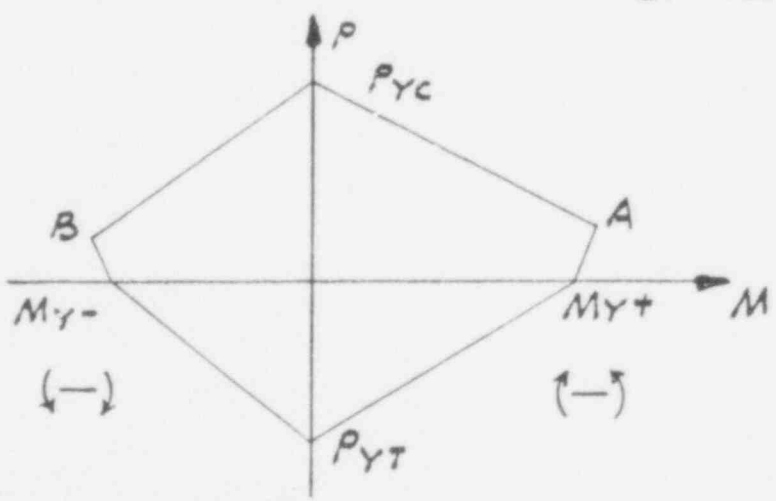

c. SHAPE CODE = 3

528 048

YIELD INTERACTION SURFACES

NRC/NONLIN

FIGURE 2.9

3. SIMPLIFIED NONLINEAR ANALYSIS OF FOUR HYPOTHETICAL STRUCTURES

3.1 Introduction

This chapter describes the analysis of four hypothetical structures: a 1-story plane frame, a 4-story plane frame, a 2-story shear wall, and a three-dimensional, nonsymmetrical 4-story building. Each structure was analyzed using the four simplified nonlinear analysis methods described in Chapter 2. The resulting predicted ductilities are compared to ductilities obtained from rigorous nonlinear analyses of the same structures (Chapters 4 and 5) to facilitate the selection of a simplified nonlinear analysis method for Category I nuclear power plant structures.

3.2 Simplified Nonlinear Analysis of a 1-Story Reinforced Concrete Frame

3.2.1 Description of the Structure. The first hypothetical structure considered in this study is the 1-story reinforced concrete frame illustrated in Figure 3.1. This particular frame was chosen because several similar structures were tested extensively at the University of Illinois.[3.1] The Modified Substitute Structure Method of simplified nonlinear analysis was developed on the basis of those tests.

3.2.2 Description of the Input. Two different input motions were used for each of the simplified and rigorous analyses of the hypothetical 1-story frame structure. The first input was based on the spectral shapes recommended in NRC Regulatory Guide 1.60.[3.2] The NRC spectra, normalized to 0.75g, for various dampings, are plotted in Figure 3.2.

The second input motion consisted of a modified version of the N21E component of the ground acceleration recorded at the Taft, California, Lincoln School Tunnel on July 21, 1952. The modification consisted of compressing the time scale by a factor of 5 and scaling the peak ground acceleration to 2.2g. The time-history and response spectra for this modified Taft record are shown in Figures 3.3 and 3.4. The modified Taft accelerogram was used by researchers at the University of Illinois for shaking table testing of the 1-story frame.

528 049

3.2.3 Structure Capacity Calculations. The four simplified nonlinear analysis methods considered here require information concerning a structure's load-resisting capacity. The calculation of structural capacity is based on the mathematical model of the structure shown in Figure 3.5. The stiffness of the model was adjusted to give an elastic period of 0.11 sec, corresponding to the period measured just prior to yield in the Illinois tests. A structural analysis, summarized in Table 3.1, showed that the applicaiton of a 1-kip base shear to the mathematical model resulted in beam and column moments of 7.7 kip-in. and 7.1 kip-in., respectively. By computing the ratio of these moments to the corresponding yield moments, it is deduced that the base shear causing column yielding is 5.63 kip. Yielding of the column is critical and is identified as the onset of the inelastic response, i.e., the point where $\mu = 1$.

The spectral acceieration corresponding to column yielding is 1.3g. The yield displacement, here defined as the displacement corresponding to $\mu = 1$, was calculated to be 0.14 in. In this case, yield displacement is identical with the yield spectral displacement although this does not hold true for multidegree-of-freedom structures.

For the Elasto-Plastic Spectrum Method (EPSM) and the Modified Substitute Structure Method, the required structural capacity information consists of period, T, and yield spectral acceleration, S_{ay}. For the 1-story frame, T = 0.11 sec and S_{ay} = 1.3g.

For the Reserve Energy Technique (RET) and the Approximate Inelastic Response Method (AIRM), more specific post-elastic capacity information is generally required. In this case, the nonlinear response of the structure was based on a bilinear force-deformation diagram, as shown in Figure 3.6. For the AIRM, the slope of the second portion of the bilinear force-deformation diagram was varied from zero to 10% of K_o, also shown in Figure 3.6. (The intent was to make a similar set of assumptions for the RET; however, the analysis showed that in this case the results were not sensitive to the assumed bilinear slope parameter.)

528 050

Capacity in terms of spectral acceleration and period of vibration is extracted from a force-deformation diagram, as indicated in Figure 3.7.

3.2.4 Demand. The demand response spectra are summarized in Figure 3.2 for the analysis using NRC spectra and in Figure 3.4 for the Taft analysis. The NRC spectra are normalized to 0.75g; the Taft spectra, to 2.2g.

3.2.5 Results of Simplified Nonlinear Analysis. Table 3.2 is a summary of the results of the analysis of the 1-story reinforced concrete frame using various simplified nonlinear analysis methods and the NRC input response spectra.

For all methods except the Modified Substitute Structure Method, damping ratios of 5%, 7%, and 10% were used. (The Modified Substitute Structure Method involves the calculation of damping as part of the analysis.) The period of vibration is calculated as part of the RET, the AIRM, and the Modified Substitute Structure Method. The EPSM specifically recommends that the inelastic analysis be made using the initial elastic period. The ductilities predicted by the various methods range from 1.0 to 16.0. The RET and EPSM give similar results, and the Modified Substitute Structure ductility and AIRM ductility for 10% damping are identical.

Table 3.3 summarizes the results of the simplified analysis of the 1-story frame for the analysis using modified Taft input spectra. For the RET, AIRM, and EPSM, 7% damping was assumed; 12% damping was calculated as part of the Modified Substitute Structure analysis. Considering the accuracy that can reasonably be expected from simplified nonlinear analysis, it is concluded that the RET, the EPSM, and the Modified Substitute Structure Method give essentially the same result in this case. The ductility factor predicted by the AIRM ($\mu = 9$) is well beyond the range predicted by the other methods.

The results of the simplified analyses are compared with rigorous analysis of this structure in Chapter 5.

528 051

3.3 Simplified Nonlinear Analysis of a 4-Story Reinforced Concrete Frame

3.3.1 Description of the Structure. The 4-story reinforced concrete frame used in this analysis is identical to one longitudinal frame of a full-scale 4-story test structure that was built in 1964 at the Department of Energy's Nevada Test Site.[3.3] Overall plans of the 4-story test structure are illustrated in Figure 3.8. The frame shown in the east elevation was used in this analysis. Column and beam details are shown in Figures 3.9 and 3.10. The following material properties were assumed:

f'_c = 4,500 psi

f_y = 50,000 psi

E_s = 30 x 10^6 psi

E_c = 4 x 10^6 psi

3.3.2 Load Capacity Calculations. Calculations of structural load capacity were based on the mathematical model shown in Figure 3.11.

The fundamental mode period of the model was computed to be 0.5 sec. Vibration tests of the 4-story test structure resulted in a measured fundamental mode period of 0.55 sec just prior to major yielding and structural damage.[3.4] Hence, the model appears to be an adequate representation of the pre-yield response of the structure.

A study was conducted to determine the error that might be introduced into this analysis from neglecting higher modes of vibration. The results of a single-mode analysis were compared with those of a multimode analysis. The comparison showed that a 12% error in the member forces might result from neglecting higher modes. This error is not considered to be significant relative to the approximations inherent in the various simplified analysis methods; hence, higher modes were neglected in this study.

Calculations to determine the yield capacity of the 4-story frame are summarized in Table 3.4. This analysis shows that beam 2 and beam 1 both yield at zero period acceleration of approximately 0.18g. This is equivalent to a spectral acceleration of 0.54g at 5% damping and T = 0.5 sec. Correspond-

528 052

ing yield forces, displacement, and accelerations of the 4-story frame are summarized in Table 3.5.

The data presented in Table 3.5 are adequate for the EPSM and the Modified Substitute Structure Method. The RET requires additional data. In this case, the shears that cause yield in each story are needed; the values are summarized in Table 3.6. These values were used in calculating story ductility factors by the method outlined in Appendix B.

The additional data necessary for the AIRM were obtained by modifying the original elastic model. The modification consisted of reducing the moment of inertia of beams 1 and 2 to 5% of the initial value. Subsequent analysis showed that only a small amount of lateral force could be added to the modified model before yielding occurred in the third-story beam and the bottom of the first-story column. The stiffness of these elements was reduced to 5% of their initial value, and the additional load required to yield the fourth-story beam was calculated. This was assumed to be the failure point, and the analysis was stopped here. Each time the model was modified and reanalyzed, the spectral acceleration, spectral displacement, and period of vibration were noted. These data are plotted in Figure 3.12.

3.3.3 Description of Input Ground Motion. Input for the various simplified analyses of the 4-story reinforced concrete frame consisted of the NRC Regulatory Guide 1.60 response spectra. Two separate analyses, one with a zero period acceleration of 0.5g and another with a zero period acceleration of 1.0g, were conducted using each simplified method. Damping of 7% of critical was used in all cases except the analyses using the Substitute Structure Method.

3.3.4 Summary of Results of 4-Story Reinforced Concrete Frame. Predicted ductilities for the various simplified methods (rounded to the nearest whole number) are summarized in Table 3.7. Results for 0.5g and 1.0g are given. The data shown in this table indicate identical results for the EPSM and the RET. There is also a close correspondence between the results for the AIRM and Modified Substitute Structure analyses. Similar trends were also noted in the results of the simplified analyses of the 1-story frame.

528 053

3.4 Simplified Nonlinear Analysis of a 2-Story Shear Wall

3.4.1 Description of Structure. Details of a 2-story shear wall are illustrated in Figure 3.13. This wall is similar to a wall recently tested by the Portland Cement Association (PCA) as part of a large-scale investigation of shear wall behavior.[3.5] (The PCA tested a 1-story version of this wall.) An arbitrary weight of 475 kip was assigned to each story; this results in a fundamental mode period of approximately 0.15 sec. Material and reinforcing properties for this shear wall are listed in Table 3.8.

3.4.2 Load Capacity Calculations. This section is divided into three subsections describing ultimate strength calculations, stiffness and period calculations, and post-ultimate load behavior.

3.4.2.1 Strength Calculations. Flexural strength calculations were based on the assumptions of section 10.2 of ACI 318-71.[3.6] The following formula for flexural strength was adapted from Reference 3.7:

$$M_u = A_s f_y l_w \left[\left(1 + \frac{N_u}{A_s f_y} \right) \left(\frac{1}{2} - \frac{\beta_1 c}{2 l_w} \right) - \frac{c^2}{l_w^2} \left(1 + \frac{\beta^2}{3} - \beta_1 \right) \right]$$

where:

$$\frac{c}{l_w} = \frac{q + a}{2q + 0.85\beta_1}$$

$$q = \frac{A_s f_y}{l_w h f'_c}$$

$$a = \frac{N_u}{l_w h f'_c} \text{ and } \beta = \frac{f_y}{87{,}000}$$

M_u = ultimate moment capacity, in.-lb

A_s = total area of vertical reinforcement at section, in.^{2}

f_y = specified yield strength of vertical reinforcement, psi

l_w = horizontal length of shear wall, in.

528 05.

c = distance from extreme compression fiber to neutral axis, in.

d = distance from extreme compression fiber to resultant of tension force, in.

h = thickness of shear wall, in.

N_u = design axial load, positive in compression, lb

f'_c = specified compressive strength of concrete, psi

β_1 = 0.85 for strength f'_c up to 4,000 psi and reduced continuously to a rate of 0.05 for each 1,000 psi of strength in excess of 4,000 psi

The shear strength provisions were taken directly from ACI-318-71:

$$v_c = 3.3\sqrt{f'_c} + \frac{N_u}{4\ell_w h}$$

$$v_s = \rho F_y$$

$$v_u = v_c + v_s < 10\sqrt{f'_c}$$

$$V_u = v_u h d$$

where:

v_c = shear stress carried by concrete, psi

v_s = shear stress carried by reinforcing steel, psi

ρ = ratio of horizontal reinforcing

v_u = combined ultimate shear strength, $< 10\sqrt{f'_c}$, psi

V_u = ultimate shear load, lb

Applying these provisions to the shear wall resulted in the following computed strengths:

M_u = 8,243 kip-in. (moment strength)

V_u = 172 kip (shear strength)

05

A base shear equal to 120 kip corresponds to M_u = 8,243 kip-in., which is less than the ultimate shear strength. Hence, this wall fails in a flexural mode with a base shear of 120 kip and an overturning moment of 8,243 kip-in. Assuming $C_b/S_a = 0.9$, the spectral acceleration corresponding to the ultimate load capacity is computed as follows:

$$S_{au} = \left[\frac{V_u}{W}\right] C_b/S_a = \frac{120}{475 \times 2} \times 0.9 = 0.11g$$

3.4.2.2 Stiffness and Period Calculations. Period calculations were based on the two-degree-of-freedom model shown in Fibure 3.14. Assuming equal mass and stiffness for each story, the equations of motion for free vibration may be solved for the fundamental mode period as follows:

$$\left(\frac{2\pi}{T}\right)^2 = 0.382 \frac{K}{m}$$

where:

T = fundamental mode period
K = story stiffness
m = story mass

Approximate calculations of the elastic story stiffness for this shear walls with edgemembers were based on the axial stiffness of an equivalent compression strut. The characteristics of the strut were determined by a method developed by Klingner and Bertero.[3.8] Details are given in Appendix C.

For shear walls without edgemembers, the elastic stiffness can be approximated as follows:

$$K = \frac{A_s G}{H}$$

where:

A_s = shear area of the wall
G = shear modulus
H = interstory height

528

These approximate elastic stiffness formulas may be used in lieu of a more precise stiffness evaluation, which might involve an elastic mathematical model of the structure being considered.

3.4.2.3 Postultimate Load Behavior. The post-ultimate load behavior of reinforced concrete shear walls is discussed in detail in Appendix C. The limited data on this subject suggest that shear walls without edgemembers are essentially elasto-plastic as shown in Figure 3.15a. Different behavior was observed from the data on shear walls with edgemembers, and the load-deflection curve illustrated in Figure 3.15b was chosen to represent these data. Details are given in Appendix C.

Calculations that were performed using the load-deflection curve for shear walls with edgemembers (Figure 3.15b) demonstrated that the ultimate load according to the ACI code was often not substantially greater than the strength calculated by considering only the horizontal reinforcing steel. Furthermore, the transition between these two plateaus (see Figure 3.15b) occurred at a range of deflections that was judged to be excessive; i.e., the wall would be considered unserviceable in this range of deflections. Hence, the load-deflection curve that was initially postulated for shear walls with edgemembers is not practical. For this study, all shear walls were considered to have elasto-plastic force-deformation characteristics.

3.4.3 Description of Input Motion. Motion input for the simplified analyses of this 2-story shear wall consisted of the NRC Regulatory Guide 1.60 response spectra normalized to 0.20g. Damping of 7% critical was used in all cases except the analyses using the Substitute Structure Method.

3.4.4 Results of Simplified Analyses. Table 3.9 summarizes the simplified analyses of a 2-story shear wall. The EPSM and the RET essentially gave the same result; extremely large ductility factors were obtained using the AIRM and the Modified Substitute Structure Method. The numerical values of the ductility factors obtained with the latter two methods have little meaning in this case because these two simplified analysis methods essentially are predicting collapse.

3.5 Simplified Nonlinear Analysis of a Torsion Building

3.5.1 Description of the Structure. The purpose of these analyses was to investigate the application of the various simplified nonlinear analysis methods to a three-dimensional, nonsymmetrical structure; i.e., a torsion building. A modified version of the 4-story building shown in Figure 3.8 was used for this analysis; the modification consisted of increasing the stiffness of one longitudinal frame by 50%.

3.5.2 Capacity Calculations. Capacity calculations for the torsion building were similar to those performed for the analyses of the 4-story reinforced concrete frame, the only difference being that the torsion building calculations were done using a three-dimensional model. The model accounted for the actual distribution of strength and stiffness throughout the building.

Results of the capacity calculations are summarized in Tables 3.10 and 3.11 and in Figure 3.16.

3.5.3 Description of Input Motion. The input motion for the torsion building analysis consisted of the NRC Regulatory Guide 1.60 response spectrum for 7% damping normalized to 1.0g.

An identical input was used for some of the analyses of the 4-story reinforced concrete frame.

3.5.4 Summary of Results. A summary of the simplified nonlinear analyses of the torsion building is presented in Table 3.12. As was the case for the other examples, the EPSM and the RET analyses produced similar results, and the Modified Substitute Structure Method and the AIRM both predicted greater ductility factors.

This study of a torsion building indicates that the simplified methods are applicable to three-dimensional nonsymmetrical structures. Except for the additional complexities in modeling and capacity calculations, the simplified analyses of this torsion building were no different from the analyses of the other structures considered in this chapter.

528 058

REFERENCES

3.1 Gulkan, P., and M. A. Sozen, "Response and Energy Dissipation of Reinforced Concrete Frames Subjected to Strong Base Motions," *Structural Research Series* No. 377, University of Illinois, Urbana, May 1971.

3.2 U. S. Nuclear Regulatory Commission, *Design Response Spectra for Seismic Design of Nuclear Power Plants*, Regulatory Guide 1.60, Washington, D. C., December 1973.

3.3 John A. Blume & Associates Research Division, *Concrete Test Structures: First Report on Structural Response*, JAB-99-29, prepared for the Nevada Operations Office, U. S. Atomic Energy Commission, San Francisco, 1976.

3.4 Chen, C. K., R. M. Czarnecki, and R. E. School, *Vibration Tests of a 4-Story Reinforced Concrete Test Structure*, JAB-99-119, prepared for the Nevada Operations Office, U. S. Energy Research and Development Administration, San Francisco, 1976.

3.5 Barda, F., J. Hanson, and W. Corley, "Shear Strength of Low-Rise Walls with Boundary Elements," *Reinforced Concrete Structures in Seismic Zones*, ACI Publication SP-42, American Concrete Institute, Detroit, 1974.

3.6 *Building Code Requirements for Reinforced Concrete (ACI 3/8/71)*, American Concrete Institute, Detroit, 1971.

3.7 Cardenas, A. E., J. M. Hanson, W. G. Corley, and E. Hognestat, "Design Provisions for Shear Walls," *ACI Journal*, American Concrete Institute, Detroit, March 1973.

3.8 Klingner, R. E., and V. V. Bertero, *Infilled Frames in Earthquake-Resistant Construction*, EERC 76-32, Earthquake Engineering Research Center, University of California, Berkeley, 1976.

528 059

TABLE 3.1

SUMMARY OF CAPACITY CALCULATIONS: 1-STORY FRAMES

Element	Moment for 1-kip Base Shear (kip-in.)	Yield Moment (kip-in.)	Base Shear for Yield Moment (kip)	Spectral Acceleration* for Yield (g)
Beam	7.7	56	7.27	1.7
Column	7.1	40	5.63	1.3

*Assuming $C_b/S_a = 1.0$

528 060

TABLE 3.2

SUMMARY OF PREDICTED DUCTILITIES AND DISPLACEMENTS: SIMPLIFIED NONLINEAR ANALYSES OF THE 1-STORY REINFORCED CONCRETE FRAME USING NRC INPUT SPECTRA

Analysis Method	Assumed Damping (%)	Period (sec)	Ductility Factor	Displacement (in.)
Reserve Energy Technique	5	0.13	1.4	0.20
	7	0.12	1.2	0.17
	10	0.11	1.0	0.14
Approximate Inelastic Response Method*	5	0.30	16.0	2.20
	7	0.30	11.0	1.50
	10	0.20	6.0	0.80
Elasto-Plastic Spectrum Method	5	0.11**	2.0	0.28
	7	0.11**	1.5	0.21
	10	0.11**	1.2	0.17
Modified Substitute Structure Method	14***	0.26	6.0	0.80

*Results shown are for 5% bilinear slope parameter. The analysis for other slope parameters gives different results, but these do not materially affect the conclusions of this study.

**Assumed

***Calculated

528 061

TABLE 3.3

SUMMARY OF PREDICTED DUCTILITIES AND DISPLACEMENTS:
SIMPLIFIED NONLINEAR ANALYSES OF THE
1-STORY REINFORCED CONCRETE FRAME USING
MODIFIED TAFT INPUT SPECTRA

Analysis Method	Damping (%)	Period (sec)	Ductility Factor	Displacement (in.)
Reserve Energy Technique	7	0.17	3.6	0.50
Approximate Inelastic Response Method	7	0.27	9.0	1.21
Elasto-Plastic Spectrum Method	7	0.11	3.5	0.49
Modified Substitute Structure Method	12	0.20	4.4	0.62

528 062

TABLE 3.4

4-STORY REINFORCED CONCRETE FRAME:

CALCULATIONS TO DETERMINE YIELD POINT

Element*	Moment from Analysis** (kip-in.)	Yield Moment, *My* (kip-in.)	Ratio to Yield
Column 4			
Top	2,122	1,470	0.69
Bottom	1,036		1.42
Column 3			
Top	3,339	1,470	0.44
Bottom	2,764		0.53
Column 2			
Top	4,063	1,470	0.36
Bottom	3,997		0.37
Column 1			
Top	3,043	1,470	0.48
Bottom	5,840		0.25
Beam 4	2,122	989	0.47
Beam 3	4,376	989	0.23
Beam 2	6,827	1,277	0.19
Beam 1	7,041	1,277	0.18

*See Figure 3.11.

**Analysis for 5% NRC Response Spectrum normalized to 1.0g, fundamental mode only.

528 063

TABLE 3.5

4-STORY REINFORCED CONCRETE FRAME:

YIELD POINT DATA

Period (sec)	Spectral Acceleration (g)	Spectral Displacement (in.)	Base Shear (kip)	Roof Displacement (in.)
0.5	0.54	1.3	30	1.7

TABLE 3.6

4-STORY REINFORCED CONCRETE FRAME:

STORY YIELD SHEARS FOR RET ANALYSIS

Story, j	Yield Shear, V_{y_j} (kip)
4	29
3	26
2	28
1	30

528 064

TABLE 3.7

SUMMARY OF PREDICTED DUCTILITIES:
SIMPLIFIED NONLINEAR ANALYSIS OF
4-STORY REINFORCED
CONCRETE FRAME

Analysis Method	Damping (%)	0.5g Earthquake		1.0g Earthquake	
		Period (sec)	Ductility Factor	Period (sec)	Ductility Factor
Reserve Energy Technique	7	0.63	2	1.2	4
Approximate Inelastic Response Method	7	0.84	4	1.3	13
Elasto-Plastic Spectrum Method	7	0.50	2	0.5	4
Modified Substitute Structure Method	12*	1.00	4	2.0	14

*Computed

528 065

TABLE 3.8

MATERIAL PROPERTIES OF SHEAR WALL

Concrete Ultimate Strength f'_c (psi)	Steel Yield Strength, f_y (psi)	Elastic Modulus of Concrete, E_c (psi)	Shear Modulus of Concrete, G (psi)	Elastic Modulus of Steel, E_s	Web Reinforcing Ratio, ρ_w	Edgemember (flange) Reinforcing Ratio, ρ_f
4,000	75,000	3.4×10^6	1.36×10^6	29×10^6	0.005 (both ways)	0.018 (vertical)

528 066

TABLE 3.9

SIMPLIFIED NONLINEAR ANALYSIS OF 2-STORY SHEAR WALLS

Analysis Method	Predicted Ductility of 2-Story Wall with Edgemembers	Predicted Ductility of 2-Story Wall without Edgemembers
Reserve Energy Technique	8	8
Approximate Inelastic Response Method	200 (collapse)	200 (collapse)
Elasto-Plastic Spectrum Method	7	7
Modified Substitute Structure Method	60 (collapse)	60 (collapse)

528 067

TABLE 3.10
TORSION BUILDING:
YIELD POINT DATA

Period (sec)	Structural Acceleration (g)	Spectral Displacement (in.)	Base Shear (kip)	Roof Displacement (in.)
0.45	0.7	1.39	68	1.8

TABLE 3.11
TORSION BUILDING:
STORY SHEAR DATA FOR RET ANALYSIS

Story, j	Yield Shear, V_{y_j} (kip)
4	52
3	57
2	66
1	68

528 068

TABLE 3.12

TORSION BUILDING:

SUMMARY OF RESULTS

Analysis Method	Predicted Ductility
Reserve Energy Technique	4
Approximate Inelastic Response Method	16
Elasto-Plastic Spectrum Method	4
Modified Substitute Structure Method	10

528 069

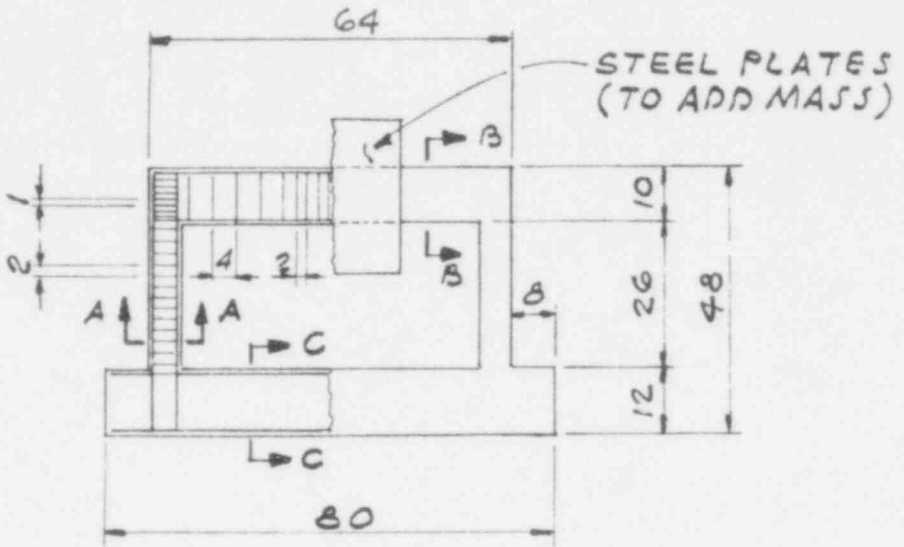

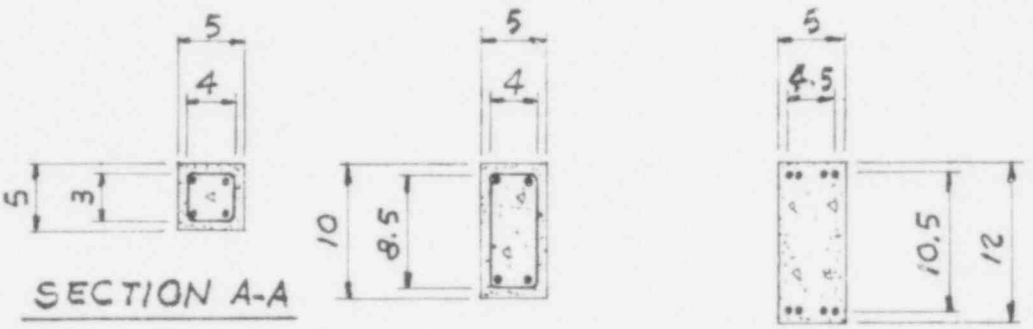

ALL DIMENSIONS IN INCHES
LONGITUDINAL REINFORCEMENT, DEF. NO. 3 BARS
TRANSVERSE REINFORCEMENT, PLAIN 1/8 IN ROUND BARS

LONGITUDINAL REINFORCING	FY = 51	KSI
TRANSVERSE REINFORCING	FY = 74	KSI
CONCRETE	Fc = 5150	PSI

HYPOTHETICAL STRUCTURE - ONE STORY FRAME

NRC, NONLIN 528 C-3 FIGURE 3.1

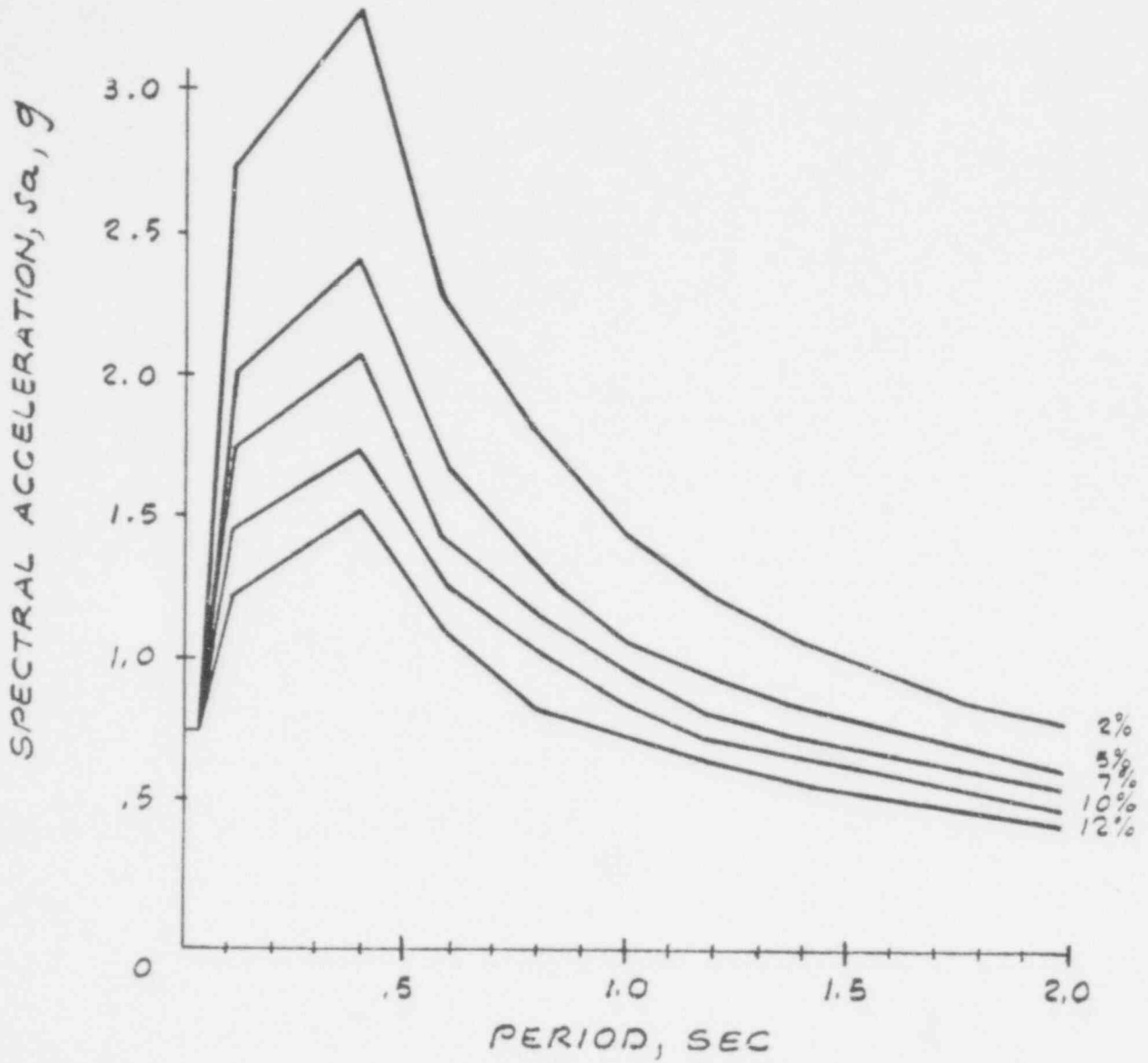

ONE-STORY FRAME INPUT SPECTRA

528 0-1

NRC/NONLIN FIGURE 3.2

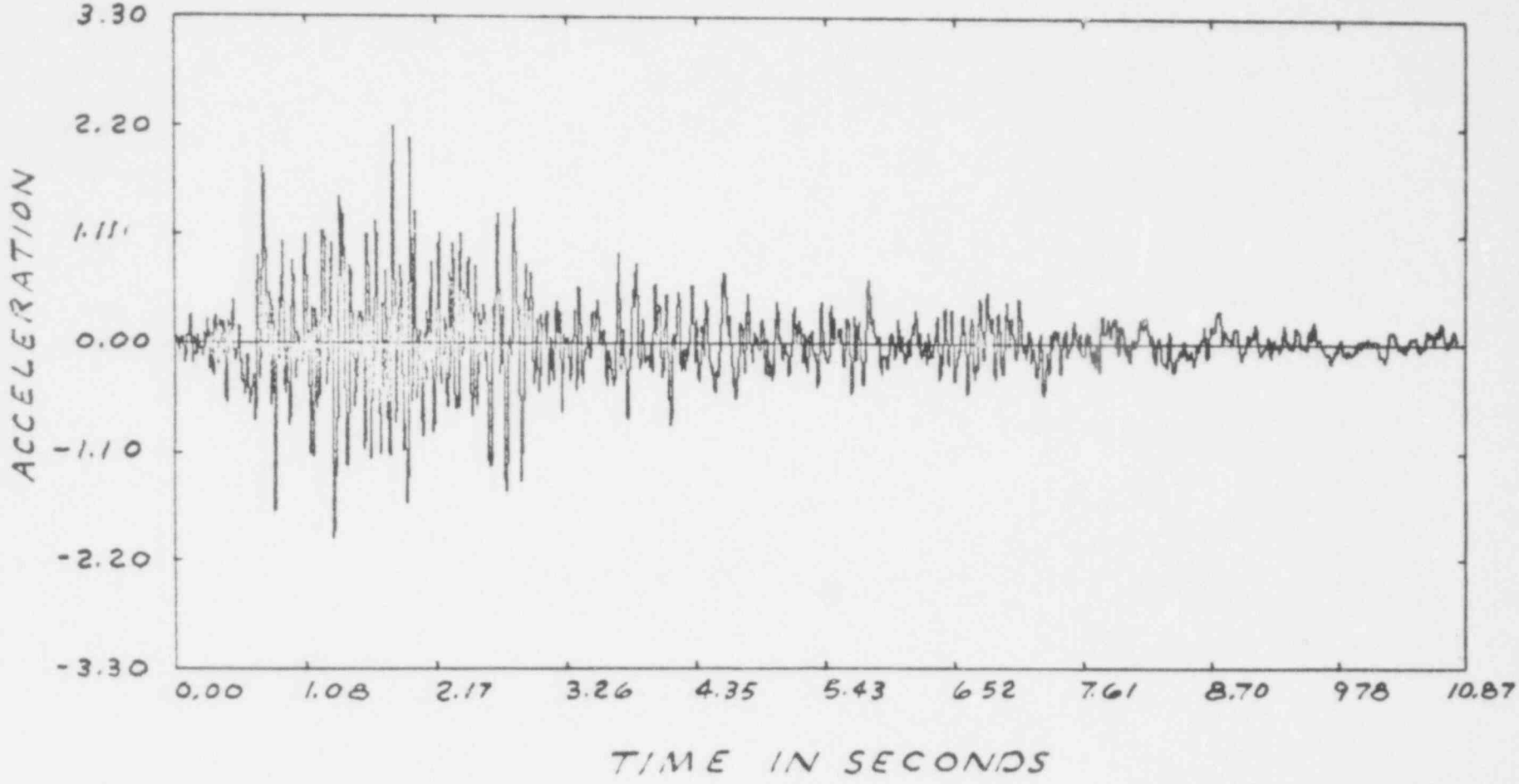

528 072

FIGURE 3.3

TAFT 1952 N21E ACCELEROGRAM
SCALED TO 2.2g TIME COMPRESSED BY 5

TAFT 1952 N21E RESPONSE SPECTRA
SCALED TO 2.26 TIME COMPRESSED DAYS
5% 7% 10% 12% DAMPING.

528 073

NRC/NONLIN

FIGURE 3.4

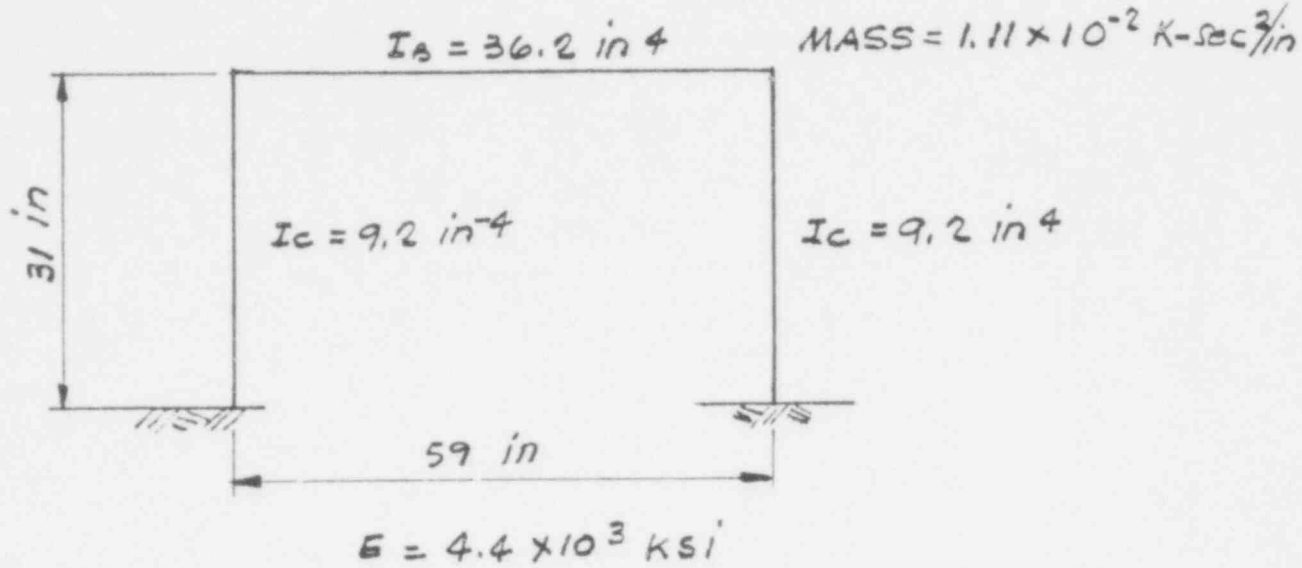

MATHEMATICAL MODEL OF ONE-STORY REINFORCED CONCRETE FRAME

528 074

NRC/NONLIN FIGURE 3.5

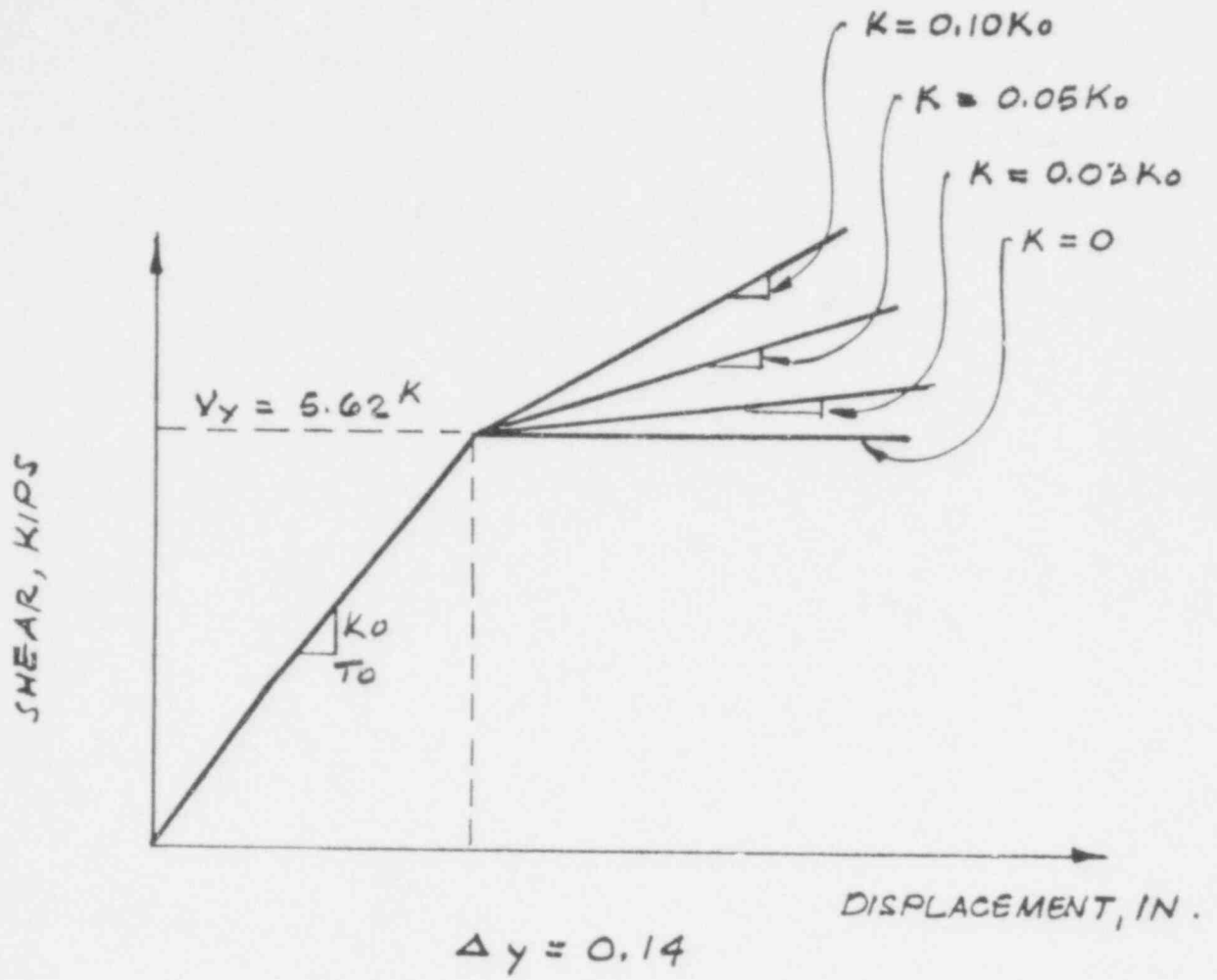

ONE-STORY FRAME FORCE-DEFORMATION DIAGRAM

528 075

NRC/NONLIN FIGURE 3.6

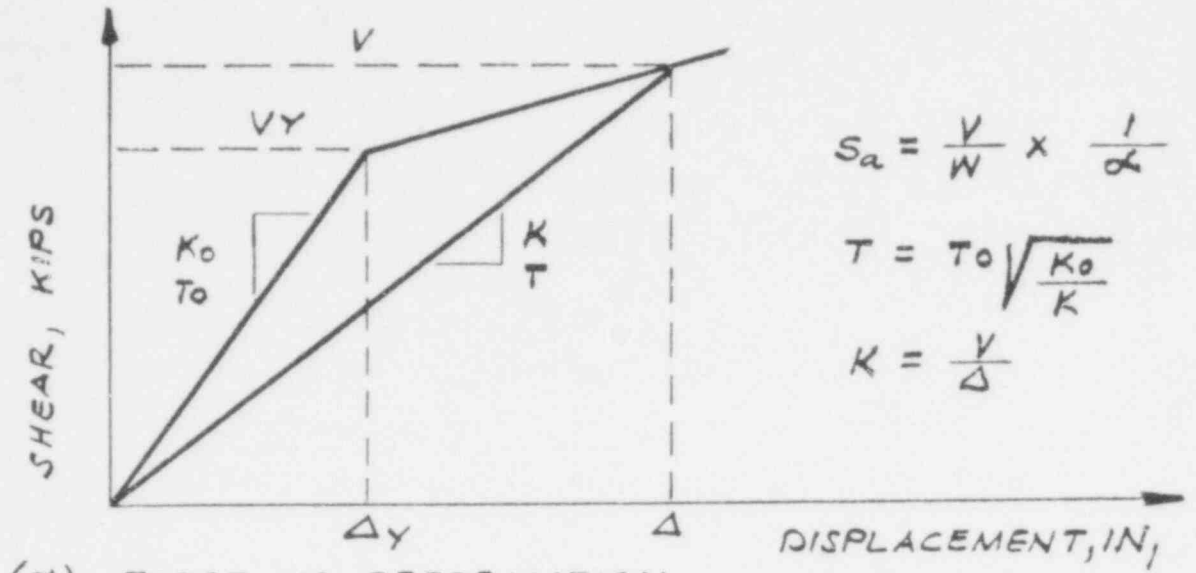

(a) FORCE VS DEFORMATION

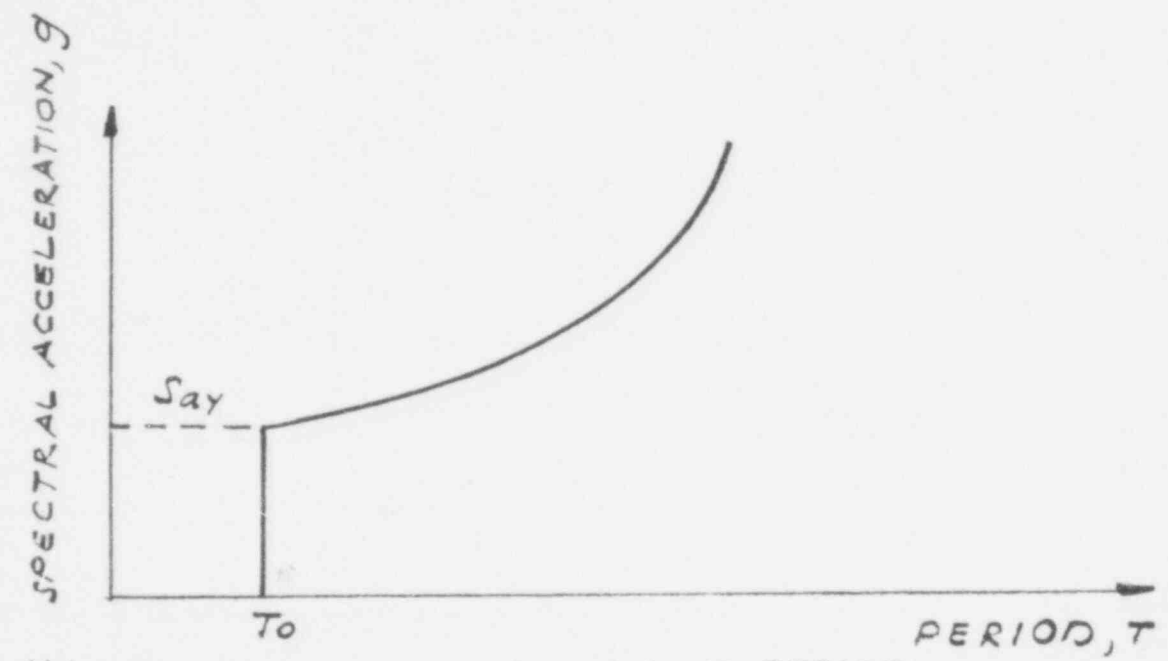

(b) SPECTRAL ACCELERATION VS PERIOD

CALCULATION OF SPECTRAL ACCELERATION VS PERIOD DIAGRAM

528 076

NRC/NONLIN

FIGURE 3.7

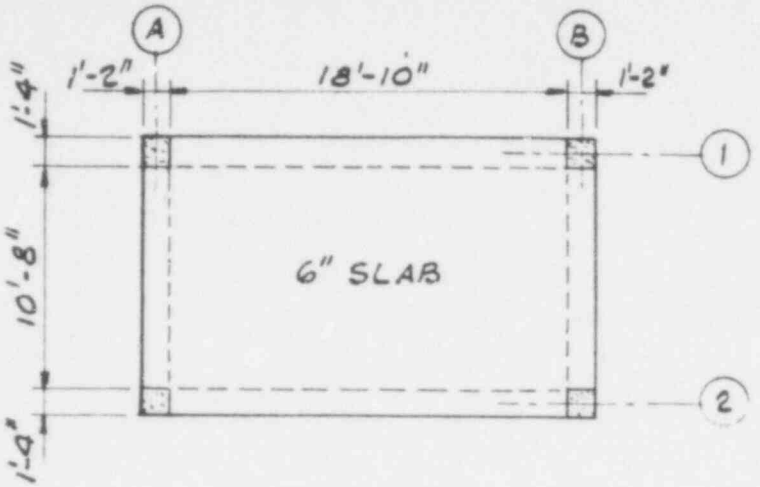

PLAN

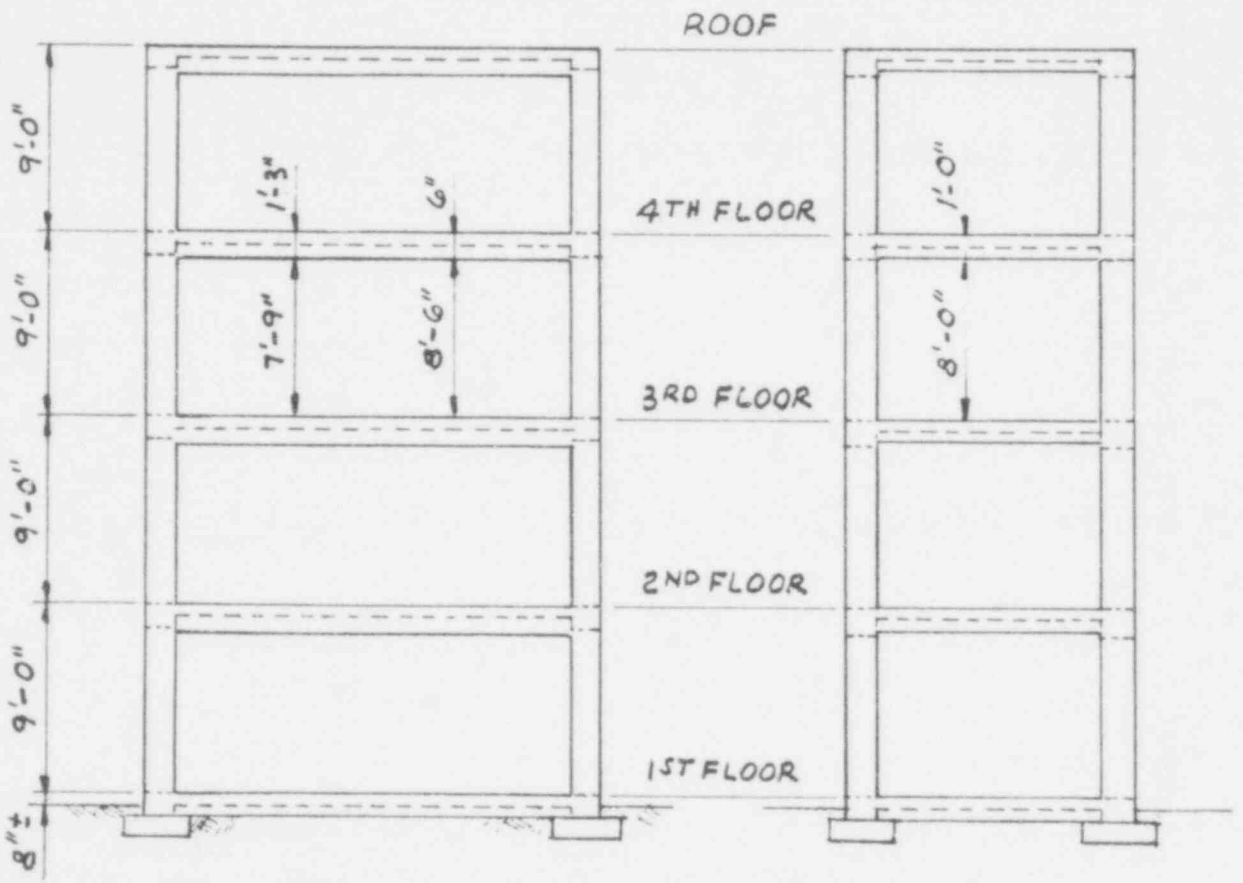

EAST ELEVATION

NORTH ELEVATION

EXAMPLE 4-STORY STRUCTURE OVERALL PLANS

NRC/NONLIN

528 077

FIGURE 3.8

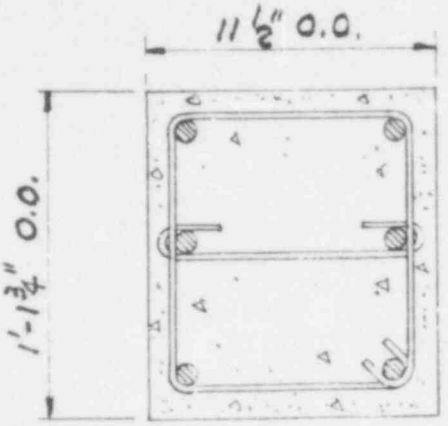

TYPICAL TIE

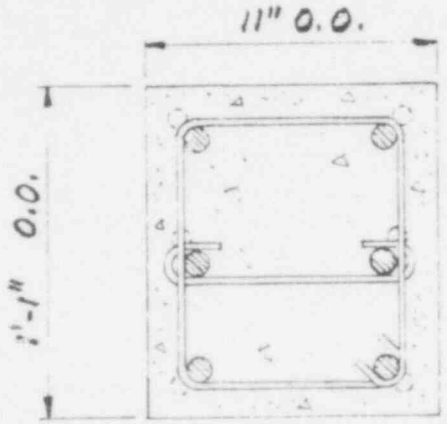

INTERMEDIATE TIE

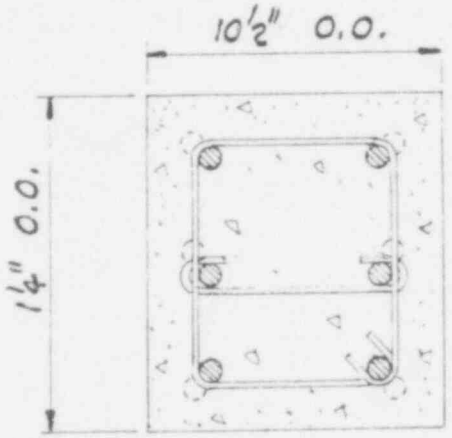

TIE AT TOP BEAM BARS

NOTE:
O.C. INDICATES OUTSIDE TO OUTSIDE MEASUREMENT

DETAILS OF COLUMN STEEL AND TIES

528 078

NRC/NONLIN

FIGURE 3.9

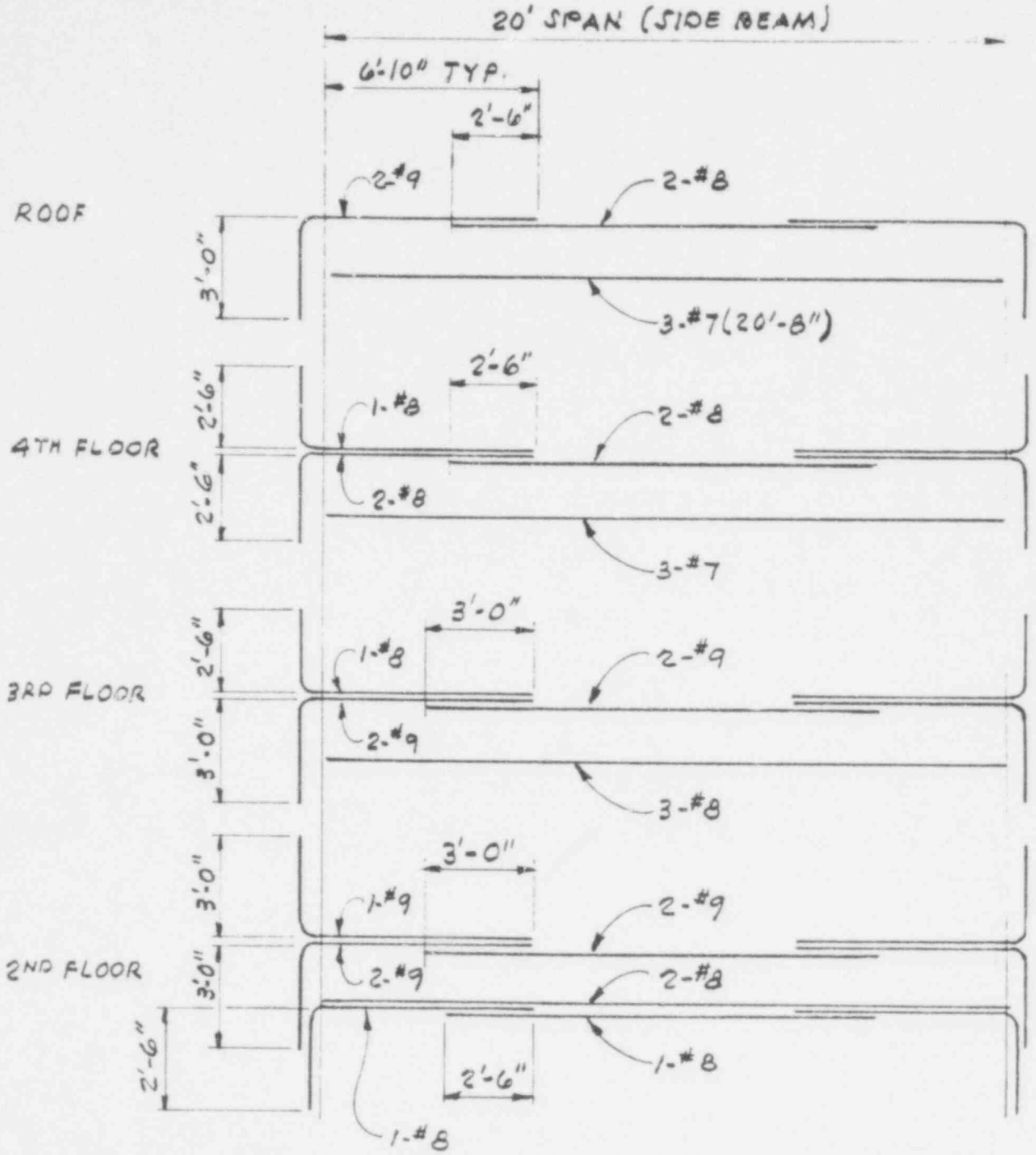

BEAM REINFORCING IN 20' SPAN

528 079

NRC/NONLIN

FIGURE 3.10

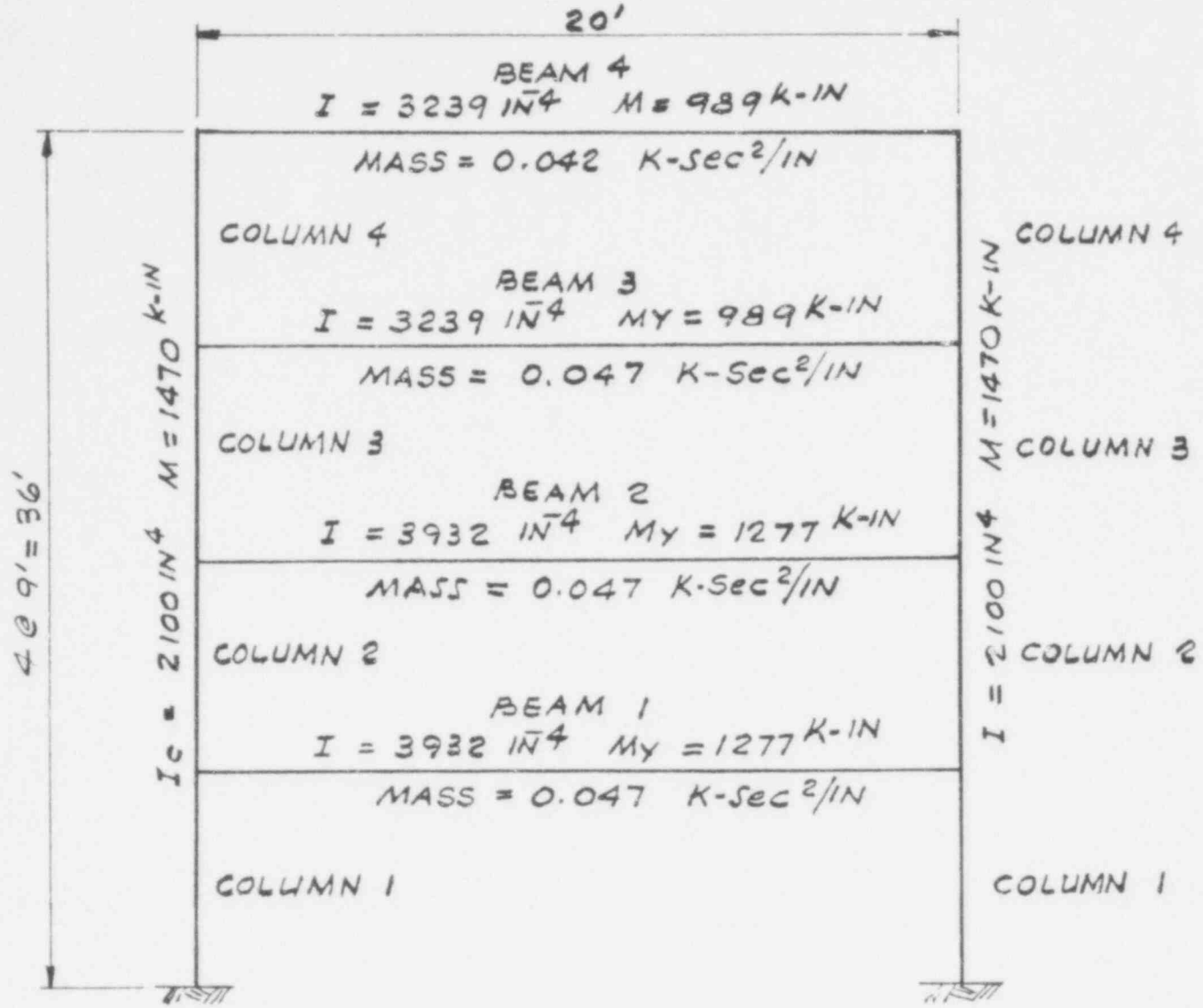

4-STORY REINFORCED CONCRETE FRAME
MATHEMATICAL MODEL FOR SIMPLIFIED ANALYSES

528 080

NRC/NONLIN FIGURE 3.11

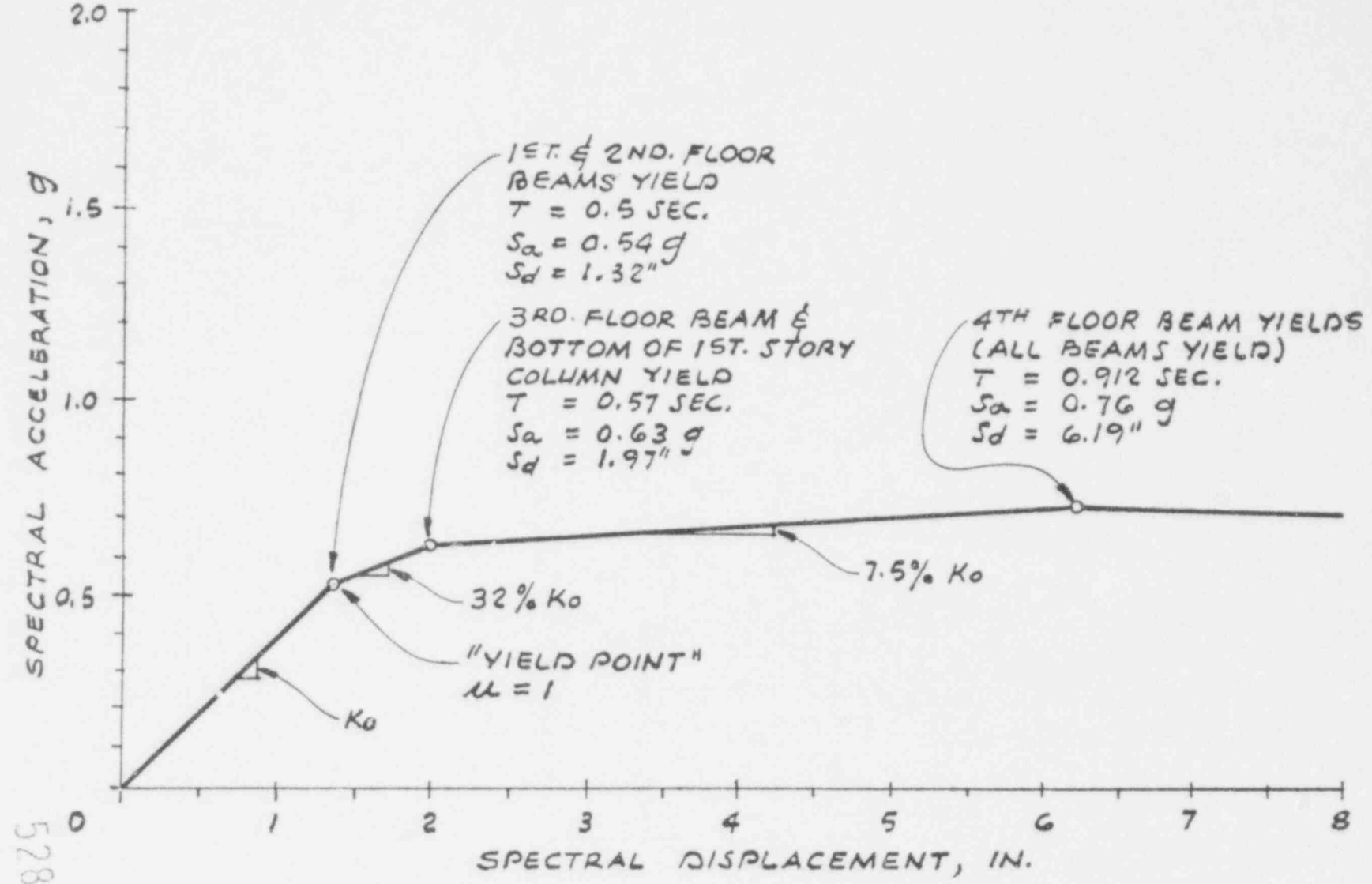

4-STORY REINFORCED CONCRETE FRAME

A.I.R.M. CAPACITY DATA

FIGURE 3.12

528 081
180

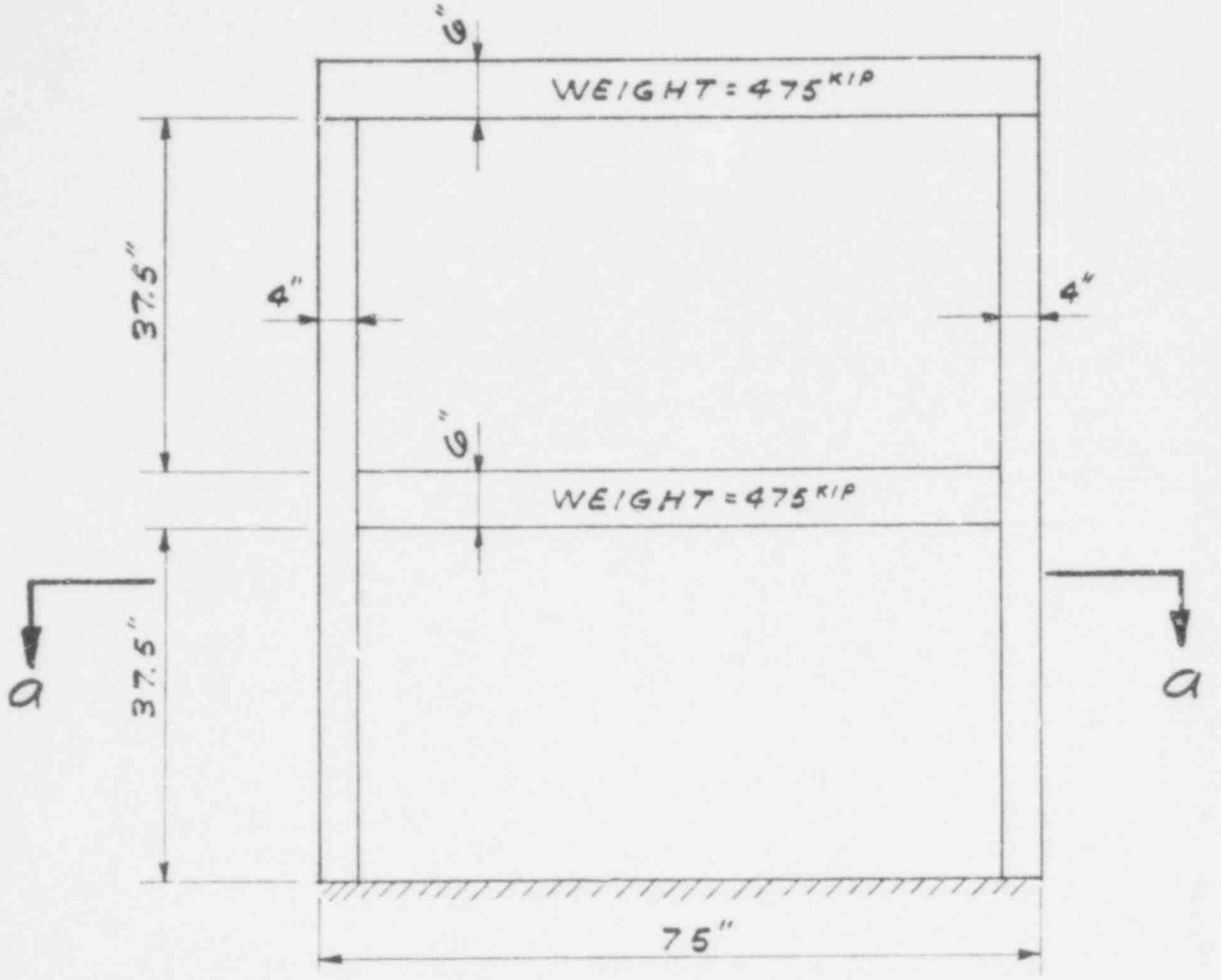

ELEVATION

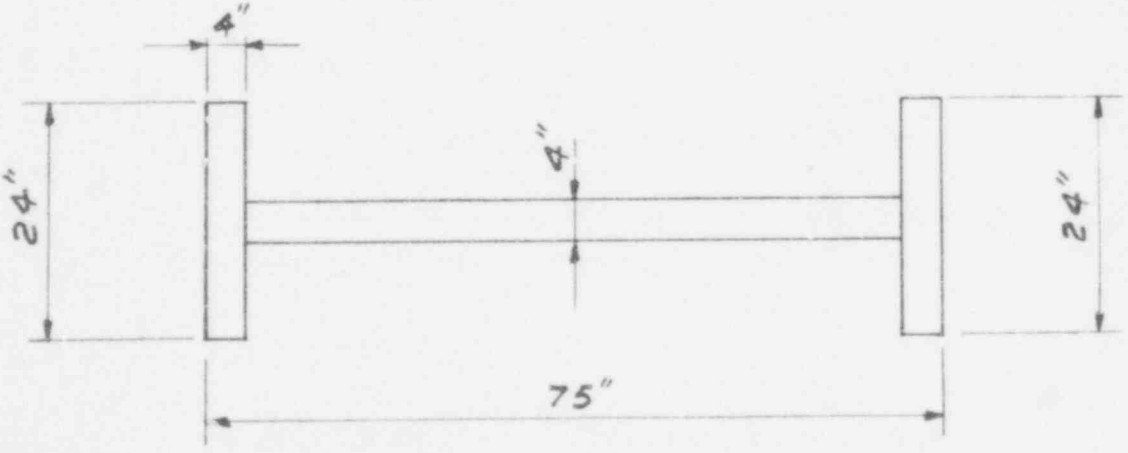

Section a-a

2-STORY SHEAR WALL
FOR SIMPLIFIED ANALYSES

528 092

NRC/NONLIN FIGURE 3.13

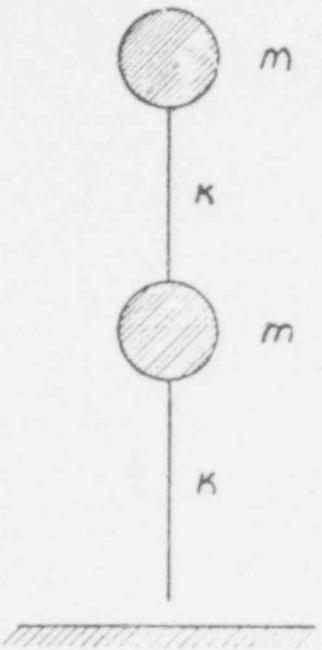

$$\left(\frac{2\pi^2}{T_1}\right) = 0.382\,\frac{K}{m}$$

TWO-DEGREE-OF-FREEDOM
MODEL FOR SHEAR WALL EXAMPLE

528 083

NRC/NONLIN FIGURE 3.14

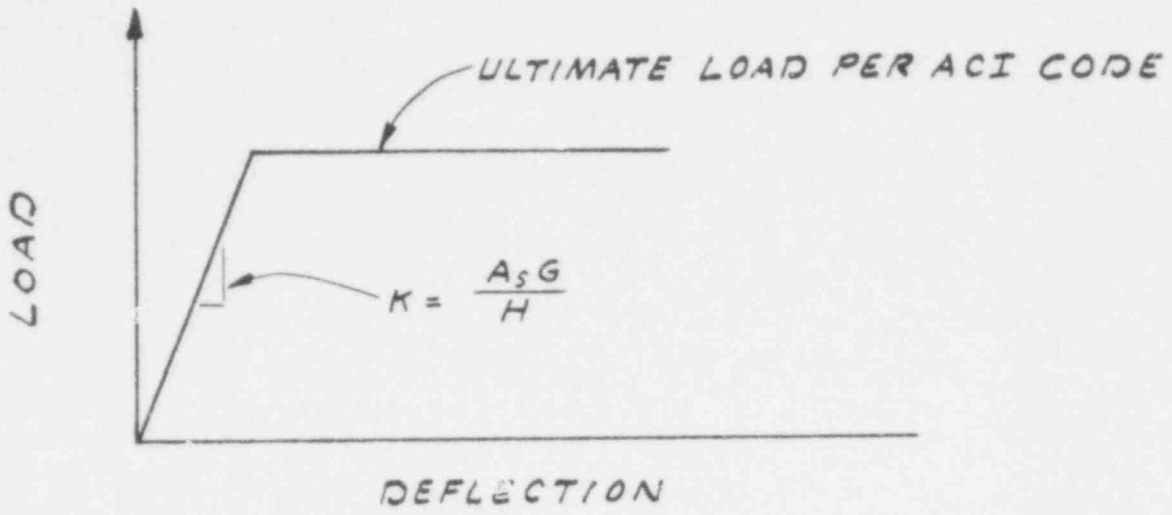

(a) WITHOUT EDGEMEMBERS

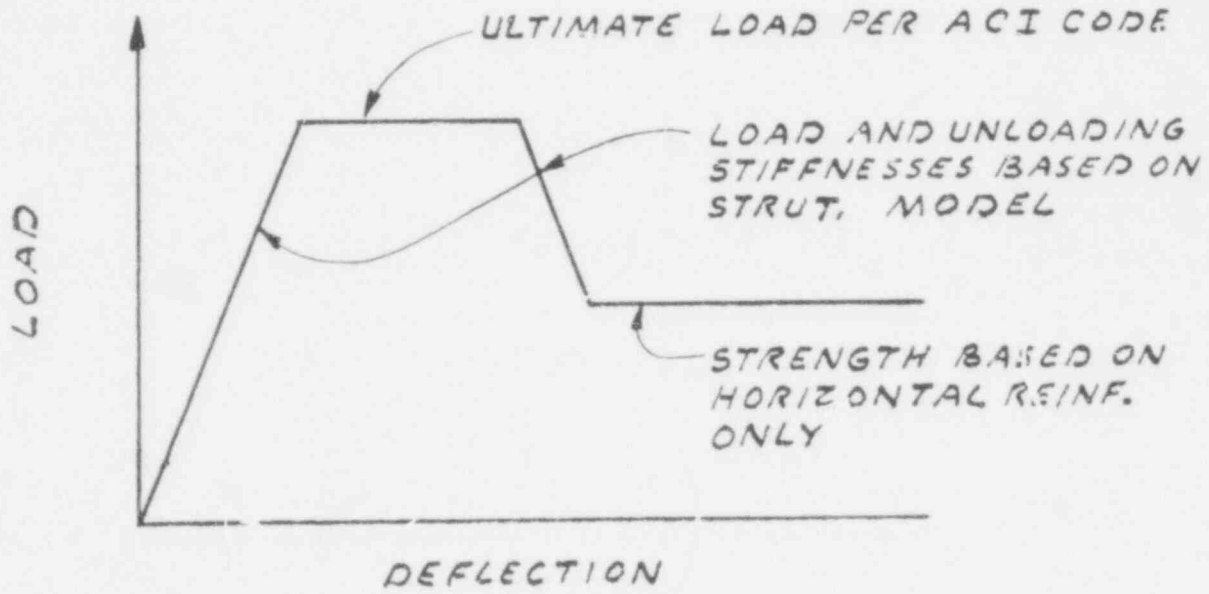

(b) WITH EDGEMEMBERS

528 084

ASSUMED LOAD BEHAVIOR
OF REINFORCED CONCRETE SHEAR WALLS

NRC/NONLIN

FIGURE 3.15

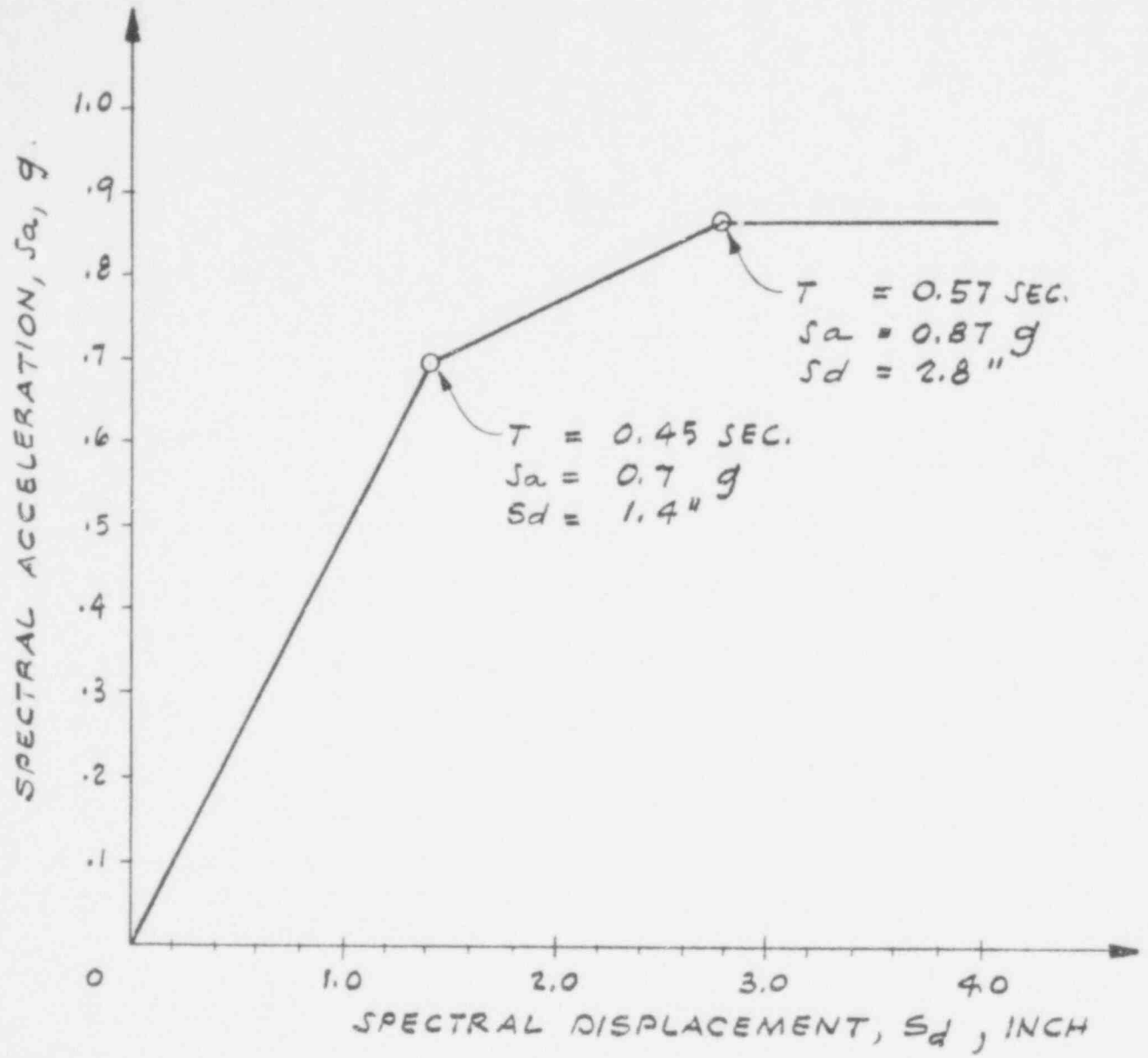

CAPACITY OF TORSION BUILDING

528 085

NRC/NONLIN FIGURE 3.16

4. RIGOROUS NONLINEAR ANALYSIS OF FOUR HYPOTHETICAL STRUCTURES

4.1 Introduction

Rigorous nonlinear analysis of four hypothetical structures is presented in this chapter. The structures analyzed are: a 1-story reinforced concrete planar frame, a 4-story reinforced concrete planar frame, a 2-story shear wall, and a three-dimensional 4-story reinforced concrete frame structure. These structures are described in detail in Chapter 3, which also discusses their analysis using the simplified nonlinear methods.

In this chapter, the modeling techniques and analytical methods applied to each of the structures and the results obtained in the process of the rigorous analysis are discussed. The main objective of the rigorous analysis was to obtain response values against which the results obtained from the various simplified nonlinear methods could be compared so that the validity, applicability, and accuracy of the simplified methods could be evaluated.

4.2 1-Story Reinforced Concrete Planar Frame

The 1-story reinforced concrete planar frame, illustrated in Figure 3.1, was chosen because it has been subjected to extensive experimental studies[4.1] at the University of Illinois.

For rigorous analysis, the structure was idealized as a beam-column system, as illustrated in Figure 4.1. The masses at the different nodal points are presented in Table 4.1.

A linear elastic analysis of the structure was carried out using the computer program SAPIV[4.2] The gross uncracked section properties were used for the beam-columns. The section and material properties used in the linear analysis are presented in Figure 4.2. The frequency of the frame was computed to be 16 Hz, and this was equal to the frequency of the frame measured during low amplitude tests. Hence, the mathematical model provides an adequate representation of the pre-yield response of the frame.

528 086

For the rigorous nonlinear analysis, several parameters have to be input by the user to the DRAIN-2D[4.3] program. These parameters are: yield moments and moments of inertia of the beam-column elements, damping, strain-hardening slope coefficient, degrading stiffness parameters for reinforced concrete subjected to cyclic loading, and shape of yield surface for beam-column elements. Some of these parameters are difficult to quantify, and the results of the analyses may be sensitive to the values used.

The yield moments prescribed for the different beam-column elements are extremely important in determining the overall structure behavior. When it is subjected to lateral ground motion, the structure under study is essentially a single-degree-of-freedom system. It is expected that plastic hinges will be formed in the columns at the base and at column-girder interface. Attention has thus been focused on the yield moments for column elements 1, 2, 3, 8, 9, and 10 (Figure 4.1). Elements 4 and 7 were assumed rigid so that the finite dimension of girder elements 5 and 6 would be modeled properly and the hinges would be formed at node points 4 and 8, which are at the interface of the girder and columns.

Three values of the yield moment for the columns were used. The first value was based on the ACI formulas assuming the yielding of tension steel and was computed to be 45 kip-in. A second value was chosen to be 38 kip-in. from a computed moment-curvature relationship,[4.1] as shown in Figure 4.3. A third value for the yield moment was based on static test results[4.1]; this was equal to 31.9 kip-in.

The moment of inertia for the columns was determined by equating secant stiffness at the yield point of the experimental $P\Delta$ curve (Figure 4.4) to the stiffness of the idealized frame. This resulted in a column moment of inertia of 8.7 $in.^4$ (Figure 4.5). The cracked moment of inertia was computed to be 38.3 $in.^4$ (Figure 4.5).

To assign a value for damping is always a problem in structural analysis; judgment and experience are relied on to obtain a reasonable number. In this study, no attempt has been made to look at damping in detail because it constitutes a major area of research in its own right. Rather, modal damping to be input into the system is assumed as some fraction of the critical value.

528 087

In DRAIN-2D, two parameters, α and β, need to be specified. These are determined from the relationships presented in Figure 4.6.

In this study, α and β were taken to be 1.166 and 0.00008. For the first two structural modes (T_1 = 0.1086 sec and T_2 = 0.0588 sec), this provides 1.2% and 1.0% damping, respectively. These values were considered adequate because the Illinois study[4.1] indicated good correlation at 1% damping. A strain-hardening slope coefficient of 1.3% obtained from the moment-curvature relationship of Figure 4.3 was used.

The behavior of reinforced concrete members under flexural load reversals, with or without axial loads, has been the subject of many studies. Takeda[4.4] proposed a complicated hysteresis model on the basis of experimental observation of a number of reinforced concrete frame structures subjected to dynamic tests to failure. This model has been incorporated into DRAIN-2D. This is essentially a degrading-stiffness model with increasing cycles of loading.

During experimental investigations, this structure was subject to a base motion simulating a modified version of the N21E component of the 1952 Taft record. To excite the test frame into the inelastic range, the original record was scaled. Accelerations were amplified, to a peak value of 229, and the time axis was compressed. The modified time-history is presented in Figure 4.7. The time history input into DRAIN-2D analyses for the current study is also presented in Figure 4.7. Although the same scale factors were used, the two records do not match completely. The Illinois record seems to have some high frequency noise; however, because the patterns of both records were similar, similar structural responses were expected.

Table 4.2 summarizes the results of the various DRAIN-2D runs. The main parameter varied was the column yield moment: 45.0, 38.0, and 31.9 kip-in. No yielding occurred with a column yield moment of 45.0 kip-in. Yielding occurred, and plastic hinges were formed at the top and the base of the column, for runs with column yield moments of 38.0 and 31.9 kip-in. The ductility ratios for these yield moments were computed to be 2.94 and 3.78, respectively. The experimental ductility was 3.94. The ductility ratio was

528 088

computed as the ratio of the maximum lateral displacement at the roof to the lateral displacement at first yield.

The roof displacement time histories are presented in Figure 4.8 for the analyses with column yield moments of 38.0 kip-in., 31.9 kip-in., and the experimentally obtained response. The computed time histories indicate trends similar to the experimental data; the model with a yield moment of 31.9 kip-in. shows better correspondence with the experimental record. Discrepancies occur mainly in the amplitudes of the displacements and may be partly due to the dissimilarities in the input time histories.

The analyses also indicate that the results are rather sensitive to one input parameter: yield moment of the columns. For a structure with more redundancies, such sensitivity to a single parameter is not expected.

4.3 4-Story Reinforced Concrete Planar Frame

The 4-story reinforced concrete frame used in this analysis is identical to the one longitudinal frame of a full-scale, 4-story test structure that was built in 1964 at the U.S. Department of Energy's Nevada Test Site. A detailed description of this structure is given in Section 3.3.

Figure 4.9 presents the mathematical model used for the DRAIN-2D analysis. The model consisted of beam-column elements. The mass assigned to each node is listed in Table 4.3. Beam-column flexural stiffnesses (i.e., moments of inertia) are presented in Table 4.4; computation of moments of inertia was based on the assumption of cracked sections. The yield moments are also presented in Table 4.4. These were based on first yielding in tension steel of the section. Sample calculations for the column properties are presented in Figure 4.10.

A linear analysis of the model was performed with the SAPIV computer program. The computed fundamental period, 0.48 sec, compares well with the measured fundamental period (0.55 sec) prior to major yielding and structural damage. Hence, the model appears to be an adequate representation of the pre-yield response of the structure.

528 089

For the nonlinear analysis, the program DRAIN-2D was used. Beam-column elements with degrading-stiffness hysteretic behavior under cyclic loading were used.

Input for the seismic excitation was obtained from a synthetic time history (Figure 4.11) obtained from NRC Regulatory Guide 1.60 response spectra (Figure 4.12). The response spectra from the synthetic time history show good correspondence with the NRC spectra at 2% and 5% damping (Figures 4.13 and 4.14). Two separate analyses, one using a peak ground acceleration of 0.5g and another with 1.0g acceleration, were conducted. Three damping values for the structure were specified: 2%, 4%, and 5% of critical.

The results for the six analyses are presented in Table 4.5. These indicate ductility ratios of approximately 2 and 4 at input acceleration levels of 0.5g and 1.0g, respectively. The ductility ratio at a particular acceleration level decreases with damping. The plastic hinges seemed to be forming at about 1.0 sec at column joints at the first-, second-, and third-floor levels for 1.0g input acceleration. Plastic hinges at the roof level seemed to be forming at around 6.5 sec. For the 0.5g input acceleration, no plastic hinges formed at the roof level.

4.4 2-Story Reinforced Concrete Shear Wall

Details of the 2-story, one-bay reinforced concrete shear wall structure are presented in Section 3.4. The mathematical model used for DRAIN-2D analysis is presented in Figure 4.15. This model consists of column elements 1, 3, 7, and 9; beam elements 5, 10, and 11; rigid links 2, 4, 6, and 8; and panel elements 1p and 2p. The column elements represent edgemembers; the panel elements represent the shear walls. The beam elements represent the slabs at the floor levels. Rigid links are provided to correctly specify the masses at the centers of mass. The nodal coordinates and the masses are presented in Table 4.6.

The nonlinear analysis was conducted using the DRAIN-2D program. The input motion used was the synthetic time history (Figure 4.11) generated from the NRC Regulatory Guide 1.60 response spectra, normalized to 0.2g peak ground acceleration. Damping specified for the structure was 5% of critical.

528 090

The results of the analysis are presented in Figure 4.16. Ductility ratios of 12 and 7 were obtained at the first and second level. The bottom panel yielded at 0.94 sec; the top panel yielded at 5.90 sec. The maximum deflection at both levels occurred at 10.34 sec with formation of hinges at the column joints at level 1.

4.5 Three-Dimensional 4-Story Reinforced Concrete Frame

The structure used for this analysis is shown in Figure 4.17. The longitudinal frames are the same as those shown in Figure 4.9 and used for the planar-frame analysis. The stiffness and dimensions of the members in frame II were increased in order to develop a nonsymmetrical three-dimensional model.

The structure was first analyzed using a linear elastic program called TABS[4.5] to determine the fundamental period. All horizontal inertial masses were assumed to be lumped at the diaphragms, as shown in Table 4.7. The moments of inertia of the column elements were computed assuming gross, uncracked sections; beam elements were assumed to have cracked. The first two periods from the TABS analysis were 0.452 sec and 0.411 sec. These values were used to compute damping coefficients for the nonlinear analysis. Both 2% and 4% of critical damping were considered.

Nonlinear analysis of the model was performed with the program DRAIN-TABS[4.6] using a synthetic time history (Figure 4.11) that corresponds to NRC Regulatory Guide 1.60 spectra normalized to the peak ground acceleration of 1.0g. Yield moments were computed assuming first yielding of the tensile steel. Figure 4.18 presents the lateral displacements at various floor levels. Frame II, being stiffer, shows less displacement than frame I. Displacements are also higher for the analysis at 2% structural damping.

Table 4.8 presents the ductilities at various floor levels. Again, the 2%-damped model shows slightly higher ductility ratios for the same excitation when compared to the 4%-damped model.

528 091

REFERENCES

4.1 Gulkan, P., and M. A. Sozen, "Response and Energy Dissipation of Reinforced Concrete Frames Subjected to Strong Base Motions," *Structural Research Series* No. 377, University of Illinois, Urbana, May 1971.

4.2 Bathe, K. J., E. L. Wilson, and F. E. Peterson, *SAPIV, a Structural Analysis Program for Static and Dynamic Response of Linear Structures*, EERC 73-11, Earthquake Engineering Research Center, University of California, Berkeley, 1973.

4.3 Kanaan, A. E., and G. H. Powell, *DRAIN-2D, a General-Purpose Computer Program for Dynamic Analysis of Inelastic Plane Structures*, EERC 73-6, Earthquake Engineering Research Center, University of California, Berkeley, 1973.

4.4 Takeda, T., "Study of the Load-Deflection Characteristics of Reinforced Concrete Beams Subjected to Alternating Loads," *Transactions, Architectural Institute of Japan*, Volume 76, September 1962.

4.5 Wilson, E. L., and H. H. Dovey, *Static and Earthquake Analysis of Three-Dimensional Frame and Shearwall Buildings*, EERC 72-8, Earthquake Engineering Research Center, University of California, Berkeley, 1972.

4.6 Israel, G. R., and G. H. Powell, *DRAIN-TABS, a Computer Program for Inelastic Earthquake Response of Three-Dimensional Buildings*, UCB/EERC-77/08, Earthquake Engineering Research Center, University of California, Berkeley, 1977.

528 092

TABLE 4.1

1-STORY, ONE-BAY REINFORCED CONCRETE FRAME:

LUMPED MASSES

Node Point	Lumped Mass ($lb\text{-}sec^2/in.$)
1	0.024
2	0.049
3	0.049
4	0.024
5	0.166
6	10.680
7	0.166
8	0.024
9	0.049
10	0.049
11	0.024

528 093

TABLE 4.2

1-STORY, ONE-BAY REINFORCED CONCRETE FRAME:

SUMMARY OF RESULTS

Column Yield Moment (kip-in.)	DRAIN-2D Results			Experimental Results		
	Maximum Deflection (in.)	Yield Deflection (in.)	Ductility	Maximum Deflection (in.)	Yield Deflection (in.)	Ductility
45.0	No Yielding	No Yielding	No Yielding	0.615	0.165	3.94
39.0	0.435	0.148	2.94	0.615	0.165	3.94
31.9	0.501	0.133	3.78	0.615	0.165	3.94

Note:

I_{column} = 10.4 in.^{4}

Damping = 1%

Slope Coefficient = 1.3%

Takeda Model for Degrading Stiffness

Ductility, $\mu = \frac{\text{maximum deflection}}{\text{yield deflection}}$

528 094

TABLE 4.3

4-STORY STRUCTURE:

NODE WEIGHTS, MASSES, AND INERTIAS

Node	Weight, x and y (lb)	Mass, x and y (lb-sec^2/in.)	Mass Moment of Inertia (lb-sec^2-in.)
1	1,050.0	2.72	704.7
2	1,050.0	2.72	704.7
3	2,100.0	5.43	1,409.0
4	2,100.0	5.43	1,409.0
5	10,087.0	26.11	18,409.0
6	10,087.0	26.11	18,409.0
7	2,100.0	5.43	1,409.0
8	2,100.0	5.43	1,409.0
9	10,087.0	26.11	18,409.0
10	10,087.0	26.11	18,409.0
11	2,100.0	5.43	1,409.0
12	2,100.0	5.43	1,409.0
13	10,087.0	26.11	18,409.0
14	10,087.0	26.11	18,409.0
15	2,100.0	5.43	1,409.0
16	2,100.0	5.43	1,409.0
17	9,037.5	23.39	17,704.0
18	9,037.5	23.39	17,704.0
19	12,242.0	31.68	33,997.0
20	12,242.0	31.68	33,997.0
21	12,242.0	31.68	33,997.0
22	12,242.0	31.68	33,997.0

528 095

TABLE 4.4

4-STORY FRAME:

MOMENTS OF INERTIA AND YIELD MOMENTS

Member	I^*_{pos} (in.)	I^*_{neg} (in.)	$+My$ (kip-in.)	$-My$ (kip-in.)
Column	4,778	4,778	1,500	1,500
Second Floor Beam	1,484	1,770	1,242	1,567
Third Floor Beam	1,482	1,670	1,243	1,458
Fourth Floor Beam	1,220	1,479	976	1,248
Roof Beam	1,218	1,294	977	1,069

*Gross section is used for moment of inertia calculation in columns; cracked section is used in the beams.

Note:

f'_c = 4.5 ksi $\quad E_c$ = 4 x 10^3 ksi

f_y = 50 ksi $\quad E_s$ = 29 x 10^3 ksi

528 026

TABLE 4.5
4-STORY FRAME:
SUMMARY OF RESULTS

Ground Acceleration (g)	Damping (%)	Yield Element #1		Yield Element #17		Yield Element #19		Yield Element #21		Yield Element #23		Maximum Top Deflection (in.)	Yield Top Deflection (in.)	Ductility μ
		Time	Node Point	Time	Node Point	Time	Node Point	Time	Node Point	Time	Node Point			
1.0	2	1.00	1	1.02	5	1.01	9	[illegible]	13	NA	17	7.77 (@ 7.03 sec)	1.79	4 [illegible]
1.0	4	1.00	1	1.03	5	1.01	9	1.02	13	6.54	17	7.16 (@ 9.02 sec)	1.69	4.24
1.0	5	1.00	1	1.03	5	1.02	9	1.03	13	6.55	17	6.80 (@ 9.01 sec)	1.65	4.12
0.5	2	1.7	1	1.77	5	1.28	9	1.81	13	NY*	--	3.32 (@ 10.67 sec)	1.53	2.17
0.5	4	[illegible]	1	1.78	5	1.29	9	10.58	13	NY*	--	2.94 (@ 10.61 sec)	1.41	2.09
0.5	5	1.28	1	8.90	5	1.30	9	10.58	13	NY*	--	2.78 (@ 10.60 sec)	1.59	1.75

*No yield

528 097

TABLE 4.6

2-STORY SHEAR WALL:

COORDINATES AND MASSES

Node Point	x Coordinate	y Coordinate	Lumped Weight (kip)	Mass (kip-sec^2/in.)
1	0	0	0	0
2	0	37.5	118.75	0.307
3	0	43.5	118.75	0.307
4	0	81.0	0	0
5	0	84.0	237.50	0.614
6	67.0	84.0	237.50	0.614
7	67.0	81.0	0	0
8	67.0	43.5	118.75	0.307
9	67.0	37.5	118.75	0.307
10	67.0	0	0	0

528 098

TABLE 4.7

4-STORY TORSION MODEL:

INPUT PROPERTIES

Lev	Properties Lumped at Diaphragms				
	Center of Mass		Mass	Weight	Rotational Inertia
	$\bar{X}$, in.	$\bar{Y}$, in.	(kip-sec^2/in.)	(kip)	(kip-sec^2-in.)
Roof	120.0	74.59	0.087	33.66	855.4
4	120.0	75.15	0.099	38.31	1,090.9
3	120.0	75.15	0.099	38.31	1,090.9
2	120.0	75.15	0.099	38.31	1,090.9

Frame	Member Properties					
	Member	A (in.^{2})	A_v (in.^{2})	I (in.^{4})	$+M_y$ (kip-in.)	$-M_y$ (kip-in.)
I	Column I	224.0	187.0	3,659	1,500	-1,500
	Beam-Roof	240.0	200.0	2,500	977	-1,069
	4	240.0	200.0	2,500	976	-1,248
	3	240.0	200.0	2,950	1,243	-1,458
	2	240.0	200.0	2,950	1,242	-1,567
II	Column II	272.25	227.0	6,177	1,895	-1,895
	Beam-Roof	280.50	234.0	3,405	1,267	-1,260
	4	280.50	234.0	3,405	1,267	-1,280
	3	280.50	234.0	4,092	1,590	-1,755
	2	280.50	234.0	4,092	1,590	-1,870
III & IV	Column I	224.00	187.0	4,779	1,180	-1,180
	II	272.25	227.0	6,177	1,562	-1,562
	Beam-Roof	168.00	140.0	2,550	544	-386
	4	168.00	140.0	2,550	544	-661
	3	168.00	140.0	2,695	712	-629
	2	168.00	140.0	2,695	712	-930

528 099

TABLE 4.8

4-STORY TORSION STRUCTURE:

SUMMARY OF DUCTILITY RESULTS

Damping (%)	Level	Δ_{max}	Time of Maximum Displacement	Δ_{yield}	Time of First Yield	Ductility*, μ
2	Roof	7.668	9.02	1.593	0.99	4.81
	4	5.946	9.03	1.265	0.99	4.70
	3	3.939	9.05	0.797	0.99	4.94
	2	1.849	9.06	0.298	0.99	6.20
4	Roof	6.812	9.01	1.495	0.99	4.56
	4	5.376	9.01	1.198	0.99	4.49
	3	3.582	9.02	0.168	0.99	4.66
	2	1.670	9.03	0.291	0.99	5.74

$$*\mu = \frac{\text{Maximum Diaphragm Deflection}}{\text{Diaphragm Deflection at First Yield}}$$

528 100

DRAIN-2D MODEL FOR ONE-STORY, ONE-BAY
REINFORCED CONCRETE FRAME
NRC / NONLIN
FIGURE 4.1
528
101
31.0"
8.67"
8.67"
8.67"
5.0"
59.0"
29.5"
X
Y

MATERIAL PROPERTIES:

$E = 3.82 \times 10^6$ PSI

$\nu = 0.15$

SECTION PROPERTIES

COLUMNS:

AXIAL AREA = 25.00 IN^2

SHEAR AREA = 20.83 IN^2

MOMENT OF INERTIA = 52.08 IN^4

BEAMS:

AXIAL AREA = 50.00 IN^2

SHEAR AREA = 41.67 IN^2

MOMENT OF INERTIA = 104.17 IN^4

MATERIAL AND SECTION PROPERTIES USED FOR LINEAR ANALYSIS OF ONE-STORY FRAME

528 102

NRC / NONLIN FIGURE 4.2

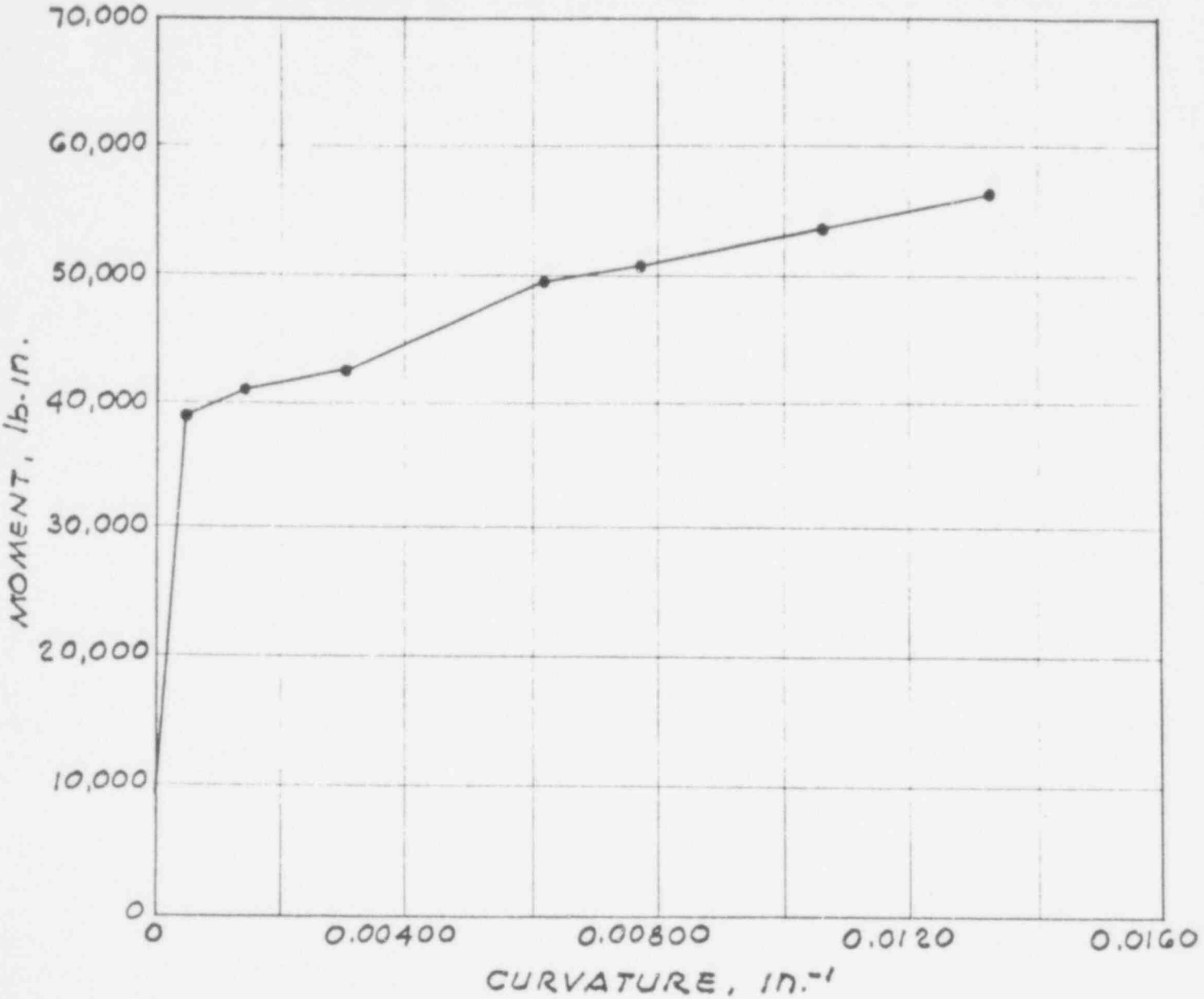

CALCULATED MOMENT-CURVATURE RELATIONSHIP FOR THE ONE-STORY, ONE-BAY REINFORCED CONCRETE FRAME

NRC / NONLIN

FIGURE 4.3

528 103

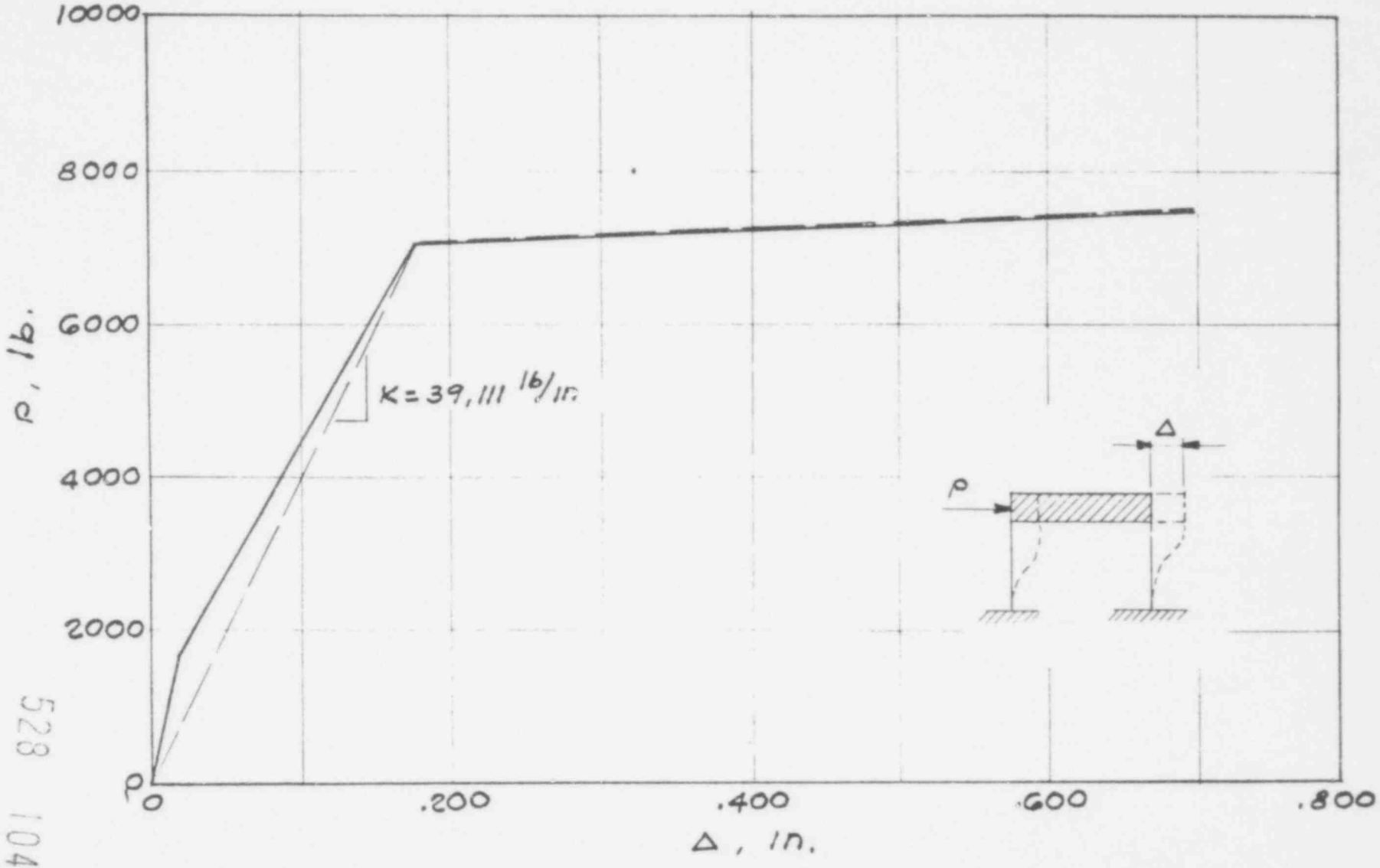

MEASURED PRIMARY CURVE (P vs. Δ) FOR ONE-STORY, ONE-BAY REINFORCED CONCRETE FRAME

FIGURE 4.4

528 104

(a) CRACKED SECTION

$A_s = 0.22\ IN.^2$

$n = 15$

$nA_s = 3.3\ IN.^2$

$(n-1)A_s = 3.08\ IN.^2$

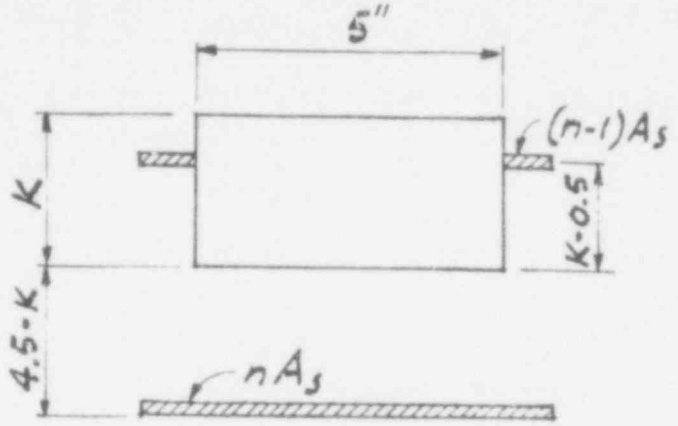

$$\Sigma A\bar{y} = 0 \quad 5K\left(\frac{K}{2}\right) + 3.08(K-0.5) = 3.3(4.5-K)$$

$$K = 1.59$$

$$I_{CR} = \frac{5(1.59)^2}{3} + 3.08(1.59-0.5)^2 + 3.3(4.5-1.59)^2$$

$$= 38.3\ IN.^4$$

(b) AT YIELD

ASSUME BEAM TO BE RIGID

$V = K\Delta \quad K = \frac{24EI}{L^3}$

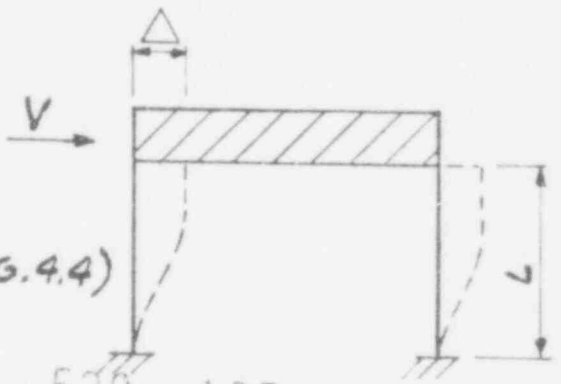

FROM ILLINOIS TEST RESULTS (FIG. 4.4)

$K = 39111\ LB/IN.$

$E = 3.3 \times 10^6\ PSI$

$$I_y = \frac{(39111)(26)^3}{(24)(3.3\times10^6)} = 8.7\ IN.^4$$

528 105

MOMENT OF INERTIA CALCULATIONS FOR ONE STORY FRAME COLUMNS

NRC/NONLIN

FIGURE 4.5

$$[c] = \alpha[M] + \beta[K] \qquad (4.1)$$

$$\alpha = \frac{4\pi (T_j \lambda_j - T_i \lambda_i)}{T_j^2 - T_i^2} \qquad (4.2)$$

$$\beta = \frac{T_i T_j (T_j \lambda_i - T_i \lambda_j)}{\pi (T_j^2 - T_i^2)} \qquad (4.3)$$

$$\lambda_i = \frac{\alpha T_i}{4\pi} + \frac{\beta \pi}{T_i} \qquad (4.4)$$

$$\lambda_j = \frac{\alpha T_j}{4\pi} + \frac{\beta \pi}{T_j} \qquad (4.5)$$

WHERE, α = MASS PROPORTIONAL DAMPING COEFFICIENT

β = STIFFNESS PROPORTIONAL DAMPING COEFFICIENT

$[M], [C], [K]$ = MASS, DAMPING AND STIFFNESS MATRICES

T_i, T_j = STRUCTURE PERIODS IN i & j^{th} MODES

λ_i, λ_j = STRUCTURE DAMPING IN i & j^{th} MODES

528 106

DAMPING COEFFICIENTS FOR INPUT-TO DRAIN-2D MODEL OF ONE-STORY FRAME

NRC/NONLIN FIGURE 4.6

TIME HISTORY FOR DRAIN-2D ONE-STORY ONE-BAY REINFORCED CONCRETE MODEL

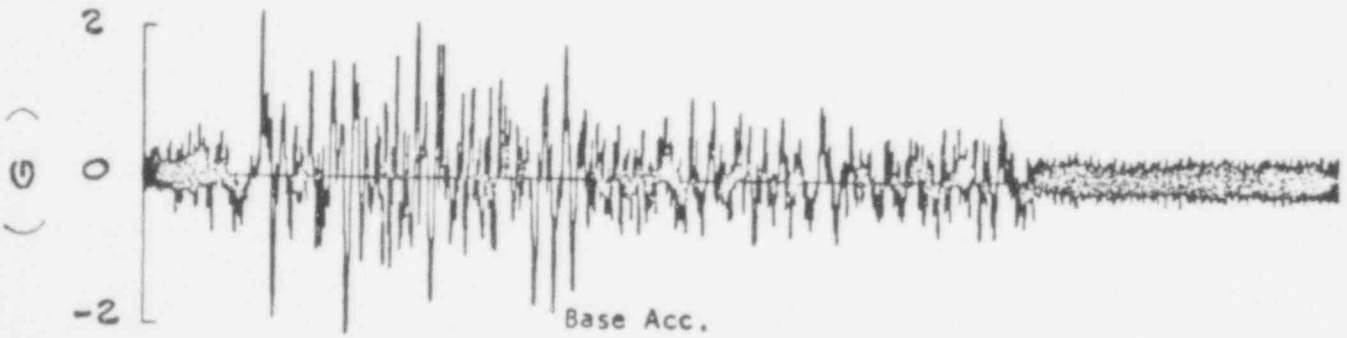

528 107

ILLINOIS TIME HISTORY INPUT

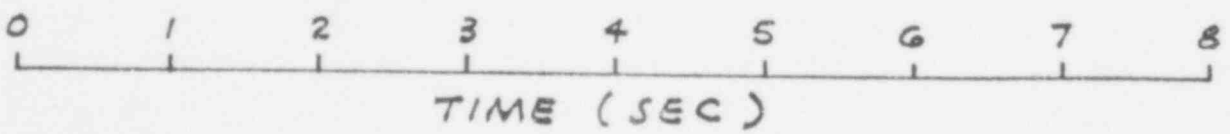

NRC / NONLIN

FIGURE 4.7

ROOF DISPLACEMENT TIME HISTORY FOR ONE-STORY ONE-BAY REINFORCED CONCRETE FRAME My=38.0 KIP-IN

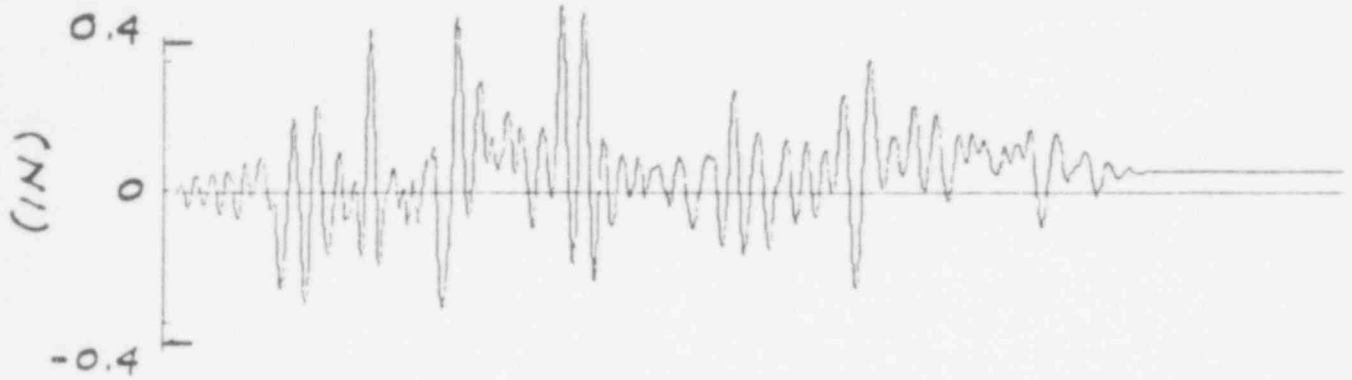

ROOF DISPLACEMENT TIME HISTORY FOR ONE-STORY, ONE-BAY REINFORCED CONCRETE FRAME My = 31.85 KIP-IN

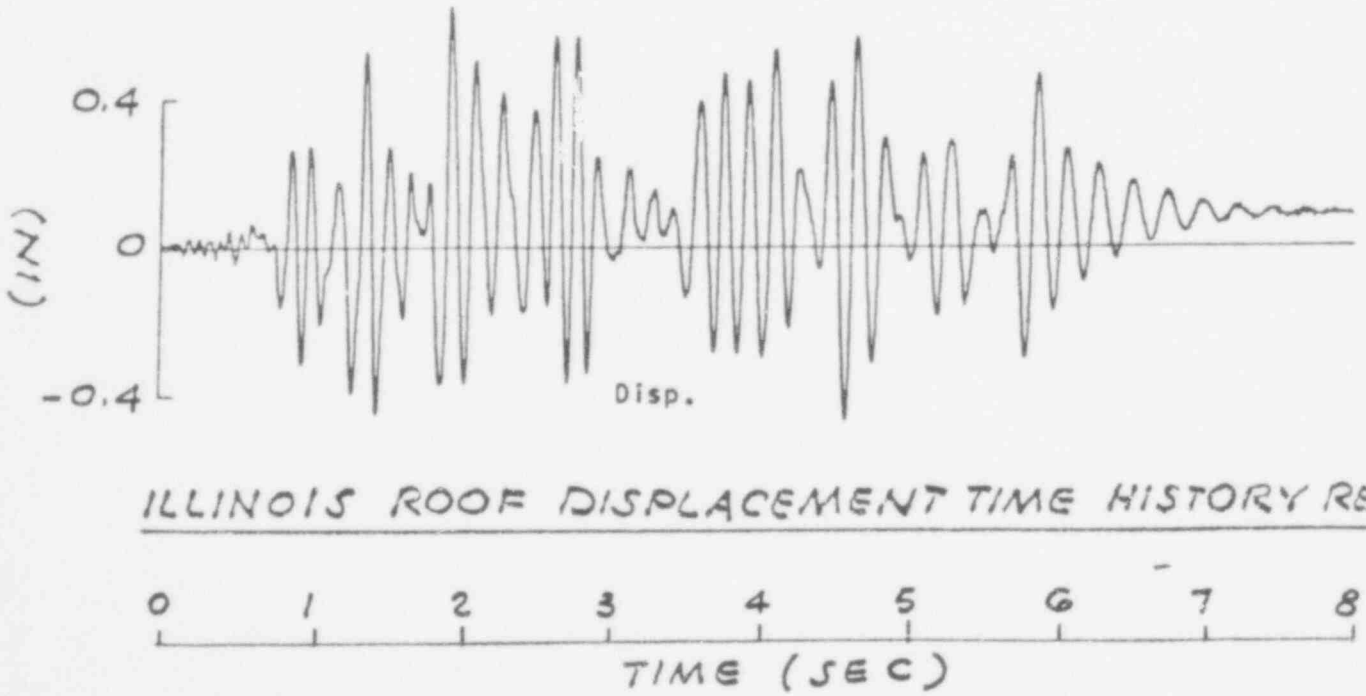

ILLINOIS ROOF DISPLACEMENT TIME HISTORY RESULTS

NRC / NONLIN FIGURE 4.8

528 108

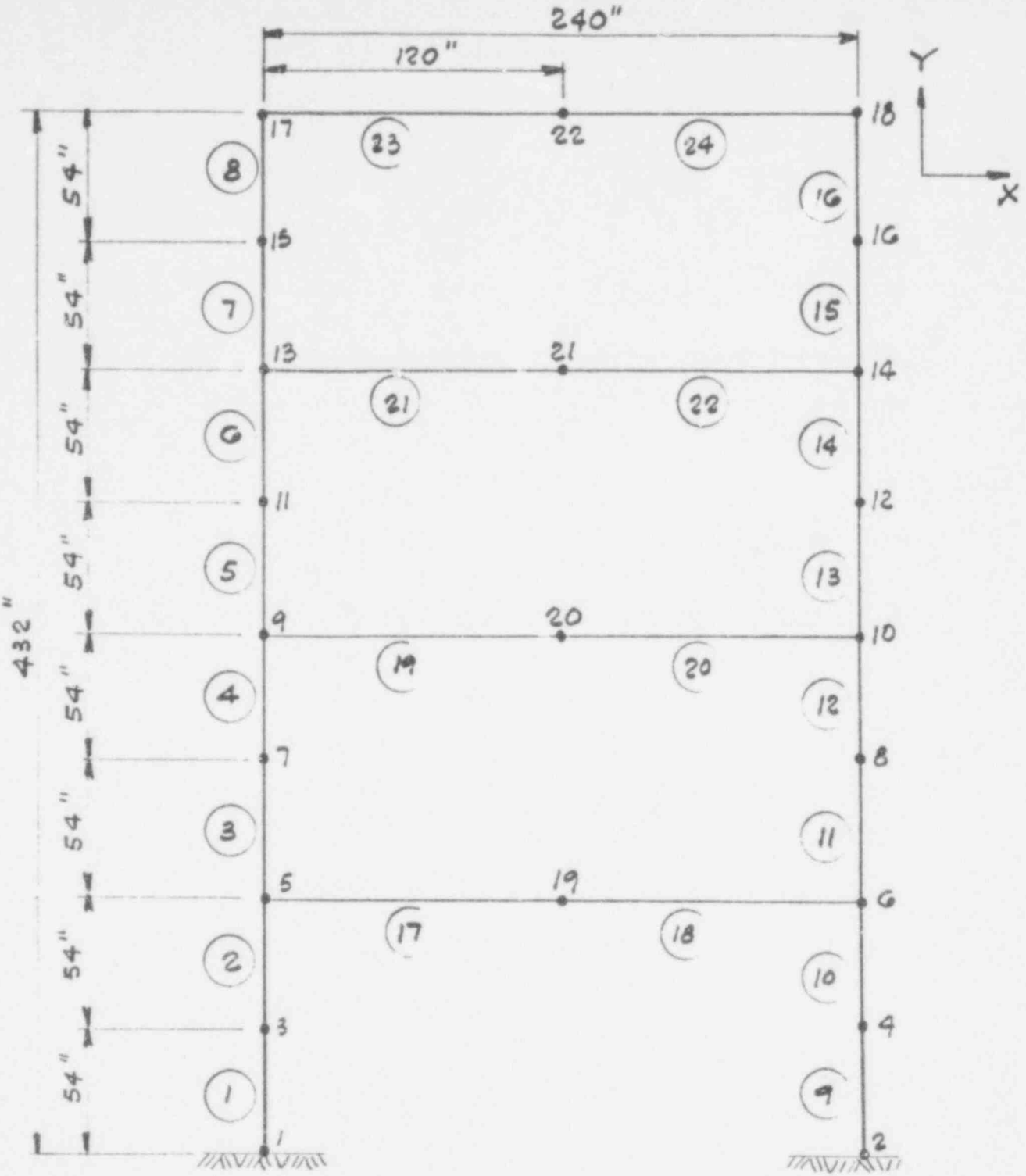

FOUR-STORY, ONE-BAY REINFORCED CONCRETE COMPUTER MODEL

528 109

NRC / NONLIN FIGURE 4.9

2ND FLOOR BEAM

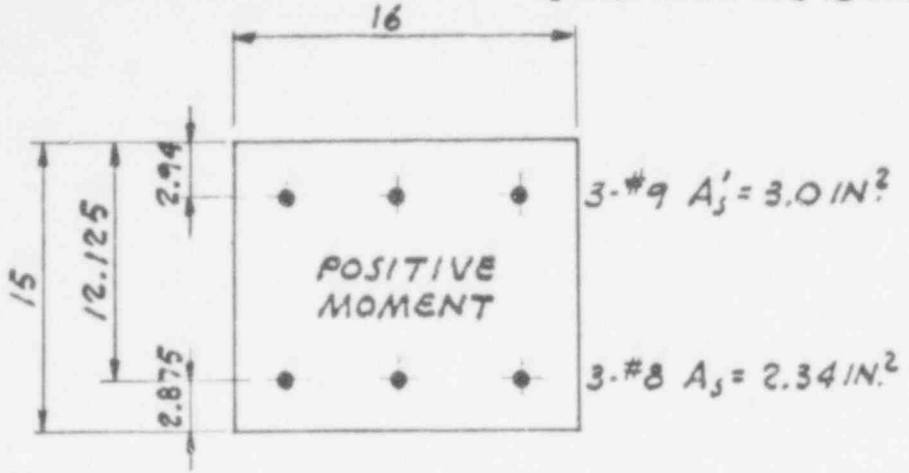

ASSUME 2" CLEAR

DIST. TO C.L. = COVER + STIR. + $\frac{1}{2} d_b$

$d_{\#9} = 2 + .375 + \frac{1.128}{2}$

$= 2.94"$

$d_{\#8} = 2. + .375 + \frac{1}{2}$

$= 2.875$

$f_c' = 4.5\ KSI \quad E_c = 4 \times 10^3\ KSI$

$f_y = 50\ KSI \quad E_s = 29 \times 10^3\ KSI$

$f_c = \epsilon_c \times 4 \times 10^3$

$\epsilon_c = x_y \left(\frac{.00172}{12.125 - x_y}\right)$

$\epsilon_s' = (x_y - 2.94)\left(\frac{.00172}{12.125 - x_y}\right)$

$\epsilon_s' = \frac{.00172 x_y - .00506}{12.125 - x_y}$

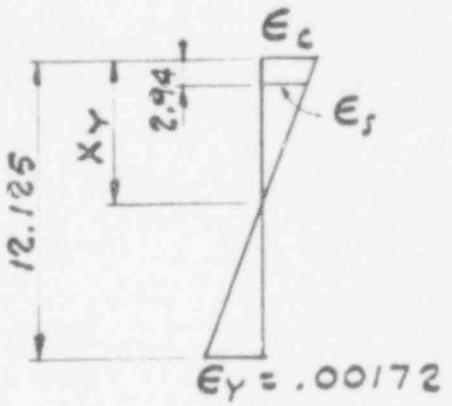

$T = A_s f_y = C = \frac{1}{2} f_c\, 16 x_y + (E_s - E_c) A_s' \epsilon_s'$

$2.34(50) = 8 \times 4 \times 10^3 \times x_y^2 \left(\frac{.00172}{12.125 - x_y}\right) + 3.0(29 - 4) \times 10^3 \left[\frac{.00172 x_y - .00506}{12.125 - x_y}\right]$

$55.04\, x_y^2 + 246.\, x_y - 1798.125 = 0$

$x_y = \frac{-246 + \sqrt{246^2 + 4 \times 55.04 (-178.125)}}{2(55.04)}$

528 110

SAMPLE CALCULATIONS FOR BEAM PROPERTIES

NRC/NONLIN FIGURE 4.10c

$X_y = 3.90$ IN.

$\epsilon_c = .0082$ $\quad C_c = \epsilon_c E_c \frac{1}{2} X_y (16) = 101.93$

$\epsilon_s = .0020$ $\quad C_s = (E_s - E_c)\epsilon'_s A_s = 15.10$

$\underline{117.03} = T$

$M_y = C_s (12.125 - 2.94) + C_s \left(12.125 - \frac{X_y}{3}\right)$

$M_y = 1242$ KIP-IN.

$I_{CR} = \frac{bh^3}{3} + Ad^2$

$I_{CR} = 1484$ IN.^{3}

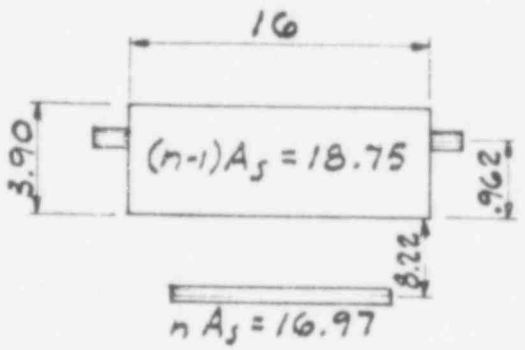

SIMILAR CALCULATIONS FOR TENSION ON TOP GAVE

$X_y = 4.30$ IN.

$M_y = 1566$ KIP-IN

$I_{CR} = 1769.5$ IN.^{4}

528

SAMPLE CALCULATIONS FOR BEAM PROPERTIES (CONT.)

NRC/NONLIN FIGURE 4.10b

TIME HISTORY FROM NRC SPECTRA

NRC/NONLIN

528 112

FIGURE 4.11

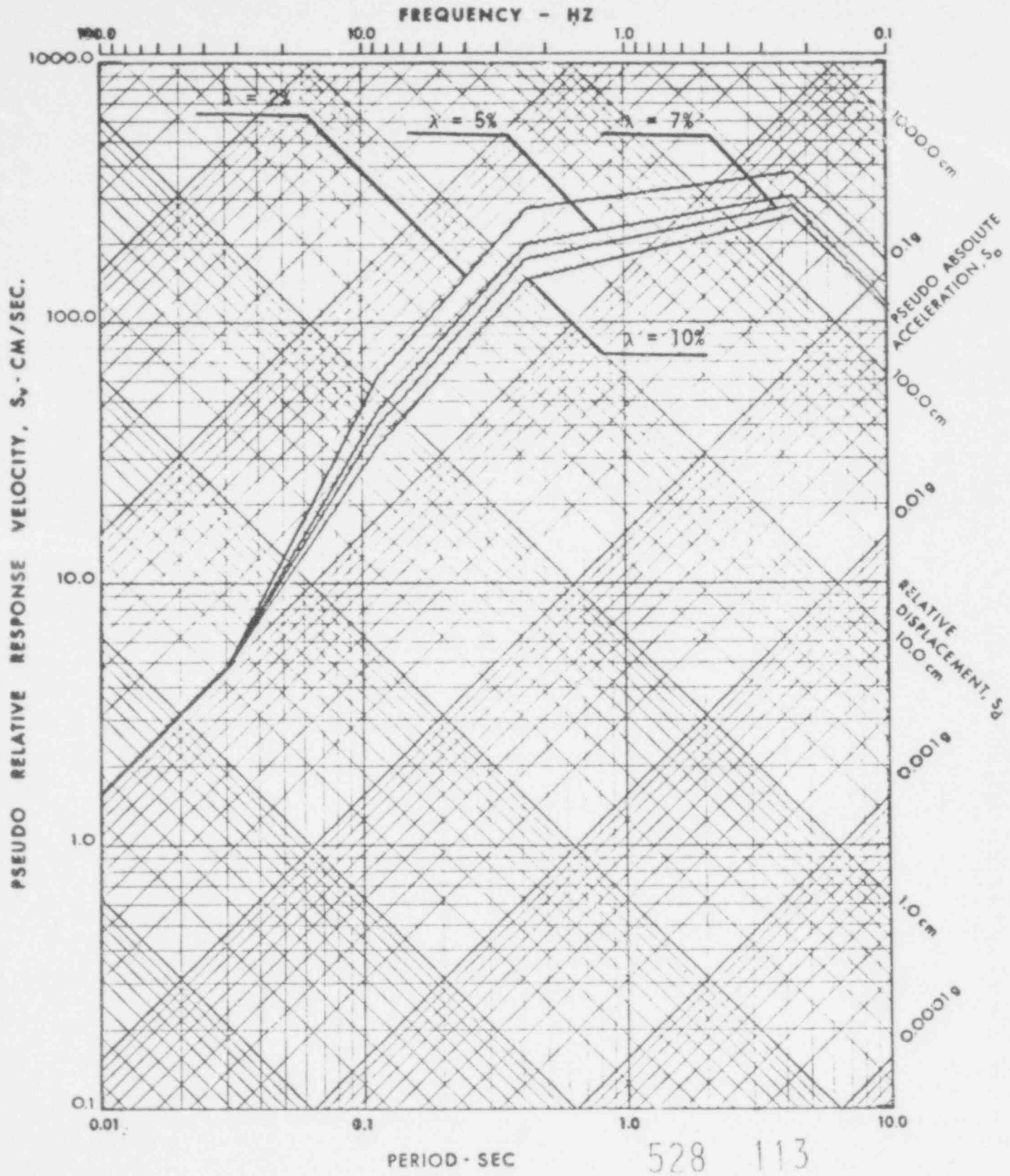

528 113

NRC RESPONSE SPECTRA 1.0 x GRAVITY

NRC/NONLIN FIGURE 4.12

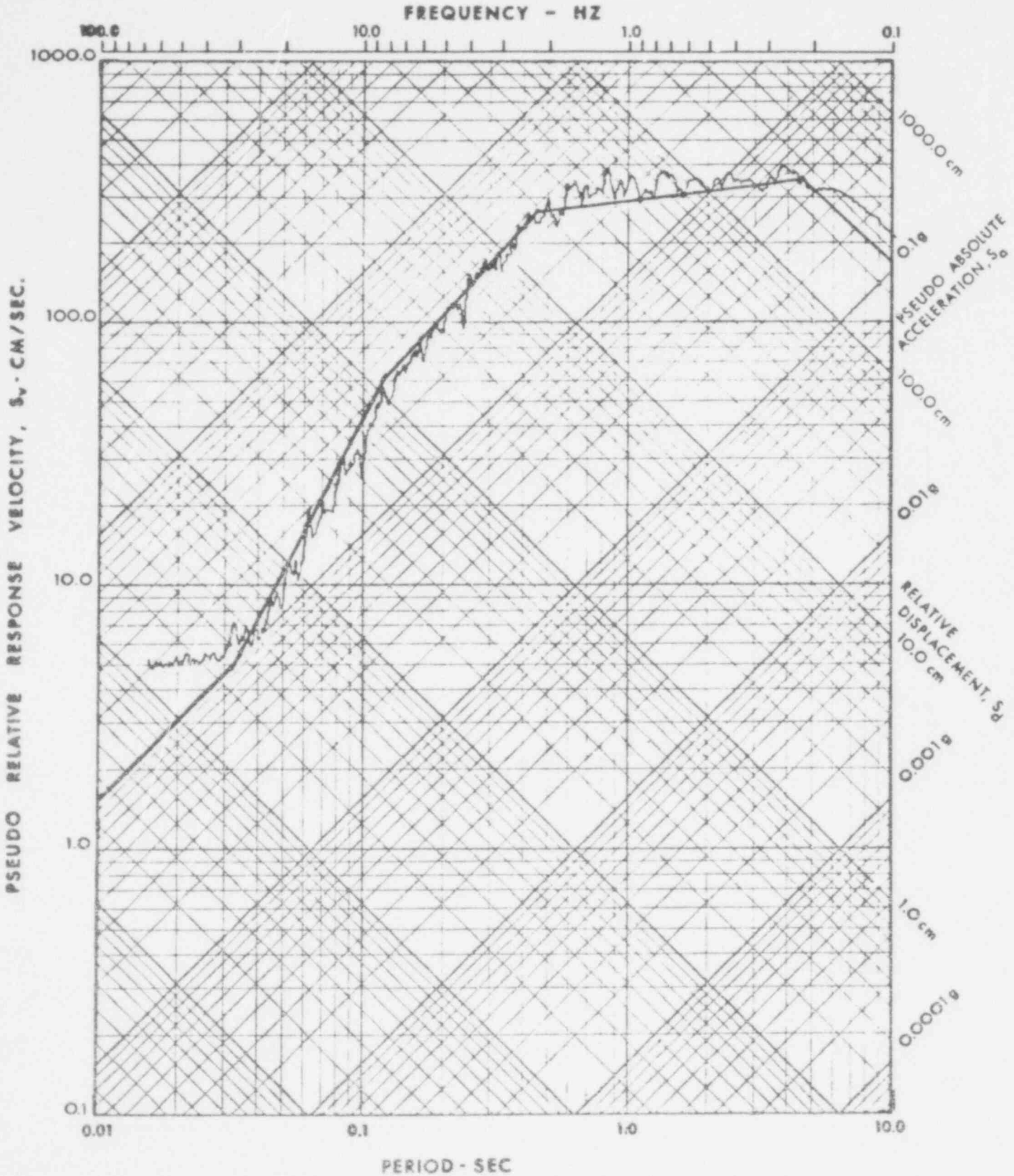

NRC LINE SPECTRA/SPECTRA OF TIME HISTORY
2 PERCENT DAMP

NRC/NONLIN

FIGURE 4.13

528 114

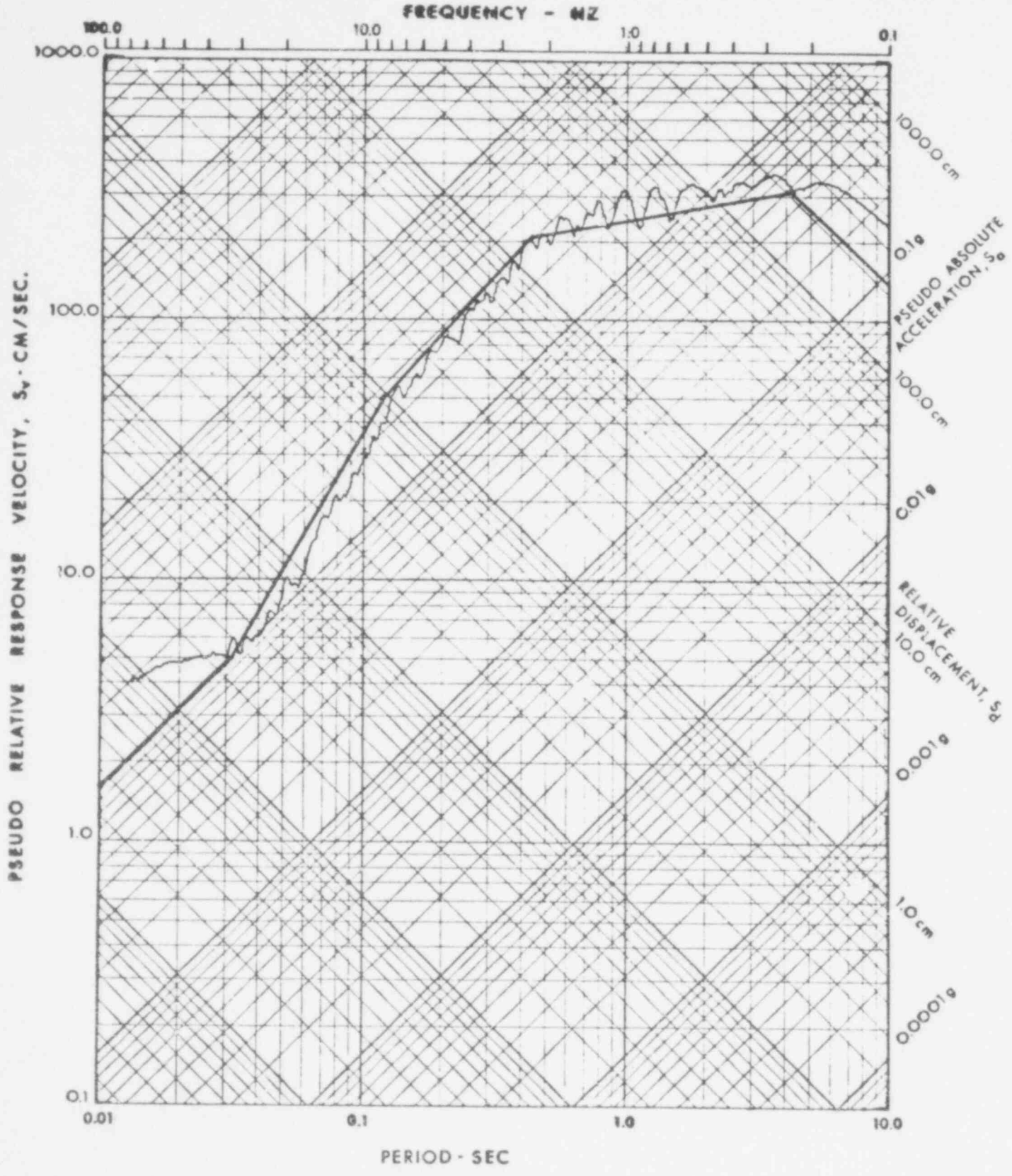

NRC LINE SPECTRA/SPECTRA OF TIME HISTORY
5 PERCENT DAMP

NRC/NONLIN

FIGURE 4.14

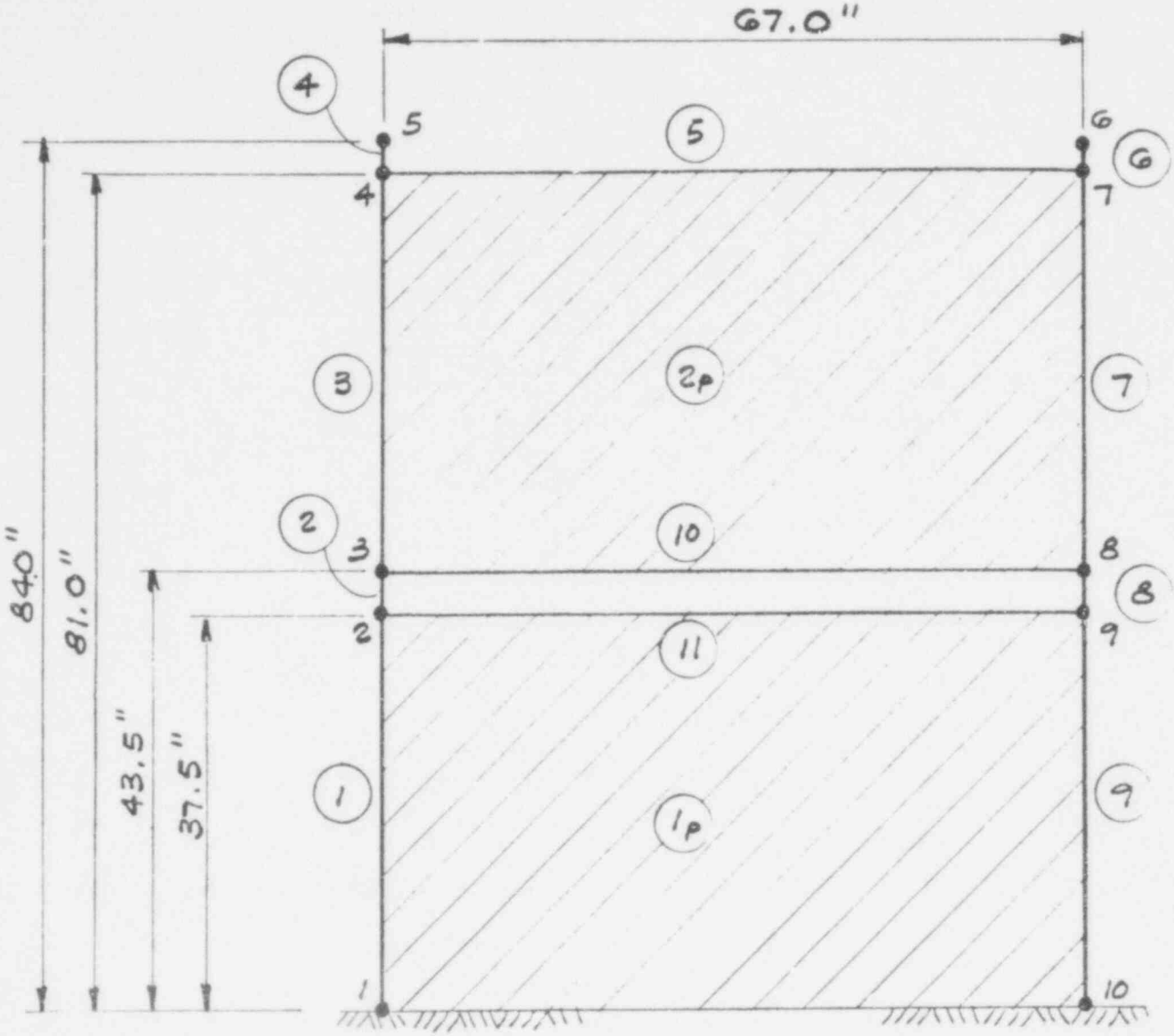

TWO-STORY, ONE-BAY REINFORCED CONCRETE SHEAR WALL COMPUTER MODEL

528 116

NRC / NONLIN

FIGURE 4.15

LEVEL	Δ MAX (IN)	TIME (SEC)	Δ YIELD (IN)	TIME (SEC)	μ
2	.1962	10.34	.0260	.93	7.5
			.0324	.94	6.0
				AVG.	6.8
1	.1773	10.34	.0135	.93	13.1
			.0170	.94	10.4
				AVG.	11.8

$$\mu = \frac{\Delta \text{ MAX}}{\Delta \text{ YIELD}}$$

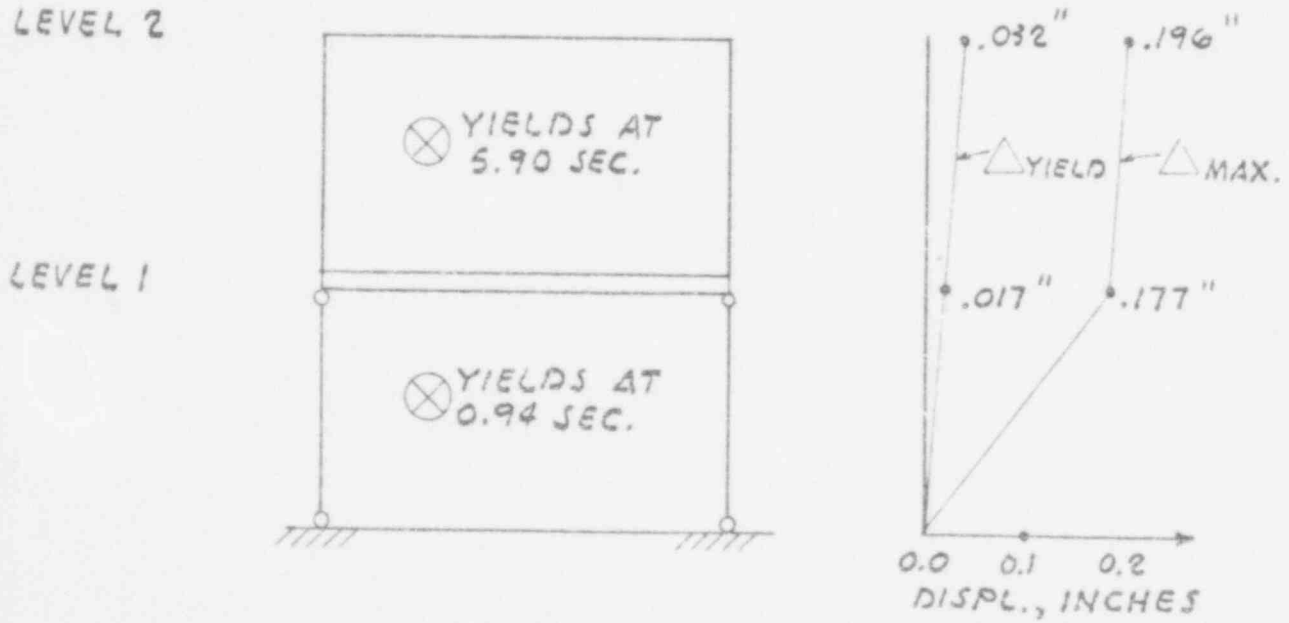

TWO STORY WALL RESULTS

NRC/NONLIN

FIGURE 4.16

528 117

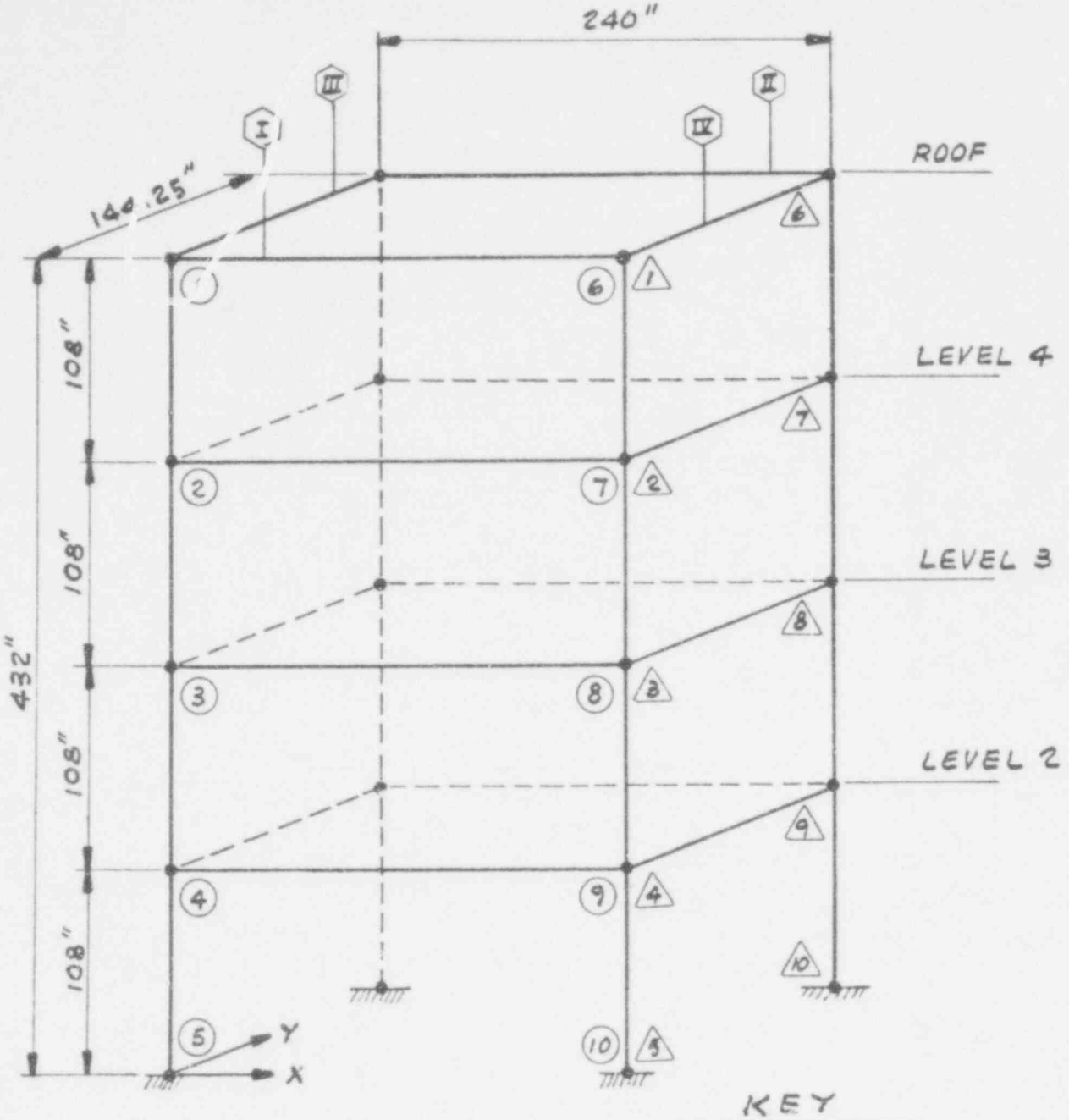

THREE - DIMENSIONAL, FOUR-STORY REINFORCED CONCRETE FRAME TORSION MODEL

528 118

NRC/NONLIN FIGURE 4.17

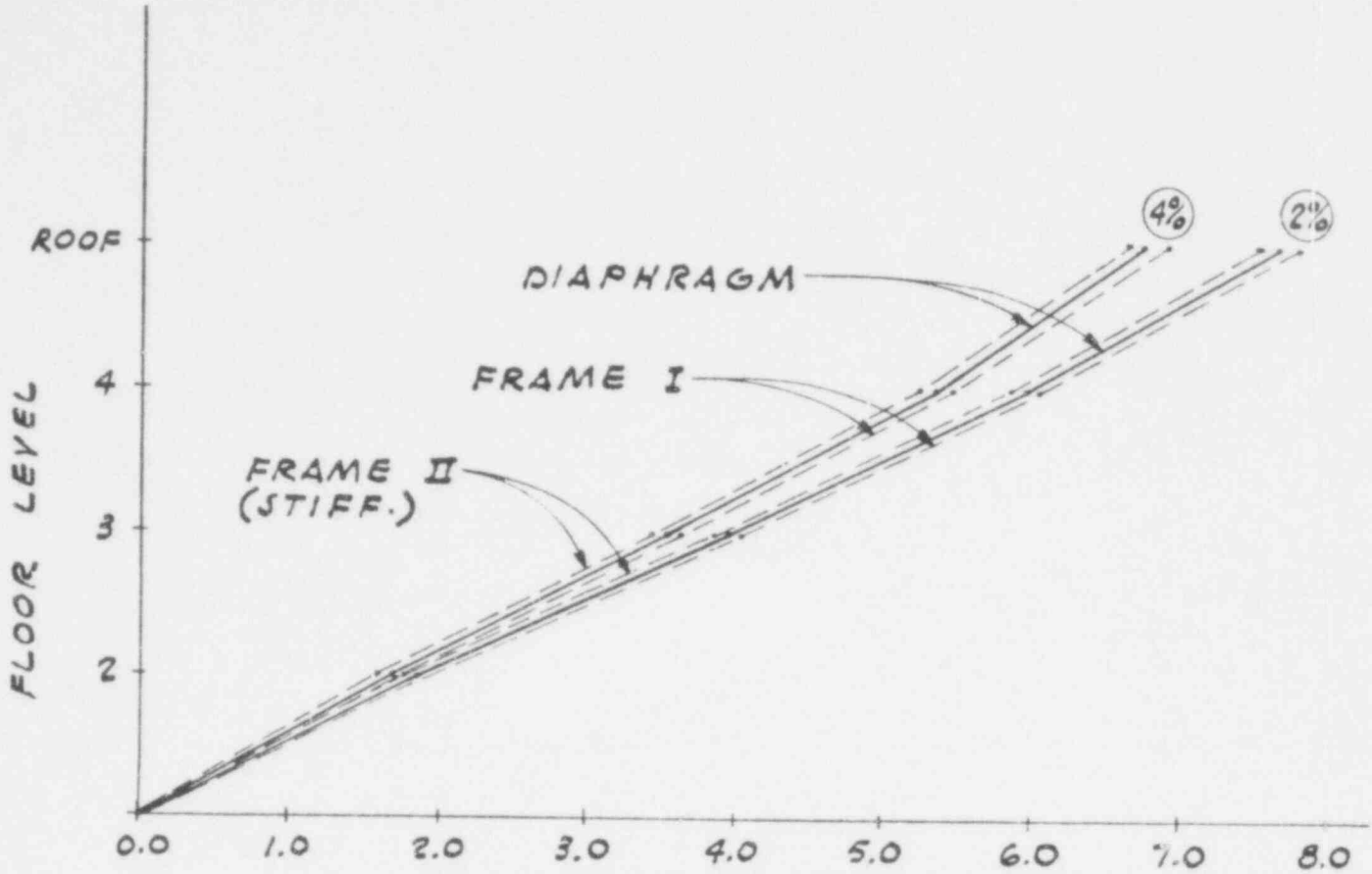

DAMPING		FRAME I		DIAPHRAGM		FRAME II	
		X	TIME	X	TIME	X	TIME
4%	ROOF	6.92	9.01	6.81	9.01	6.71	9.01
	4	5.47	9.01	5.38	9.01	5.29	9.01
	3	3.65	9.01	3.58	9.02	3.53	9.02
	2	1.69	9.02	1.67	9.03	1.65	9.03
2%	ROOF	7.79	9.02	7.67	9.02	7.56	9.03
	4	6.05	9.03	5.95	9.03	5.86	9.03
	3	3.99	9.04	3.94	9.05	3.89	9.05
	2	1.87	9.05	1.85	9.06	1.83	9.06

LATERAL DISPLACEMENTS T DIFFERENT LEVELS OF FOUR-STORY TORSION STRUCTURE

NRC/NONLIN

FIGURE 4.18

528 119

5. COMPARISON OF SIMPLIFIED AND RIGOROUS ANALYSIS RESULTS AND RECOMMENDATION OF A SIMPLIFIED NONLINEAR ANALYSIS METHOD FOR CATEGORY I NUCLEAR POWER PLANT STRUCTURES

5.1 Comparison and Recommendation

The previous chapters described rigorous and simplified nonlinear analyses of four hypothetical structures. A comparison of the results from the two types of analyses is presented in Table 5.1. In most of the cases considered, ductility factors predicted using the Modified Substitute Structure Method and the Approximate Inelastic Response Method (AIRM) were greater than those obtained from the rigorous analysis. For this reason, both methods were eliminated from consideration. Ductility factors obtained using the Elasto-Plastic Spectrum Method (EPSM) and those obtained from the Reserve Energy Technique (RET) are in close agreement with each other and with the results from the rigorous analysis. This suggests that the RET and the EPSM are equally suitable for simplified analysis of Category I nuclear power plant structures. The RET is recommended for several reasons:

- The RET involves a more detailed structural analysis than is required by the EPSM. This is advantageous because a detailed analysis is likely to identify critical weak or nonductile structural members that might otherwise go unnoticed.
- The RET considers all types of nonlinear behavior whereas the EPSM is appropriate only for elasto-plastic structures.
- The RET predicts ductility factors for various parts of structures (maximum values are shown in Table 5.1) whereas the EPSM predicts a single value for the entire structure.
- The RET was developed for the analysis, design, and evaluation of nonlinear response whereas the EPSM was originally intended exclusively for design. For this reason, the basic formulation of the RET if more suitable for analysis of structures.

Hence, the RET is recommended for the simplified nonlinear analysis of Category I structures because it gives sufficiently accurate results and also because it is capable of providing detailed nonlinear response information for a wide variety of structures.

528 120

5.2 Theoretical Background, Mathematical Formulation, and Basic Assumptions of the RET[5.1-5.4]

The theoretical background for the RET is taken from a basic law of physics: the conservation of energy. In this case, energy supplied by a dynamic disturbance must be balanced by the energy dissipated within the structure plus the energy radiated away from the structure. The energy balance equation may be written as follows:

$$E_I = E_D + E_R \tag{5.1}$$

or:

$$E_D = E_I - E_R \tag{5.2}$$

where:

E_I = energy input by a dynamic disturbance

E_D = energy dissipated by the structure

E_R = energy radiated away from the structure

E_D is the quantity of interest because it determines structural behavior and response. The underlying theoretical principle of the RET is that structures will respond dynamically in a manner that satisfies Equation (5.2).

Using state-of-the-art time-series methods of analysis, it is theoretically possible to perform rigorous energy balance calculations. However, because their accuracy is currently limited by the lack of precise knowledge concerning the dissipation and radiation of energy, such calculations are not yet practical. Even so, the energy balance concept remains extremely useful as a tool for the prediction of nonlinear structural response. The RET was developed to take advantage of this principle while avoiding lengthy, and possibly imprecise, rigorous calculations. Several approximations and assumptions are used to accomplish this, as outlined below.

The term $E_I - E_R$ from Equation (5.2) is the energy demand, or the net energy affecting the structure. Linear elastic behavior is assumed in the demand calculations. The energy capacity of a structure (its capacity to dissipate

528 121

energy) is a function of the response; usually, greater response implies greater energy dissipation. The nonlinear response characteristics of a structure are reflected in its energy capacity.

Both demand and capacity calculations are based on a force-deflection diagram. An illustrative example is shown in Figure 5.1. An example single-degree-of-freedom system, consisting of a mass, m, and an elasto-plastic spring, is shown in Figure 5.1a. The force-deflection characteristics of the spring are shown in Figure 5.1b. The yield point is identified as the point corresponding to the force = V_y and the deflection = Δ_y. For forces less than V_y, the spring has a constant stiffness, K. Note that K is equal to the ratio V_y/Δ_y. The elastic period of vibration, T, of the single degree of freedom is computed as follows:

$$T = 2\pi\sqrt{\frac{m}{K}} \tag{5.3}$$

The force-deflection diagram of Figure 5.1b is elasto-plastic, and a force greater than V_y cannot be developed. (Deflections greater than Δ_y can occur without additional resistance.) The effective linear stiffness of the plastic response is defined as K', and this is equal to the ratio V_y/Δ, where Δ is any deflection greater than Δ_y. The effective period of the nonlinear response is computed as follows:

$$T' = 2\pi\sqrt{\frac{m}{K'}} \tag{5.4}$$

The demand is calculated as the area under the force-deflection curve, assuming the system remains elastic. For example, assume that the single-degree-of-freedom system is subjected to a peak acceleration, α. The corresponding force in the spring, assuming elastic response, is computed as follows:

$$V = m\alpha \tag{5.5}$$

The energy demand is:

$$\text{Energy Demand} = \frac{1}{2}\frac{V^2}{K} \tag{5.6}$$

528 123

Hence, the demand is calculated on the fictitious assumption of elastic behavior. The capacity is calculated as the area under the actual (in this case, elasto-plastic) force-deflection diagram. The energy capacity for a given deflection Δ is computed as follows:

$$\text{Energy Capacity} = \frac{1}{2} V_y \Delta_y + V_y(\Delta - \Delta_y) \tag{5.7}$$

where:

V_y = yield level shear force

Δ_y = yield level deflection

Δ = maximum deflection

Equating demand and capacity gives the following results:

$$\frac{1}{2} \frac{V}{K^2} = \frac{1}{2} V_y \Delta_y + V_y(\Delta - \Delta_y) \tag{5.8}$$

The ductility factor is defined as $\mu = \Delta/\Delta_y$. Equation (5.8) can be rewritten as follows:

$$\frac{V^2}{K} = V_y \Delta_y + V_y \Delta_y (2\mu - 2) \tag{5.9}$$

Substituting the ratio V_y/K for Δ_y and solving for μ gives the following:

$$\mu = \frac{1}{2} \frac{V^2}{V_y^2} + \frac{1}{2} \tag{5.10}$$

The ductility factor, $\mu = \Delta/\Delta_y$, is the result of an RET analysis. This quantity provides a measure of the nonlinear response.

The foregoing example for an elasto-plastic single-degree-of-freedom system can be easily generalized to multistory structures with various types of force-deformation relationships. For a multistory application, the RET calculates a ductility factor, μ_j, for each story, j, on the basis of the dynamic story shear, DV_j:

123

$$DV_j = \frac{C_b}{S_a}\left(1 + \frac{N-1}{100}\right) S_a W_b \frac{\sum_{j}^{N} m_j \phi_j}{\sum_{1}^{N} m_j \phi_j} \qquad (5.11)$$

where:

C_b = fundamental mode dynamic base shear coefficient

S_a = spectral acceleration (g)

N = total number of stories

W_b = total dynamic weight (kip)

ϕ_j = fundamental mode-shape deflection for story j

m_j = dynamic mass for story j

The expression for the story ductility, μ_j, is similar to Equation (5.10):

$$\mu_j = \frac{P_j \alpha^2 (DV_j)^2}{2(V_{yj})^2} + \frac{1}{2} \qquad (5.12)$$

where:

μ_j = ductility factor for story j

P_j = ratio of effective energy-absorption capacity in story j to the sum of same for that story plus all superimposed stories

α = a factor to convert elasto-plastic to bilinear softening values

V_{yj} = yield shear or yield force of story j (kip)

The ratio C_b/S_a in Equation (5.11) is called the modal weight ratio; this term is a constant, depending on the fundamental mode shape and the distribution of mass. The term:

$$1 + \frac{N-1}{100}$$

528 124

is introduced to account approximately for the effect of higher modes of vibration, which are otherwise ignored in this analysis. Thus, the first terms on the right side of Equation (5.11), i.e.,:

$$\frac{C_b}{S_a}\left(1 + \frac{N-1}{100}\right) S_a W_b$$

are equal to the approximate multimode base shear. The final term in this equation, the ratio of the sum of mass times mode-shape deflections, is a factor that distributes the total base shear to the various stories. This is similar in principle to the shear distribution adopted by the *Uniform Building Code*.

A ductility factor may be predicted for each story using Equation (5.12). This equation is based on energy considerations of a single-degree-of-freedom system; the term P_j is a factor that accounts for the effective energy-absorption capacity of a single story of a multistory structure. The equation for story ductility was also based on elasto-plastic conditions, and the term α is introduced to account for other types of force-deformation relationships:

$$\alpha = \frac{A_{ep}(\Delta)}{A(\Delta)} \tag{5.13}$$

where:

$A_{ep}(\Delta)$ = the area under an elasto-plastic force-deflection curve up to a deflection Δ

$A(\Delta)$ = the area under the actual force-deflection curve up to the deflection Δ

The factor α may be a function of Δ; however, for practical force-deflection curves, it is a constant. Appendix B gives more specific information on the factors α and P_j and on the calculation of story ductilities.

For many types of dynamic loads, the story accelerations (and also the story shears and demand energies) depend on the period of vibration. The RET requires that the effective period of the nonlinear response be used in the

528 125

calculation of demand energy. By manipulating Equations (5.4) and (5.5), the effective nonlinear period can be expressed as follows:

$$T' = T\sqrt{K/K'} \tag{5.14}$$

where:

T' = effective nonlinear period
T = linear elastic period
K = linear elastic stiffness
K' = effective nonlinear stiffness

For simplicity, the ratio of K/K' for the first story may be used to calculate T'.

Note that K' and T' depend on the peak deflection (see Figure 5.1b) and that this quantity is not known at the start of an RET analysis. Hence, it is necessary to perform iterative calculations as follows:

(1) Calculate the demand from the initial elastic stiffness, K, and period, T.

(2) Evaluate Equation (5.12) for the ductility.

(3) Calculate the peak displacement, $\Delta = \mu\Delta_y$, and evaluate the effective nonlinear stiffness.

(4) Calculate the effective nonlinear period.

(5) Calculate the demand from the effective nonlinear stiffness, K', and period, T'.

(6) Repeat steps 2 through 5 until the same ductility is calculated on two successive cycles. Note that, due to the various assumptions and approximations of RET analysis, convergence of μ to only one, or at most two, significant figures is required.

Examples of these iterative calculations are given in the section dealing with analysis of the benchmark problems.

5.3 Analytical Models and Capacity Calculations

The application of the RET requires the use of a mathematical model of the structure being analyzed. The model is used to calculate the initial elastic

dynamic characteristics as well as to calculate the story shears and interstory displacement for the initiation of inelastic action.

A mathematical model for RET analysis may be quite complex, or it may be very simple, depending on the nature of the structure being analyzed and the level of sophistication required. The accuracy of final results (i.e., ductility) is affected by the assumptions and approximations of the model. Generally, a stick model such as shown in Figure 5.2 is adequate. A lumped mass, m, is included to represent the dynamic mass of each floor, and the spring constant, K, is the interstory stiffness: the shear required to cause a unit deflection of one story relative to an adjacent story. The constant K may be determined by approximate methods or by computer analysis. Section properties used to calculate K should be representative of those that will occur at or near the yield point. For reinforced concrete, this means that moments of inertia should be based on cracked-section calculations for beams. Columns and slabs may be considered as uncracked; however, it is wise to verify this assumption. For nonsymmetrical buildings, a more complex, three-dimensional model is usually required to model torsional effects correctly.

An eigenvalue analysis of the model must be performed to extract the frequencies and mode shapes. This may consist of a hand analysis using the Rayleigh Method [5.6], or any one of a number of available computer routines may be used. Only the fundamental mode properties are required for an RET analysis; however, it is usually wise to obtain several modes and to estimate the relative contribution of each to the total response.

The model may also be used to determine the story shear and displacement that cause the initiation of significant nonlinear response. To do this, it is necessary to calculate the moment and shear capacity of each element in the story. These element capacities should be computed by conventional methods such as those recommended by the ACI or the AISC. Element capacities are compared to the element moments and shear resulting from an analysis for a unit story shear. The minimum story shear causing significant yielding in the story can be calculated by simple ratio. The corresponding interstory displacement is obtained by dividing the yield shear by the interstory stiffness, K.

528 127

Application of the RET also requires knowledge of the force-deflection characteristics of the structure in the post-elastic range. Selection of one of of the 12 cases outlined in Appendix B is usually adequate. Adopting one of these will eliminate the need for further calculations; otherwise, additional calculations to determine the postelastic force deformations for each story will be necessary. Such analyses may consist of a series of linear approximations of the nonlinear response. At the end of each linear analysis, members that have yielded are identified and replaced with dummy elements having a fraction of the original member's stiffness. An advantageous by-product of such analysis is the opportunity to identify (and correct for design) weak or nonductile elements.

The demand calculations of the RET require an assumption concerning damping. In general, the damping ratios recommended in NRC Regulatory Guide 1.61[5.5] for structures at or near the yield point may be used for an RET analysis. However, other damping values may be used where justified.

5.4 Methods of Solution and Interpretation of Results

The analysis of a building using the RET may be performed in various ways; all are based on the energy balance concept. The calculation sheet shown in Figure 5.3 is a useful tool for organizing and performing reserve-energy calculations. A description of the input data and various calculations required on this sheet is given in Appendix B along with various examples.

Note that the RET does not require that the ductility of each story be calculated. The number of stories that are included in the analysis is an option. An expedient scheme for an RET analysis consists of first performing the iterative calculations for the period using only the first story, and, after this solution converges (see section 5.2), calculating ductilities in other parts of the building. This scheme avoids the unnecessary complications that would be introduced by iterative calculations using all the stories.

The results of the RET are ductility factors for the various stories considered in the analysis. (The ratio of peak interstory displacement to interstory displacement at yield is defined as the ductility factor.) The duc-

528 128

tility factor applies to the story as a whole and is not necessarily indicative of the ductility demand on a given element. Note that the interpretation of the story ductility factor depends on the criterion used to identify $\mu = 1$ (the initiation of inelastic response). For example, if $\mu = 1$ is assigned to an interstory displacement causing the weakest element to reach yield, the story ductility resulting from the RET will also be the ductility demand for the weakest element. In this case, the ductility demand for other elements would be less than the story ductility. Alternatively, a ductility factor of 1 may be assigned to an interstory displacement that is sufficient to cause yielding of several members. In this case, an RET analysis will result in a ductility factor indicative of the minimum ductility demand of the members whose yielding identified $\mu = 1$. In either case, members that do not yield for $\mu = 1$ have ductility demands that are less than the story ductility predicted by the RET.

Load-versus-deflection diagrams for structures that possess a great deal of redundancy do not generally have a definite yield point where there is a drastic reduction in structural stiffness. For these structures, judgment is required to establish the point where $\mu = 1$, i.e., the initiation of inelastic action. In general, $\mu = 1$ may be assigned to a point on the load-versus-deflection diagram that corresponds to the overstressing of several important structural members. The tangent stiffness at this point should be 30% to 50% of the elastic tangent stiffness.

For structures with less redundancy, $\mu = 1$ can be assigned to the overstressing of a single major structural element inasmuch as this normally corresponds with a drastic reduction in stiffness. Because of the general lack of redundancy, this criterion for $\mu = 1$ is used in the analysis of the benchmark problems.

From the ductilities and corresponding displacements predicted by the RET, it is possible to calculate moments, shears, stresses, and strains in structural members. These calculations may be performed by various methods; however, specific details are beyond the scope of RET analysis.

129

The computed ductilities may be used as a criterion to judge the acceptability of a structure that has been analyzed using the RET. While this study is not intended to establish allowable or acceptable ductilities, it is possible to provide some general guidelines on this subject as it pertains to the RET. The following factors will generally influence an allowable ductility criterion.

(1) Type of Building. Buildings with redundant structural elements can be allowed a higher ductility than those without alternative load paths. For example, a ductile frame might have several redundant load paths, but this may not be the case for a shear wall structure.

(2) Function of Building. Noncritical buildings can be allowed higher ductilities than critical buildings. Category structures (the subject of this report) are all important buildings, but certain parts of these structures are undoubtedly more critical than others. Various allowable ductility factors may be assigned on this basis. The determination must necessarily be made by others who are responsible for the operational and safety aspects of nuclear power plants.

(3) Material of Construction. Structural steel is generally considered to be the most ductile material used in nuclear power plants. Properly detailed and carefully placed reinforced concrete may also be quite ductile. The various types of masonry construction are all considered to be less ductile than reinforced concrete unless specially reinforced.

(4) Type of Failure. This criterion for allowable ductility is also related to material of construction. For example, a bending failure may be quite ductile in an under-reinforced concrete beam or a steel beam, but failure might be sudden for bending of an over-reinforced concrete beam. A compression failure in a steel column might be nonductile if buckling occurs; however, a spiral reinforced concrete column can exhibit considerable ductile behavior.

528 130

There has been a considerable amount of research on the extent of ductile behavior that can be safely allowed.[5.2, 5.7-5.13] Interstory or total displacement ductility factors between 2 and 8 have been sustained by conventional structures without loss of structural integrity; however, these tests were generally inconclusive regarding the details of structural performance associated with a given displacement ductility factor. Hence, the following ductility criteria are established with concern for overall structural integrity, and details such as cracking, spalling, and permanent set are not given specific consideration.

General guidelines for allowable ductilities for Category I nuclear power plant structures may be presented as shown in Tables 5.2 and 5.3. Table 5.2 applies to buildings that resist lateral forces through frame action; Table 5.3 is for shear wall structures. Each table lists acceptable and unacceptable ductility factors for various performance criteria. A structure may be considered acceptable if an RET analysis results in values less than or equal to those presented in the "acceptable ductility" column. A structure with ductility factors equal to or greater than those shown in the "unacceptable ductility" column should be considered unacceptable. A detailed analysis is generally necessary to demonstrate the adequacy of structures whose RET ductility factors are between the acceptable and unacceptable values.

Performance criteria listed in the tables consist of safe shutdown and noncollapse. The function of a building determines which of the performance criteria must be satisfied. For example, certain noncritical buildings may be required only to remain standing after a severe earthquake. In this case, the noncollapse performance criterion would apply. Other buildings or elements are required to provide containment or safe shutdown of the plant; hence, more restrictive ductilities would apply.

Note that the values presented in Tables 5.2 and 5.3 are only general guidelines. The ductility criterion used for a specific building may differ, depending upon the degree of redundancy, the presence or absence of brittle elements, and the material of construction. Following an RET analysis of a specific structure, it is wise to take a critical look at the building to

528 131

identify the elements that have failed or have been severely damaged. Is there a safe-load path remaining to transfer lateral forces to the ground? If not, the building is unacceptable regardless of the computed ductility. In such cases, the building should be redesigned or otherwise strengthened. These considerations, in addition to the ductility criteria presented in Tables 5.2 and 5.3, must be included in evaluating the results of an RET analysis.

The energy balance concepts of the RET appear useful for analyzing a broad range of structural problems and thus has little limitation in applicability. However, a successful RET analysis requires careful selection of modeling parameters, calculation of structural capacity, calculation of demand, specification of inelastic behavior characteristics, and interpretation of results. The lack of adequate consideration of these factors will limit the applicability of an RET analysis. The degree of care reflected in the analysis presented in this report will generally ensure reliable results at least within the range of the acceptable ductility factors listed in Tables 5.2 and 5.3.

528 132

REFERENCES

5.1 Blume, J. A., "A Reserve Energy Technique for the Earthquake Design and Rating of Structures in the Inelastic Range," *Proceedings, Second World Conference on Earthquake Engineering*, Tokyo, 1960.

5.2 Blume, J. A., N. M. Newmark, and L. H. Corning, *Design of Multistory Reinforced Concrete Buildings for Earthquake Motions*, Portland Cement Association, Skokie (Illinois), 1961.

5.3 Blume, J. A., "Elements of a Dynamic-Inelastic Design Code," *Proceedings, Fifth World Conference on Earthquake Engineering*, Rome, 1973.

5.4 Blume, J. A., "Analysis of Dynamic Earthquake Response," State of Art Report No. 3, Technical Committee 6, Earthquake Loading and Response, *Proceedings, ASCE-IABSE International Conference on the Planning and Design of Tall Buildings*, August 1972.

5.5 U. S. Nuclear Regulatory Commission, *Damping Values for the Design of Nuclear Power Plants*, Regulatory Guide 1.61, Washington, D.C., October 1973.

5.6 Biggs, J. M., *Introduction to Structural Dynamics*, McGraw-Hill, New York, 1964.

5.7 John A. Blume & Associates Research Division, *Response of Two Identical Seven-Story Structures to the San Fernando Earthquake of February 9, 1971*, JAB-99-98, prepared for the Nevada Operations Office, U.S. Atomic Energy Commission, San Francisco, October 1973.

5.8 Mahin, S. A., and V. V. Bertero, "Nonlinear Seismic Response Evaluation - Charaima Building, *Journal of the Structural Division*, American Society of Civil Engineers, June 1974.

528 133

5.9 Chen, C. K., R. M. Czarnecki, and R. E. Scholl, *Vibration Tests of a 4-Story Reinforced Concrete Test Structure*, JAB-99-119, prepared for the Nevada Operations Office, U. S. Energy Research and Development Administration, San Francisco, January 1976.

5.10 Gulkan, P., and M. A. Sozen, "Response and Energy Dissipation of Reinforced Concrete Frames Subject to Strong Base Motion," *Structural Research Series* No. 377, University of Illinois, Urbana, May 1971.

5.11 Popov, E. P., V. V. Bertero, and S. Vinathanatepa, "Analytic and Experimental Hysteretic Loops for R/C Subassemblies," *Proceedings, Fifth European Conference on Earthquake Engineering*, September 1975.

5.12 Newmark, N. M., and E. Rosenblueth, *Fundamentals of Earthquake Engineering*, Prentice-Hall, Englewood Cliff (New Jersey), 1971.

5.13 *Tentative Provisions for the Development of Seismic Regulations for Buildings*, prepared by the Applied Technology Council associated with the Structural Engineers Association of California, 1978.

528 134

TABLE 5.1
COMPARISON OF RIGOROUS AND SIMPLIFIED RESULTS

1-Story Frame			4-Story Frame		
	Taft (2.2g) Input	NRC (1.0g) Input		0.5g Input	1.0g Input
Rigorous Analysis	$\mu = 4$	$\mu = 1.5$	Rigorous Analysis	$\mu = 2$	$\mu = 4$
Simplified Analysis			Simplified Analysis		
Elasto-Plastic Spectrum Method	$\mu = 3.5$	$\mu = 1.5$	Elasto-Plastic Spectrum Method	$\mu = 2$	$\mu = 4$
Modified Substitute Structure Method	$\mu = 4.0$	$\mu = 6.0$	Modified Substitute Structure Method	$\mu = 4$	$\mu = 14$
Reserve Energy Technique	$\mu = 3.6$	$\mu = 1.2$	Reserve Energy Technique	$\mu = 2$	$\mu = 4$
Approximate Inelastic Response Method	$\mu = 9.0$	$\mu = 11$	Approximate Inelastic Response Method	$\mu = 4$	$\mu = 13$

2-Story Shear Wall (0.2g Input)		Torsion Building (1.0g Input)	
Rigorous Analysis	$\mu = 12$	Rigorous Analysis	$\mu = 5$
Simplified Analysis		Simplified Analysis	
Elasto-Plastic Spectrum Method	$\mu = 7$	Elasto-Plastic Spectrum Method	$\mu = 4$
Modified Substitute Structure Method	$\mu = 60$ (collapse)	Modified Substitute Structure Method	$\mu = 10$
Reserve Energy Technique	$\mu = 8$	Reserve Energy Technique	$\mu = 4$
Approximate Inelastic Response Method	$\mu = 200$ (collapse)	Approximate Inelastic Response Method	$\mu = 16$

528 135

TABLE 5.2

ALLOWABLE DUCTILITIES AND LIMITS OF APPLICABILITY

FOR REINFORCED CONCRETE MOMENT-RESISTING FRAME BUILDINGS

Performance Criteria	Acceptable Ductility	Unacceptable Ductility
Noncollapse	5	10
Safe Shutdown	2	6

TABLE 5.3

ALLOWABLE DUCTILITIES AND LIMITS OF APPLICABILITY

FOR REINFORCED CONCRETE SHEAR WALL BUILDINGS

Performance Criteria	Acceptable Ductility	Unacceptable Ductility
Noncollapse	4	7
Safe Shutdown	2	4

528 136

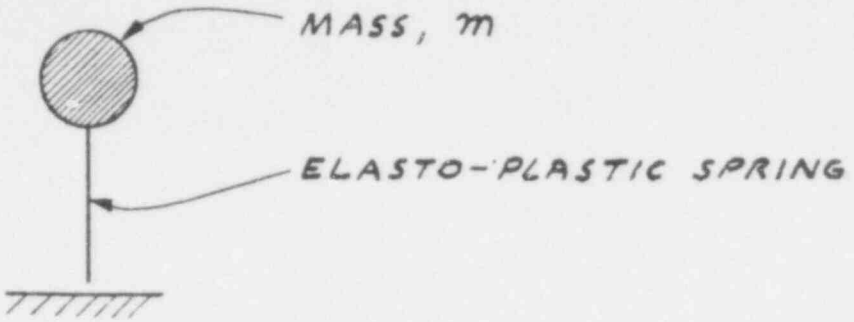

(a) EXAMPLE SINGLE-DEGREE OF FREEDOM SYSTEM

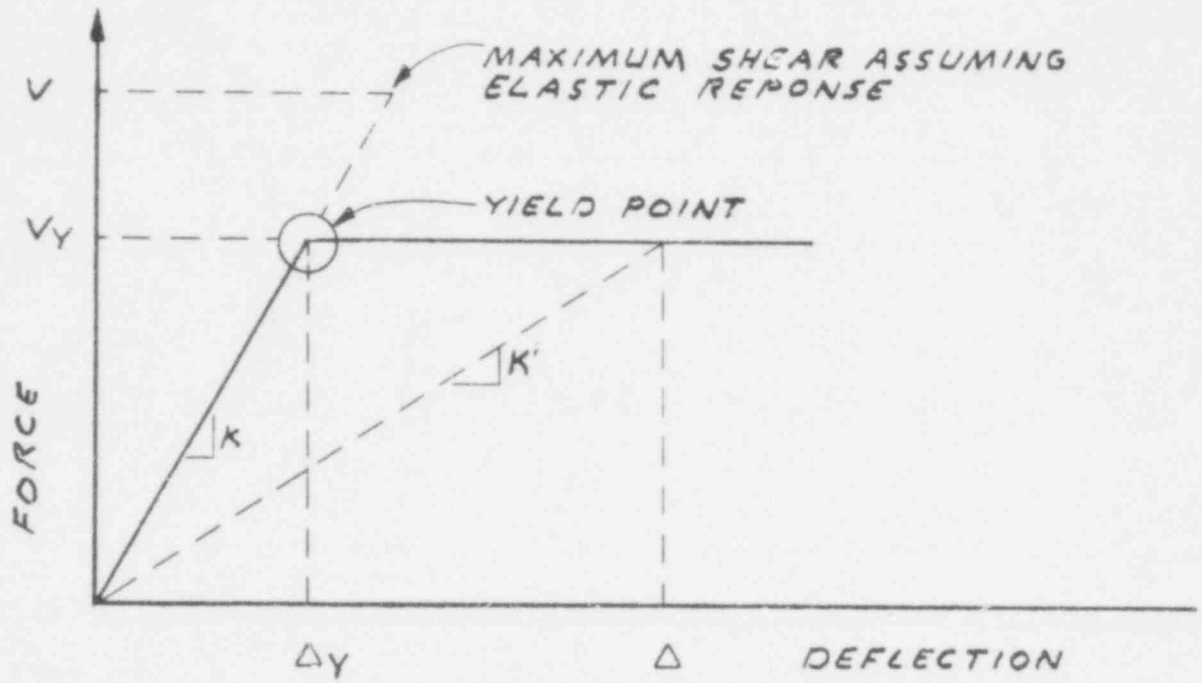

(b) FORCE DEFLECTION DIAGRAM

EXAMPLE SINGLE-DEGREE OF FREEDOM SYSTEM AND FORCE-DEFLECTION

528 137

NRC/NONLIN FIGURE 5.1

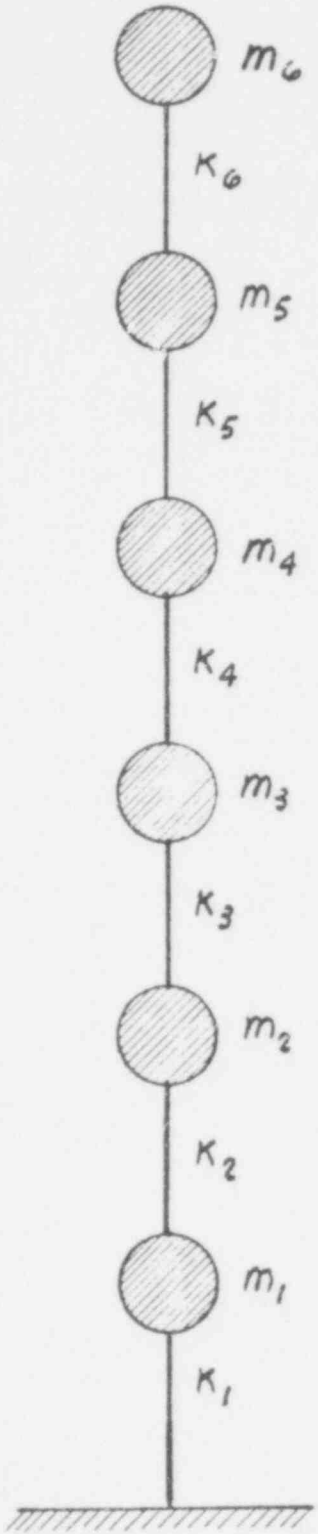

528 138

EXAMPLE STICK MODEL

NRC/NONLIN FIGURE 5.2

NRC / NONLIN

RET CALCULATION FORM

Building _____ Direction _____

N = _____ Earthquake _____

Story Shear Model _____ α = _____

Level, j	MODE 1 T = S_a = Γ =		MODE 2 T = S_a = Γ =		MODE 3 T = S_a = Γ =		DV_j (kip)	V_{y_j} (kip)	$\frac{DV_j}{V_{y_j}}$	μ_j
	F (kip)	DV_{j1} (kip)	F (kip)	DV_{j2} (kip)	F (kip)	DV_{j3} (kip)				

528

139

FIGURE 5.3

6. BENCHMARK PROBLEMS

6.1 Introduction

For the preparation of the benchmark problems, structural details of nine nuclear power plants, built in the United States over the past decade, were considered. The following general conclusions regarding the main structural features of the buildings of nuclear power plants were drawn as a result of this study.

6.1.1 Turbine Building. The turbine building is a large rectangular building, typically 150 ft by 300 ft in plan. It has a mixed type of lateral-force-resisting system. A steel frame system, usually braced, supports a large overhead crane. A reinforced concrete shear wall/diaphragm system supports the two to three working floors. The turbine support system, made of massive reinforced concrete frames, is isolated from the building structural system. The foundation is of the mat type. Figure 6.1 presents the lateral-force-resisting system, composed of reinforced concrete shear walls and braced steel frames, of a hypothetical turbine building. Figure 6.2 is the proposed benchmark model of one bay of this wall, with the typical dimensions as shown.

6.1.2 Auxiliary Building. The auxiliary building is a reinforced concrete shear wall/diaphragm structure, usually rectangular or L-shaped in plan, with overall dimensions of about 200 ft by 100 ft. There are usually three to six working floors for various functions. The foundation is usually of the mat type. The shear walls and diaphragms are uniformly reinforced with about 0.3% to 0.5% reinforcement. The walls are up to 3-1/2 ft thick. Figure 6.3 shows the plan of a hypothetical auxiliary building. The building surrounds the containment building on two sides, giving it an L-shaped appearance in plan. Figures 6.4 and 6.5 show typical sections through the building. The structure has shear walls of different aspect ratios varying from 1:2 (height:width) to 1:4. Figure 6.6 shows very simplified lumped-mass models used for dynamic analysis of these complex structures. For the benchmark problem, it was decided to choose a model that represents the auxiliary building more completely (see Figure 6.7). The shear walls are

528
140

24 in. thick, and the diaphragms are 30 in. thick. The shear walls are assumed to have 0.5% reinforcement uniformly distributed on both faces.

6.1.3 Containment Building. A reinforced concrete cylindrical shell building topped by a hemispherical dome usually houses the nuclear reactor and provides containment. The building is usually about 150 ft in diameter and about 200 ft high (Figure 6.8). A massive reinforced concrete mat provides the foundation. The cylindrical reinforced concrete shell is about 30 in. to 42 in. thick and has about 3% to 6% reinforcement placed uniformly in both longitudinal and hoop directions. This structure may be modeled as a lumped-mass shear-beam structure as shown in Figure 6.8. This model was used for simplified nonlinear analysis of the hypothetical containment building.

6.2 Analysis of a Turbine Building

The hypothetical turbine building structure is made up of a braced steel frame and reinforced concrete shear panels as shown in Figure 6.2. The benchmark analyses of a turbine building structure consisted of three parts: a rigorous elastic analysis, a simplified nonlinear analysis using the Reserve Energy Technique (RET), and a rigorous nonlinear analysis. The following paragraphs discuss each of these steps.

6.2.1 Elastic Analysis and Capacity Calculations. The main purpose of this analysis is to predict the elastic response of the structure. A comparison of the elastic response with the results of simplified and rigorous nonlinear analyses will be beneficial in judging the relative merits of these analytical approaches. Elastic analyses are also performed as a prerequisite of both the rigorous and simplified nonlinear analyses. The information extracted from these elastic analyses includes: modal frequencies, mode shapes, participation factors, modal weight ratios, story stiffnesses, and story shears and displacements causing the initiation of inelastic action in each story. Note that the elastic analyses performed as a prerequisite of the simplified and rigorous nonlinear analyses are independent of the type of dynamic disturbance and level of force that cause nonlinear response.

The two-dimensional elastic model of the hypothetical turbine building shown in Figure 6.9 was developed to determine elastic response properties and to

aid in calculating structural capacity. The masses, dimensions, and member properties used in this model were the same as those used for rigorous nonlinear analysis of this structure (details are included in Section 6.2.3). The hypothetical structure was presumed to have two diagonal braces at levels 6, 5, and 4. For the elastic model, it was assumed that the diagonal braces were incapable of sustaining compressive loads. This condition was modeled by a single member that could resist equal tensile and compressive forces. The TABS computer program[6.1] was used for the elastic analysis; however, numerous other structural analysis programs could have been used to obtain the same results.

Three analyses were conducted using the elastic model. The first consisted of an eigenvalue analysis to obtain the mode shapes and periods of vibration. These results are summarized in Tables 6.1 and 6.2. The latter table also includes story masses and the calculation of participation factors, Γ, and modal weight ratios, i.e., the ratio of the base shear coefficient to the spectral acceleration. The data presented in Table 6.2 indicate that this structure is somewhat unusual in that the second mode has the largest participation factor and modal weight ratio.

The second analysis using the elastic model consisted of the calculation of the root-sum-square displacements of the various floors. These calculations are summarized in Table 6.3. Three modes are included in this analysis; spectral accelerations for these modes were obtained from the 5%-damped curve of Figure 6.10. Input data for the rigorous and simplified nonlinear analysis were based on the same spectrum. This damping ratio is considered appropriate because the structure consists of both steel and reinforced concrete elements.

The elastic model was also used to perform a static lateral-load analysis. Static lateral loads proportional to the mass times the first mode shape were applied to each story of the elastic model, and the resulting story shears, displacements, and member forces were calculated. These results are summarized in Tables 6.4 and 6.5. This analysis was conducted (1) to determine the interstory stiffness, which is equal to the story shear divided by the corresponding interstory displacement, and (2) to extrapolate from these

528 142

results the story shear and interstory displacement corresponding to the initiation of inelastic behavior in each story. The end products of this analysis (i.e., interstory stiffness, story shear, and interstory displacement) are independent of the level of lateral force applied to the model. Lateral forces that are proportional to the mass times the first mode shape result in deflections that are proportional to the first mode shape, which may provide additional insight into the response of this turbine building.

Member yield capacity data for this structure are summarized in Table 6.6. These values were obtained using provisions of the American Institute of Steel Construction for steel members and the American Concrete Institute for reinforced concrete. The yield stress of structural steel was assumed to be 36 ksi. The compressive strength of concrete was taken as 4,000 psi, and 50,000 psi was used for the yield value of reinforcing steel. The capacities of steel members are based on the yield strength, and the concrete capacities are based on ultimate strength theory.

Also shown in Table 6.6 are the ratios of element capacities to the corresponding moments and forces from Table 6.5. These ratios indicate the relative strength of the various members in this structure: weak members and members with high loads have low ratios. From these data, one can conclude that the walls at levels 1 and 2 are the weakest members in the frame. They will exceed their capacities when the total shears in levels 1 and 2 are approximately 77 times the shears reported in Table 6.4, and the corresponding displacements will be approximately 77 times the displacements in Table 6.4. Hence, the initiation of inelastic action for the building as a whole occurs when the walls at levels 1 and 2 are overstressed; the corresponding shears and total displacements are summarized in Table 6.7.

The shear and interstory displacement causing first yield in each story can also be determined from the ratios listed in Table 6.6. These values, which are the capacity input required by the RET, are summarized in Table 6.8. They are calculated by applying the minimum ratio found in each story to the shear and interstory displacement in Table 6.4. For example, the minimum ratio found in level 6 is 150.2 (Table 6.6). Hence, the shear and interstory displacement values for level 6 shown in Table 6.8 are 150.2 times the

528 143

corresponding values in Table 6.4. The values for other levels shown in Table 6.8 were computed in an analogous manner.

6.2.2 Analysis of a Turbine Building with the RET. The RET analysis of the turbine building example consisted of two parts. The first part concentrated on the first story of the structure and was principally an iterative analysis to determine the effective inelastic period of vibration. Once this was established, a full RET analysis was conducted, and a ductility value was calculated for each story. Elasto-plastic shear deformation characteristics were assumed for each story in both of these analyses.

The formulation of the RET includes rigorous consideration of only the fundamental-mode response; a correction factor is applied to account for higher modes, which is adequate for most buildings. However, this building is an exception because of the importance of the higher modes relative to the fundamental mode. The higher-mode correction factor is not sufficient in this case, and an alternative procedure must be adopted. A logical solution is to perform the RET calculations using as many modes as needed. In this case the lowest three modes were sufficient because the modal weight ratios listed in Table 6.2 indicate that the combination of these modes comprises 96% of the total modal weight.

Iterative calculations for the periods of vibration are summarized in Figure 6.11. Note that these calculations consider three modes and only the first story. Modal periods from the elastic analysis were used for the first cycle, and spectral accelerations were obtained from the 5%-damped spectral curve shown in Figure 6.10. The spectral acceleration for each mode times the modal weight ratio, C_b/S_a, times the total building weight is equal to the dynamic base shear for that mode. The total dynamic base shear, DV, was obtained by a root-sum-squares combination of the modal contributions. The shear capacity of the base story is listed in Table 6.7 as 911 kip. The ductility calculation, from Equation (5.12) resulted in a value of 3.7 for the first cycle of this iteration. The corresponding interstory displacement, δ, and story stiffness, K', were computed as shown in Figure 6.11. For cycle 2, the elastic periods are adjusted by the square root of the ratio of the original elastic stiffness to the effective stiffness, K'. The calculations for cycle 2 are similar to those performed for cycle 1 except that the

528 144

spectral accelerations used for cycle 2 were obtained from the 5%-damped spectral curve of Figure 6.10 at the adjusted periods for cycle 2.

This iteration was continued until the same ductility factor (rounded off to the nearest whole number) was calculated on two successive cycles. In this case, the solution converges to a first-story ductility factor of 4.

The calculations of ductility factors for each story are shown in Figure 6.12. These calculations were based on the adjusted periods determined by the iterative calculations. The dynamic story shears, DV_j, were calculated as shown in Figure 6.12 using a root-sum-squares combination of the modal story shear.

The last column of Figure 6.12 shows interstory ductilities, which indicate the degree of inelastic action in each story. Ductilities for stories 4, 5, and 6 result from tensile yielding of the diagonal braces, and the values listed in Figure 6.12 are considered to be acceptable for this type of inelastic response. The ductilities calculated for stories 1, 2, and 3 are for the reinforced concrete panels. These values are slightly above the range of ductilities normally considered to be safe for concrete shear walls. Hence, a rigorous nonlinear analysis would be necessary to verify the adequacy of this structure.

The story ductilities listed in Figure 6.12 are the ratio of the maximum interstory displacement to the interstory displacement causing inelastic behavior in that story. A slightly different definition of ductility factor is the ratio of total story displacement to the displacement of that story when first yield occurs anywhere in the building. The total displacement is defined as the actual displacement of a story relative to the base. It is also equal to the sum of the interstory displacements for the stories below the one being considered. The values in Figure 6.12 can be converted to the latter definition of ductility, as shown in Table 6.9. The total-ductility factors in Table 6.9 (so called because they are based on total rather than interstory displacement) are of interest because they can be compared to the rigorous nonlinear analysis results of this building.

528 145

The foregoing analysis considered the lowest three modes of vibration. To assess the importance of the higher modes, an RET analysis was conducted using only the first mode; these results are summarized in Table 6.10. Note that the higher-mode correction factor recommended by the RET was included in the calculations. The single-mode analysis resulted in values that are up to a factor of 2 lower than the multimode results. The conclusion from this comparison is that it is very important to include the higher modes in the analysis of this type of building.

6.2.3 Rigorous Nonlinear Analysis of a Turbine Building. The rigorous nonlinear analysis of the turbine building was based on the mathematical model shown in Figure 6.13. Nodal geometry and lumped masses are listed in Table 6.11. The model consists of beam-column elements 1 through 24, diagonal brace elements 1 through 6, and panel elements 1, 2, and 3.

Diagonal brace properties are listed in Table 6.12. The braces consist of two 6-in. by 6-in. angles 9/16 in. thick having an area of 12.9 in.^{2} and a minimum radius of gyration of 1.85 in. Tensile yield strength of 36 ksi was assumed, and a compressive strength (i.e., buckling) of 3 ksi was obtained by applying the buckling criteria specified by the American Institute of Steel Construction. Because elasto-plastic behavior was assumed, the hardening ratio was taken to be zero.

Reinforced concrete panel element properties are listed in Table 6.13. Concrete of normal weight with a compressive strength of 4,000 psi was assumed. Strength calculations were based on the following:

$$\text{Young's Modulus } E = W^{1.5}\, 33\sqrt{f'_c} = 3{,}834 \text{ ksi}$$

$$\text{Shear Modulus } G = 0.4E = 1{,}534 \text{ ksi}$$

The shear and moment capacities of the panels were calculated according to the procedures outlined in Chapter 3, and the results of these calculations are listed in Table 6.6. The ratios listed in this table indicate that the panels fail in bending before attaining their shear capacity. These ratios may be applied to the wall shears of Table 6.5 to calculate the wall shear associated with bending failures. These calculations are summarized below.

528 146

Panel Element 1:

ratio for moment failure = 82.44

wall shear at moment failure = 82.44 x 8.5 = 700.7 kip

shear stress = 700.7/12 x 327.25 = 0.178 ksi

Panel Element 2:

ratio for moment failure = 78.18

wall shear at moment failure = 78.18 x 9.97 = 779.5 kip

shear stress = 779.5/12 x 327.25 = 0.198 ksi

Panel Element 3:

ratio for moment failure = 77.23

wall shear at moment failure = 77.23 x 11.38 = 878.9 kip

shear stress = 878.9/22 x 327.25 = 0.122 ksi

The shear stress values are shown in Table 6.13 and were used in the nonlinear analysis. A hardening ratio of zero was assumed, resulting in elastoplastic response.

Properties of the beam-column elements are shown in Table 6.14. The yield moments were based on elastic section moduli and an assumed yield stress of 36.0 ksi. The positive yield force, P_y (i.e., tension), was calculated as the area times 36 ksi. The negative yield force was calculated from the buckling criteria of the American Institute of Steel Construction. Yield forces were not required input for horizontal beam-column elements because axial forces are neglected in these members.

The time history shown in Figure 6.14 was used as input for the rigorous nonlinear dynamic analysis. The peak acceleration of this accelerogram is 1.0g, and the response spectrum of this time history for 5% damping generally conforms to the 5%-damped curve shown in Figure 6.10. The nonlinear structural analysis computer program DRAIN-2D[2•6] was used in this analysis.

The qualitative aspects of the nonlinear analysis results are quite similar to the results from the RET analysis. For example, both analyses predict that the concrete panels in the lower three stories will be the first elements of the structure to exceed their capacity. Both analyses also predict

528 147

extreme inelastic response in these panels. The rigorous analysis predicts yielding in the steel columns of the lower two stories. The RET analysis predicts that the columns in stories 3 and 2 will yield and that the columns in level 1 are within 90% of yield stress. (Conclusions concerning column yielding are not a direct result of the RET analysis presented in Section 6.2.2. These conclusions are inferred from the peak interstory displacements predicted by the RET.) A difference between the rigorous and simplified nonlinear analyses is that the latter predicts yielding in the diagonal braces while the former does not. The reason for this difference is that the RET analysis distributes the total base shear to the various stories in accordance with the original elastic model. This distribution is not realistic because early yielding in the lower stories tends to isolate the diagonal braces in the upper stories from extreme loads. After yielding, the lower levels behave as so-called soft stories. The rigorous analysis method is capable of recognizing and accounting for this phenomenon; however, this is not possible with the current version of the RET. It is entirely feasible that the RET could be modified to account for the development of soft stories due to inelastic action. However, this is beyond the scope of the current effort.

Total displacements resulting from the rigorous nonlinear analysis and the RET are compared in Table 6.15. Also listed in the table are the displacements that resulted from a rigorous elastic analysis, a multimode simplified nonlinear analysis, and a single-mode simplified analysis. By coincidence, the displacements from the rigorous elastic analysis closely correspond to the results of the single-mode simplified analysis. Both these analyses resulted in considerably lower displacements than those of the rigorous analysis. In the lower stories, the displacements from the elastic and single-mode nonlinear analysis are 20% to 30% of the rigorous nonlinear analysis results. For this reason, the former two analysis schemes are judged to be unacceptable.

In the upper three stories, the results of the multimode simplified nonlinear analysis compare favorably with the rigorous nonlinear analysis. However, in the lower stories, the simplified results are only 40% to 60% of the rigorous analysis displacements. The main reason for the discrepancy is the improper distribution of story shears previously discussed. However, on an

528 148

overall basis, the displacements resulting from the multimode simplified nonlinear analysis compare favorably with the rigorous analysis results. Hence, the simplified analysis can be used with confidence.

6.3 Analysis of an Auxiliary Building

An auxiliary building is a massive reinforced concrete structure such as shown in Figures 6.15 and 6.16. The building hypothesized for this example is made up of 24-in.-thick reinforced concrete shear walls and 30-in.-thick roof and floor slabs. The walls and slabs are bounded by reinforced concrete beams and columns (i.e., edge members).

The benchmark analyses of this hypothetical auxiliary building consisted of a rigorous elastic analysis, a simplified nonlinear analysis using the RET, and a rigorous nonlinear analysis. Each of these is discussed in the following paragraphs.

6.3.1 Elastic Analysis and Capacity Calculations. The main purpose of this analysis is to predict the elastic response of the auxiliary structure. A comparison of the elastic response with the results of simplified and rigorous nonlinear analyses will be beneficial in judging the relative merits of these analytical approaches.

Elastic analyses are also performed as a prerequisite of both the rigorous and the simplified nonlinear analyses. Information extracted from these elastic analyses includes: periods of vibration, mode shapes, participation factors, modal weight ratios, elastic stiffnesses, and the shears and interstory displacements that cause the onset of inelastic response in each story. The masses, dimensions, and elastic member properties used in the elastic model were the same as those used for the rigorous nonlinear analysis of this structure (details are provided in Section 6.3.3). The TABS[6.1] computer program was used for the elastic analysis; however, numerous other structural analysis computer programs could have been used to obtain the same results.

Three analyses were conducted using the elastic model. The first consisted of an eigenvalue analysis to obtain the mode shapes and periods of vibration.

528 149

These results are summarized for the lowest three modes in Tables 6.16 and 6.17. The first two modes of this structure involve rotation and y translation whereas the third is the lowest x-translation mode. For the simplified nonlinear analysis using the RET, modes 1 and 2 were used for the y direction, and mode 3 was used for the x direction. Participation factors and modal weight ratios, C_b/S_a are listed in Table 6.18. The modal weight ratio for mode 3 is sufficiently high to justify the assumption of single-mode behavior in the x direction of the building.

The second analysis using the elastic model consisted of the calculation of the root-sum-square displacements of the center of mass of the various floors. These calculations are summarized in Table 6.19. The lowest two modes contribute to the deflection in the y direction whereas only the third mode is considered in the x direction. Spectral accelerations were obtained from the NRC response spectrum for 7% damping normalized to 0.5g. The input data for the rigorous and simplified nonlinear analyses were based on the same spectrum.

The elastic model was also used to perform static lateral load analyses. The purpose of these analyses was to provide the data necessary to calculate the elastic story stiffness and the story shears and interstory displacements that cause the initiation of inelastic behavior in each story. Static lateral loads proportional to the mass times the first mode shape were applied in the y direction, and loads proportional to the mass times the third mode shape were applied in the x direction. (Note that the resulting lateral deflections are proportional to the respective mode shapes.) The resulting shears, deflections, and interstory stiffnesses are summarized in Table 6.20; corresponding member forces are listed in Table 6.21. Only the wall shears and moments are presented because these elements comprise the lateral-load-resisting system of the structure.

Member capacity data for this structure are given in Table 6.22. These values were obtained using the ultimate strength provisions of the American Concrete Institute. The compressive strength of concrete was taken as 5,000 psi, and the yield strength of reinforcing steel was assumed to be 50,000 psi. Horizontal and vertical reinforcing steel ratios equal to 0.005 were assumed for all walls.

528 150

Also shown in Table 6.22 are the ratios of element capacities to the corresponding moments and shears from Table 6.21. These ratios indicate the relative strength of the various walls: weak walls and walls with high loads have low ratios. For the x direction, the shear ratios are lower than the corresponding moment ratios, indicating that these walls fail in shear. The lowest ratio in the x direction is 50.49 for level 1. This means that the x-direction walls in level 1 will exceed their shear capacities when the shears and displacements are 50.49 times the values given in Table 6.20. Overstressing of the x-direction walls in levels 2 and 3 would occur when the shears and displacements are 76.41 and 96.94 times the values shown in Table 6.20.

The ratios given in Table 6.22 for the y direction indicate that these walls are expected to fail in bending. First overstressing is expected in level 1 of wall A and is followed by progressive overstressing in level 1 of walls B, C, and D. This failure pattern is a result of torsional response that increases the load at one end of the building and decreases it at the other. The conclusion from these data is that all of the y-direction walls in level 1 are approximately simultaneously overstressed when the shear in level 1 reaches 9.15 times the shear shown in Table 6.20.

The story shears and total displacements for first overstressing are summarized in Table 6.23. The values for the x direction are 50.49 times the x-direction shears and displacements of Table 6.20. For the y direction, a factor of 9.15 was used to obtain the values shown in Table 6.23. Note that the values in Table 6.23 are the shears and displacements corresponding to overstressing in the first level in the x and y directions. Overstressing in the upper stories of the building would occur at forces that are higher than those shown in the table. The forces and interstory displacements that cause overstressing in each story are listed in Table 6.24. The values in Table 6.24 are used as input to the RET.

528 151

6.3.2 Analysis of an Auxiliary Building with the RET. Separate RET analyses were conducted for each direction of the hypothetical auxiliary building. The input ground motion for each direction consisted of the NRC Regulatory Guide 1.60 response spectra normalized to 0.5g. The response

spectra used for this analysis were exactly one-half of the curves shown in Figure 6.10. A damping ratio of 7% was used in each case. Elasto-plastic force-deformation characteristics were assumed for all walls.

Calculations for the x direction are summarized in Figure 6.17. Note that mode 3 is the lowest mode in the x direction. For each story in the x direction, the ratio of DV_j/V_{y_j} is less than 1, which indicates no overstressing. Calculations indicate that overstressing would occur in the x direction if the seismic input acceleration spectra were approximately 7 times the input used in this analysis. For this reason, a rigorous nonlinear analysis in the x direction was not performed.

The RET analysis for the y direction consisted of an iterative analysis for the effective periods and computation of a ductility factor for each level. The iterative calculations, which deal with the lowest two modes and only the first story, are summarized in Figure 6.18. The elastic periods of vibration were used for the first cycle. Spectral accelerations were obtained from a 7%-damped response spectrum curve. The spectral acceleration for each mode times the modal weight ratio, C_b/S_a, times the total building weight is equal to the dynamic base shear for that mode. The total dynamic base shear, DV, was obtained by a root-sum-squares combination of the modal contributions. The ductility factor, μ_j, was computed in accordance with the procedure outlined in Chapter 5. The interstory displacement, δ, and effective stiffness, K', were computed, and new periods were calculated from the original periods and the square root of the ratio of the original elastic stiffness to the effective stiffness. The new periods were used in the second cycle of the analysis. The calculation converges in three cycles to a first-level ductility factor of approximately 1.5.

The calculations of interstory ductility factors are summarized in Figure 6.19. These calculations were based on the adjusted periods that resulted from the iterative calculations. The dynamic story shears, DV_j, were calculated by taking a root-sum-squares combination of the story shears of modes 1 and 2. The interstory ductility factors in Figure 6.19 are the ratios of the maximum interstory displacements to the corresponding

528 152

values for the initiation of inelastic action in each story. The analysis shows that inelastic response is confined to the first story.

An alternative definition of ductility factor is the ratio of total story deflection to the deflection of that story when first overstressing occurs anywhere in the structure. The values in Figure 6.19 can be converted to the latter definition of ductility; these calculations are summarized in Table 6.25. The total-ductility factors of Table 6.25 (so called because they are based on total rather than interstory displacements) are of interest because they can be compared to the rigorous analysis results for this building. The total-ductility factors alone do not indicate what portions of the building are overstressed; this information is explicit in the interstory ductility factors. Note that both the interstory ductility factors (Figure 6.19) and the total ductility factors (Table 6.25) are quite low. These values are within the range that is considered acceptable for this type of building.

The foregoing analysis for the y direction considered the lowest two modes of vibration. To assess the importance of the higher modes, an RET analysis was conducted using only the first mode; these results are summarized in Table 6.26. Note that the higher-mode correction factor was included in these calculations. The ductility factors from the single-mode analysis are equal to the ductility factors from the multimode analysis, and the total inelastic displacements from these two analyses are nearly identical. Hence, a single-mode analysis using the higher-mode correction factor is adequate for this building.

6.3.3 Rigorous Nonlinear Analysis of an Auxiliary Building. A rigorous nonlinear analysis of the hypothetical auxiliary building shown in Figure 6.15 was conducted to verify the results of the RET analyses. A mathematical model of the building was developed. It included the walls located on lines 1, 2, A, B, C, and D of Figure 6.15. Each wall was modeled by an assembly of node points that were connected by beam-column elements. The beam-column elements surrounded reinforced concrete panel elements. The node configuration, panel numbers, and beam-column elements are shown in Figure 6.20.

528 153

Each node was assigned three degrees of freedom: horizontal translation in two directions and rotation about a vertical axis. The translational masses and rotational mass moment of inertia were assumed to be concentrated at the center of mass of each floor diaphragm. These data are summarized in Table 6.27. The floor diaphragms were assumed to be infinitely rigid, and the translational masses and rotational inertias were assigned to the various nodes on the basis of that assumption.

The panel elements are the major lateral-load-resisting members of this building. A shear modulus of 1,612 ksi was assumed, and the elastic stiffness of the panel was calculated using this value. The yield stress of each panel is given in Table 6.28. These values were obtained by multiplying the story shears from Table 6.21 by the minimum ratio for each story from Table 6.22. The product was divided by the area of the wall. For example, 0.150 ksi is given in Table 6.28 as the shear capacity of panel 2 of wall B. Checking Figure 6.20 reveals that this panel is in level 2. Table 6.22 shows that the minimum ratio for wall B at level 2 is 19.91; this value is associated with moment failure. Table 6.21 gives the shear in wall B at level 2 as 49.94 kip. Figure 6.16 indicates that the area of wall B is 24 x (300 - 24) = 6,624 in^2. These data are assembled to calculate the yield stress as follows:

$$\tau_y = 49.94 \times 19.91/6,624 = 0.150 \text{ ksi}$$

Elasto-plastic nonlinear characteristics were assumed for all walls; hence no stresses in excess of the values shown in Table 6.28 were allowed.

The panels were assumed to carry only horizontal shear forces, i.e., axial loads and bending were not allowed in the walls. The effective axial and bending stiffnesses of the panels were modeled by assuming fictitious properties for the beams and columns that surround the panels. The columns were assumed to have no shear stiffness; hence, all of the horizontal shear was applied to the panels. The various types of beam-column properties used in the model are listed in Table 6.29. Table 6.30 shows the types of

528 154

beam-column properties assigned to various elements of the model.

The rigorous nonlinear analysis computer program DRAIN-TABS[6.3] was used for analysis of this structure. A time history of ground acceleration having a maximum value of 0.5g was input at the base of the nonlinear model. The accelerogram used in this analysis was the same as that shown in Figure 6.14 except that the accelerations were scaled by a factor of 0.5. The analysis routine approximates the nonlinear response of the structure by a series of linear calculations. For each time step (ΔT = 0.01 sec), the stiffness of the structure is reevaluated. Elements that have exceeded their assigned capacity are assumed to be elasto-plastic whereas the unyielded members retain their original elastic stiffness. The response of the structure during a given time step is based on the stiffness of the structure at the beginning of that step. The stiffness is reevaluated at the end of each time step.

Qualitatively, the results of the rigorous nonlinear analysis are very similar to the results of the simplified nonlinear analysis. Both the RET and the rigorous analyses predict overstressing in the walls that are oriented in the y direction in level 1. The rigorous nonlinear analysis provides more details on this point; it indicates overstressing in walls A and B in level 1.

Total displacements resulting from the rigorous analyses are listed in Table 6.31. Also given in the table are the displacements resulting from a rigorous elastic analysis, a multimode RET analysis, and a single-mode RET analysis. The displacements obtained by the two RET analyses compare favorably with the rigorous analysis. The elastic analysis resulted in lower displacement values. These results suggest that the RET analysis can be used with confidence for this type of building.

6.3.4 Rigorous and Simplified Analyses of an Auxiliary Building for 1.0g. In addition to the analyses reported in the previous sections, the auxiliary building was analyzed using an input motion with a peak ground acceleration of 1.0g. This input was twice that used in the previous analyses. The following paragraphs present a summary of the analyses for 1.0g.

528 155

The simplified analyses using the RET indicated no yielding in the x direction for 1.0g. The RET analysis predicted a ductility factor of 5 at the first story and 2 at the second story. Overstressing in level 3 was not predicted. Comparing these predicted ductility factors with the criteria for shear wall buildings (Chapter 5) indicates that the building is either marginal or unacceptable, depending upon the applicable performance criterion. Engineering judgment suggests that the building be considered unacceptable unless a rigorous analysis indicates otherwise.

A rigorous analysis of the structure was conducted using a ground motion accelerogram with a peak value of 1.0g. The results of this analysis were quite different from the RET analysis. The rigorous analysis predicts widespread overstressing in both directions of the building. All the y-direction walls in the first level are overstressed quite early in the record. This greatly increases both the torsional response and the forces applied to the walls in the x direction. Later in the analysis, the x-direction walls in level 1 are overstressed; this leads to extremely large deflections. The analysis indicates structural instability; hence, the numerical values of displacements and ductility factors may be greatly in error. Small changes in the model or in the input time history would probably result in substantial changes in the results. Regardless of the numerical values, the results of the rigorous analysis indicate that the building is unacceptable and possibly hazardous for a 1.0g earthquake.

The reason for the large numerical discrepancy between the rigorous and the RET analysis results is that the RET has no provision for redistributing forces based on the yielding or failure of structural members. This was noted also in the analysis of the turbine building; therefore, it is not realistic to expect close numerical correspondence between the rigorous and simplified analyses for high values of the ductility factor. For low ductility factors (i.e., those considered acceptable in Chapter 5), force redistribution is not significant; hence, closer agreement between the rigorous and RET analyses may be expected.

528 156

Importantly, the qualitative conclusion from the analysis of the hypothetical auxiliary building for 1.0g is the same for the rigorous and RET analyses:

that the building is unacceptable. Compared with the significance of this observation, the numerical value of the computed ductility is unimportant.

6.4 Analysis of a Containment Building

An elevation view of a hypothetical containment building is shown in Figure 6.2. This reinforced concrete structure consists of a 3.5-ft-thick cylindrical shell topped by a 2.5-ft-thick hemispherical dome roof. The inside radius of the cylinder and of the dome is 70 ft; the spring line of the dome is 231 ft above the base.

The benchmark analyses of this structure consisted of an elastic analysis and a simplified nonlinear analysis using the RET. No rigorous nonlinear analysis was conducted because appropriate dynamic analysis techniques are not currently available for shell structures.

6.4.1 Elastic Analysis and Capacity Calculations. The main purpose of this analysis is to predict the elastic response of the structure. A comparison of the elastic response with the results of simplified nonlinear analyses is presented in a following section. Elastic analyses are also performed as a prerequisite of the simplified nonlinear analyses. The information extracted from the elastic analysis includes: modal frequencies, mode shapes, participation factors, modal weight ratios, internodal stiffnesses, shears, and displacements that cause the initiation of inelastic action in each element. Note that the elastic analyses that are performed as a prerequisite of the simplified nonlinear analyses are independent of the type of dynamic disturbance and level of force that cause nonlinear response.

The mathematical model used for the elastic analysis of this structure is illustrated in Figure 6.22. Nodal masses and member properties are listed in Table 6.32. Each node was assigned two degrees of freedom: x translation and z rotation.

The data in Figure 6.22 and Table 6.32 were assembled for use by the computer program SAPIV[6.4] in the elastic analysis. Numberous other structural analysis computer programs could have been used to obtain the same results.

528 157

Three analyses were conducted using the elastic model. The first consisted of an eigenvalue analysis to obtain the mode shapes and periods of vibration. The results are summarized in Tables 6.33 and 6.34. The latter table lists the nodal masses and the mode shape displacements for three modes of vibration. The calculations for the participation factors and the modal weight ratio are also illustrated. These calculations demonstrated that the fundamental mode contributes at least 76% of the total base shear.

The second analysis using the elastic model consisted of the calculation of the root-sum-square displacements of the various floors. These calculations are summarized in Table 6.35. Three modes are included in this analysis, and spectral accelerations were obtained from the 5%-damped curve of Figure 6.23. The RET analysis used the same response spectra.

The elastic model was also used to perform a static lateral load analysis. The purpose of this analysis was to determine the elastic stiffness between adjacent nodes and to calculate the shear and internodal displacements causing the initiation of inelastic action. Note that the end products of the lateral load analysis are independent of the magnitude of the lateral forces that are applied to the model. The lateral force applied to each node was proportional to the mass of that node times the first-mode displacement. This distribution of lateral forces results in a deflected shape that is proportional to the first mode shape. The results of this analysis are summarized in Table 6.36. They include total displacement, internodal displacement, shear, moment, and internodal stiffness. The last quantity is defined as shear divided by internodal displacement.

Member capacity data for this structure are summarized in Table 6.37. Also given in this table are the ratios of the shear and moment capacities to the corresponding values in Table 6.36. These ratios indicate the relative strength of various elements: weak elements and elements with high loads have low ratios.

528 158

The shear capacities were calculated according to the ACI code; the expressions for the ultimate shear strength of walls were used. This led to an ultimate shear strength which was greater than $10\sqrt{f'_c}$, the maximum value allowed by the ACI code. Hence, the maximum allowable shear strength was

taken as equal to $10\sqrt{f'_c}$, which is equal to 775 psi (111.6 ksf) in this case. The shear capacities shown in Table 6.37 are equal to the maximum allowable shear strength times the shear area (Table 6.32).

The moment capacities shown in Table 6.37 were computed by the provisions of the ACI code. It was assumed that the containment shell behaved as a cylindrical reinforced concrete beam; plane sections were assumed to remain plane. The moment capacity calculations assumed a distribution of axial strain that corresponds to yield strain at the extreme tension fiber. The location of the neutral axis was determined by equating the tensile and compressive forces corresponding to the assumed strain distribution. The effect of the weight of the structure was included. The moment capacity was calculated by summing the moments of the tensile and compressive forces about the neutral axis.

The ratios listed in Table 6.37 indicate that overstressing first occurs in element 9; the corresponding shears and displacements (see Table 6.38) are 27.05 times the values shown in Table 6.36. The shears and internodal displacements corresponding to the overstressing in each level are listed in Table 6.39. These values were obtained for each node by multiplying the shear ratio times the shear and internodal displacements from Table 6.36. The data listed in Table 6.39 are necessary for the simplified analysis of this structure using the RET.

6.4.2 Analysis of a Containment Building with the RET. The RET analysis of this containment building consisted of two parts. The first part was to perform iterative calculations to determine the effective period of vibration. The second part of the analysis was a complete RET evaluation, which resulted in a ductility calculation for each level. Both of these analyses used the 5%-damped spectral response curve shown in Figure 6.23. Elasto-plastic stiffness characteristics were assumed for all elements.

The iterative period calculations are summarized in Figure 6.24. In the first cycle, the demand, DV, and internodal ductility factor, μ, are based on the elastic periods of the lowest three modes. The periods for the next cycle are obtained by multiplying the elastic periods times the

528 159

square root of the ratio of the initial stiffness, K, to the effective stiffness, K'. The demand and ductility computations for cycle 2 are based on the adjusted period. The iteration shown in Figure 6.24 converges in two cycles.

Calculation of internodal ductility factors at each level is demonstrated in Figure 6.25. Note that ductility factors are not computed if DV_j/V_{yj} is less than or equal to 1.0. The ductilities computed in Figure 6.25 are quite low and are within the range considered to be acceptable for this type of structure.

The ductility factors listed in Figure 6.25 are the ratios of internodal displacement to internodal displacement at yield. The ductility factor may alternatively be defined as the ratio of total displacement to the total displacement when yield occurs anywhere in the structure. Total displacement is defined as the displacement of a point on the structure relative to the base. It is equal to the sum of the internodal displacements below the point in question. The internodal ductility factors listed in Figure 6.25 may be converted to total ductility factors; these calculations are summarized in Table 6.40.

Table 6.41 presents a comparison of displacements of this structure computed from an elastic and an RET analysis. The RET displacements are from 5% to 10% larger than the displacements derived from an elastic analysis. The difference between the two analyses is small, which suggests that the elastic analysis alone would be sufficient in this case. However, this conclusion depends on the relative intensity of the ground motion compared with the strength of the structure being considered. The discrepancy between an elastic and an RET analysis would increase if the intensity of the ground motion were increased or the strength of the structure were decreased.

528 160

REFERENCES

6.1 Wilson, E. L., and H. H. Dovey, *Static and Earthquake Analysis of Three-Dimensional Frame and Shearwall Buildings*, EERC 72-8, Earthquake Engineering Research Center, University of California, Berkeley, 1972.

6.2 Kanaan, A. E., and G. H. Powell, *DRAIN-2D, a General Purpose Computer Program for Dynamic Analysis of Inelastic Plane Structures*, EERC 73-6, Earthquake Engineering Research Center, University of California, Berkeley, 1973.

6.3 Israel, G. R., and G. H. Powell, *DRAIN-TABS, a Computer Program for Inelastic Earthquake Response of Three-Diminsional Buildings*, UCB/EERC-77/08, Earthquake Engineering Research Center, University of California, Berkeley, 1977.

6.4 Bathe, K. J., E. L. Wilson, and F. E. Peterson, *SAPIV, a Structural Analysis Program for Static and Dynamic Response of Linear Structures*, EERC 73-11, Earthquake Engineering Research Center, University of California, Berkeley, 1973.

528 16.

TABLE 6.1

ELASTIC ANALYSIS OF A TURBINE BUILDING:

PERIODS OF VIBRATION

Mode	Period (sec)
1	0.226
2	0.115
3	0.044
4	0.039
5	0.025
6	0.017

162

TABLE 6.2

ELASTIC ANALYSIS OF A TURBINE BUILDING:

MASSES, MODE SHAPES, PARTICIPATION FACTORS, AND MODAL WEIGHT RATIOS

Level	Mass (kip-sec^2/in.)	Mode Shapes											
		ϕ_1	ϕ_2	ϕ_3	ϕ_4	ϕ_5	ϕ_6	$m\phi_1$	$m\phi_2$	$m\phi_3$	$m\phi_4$	$m\phi_5$	$m\phi_6$
6	0.12	2.07	1.26	0.54	1.54	0.02	0.32	0.25	0.15	0.06	0.18	.002	0.04
5	0.10	1.63	0.69	-0.48	-2.36	-0.10	-1.11	0.16	0.07	-0.05	-0.24	-0.01	-0.11
4	0.03	0.91	-0.22	-0.84	-1.91	0.21	5.63	0.03	-0.01	-0.03	-0.06	0.01	0.17
3	1.14	0.40	-0.69	-0.41	0.19	0.18	-0.09	0.46	-0.79	-0.47	0.22	0.21	-0.10
2	1.07	0.18	-0.41	0.52	-0.09	-0.67	0.03	0.19	-0.44	0.56	-0.10	-0.72	0.03
1	1.52	.06	-0.17	0.54	-0.14	0.56	-0.01	0.09	-0.26	0.82	-0.21	0.85	-0.02
	Σm = 3.98							Γ_1 =	Γ_2 =	Γ_3 =	Γ_4 =	Γ_5 =	Γ_6 =
								1.18	-1.28	0.89	-0.21	0.34	0.02

Modal Weight Ratio Calculation

$$\frac{C_b}{S_a} = \frac{(\Gamma_i)^2}{\Sigma m}$$

Mode 1

$$\frac{C_b}{S_a} = (1.18)^2/3.98 = 0.35$$

Mode 2

$$\frac{C_b}{S_a} = (-1.28)^2/3.98 = 0.41$$

Mode 3

$$\frac{C_b}{S_a} = (0.89)^2/3.98 = 0.20$$

Mode 4

$$\frac{C_b}{S_a} = (-0.21)^2/3.98 = 0.01$$

Mode 5

$$\frac{C_b}{S_a} = (0.34)^2/3.98 = 0.03$$

Mode 6

$$\frac{C_b}{S_a} = (0.02)^2/3.98 = .0001$$

528 163

TABLE 6.3

ELASTIC ANALYSIS OF A TURBINE BUILDING:

DISPLACEMENT FOR NRC SPECTRUM ANALYSIS

Level	Mode 1* Δ_1 (in.)	Mode 2** Δ_2 (in.)	Mode 3† Δ_3 (in.)	RSS†† Δ (in.)
6	3.60	-0.62	0.01	3.65
5	2.84	-0.34	-0.01	2.86
4	1.58	0.11	-0.02	1.58
3	0.70	0.34	-0.01	0.78
2	0.31	0.20	0.01	0.37
1	0.10	0.08	0.01	0.13

*Mode 1

T = 0.23 sec; S_a = 2.85g; Γ = 1.18; $\Delta_j = \Gamma\phi_j S_a \left(\frac{T}{2\pi}\right)^2 = 1.74\phi_j$

**Mode 2

T = 0.12 sec; S_a = 2.74g; Γ = -1.28; $\Delta_j = \Gamma\phi_j S_a \left(\frac{T}{2\pi}\right)^2 = -0.49\phi_j$

†Mode 3

T = 0.044 sec; S_a = 1.38g; Γ = 0.89; $\Delta_j = \Gamma\phi_j S_a \left(\frac{T}{2\pi}\right)^2 = 0.023\phi_j$

††$RSS\Delta = (\Delta_1^2 + \Delta_2^2 + \Delta_3^2)^{1/2}$

528 164

TABLE 6.4

ELASTIC ANALYSIS OF A TURBINE BUILDING:

STATIC FORCES, SHEARS, AND DISPLACEMENTS

Level	Force (kip)	Shear (kip)	Total Displacement (in.)	Interstory Displacement (in.)	Interstory Stiffness (kip/in.)
6	2.5	2.5	.02768	.00587	425.9
5	1.6	4.1	.02181	.00967	424.0
4	0.3	4.4	.01214	.00684	643.3
3	4.6	9.0	.00530	.00293	3,071.7
2	1.9	10.9	.00237	.00152	7,171.1
1	0.9	11.8	.00085	.00085	13,882.4

528 165

TABLE 6.5

ELASTIC ANALYSIS OF A TURBINE BUILDING:

MEMBER FORCES AND MOMENTS*

Level	Element	Moment (kip-in.)	Shear (kip)	Axial Load (kip)
	Diagonal	--	--	3.09
6	Beam	2.97	--	--
	Column	24.94	0.14	1.39
	Diagonal	--	--	4.40
5	Beam	3.44	--	--
	Column	43.23	0.29	4.06
	Diagonal	--	--	3.04
4	Beam	69.30	--	--
	Column	190.85	0.95	6.22
	Wall	2,717.18	8.50	--
3	Column	40.85	0.25	5.76
	Wall	3,523.98	9.97	--
2	Column	56.78	0.47	9.20
	Wall	6,201.10	11.38	--
1	Column	39.07	0.21	9.34

*Corresponding to shears and displacements shown in Table 6.4.

528 166

TABLE 6.6

ELASTIC ANALYSIS OF A TURBINE BUILDING:

MEMBER CAPACITIES AND RATIOS

Level	Element	Moment		Shear		Axial Load	
		Capacity (kip-in.)	Ratio*	Capacity (kip)	Ratio*	Capacity (kip)	Ratio*
6	Diagonal	--	--	--	--	464	150.2
	Beam	1,656	557.60	--	--	--	--
	Column	47,238	1,894.10	--	--	--	--
5	Diagonal	--	--	--	--	464	105.5
	Beam	1,656	481.40	--	--	--	--
	Column	47,238	1,092.70	--	--	--	--
4	Diagonal	--	--	--	--	464	152.6
	Beam	12,816	184.90	--	--	--	--
	Column	47,238	247.50	--	--	--	--
3	Wall	224,000	82.44	1,936	227.8	--	--
	Column	47,238	1,155.40	--	--	-	--
2	Wall	275,500	78.18	2,038	204.4	--	--
	Column	47,238	831.90	--	--	--	--
1	Wall	478,890	77.23	3,687	324.0	--	--
	Column	47,238	1,209.10	--	--	--	--

*Ratio of member capacities given in this table to the corresponding forces and moments of Table 6.5.

528 167

TABLE 6.7

ELASTIC ANALYSIS OF A TURBINE BUILDING:
SHEARS AND DISPLACEMENTS CORRESPONDING
TO OVERSTRESSING OF THE WALLS AT LEVELS 1 AND 2

Level	Shear (kip)	Total Displacement (in.)
6	193	2.13
5	317	1.68
4	540	0.93
3	695	0.41
2	842	0.18
1	911	0.07

528 168

TABLE 6.8

ELASTIC ANALYSIS OF A TURBINE BUILDING:
STORY SHEARS AND INTERSTORY DISPLACEMENTS
CORRESPONDING TO OVERSTRESSING IN EACH STORY

Level	Shear Capacity (kip)	Interstory Displacements (in.)
6	376	0.88
5	433	1.02
4	672	1.05
3	742	0.24
2	852	0.12
1	911	0.07

TABLE 6.9

RET ANALYSIS OF A TURBINE BUILDING:

CALCULATION OF TOTAL DUCTILITY FACTOR FROM

INTERSTORY DUCTILITY FACTOR

Story	Interstory* Ductility Factor	Yield** Interstory Displacement (in.)	Inelastic Interstory Displacement (in.)	Inelastic Total Displacement (in.)	Yield† Total Displacement (in.)	Total Ductility Factor
6	1.00	0.88	0.88	4.68	2.13	2.2
5	1.50	1.02	1.53	3.80	1.68	2.3
4	0.95††	1.05	1.00	2.27	C.93	2.4
3	2.40	0.24	0.58	1.27	0.41	3.1
2	3.30	0.12	0.40	0.69	0.18	3.8
1	4.10	0.07	0.29	0.29	0.07	4.1

*From Figure 6.12

**From Table 6.8

†From Table 6.7

††Use DV_j/V_j for $\mu < 1.0$

528 170

TABLE 6.10

RLT ANALYSIS OF A TURBINE BUILDING:

SUMMARY OF AN ANALYSIS CONSIDERING

ONLY THE FIRST MODE

Story	Interstory Ductility Factor	Inelastic Total Displacement (in.)	Total Ductility Factor
6	0.88†	3.77	1.8
5	1.28	3.00	1.8
4	0.87†	1.69	1.8
3	1.79	0.78	1.9
2	1.93	0.35	1.9
1	1.74	0.12	1.7

†DV_j/V_{y_j} is given when $\mu < 1$.

528 171

TABLE 6.11

RIGOROUS NONLINEAR ANALYSIS OF A TURBINE BUILDING:

NODE GEOMETRY AND MASSES

Node	Node Geometry		Node Masses	
	x Coordinate (in.)	y Coordinate (in.)	x Mass (kip-sec^2/in.)	y Mass (kip-sec^2/in.)
1	0	0	0	0
2	327.250	0	0	0
.3	0	228.0	1.530	0.510
4	163.625	228.0	0	0.510
5	327.250	228.0	0	0.510
6	0	408.0	1.050	0.350
7	163.625	408.0	0	0.350
8	327.250	408.0	0	0.350
9	0	660.0	1.140	0.380
10	163.625	660.0	0	0.380
11	327.250	660.0	0	0.380
12	0	888.0	0.027	0.009
13	163.625	888.0	0	0.009
14	327.250	888.0	0	0.009
15	0	1,134.0	0.099	0.033
16	163.625	1,134.0	0	0.033
17	327.250	1,134.0	0	0.033
18	0	1,296.0	0.117	0.039
19	163.625	1,296.0	0	0.039
20	327.250	1,296.0	0	0.039

528 172

TABLE 6.12

RIGOROUS NONLINEAR ANALYSIS OF A TURBINE BUILDING:

BRACE ELEMENT PROPERTIES

Element Number	Young's Modulus (ksi)	Hardening Ratio	Area ($in.^2$)	Tensile Yield Stress (ksi)	Compression Yield Stress (ksi)
1	29×10^3	0	12.9	36	-3
2	29×10^3	0	12.9	36	-3
3	29×10^3	0	12.9	36	-3
4	29×10^3	0	12.9	36	-3
5	29×10^3	0	12.9	36	-3
6	29×10^3	0	12.9	36	-3

528 173

TABLE 6.13

RIGOROUS NONLINEAR ANALYSIS OF A TURBINE BUILDING:

REINFORCED CONCRETE PANEL ELEMENT PROPERTIES

Element Number	Shear Modulus	Hardening Ratio	Panel Thickness (in.)	Yield Stress (ksi)
1	1,534	0	12	0.178
2	1,534	0	12	0.198
3	1,534	0	22	0.122

528 174

TABLE 6.14

RIGOROUS NONLINEAR ANALYSIS OF A TURBINE BUILDING:

BEAM-COLUMN ELEMENTS

Element Number	Young's Modulus (ksi)	Hardening Ratio	Area ($in.^2$)	Moment of Inertia ($in.^4$)	Positive M_y (kip-in.)	Negative M_y (kip-in.)	Positive P_y (kip)	Negative P_y (kip)
1	29×10^3	0	99.0	26,244	47,232	-47,232	3,564	-2,722
2	29×10^3	0	99.0	26,244	47,232	-47,232	3,564	-2,722
3	29×10^3	0	99.0	26,244	47,232	-47,232	3,564	-2,722
4	29×10^3	0	99.0	26,244	47,232	-47,232	3,564	-2,722
5	29×10^3	0	99.0	26,244	47,232	-47,232	3,564	-2,722
6	29×10^3	0	99.0	26,244	47,232	-47,232	3,564	-2,722
7	29×10^3	0	99.0	26,244	47,232	-47,232	3,564	-2,722
8	29×10^3	0	99.0	26,244	47,232	-47,232	3,564	-2,722
9	29×10^3	0	99.0	26,244	47,232	-47,232	3,564	-2,722
10	29×10^3	0	99.0	26,244	47,232	-47,232	3,564	-2,722
11	29×10^3	0	99.0	26,244	47,232	-47,232	3,564	-2,722
12	29×10^3	0	99.0	26,244	47,232	-47,232	3,564	-2,722
13	29×10^3	0	10.6	281	1,656	-1,656	--	--
14	29×10^3	0	10.6	281	1,656	-1,656	--	--
15	29×10^3	0	10.6	281	1,656	-1,656	--	--
16	29×10^3	0	10.6	281	1,656	-1,656	--	--
17	29×10^3	0	34.8	5,900	12,816	-12,816	--	--
18	29×10^3	0	34.8	5,900	12,816	-12,816	--	--
19	29×10^3	0	1×10^8	1×10^8	1×10^8	-1×10^8	--	--
20	29×10^3	0	1×10^8	1×10^8	1×10^8	-1×10^8	--	--
21	29×10^3	0	1×10^8	1×10^8	1×10^8	-1×10^8	--	--
22	29×10^3	0	1×10^8	1×10^8	1×10^8	-1×10^8	--	--
23	29×10^3	0	1×10^8	1×10^8	1×10^8	-1×10^8	--	--
24	29×10^3	0	1×10^8	1×10^8	1×10^8	-1×10^8	--	--

528 175

TABLE 6.15

SUMMARY OF ANALYSES OF A TURBINE BUILDING*

Level	Displacement			
	Rigorous Elastic Analysis (in.)	Multimode RET Analysis (in.)	Single-Mode RET Analysis (in.)	Rigorous Nonlinear Analysis (in.)
6	3.65	4.68	3.77	4.17
5	2.86	3.80	3.00	3.47
4	1.58	2.27	1.69	2.43
3	0.78	1.27	0.78	1.72
2	0.37	0.69	0.35	1.08
1	0.13	0.29	0.12	0.70

*All analyses based on 1.0g input ground motion.

528 176

TABLE 6.16

ELASTIC ANALYSIS OF AN AUXILIARY BUILDING:

PERIODS OF VIBRATION

Mode	Period (sec)
1	0.086
2	0.056
3	0.044

528 177

TABLE 6.17

ELASTIC ANALYSIS OF AN AUXILIARY BUILDING:

MODE SHAPES

Level	Direction	Mode 1	Mode 2	Mode 3
3	x	0.000000	0.000000	0.480054
2	x	0.000000	0.000000	0.350775
1	x	0.000000	0.000000	0.194621
3	y	0.581407	-0.264140	0.000000
2	y	0.329946	0.192597	0.000000
1	y	0.138050	0.100779	0.000000
3	Rotational	0.000304	-0.001279	0.000000
2	Rotational	0.000245	-0.001000	0.000000
1	Rotational	0.000099	-0.000456	0.000000

528 178

TABLE 6.18

ELASTIC ANALYSIS OF AN AUXILIARY BUILDING:

PARTICIPATION FACTORS AND C_b/Sa

Mode	Participation Factor, Γ	Modal Weight Ratio, C_b/Sa
1	2.84	0.74
2	1.07	0.10
3	3.13	0.89

528 179

TABLE 6.19

ELASTIC ANALYSIS OF AN AUXILIARY BUILDING:

DISPLACEMENTS FOR NRC SPECTRUM ANALYSIS

Level	Mode 1* Deflection (in.)	Mode 2** Deflection (in.)	RSS Deflection in y Direction (in.)	Deflection† in x Direction (in.)
3	0.120	0.006	0.120	0.017
2	0.068	-0.005	0.068	0.012
1	0.028	-0.002	0.028	0.007

*Mode 1

T = 0.086 sec; S_a = 1.0g; Γ = 2.84; $\Delta_j = \Gamma\phi_j S_a \left(\frac{T}{2\pi}\right)^2 = 0.206\phi_j$

**Mode 2

T = 0.056 sec; S_a = 0.72g; Γ = 1.07; $\Delta_j = \Gamma\phi_j S_a \left(\frac{T}{2\pi}\right)^2 = 0.024\phi_j$

†Deflection in x Direction = Mode 3 Deflection

T = 0.044 sec; S_a = 0.60g; Γ = 3.13; $\Delta_j = \Gamma\phi_j S_a \left(\frac{T}{2\pi}\right)^2 = 0.036\phi_j$

528 160

TABLE 6.20

ELASTIC ANALYSIS OF AN AUXILIARY BUILDING:

STATIC FORCES, SHEARS, AND DISPLACEMENTS

x Direction (Longitudinal)					
Level	Force (kip)	Shear (kip)	Total Displacement (in.)	Interstory Displacement (in.)	Interstory Stiffness (kip-in.)
3	55.61	55.61	0.00231	0.00063	88,270
2	148.59	204.20	0.00168	0.00074	275,946
1	108.77	312.97	0.00094	0.00094	332,947
y Direction (Transverse)					
Level	Force (kip)	Shear (kip)	Total Displacement (in.)	Interstory Displacement (in.)	Interstory Stiffness (kip-in.)
3	67.37	67.37	0.01028	0.00404	16,681
2	139.77	207.16	0.00624	0.00363	57,069
1	77.16	284.32	0.00261	0.00261	108,935

528 181

TABLE 6.21

ELASTIC ANALYSIS OF AN AUXILIARY BUILDING:

MEMBER FORCES AND MOMENTS

x Direction (Longitudinal)			
Wall	Level	Wall Shear (kip)	Wall Moment (kip-in.)
1 and 2	3	27.81	3,336.6
	2	102.10	21,715.9
	1	156.49	49,880.9
y Direction (Transverse)			
Wall	Level	Wall Shear (kip)	Wall Moment (kip-in.)
A	3	31.85	3,822.57
	2	63.33	15,222.53
	1	85.02	30,525.62
B	3	35.54	4,264.23
	2	49.94	13,253.10
	1	74.39	26,643.76
C	2	52.87	9,517.56
	1	67.59	21,683.42
D	2	41.01	7,382.39
	1	57.32	17,700.35

528 182

TABLE 6.22

ELASTIC ANALYSIS OF AN AUXILIARY BUILDING:

MEMBER CAPACITIES AND RATIOS*

x Direction (Longitudinal)					
Wall	Level	Shear Capacity (kip)	Shear* Ratio	Moment Capacity (kip-in.)	Moment* Ratio
1 and 2	3	2,696	96.94	445,237	133.44
	2	7,804	76.41	3,851,827	177.37
	1	7,901	50.49	4,162,258	83.44
y Direction (Transverse)					
Wall	Level	Shear Capacity (kip)	Shear* Ratio	Moment Capacity (kip-in.)	Moment* Ratio
A	3	1,940	60.91	231,593	60.59
	2	1,969	31.09	256,061	16.82
	1	1,996	23.48	279,411	9.15
B	3	1,940	54.59	231,593	54.31
	2	1,978	39.61	263,902	19.91
	1	2,016	27.10	297,155	11.15
C	2	1,956	37.00	245,019	25.74
	1	1,994	29.50	278,294	12.83
D	2	1,947	47.48	237,200	32.13
	1	1,974	30.44	260,551	14.72

*Ratio of capacities shown in this table to corresponding shears and moments of Table 6.21.

528 183

TABLE 6.23

ELASTIC ANALYSIS OF AN AUXILIARY BUILDING: SHEARS AND DISPLACEMENTS CORRESPONDING TO OVERSTRESSING THE WALLS AT LEVEL 1

x Direction (Longitudinal)		
Level	Shear (kip)	Total Displacement (in.)
3	2,008	0.117
2	10,310	0.085
1	15,802	0.047

y Direction (Transverse)		
Level	Shear (kip)	Total Displacement (in.)
3	617	0.094
2	1,896	0.057
1	2,602	0.024

528 184

TABLE 6.24

ELASTIC ANALYSIS OF AN AUXILIARY BUILDING:

STORY SHEAR CAPACITIES AND INTERSTORY DISPLACEMENTS

x Direction (Longitudinal)		
Level	Shear Capacity (kip)	Interstory Displacement (in.)
3	5,391	0.061
2	15,603	0.057
1	15,802	0.048

y Direction (Transverse)		
Level	Shear Capacity (kip)	Interstory Displacement (in.)
3	3,660	0.219
2	3,484	0.061
1	2,602	0.024

528 185

528 186

TABLE 6.25

RET ANALYSIS OF AN AUXILIARY BUILDING:

CALCULATION OF TOTAL DUCTILITY FACTOR FROM

INTERSTORY DUCTILITY FACTOR

y DIRECTION

Level	$\frac{DV}{V_y}$	Interstory Ductility Factor	Yield Interstory Displacement (in.)	Inelastic Interstory Displacement (in.)	Inelastic Total Displacement (in.)	Yield Total Displacement (in.)	Total Ductility Factor
3	0.23*	--	0.219	0.050	0.132	0.094	1.4
2	0.75*	--	0.061	0.046	0.082	0.057	1.4
1	--	1.5	0.024	0.036	0.036	0.024	1.5

*Use DV/V_y when $\mu < 1$.

TABLE 6.26

RET ANALYSIS OF AN AUXILIARY BUILDING:

SUMMARY OF AN ANALYSIS CONSIDERING

ONLY THE FIRST MODE IN THE y DIRECTION

Level	Interstory Ductility Factor	Inelastic Total Displacement (in.)	Total Ductility Factor
3	0.23*	0.135	1.4
2	0.75*	0.082	1.4
1	1.50	0.036	1.5

*DV/V_y is given where $\mu < 1$.

528 187

TABLE 6.27

RIGOROUS ANALYSIS OF AN AUXILIARY BUILDING:

MASSES AND ROTATIONAL INERTIAS

Level	x Mass (kip-sec^2/in.)	y Mass (kip-sec^2/in.)	Rotational Mass Moment of Inertia$_2$ (kip-in.-sec^2)
3	1.159	1.159	29,330
2	4.236	4.236	521,700
1	5.589	5.589	651,600

528 188

TABLE 6.28

RIGOROUS ANALYSIS OF AN AUXILIARY BUILDING:

PANEL ELEMENT YIELD STRESS

Panel Element Number	Yield Stress (ksi)				
	Walls 1 & 2	Wall A	Wall B	Wall C	Wall D
1	0.293	0.291	0.291	0.206	0.199
2	0.295	0.161	0.150	0.131	0.127
3	0.298	0.118	0.125	--	--
4	0.295	--	--	--	--
5	0.298	--	--	--	--
6	0.295	--	--	--	--
7	0.298	--	--	--	--

528 189

TABLE 6.29

RIGOROUS ANALYSIS OF AN AUXILIARY BUILDING:

BEAM-COLUMN PROPERTY TYPES

Property Type	Area ($in.^2$)	Moment of Inertia ($in.^4$)	Shear Area
1	1,748	1.0	0
2	1×10^{15}	1×10^{15}	1×10^{15}
3	4,153	1.0	0
4	934	1.0	0

528 130

TABLE 6.30

RIGOROUS ANALYSIS OF AN AUXILIARY BUILDING:

BEAM-COLUMN ELEMENT

Beam-Column Number	Property Type*		
	Walls 1 & 2	Walls A & B	Walls C & D
1	1	4	4
2	3	4	4
3	3	4	4
4	1	4	4
5	4	4	2
6	4	4	2
7	4	2	--
8	4	2	--
9	3	2	--
10	3	--	--
11	2	--	--
12	2	--	--
13	2	--	--
14	2	--	--
15	2	--	--
16	2	--	--
17	2	--	--

*See Table 6.29.

528 191

TABLE 6.31

SUMMARY OF ANALYSES OF AN AUXILIARY BUILDING

FOR 0.5g IN THE y DIRECTION

Level	Displacement			
	Rigorous Elastic Analysis (in.)	Multimode RET Analysis (in.)	Single-Mode RET Analysis (in.)	Rigorous Nonlinear Analysis (in.)
3	0.120	0.132	0.135	0.148
2	0.068	0.082	0.082	0.087
1	0.028	0.036	0.036	0.032

528 192

TABLE 6.32

ELASTIC ANALYSIS OF A CONTAINMENT BUILDING:

NODE AND ELEMENT PROPERTIES

Node	Mass (kip-sec^2/ft)	Element	Axial Area (ft^2)	Shear Area (ft^2)	Moment of Inertia (ft^4)
1	58.57	1	1,119.2	559.6	798.0
2	130.99	2	1,119.2	559.6	2,105.0
3	131.24	3	1,119.2	559.6	2,759.0
4	160.75	4	1,570.0	785.0	4,080.0
5	190.68	5	1,570.0	785.0	4,080.0
6	190.68	6	1,570.0	785.0	4,080.0
7	190.68	7	1,570.0	785.0	4,080.0
8	174.07	8	1,570.0	785.0	4,080.0
9	156.49	9	1,570.0	785.0	4,080.0

528 193

TABLE 6.33

ELASTIC ANALYSIS OF A CONTAINMENT BUILDING:

PERIODS OF VIBRATION

Mode	Period (sec)
1	0.196
2	0.067
3	0.037
4	0.026
5	0.021

528 194

TABLE 6.34

ELASTIC ANALYSIS OF A CONTAINMENT BUILDING:

MASSES, MODE SHAPES, PARTICIPATION FACTORS, AND MODAL WEIGHT RATIOS

Node	Mass (kip-sec^2/ft)	ϕ_1	ϕ_2	ϕ_3	$m\phi_1$	$m\phi_2$	$m\phi_3$
1	58.57	0.0470	0.0487	-0.0417	2.75	2.85	-2.44
2	130.99	0.0430	0.0355	-0.0230	5.63	4.65	-3.01
3	131.24	0.0381	0.0157	0.0095	5.00	2.06	1.25
4	160.75	0.0324	-0.0064	0.0337	5.21	-1.03	5.42
5	190.68	0.0267	-0.0226	0.0298	5.09	-4.31	5.68
6	190.68	0.0205	-0.0324	0.0029	3.91	-6.18	0.55
7	190.68	0.0143	-0.0335	-0.0268	2.73	-6.39	-5.11
8	174.07	0.0084	-0.0256	-0.0367	1.46	-4.46	-6.39
9	156.49	0.0039	-0.0140	-0.0244	0.61	-2.19	-3.82
	Σm = 1,384.15		Participation Factors:		Γ_1 = 32.39	Γ_2 = -15.00	Γ_3 = -7.87

Modal Weight Ratios

Mode 1

$$C_b/S_a = \frac{32.39^2}{1{,}384.15} = 0.76$$

Mode 2

$$C_b/S_a = \frac{-15.00^2}{1{,}384.15} = 0.16$$

Mode 3

$$C_b/S_a = \frac{-7.87^2}{1{,}384.15} = 0.04$$

Note: $\Sigma M\phi^2 = 1.0$ for each mode.

TABLE 6.35

ELASTIC ANALYSIS OF A CONTAINMENT BUILDING:

DISPLACEMENT FOR NRC SPECTRUM ANALYSIS

Node	Mode 1* Δ (in.)	Mode 2** Δ (in.)	Mode 3† Δ (in.)	RSS†† Δ (in.)
1	2.00	-0.07	-0.01	2.00
2	1.83	-0.05	- -	1.83
3	1.62	-0.02	- -	1.62
4	1.38	0.01	-0.01	1.38
5	1.14	0.03	- -	1.14
6	0.87	0.05	- -	0.87
7	0.61	0.05	- -	0.61
8	0.36	0.04	0.01	0.36
9	0.17	0.02	- -	0.17

*Mode 1

T = 0.196 sec; S_a = 3.50g; Γ_1 = 32.39: $\Delta_1 = \Gamma_1 \phi_1 S_a \left(\frac{T}{2\pi}\right)^2 = 42.63\phi_1$

**Mode 2

T = 0.067 sec; S_a = 2.25g; Γ_2 = -15.00; $\Delta_2 = \Gamma_2 \phi_2 S_a \left(\frac{T}{2\pi}\right)^2 = -1.48\phi_2$

†Mode 3

T = 0.037 sec; S_a = 1.4g; Γ_3 = -7.87; $\Delta_3 = \Gamma_3 \phi_3 S_a \left(\frac{T}{2\pi}\right)^2 = -0.15\phi_3$

††$\text{RRS}\Delta = (\Delta_1^2 + \Delta_2^2 + \Delta_3^2)^{\frac{1}{2}}$

961 528 196

TABLE 6.36

ELASTIC ANALYSIS OF A CONTAINMENT BUILDING:

NODAL DISPLACEMENTS, SHEARS, AND MOMENTS

Node	Total Displacement (ft)	Internodal Displacement (ft)	Shear (kip)	Moment (kip-ft)	Internodal Stiffness kip/ft x 10^5
1	0.00459	0.000390	275	6,647	7.1
2	0.00420	0.000480	838	26,901	17.5
3	0.00372	0.000566	1,338	59,241	23.6
4	0.00316	0.000560	1,859	106,180	33.2
5	0.00260	0.000590	2,368	165,970	40.1
6	0.00201	0.000610	2,759	235,640	45.2
7	0.00140	0.000584	3,032	312,200	51.9
8	0.000816	0.000437	3,178	378,140	72.7
9	0.000379	0.000379	3,239	445,350	85.5

TABLE 6.37

ELASTIC ANALYSIS OF A CONTAINMENT BUILDING:

ELEMENT CAPACITIES AND RATIOS*

Element	Shear Capacity (kip)	Shear Ratio*	Moment Capacity (kip-ft)	Moment Ratio*
1	62,451	227.09	5.08×10^6	764.25
2	62,451	74.52	8.23×10^6	305.94
3	62,451	46.67	1.13×10^7	190.75
4	87,606	47.13	1.15×10^7	108.31
5	87,606	37.00	1.16×10^7	69.89
6	87,606	31.75	1.18×10^7	50.08
7	87,606	28.89	1.19×19^7	38.12
8	87,606	27.57	1.21×10^7	32.00
9	87,606	27.05	1.22×10^7	27.39

*Ratio of shear and moment capacities to corresponding values from Table 6.36.

528 198

TABLE 6.38

ELASTIC ANALYSIS OF A CONTAINMENT BUILDING:
SHEARS AND DISPLACEMENTS CORRESPONDING
TO OVERSTRESSING OF ELEMENT 9

Node	Shear (kip)	Total Displacement (ft)
1	7,439	0.1242
2	22,668	0.1136
3	36,193	0.1006
4	50,286	0.0855
5	64,054	0.0703
6	74,631	0.0544
7	82,016	0.0379
8	85,965	0.0221
9	87,606	0.0103

528 199

TABLE 6.39

ELASTIC ANALYSIS OF A CONTAINMENT BUILDING:

SHEAR AND INTERNODAL DISPLACEMENT

FOR OVERSTRESSING AT EACH LEVEL

Node	Shear (kip)	Internodal Displacement (ft)
1	62,451	0.0886
2	62,451	0.0358
3	62,451	0.0264
4	87,606	0.0264
5	87,606	0.0218
6	87,606	0.0194
7	87,606	0.0169
8	87,606	0.0120
9	87,606	0.0103

528 200

TABLE 6.40

RET ANALYSIS OF A CONTAINMENT BUILDING:

COMPUTATION OF TOTAL DUCTILITY FACTOR

Node	Internodal Ductity Factor	Yield* Internodal Displacement (ft)	Inelastic Internodal Displacement (ft)	Inelastic Total Displacement (ft)	Yield** Total Displacement (ft)	Total Ductility Factor
1	0.18[+]	0.0886	0.016	0.179	0.121	1.4
2	0.53	0.0358	0.019	0.163	0.114	1.4
3	0.83	0.0264	0.022	0.144	0.101	1.4
4	0.81	0.0264	0.021	0.122	0.086	1.4
5	1.00	0.0218	0.022	0.101	0.070	1.4
6	1.20	0.0194	0.023	0.079	0.054	1.5
7	1.40	0.0169	0.024	0.056	0.038	1.6
8	1.40	0.0120	0.017	0.032	0.022	1.5
9	1.50	0.0103	0.015	0.015	0.010	1.5

*From Table 6.37

**From Table 6.38

[+]Use DV_j/V_{yj} when $\mu_j < 1$

523 201

TABLE 6.41

COMPARISON OF ELASTIC AND RET ANALYSIS

OF A CONTAINMENT BUILDING

Node	Displacement	
	Elastic Analysis (in.)	RET Analysis (in.)
1	2.00	2.15
2	1.83	1.96
3	1.62	1.73
4	1.38	1.46
5	1.14	1.21
6	0.87	0.95
7	0.61	0.70
8	0.36	0.38
9	0.17	0.18

528 202

TURBINE BUILDING - TYPICAL LATERAL FORCE RESISTING SYSTEM

FIGURE G.1

528 203

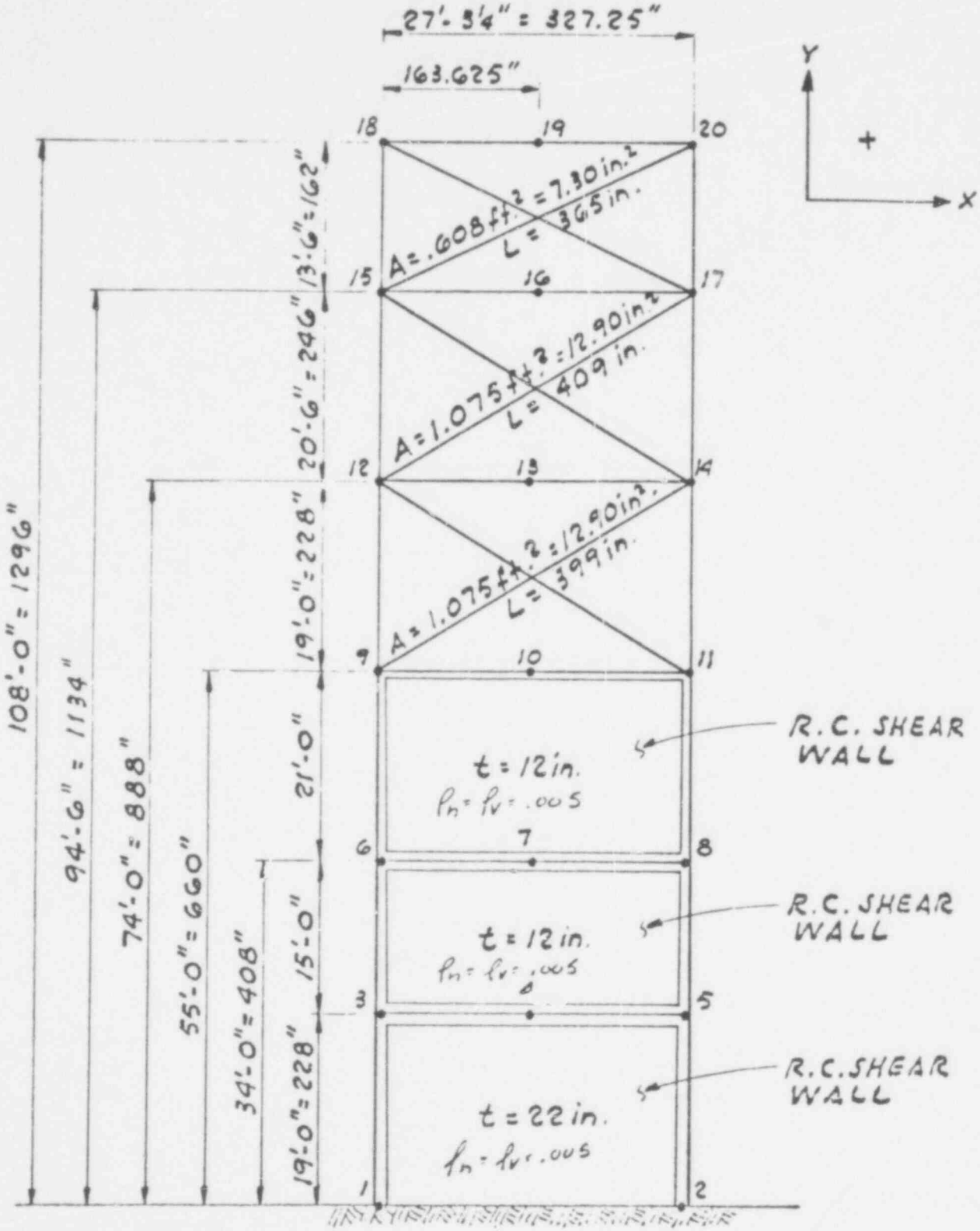

BENCHMARK PROBLEM FOR TURBINE BUILDING

NRC / NONLIN 528 204 FIGURE 6.2

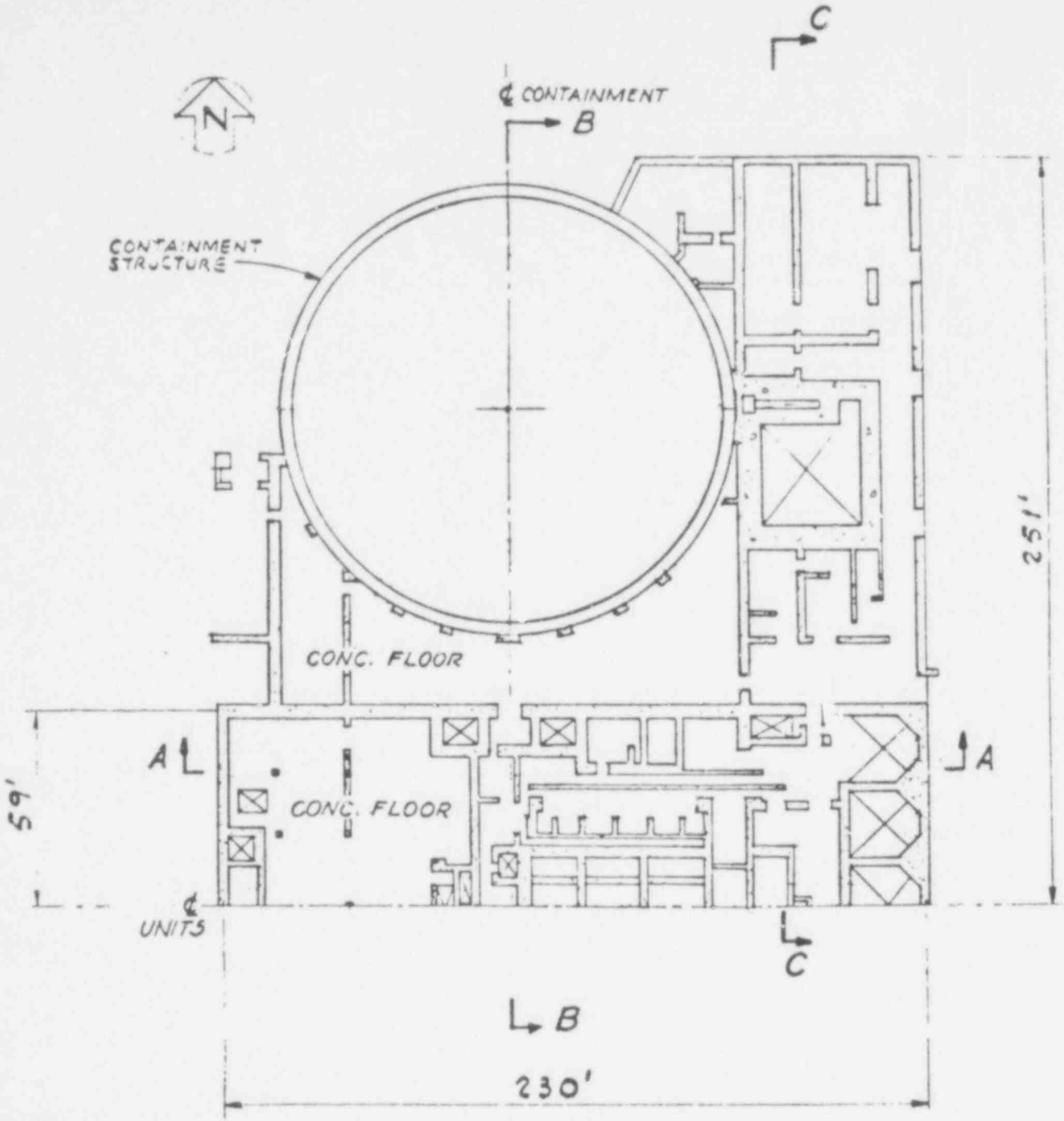

528 205

AUXILIARY BUILDING - TYPICAL PLAN

NRC / NONLIN

FIGURE 6.3

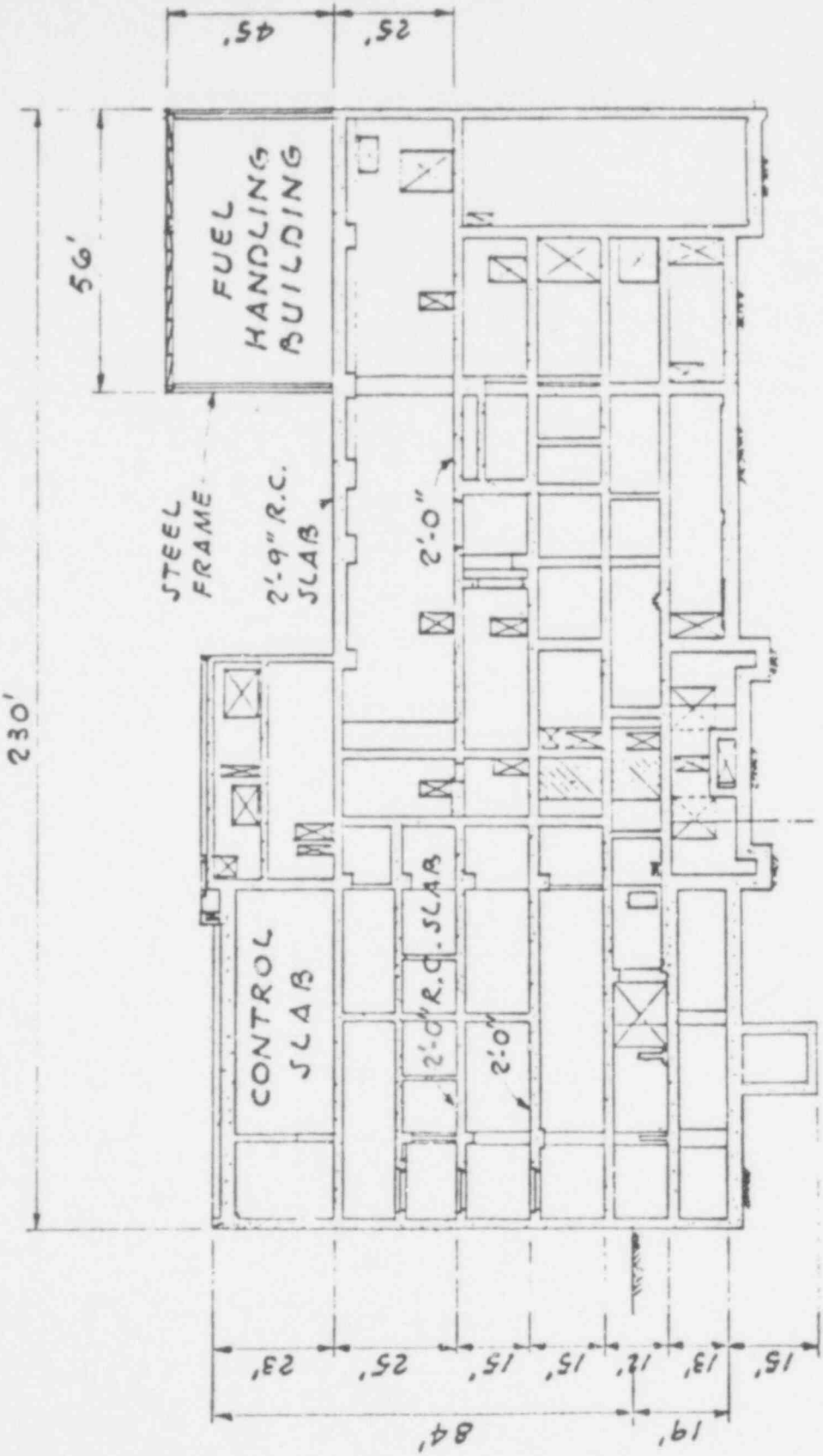

SECTION A-A

AUXILIARY BUILDING - TYPICAL SECTION

NRC / NONLIN

FIGURE 6.4

528 206

SECTION C-C

AUXILIARY BUILDING - TYPICAL SECTION

FIGURE 6.5

528 207

528 208

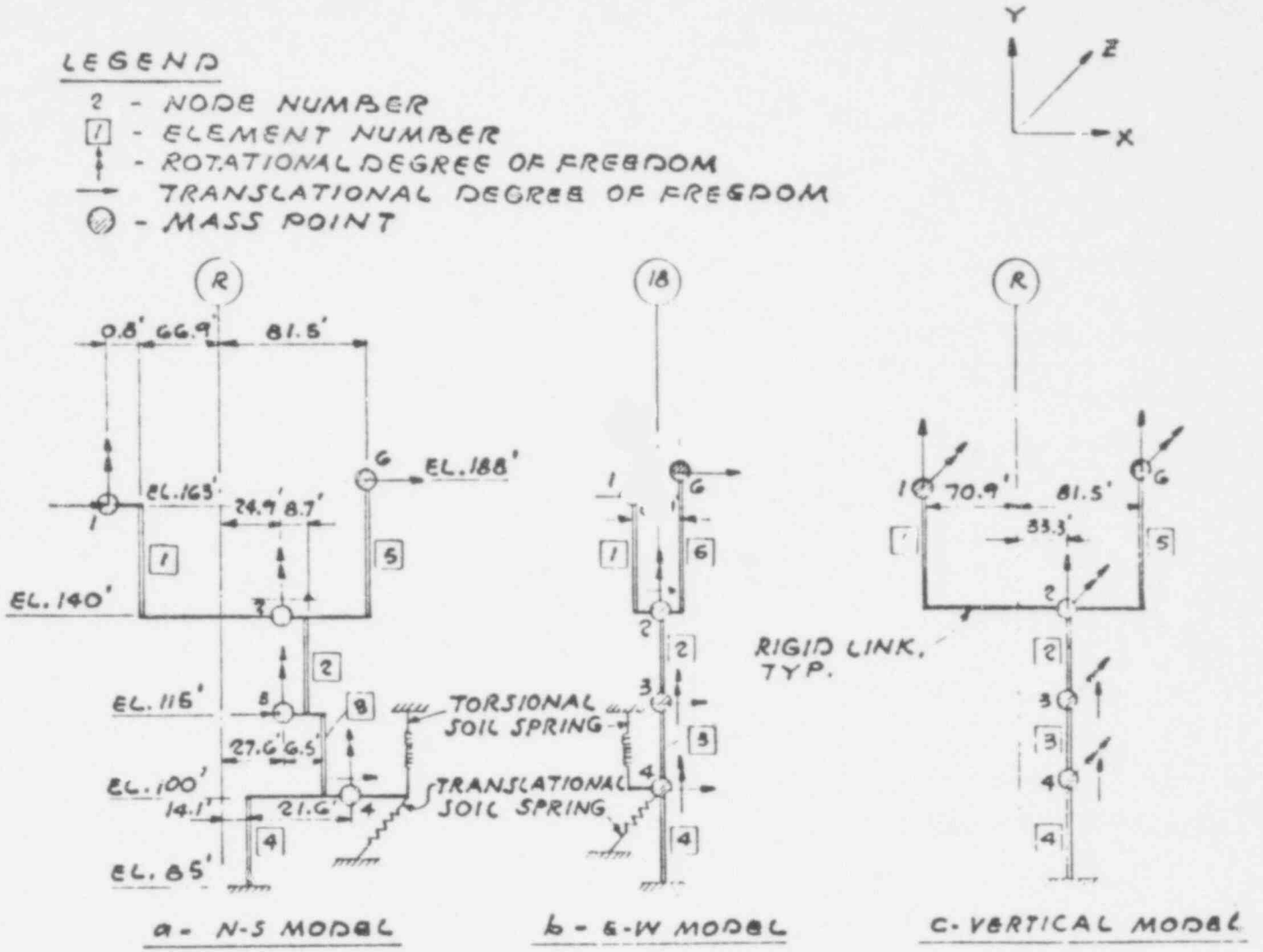

LUMPED-MASS MATHEMATICAL MODELS FOR HORIZONTAL TORSIONAL AND VERTICAL ANALYSIS OF THE AUXILIARY BUILDING

FIGURE 6.6

BENCHMARK PROBLEM FOR TYPICAL AUXILIARY BUILDING - TYPE I

FIGURE G.7

NRC / NONLIN

NRC / NONLIN

528 210

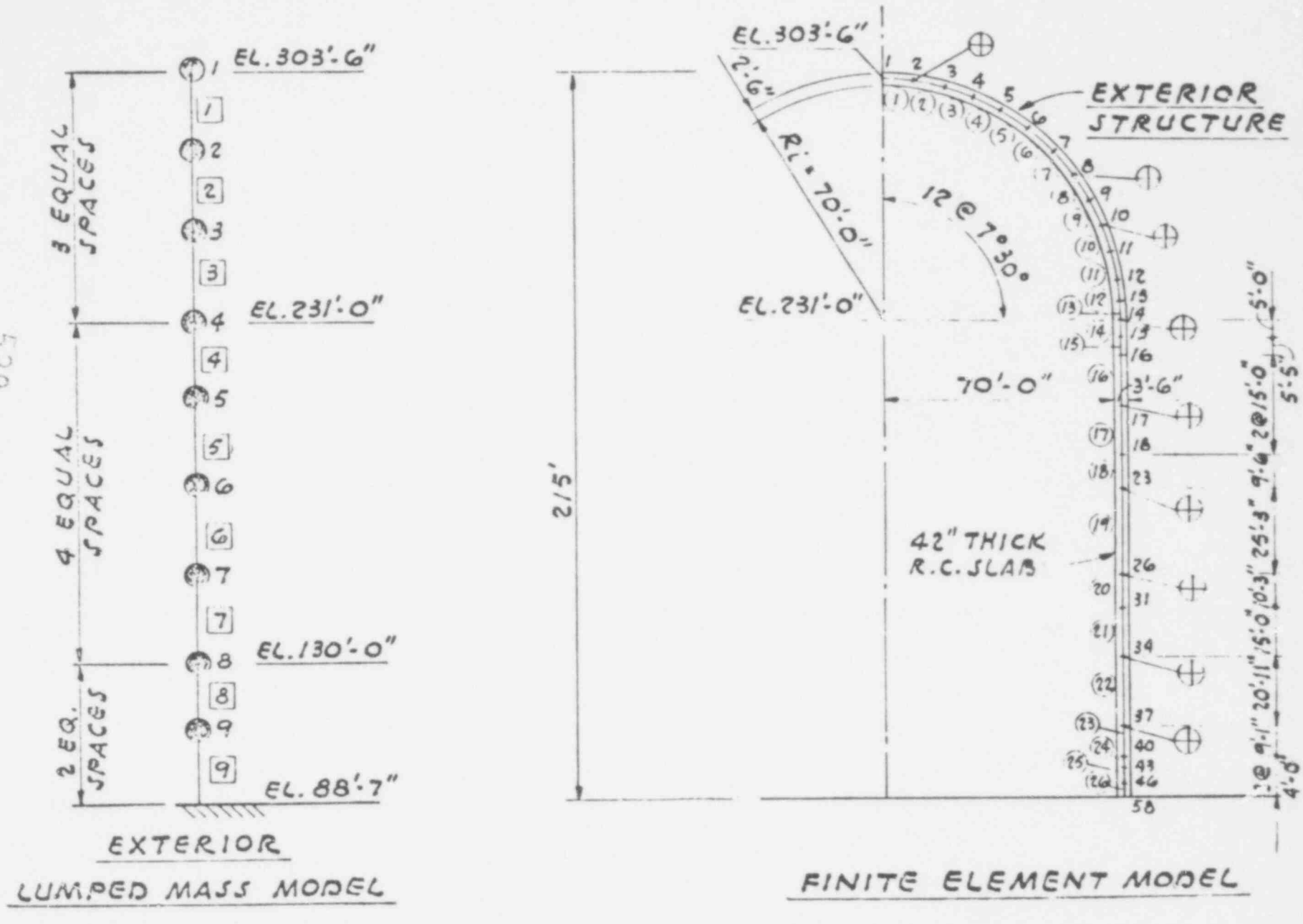

FIGURE 6.8

CONTAINMENT STRUCTURE - TYP. MODELS

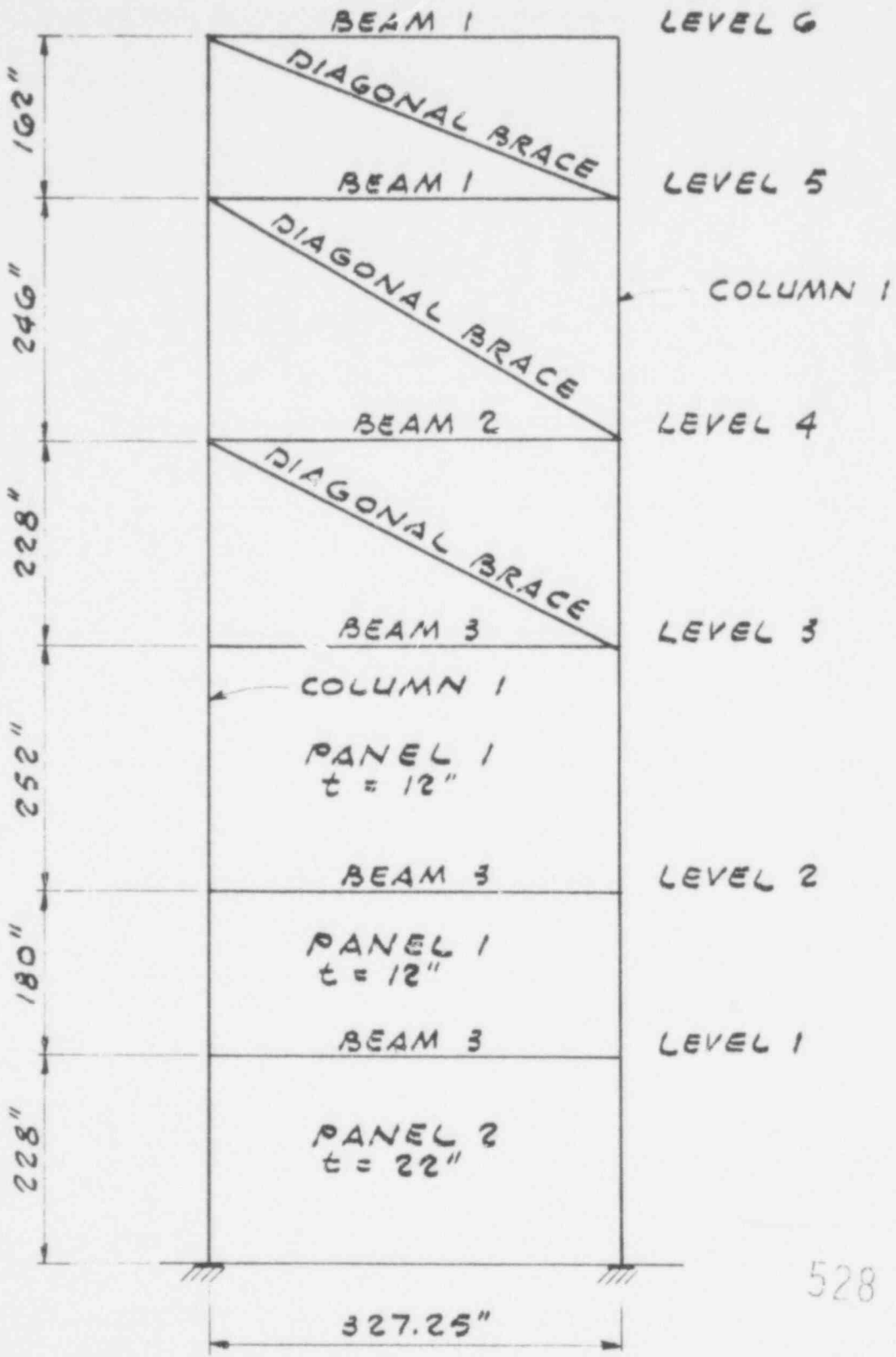

528 211

ELASTIC MODEL OF A TURBINE BUILDING

NRC/NONLIN FIGURE 6.9

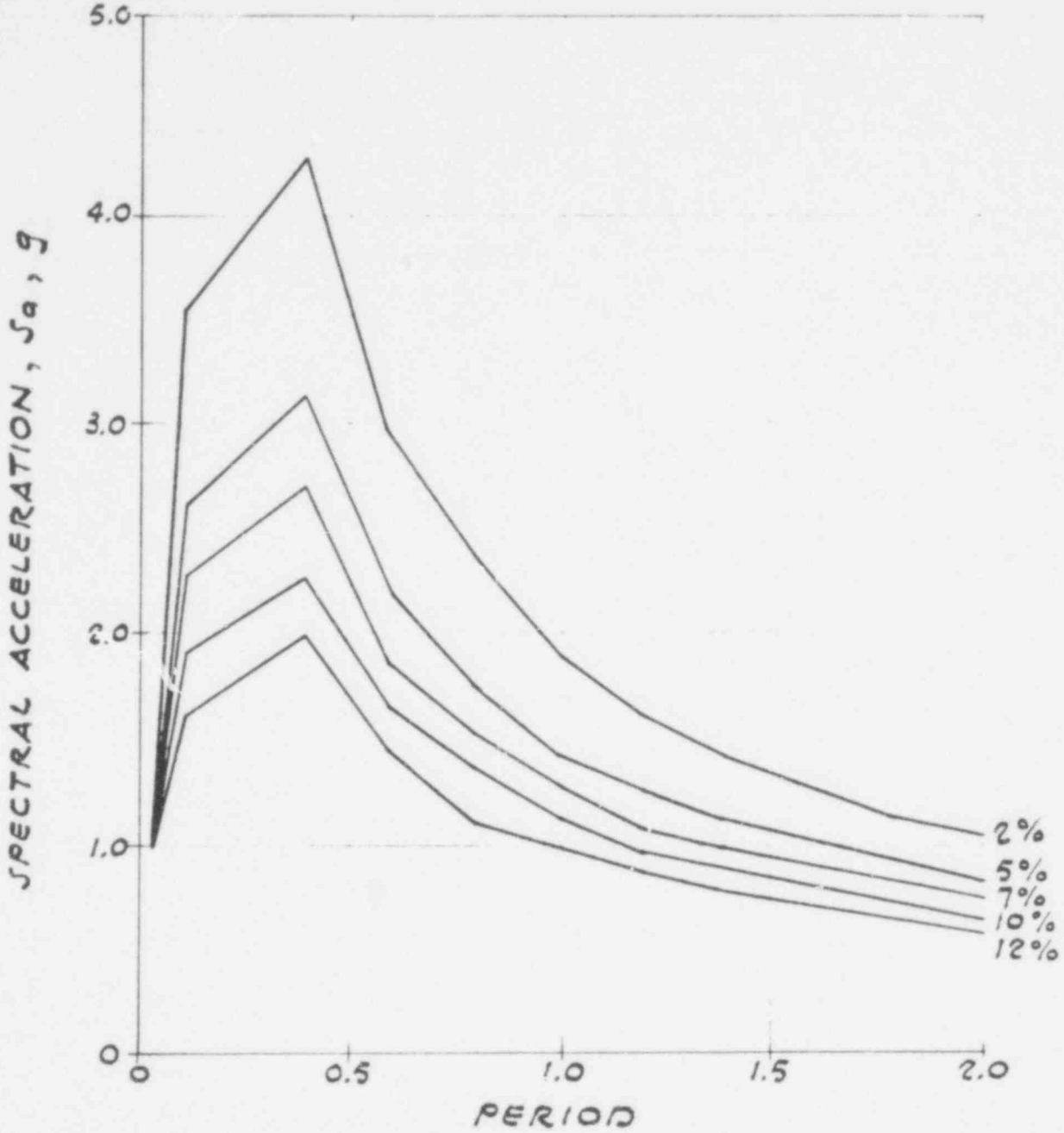

INPUT RESPONSE SPECTRA FOR THE BENCHMARK PROBLEM

NRC/NONLIN 528 212 FIGURE 6.10

	MODE 1	MODE 2	MODE 3	
CYCLE 1	$T_1 = 0.23$ SEC.	$T_2 = 0.12$ SEC.	$T_3 = 0.044$ SEC.	$W = 1537.87^K$
	$S_{a1} = 2.85g$	$S_{a2} = 2.64g$	$S_{a3} = 1.38g$	
	$\frac{C_b}{S_a} = 0.35$	$\frac{C_b}{S_a} = 0.41$	$\frac{C_b}{S_a} = 0.20$	
	$V_{B1} = 1537.87^K$	$V_{B2} = 1664.59^K$	$V_{B3} = 424.45^K$	

$DV = [1537.87^2 + 1664.59^2 + 424.45^2]^{1/2} = 2305.66^K$

$V_Y = 911^K$

$\mu = 0.5 \times \left(\frac{2305.66^2}{911^2}\right) + 0.5 = 3.70 \longrightarrow \underline{\mu = 4}$

$S_Y = .07"$ (TABLE 6.8) $S = 0.7 \times 3.70 = 0.26"$

$K' = 911/.26 = 3517.37$ $K = 13,882.4$ (TABLE 6.4)

$\sqrt{K/K'} = 1.99$

CYCLE 2	$T_1 = .23 \times 1.99 = 0.46$ SEC.	$T_2 = 0.12 \times 1.99 = 0.24$ SEC.	$T_3 = 0.044 \times 1.99 = .09$ SEC.	
	$S_{a1} = 2.80g$	$S_{a2} = 2.86g$	$S_{a3} = 2.27g$	
	$V_{b1} = 1507.11^K$	$V_{b2} = 1803.31$	$V_{b3} = 698.19$	
	$DV = 2451.69^K$	$V_Y = 911^K$		

$\mu = 4.12 \longrightarrow \underline{\mu = 4}$

SOLUTION CONVERGES TO

$T_1 = 0.46$ SEC.	$T_2 = 0.24$ SEC.	$T_3 = 0.09$ SEC.
$S_{a1} = 2.80g$	$S_{a2} = 2.86g$	$S_{a3} = 2.27g$

528 213

RET ANALYSIS OF A TURBINE BUILDING
ITERATION FOR EFFECTIVE PERIOD

NRC/NONLIN FIGURE 6.11

Building TURBINE BENCHMARK Direction NA

N = 6 Earthquake 1.0g

Story Shear Model III α = 1.0

Level, j	MODE 1 T = 0.46 SEC. S_a = 2.80g Γ = 1.18		MODE 2 T = 0.24 SEC. S_a = 2.86g Γ = -1.28		MODE 3 T = 0.09 SEC. S_a = 2.27g Γ = 0.89		DV_j (kip)	V_{y_j} (kip)	$\frac{DV_j}{V_{y_j}}$	μ_j
	F (kip)	DV_{j1} (kip)	F (kip)	DV_{j2} (kip)	F (kip)	DV_{j3} (kip)				
6	319.17	319.17	-212.18	-212.18	46.84	46.84	386.11	376	1.03	1.0
5	204.27	523.44	-99.02	-311.20	-39.03	7.81	609.01	433	1.41	1.5
4	38.30	561.74	14.15	-297.05	-23.42	-15.61	635.64	672	0.95	-
3	587.27	1149.01	1117.48	820.43	-366.90	-382.52	1462.75	742	1.97	2.4
2	242.57	1391.58	622.39	1442.82	437.16	54.65	2005.30	852	2.35	3.3
1	114.90	1506.48	367.78	1810.60	640.13	694.77	2455.70	911	2.70	4.1

RET ANALYSIS OF A TURBINE BUILDING

INTERSTORY DUCTILITY CALCULATION

FIGURE 6.12

NRC/NONLIN 528 214

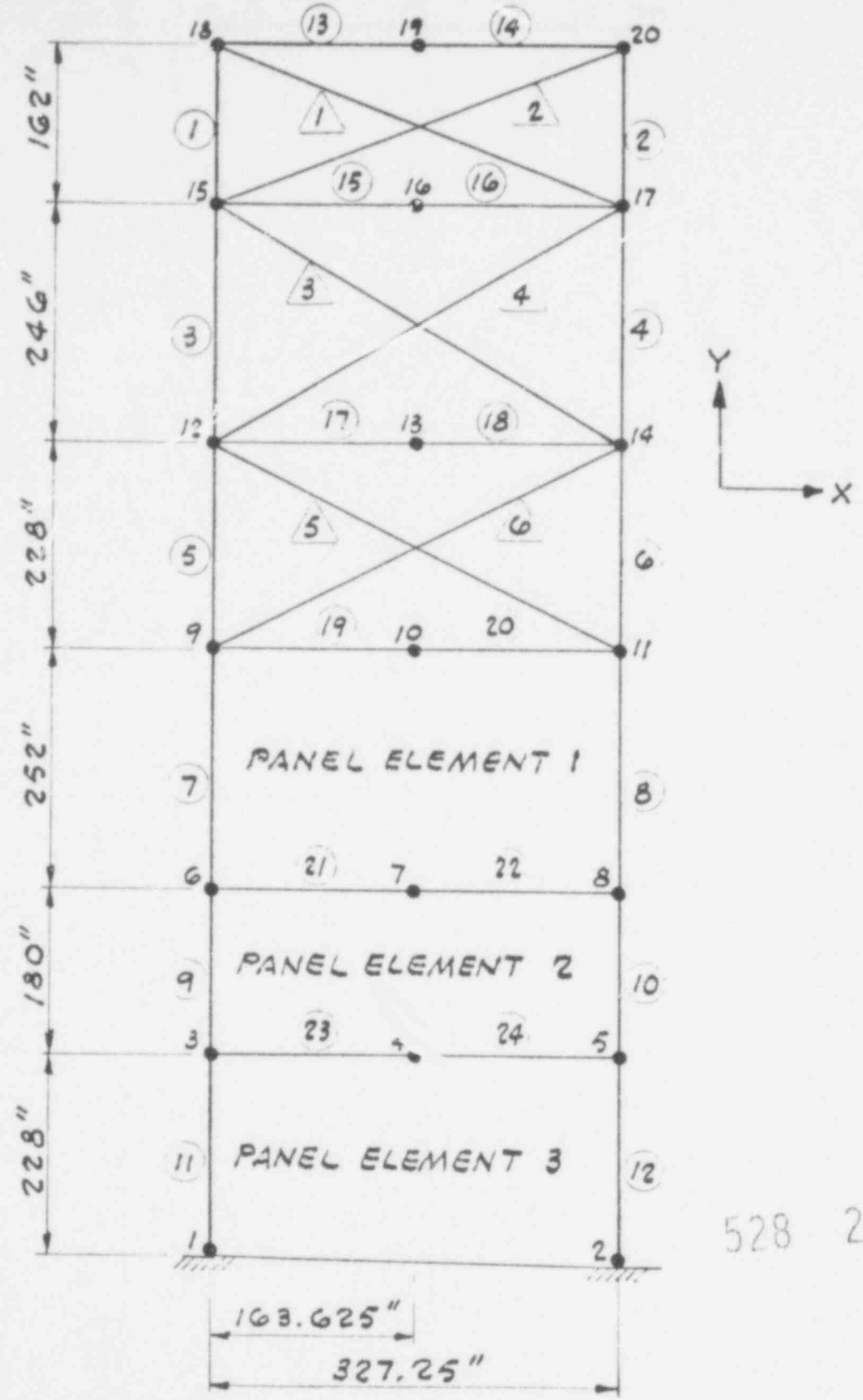

528 215

RIGOROUS NONLINEAR ANALYSIS OF A TURBINE BUILDING MATHEMATICAL MODEL

NRC/NONLIN

FIGURE 6.13

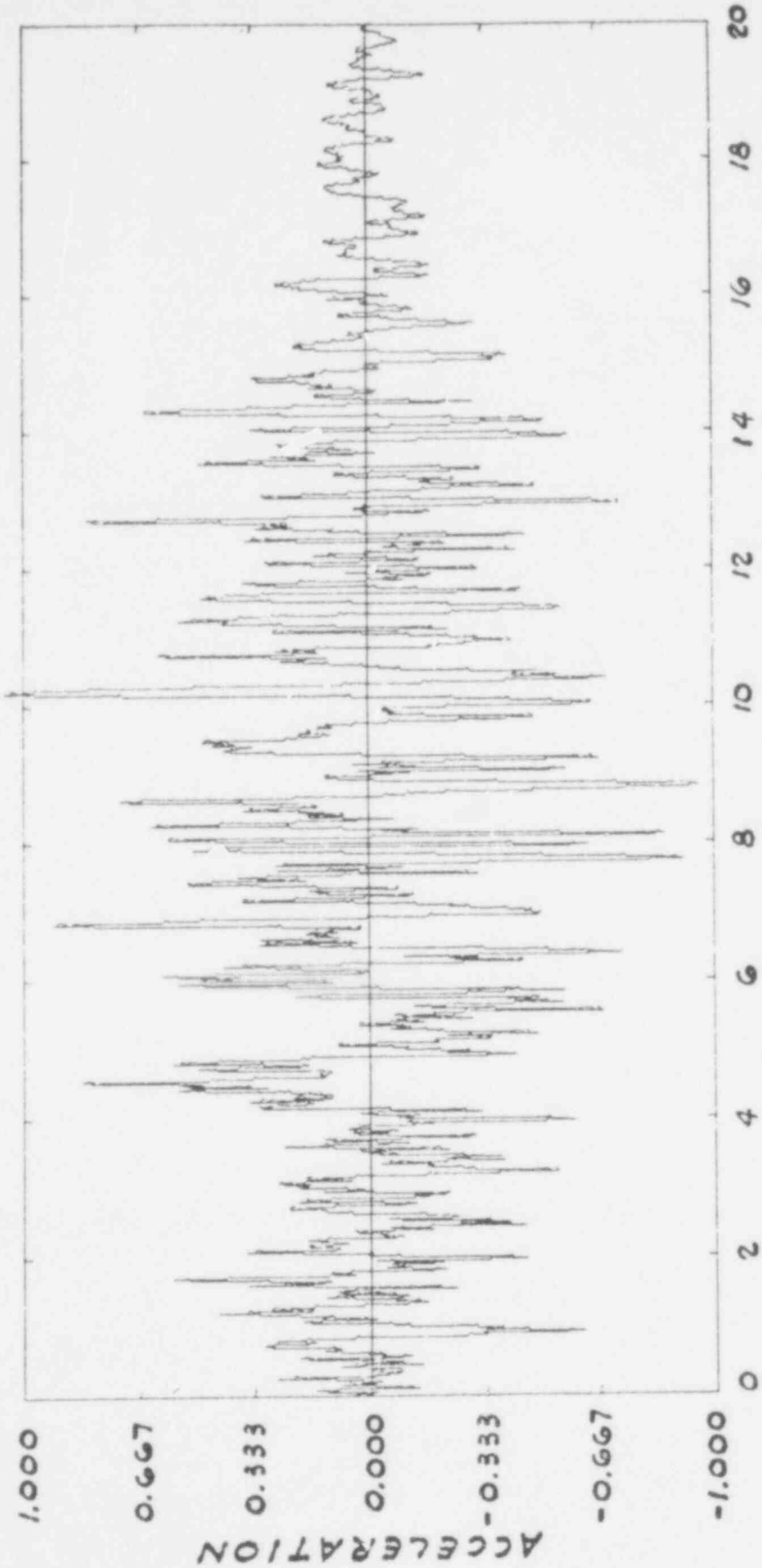

TIME HISTORY FROM NRC SPECTRA

NRC/NONLIN

FIGURE 6.14

528 216

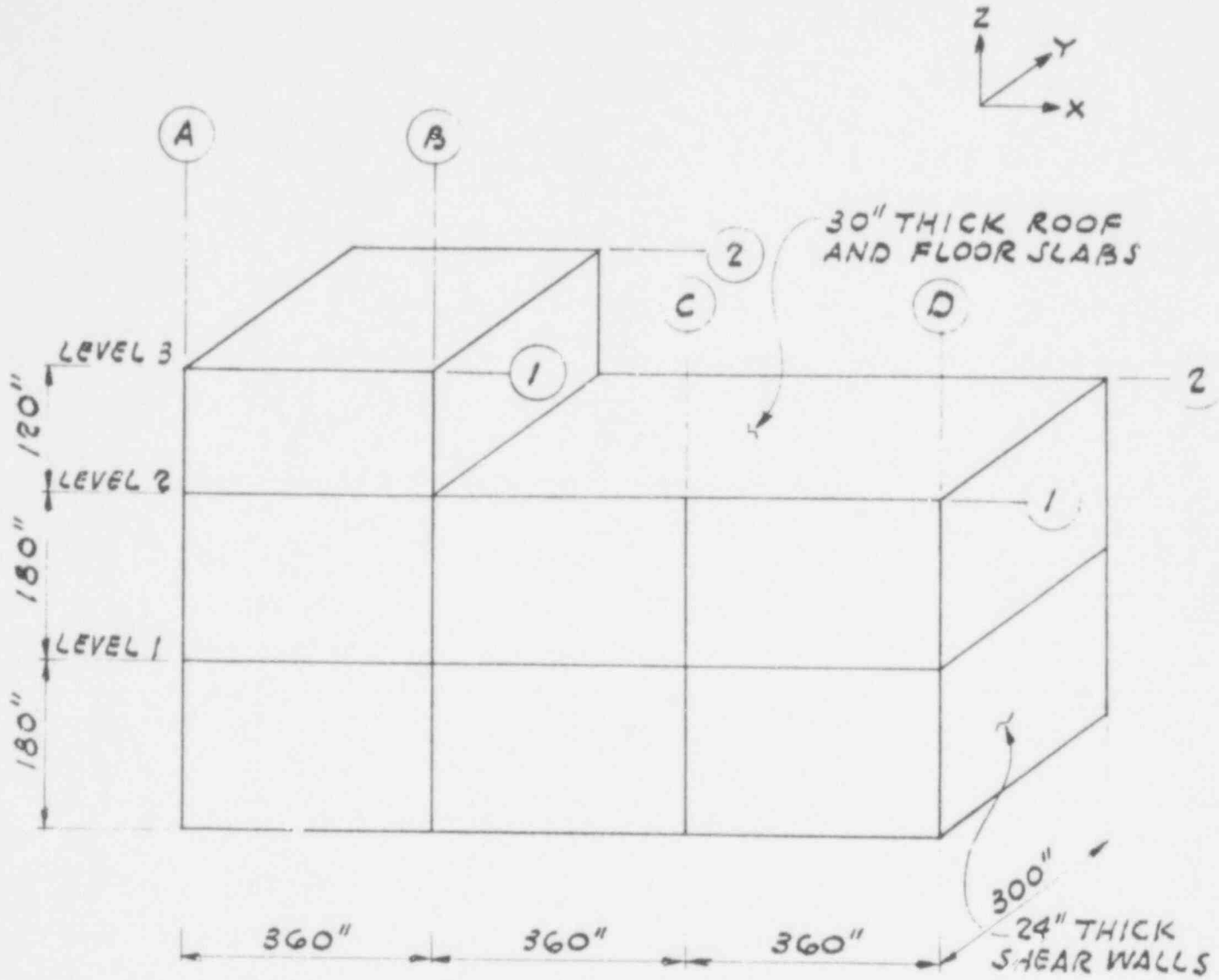

NOTE: ALL DIMENSIONS ARE CENTER-TO-CENTER

TYPICAL AUXILIARY BUILDING

528 217

NRC/NONLIN FIGURE 6.15

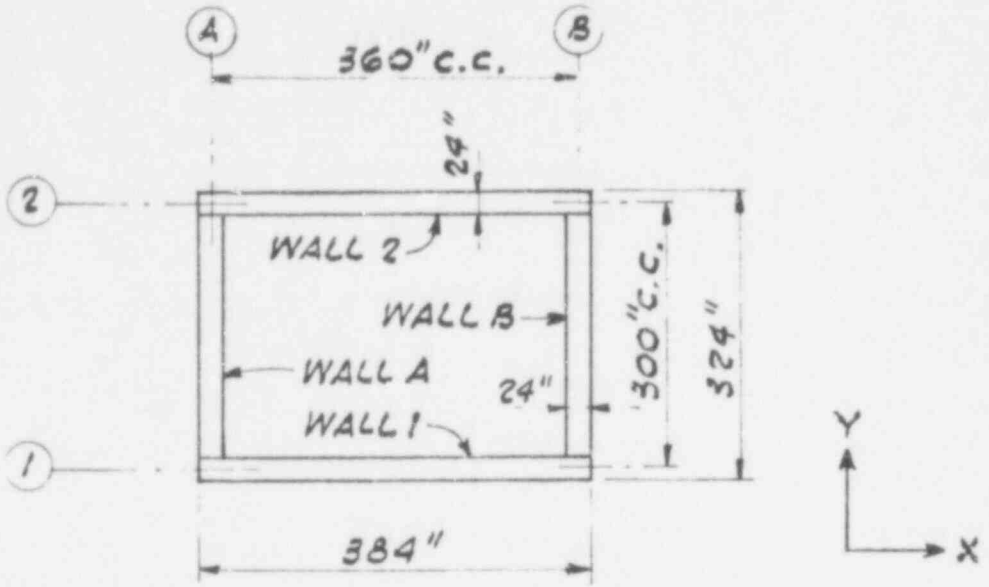

PLAN AT LEVEL 3

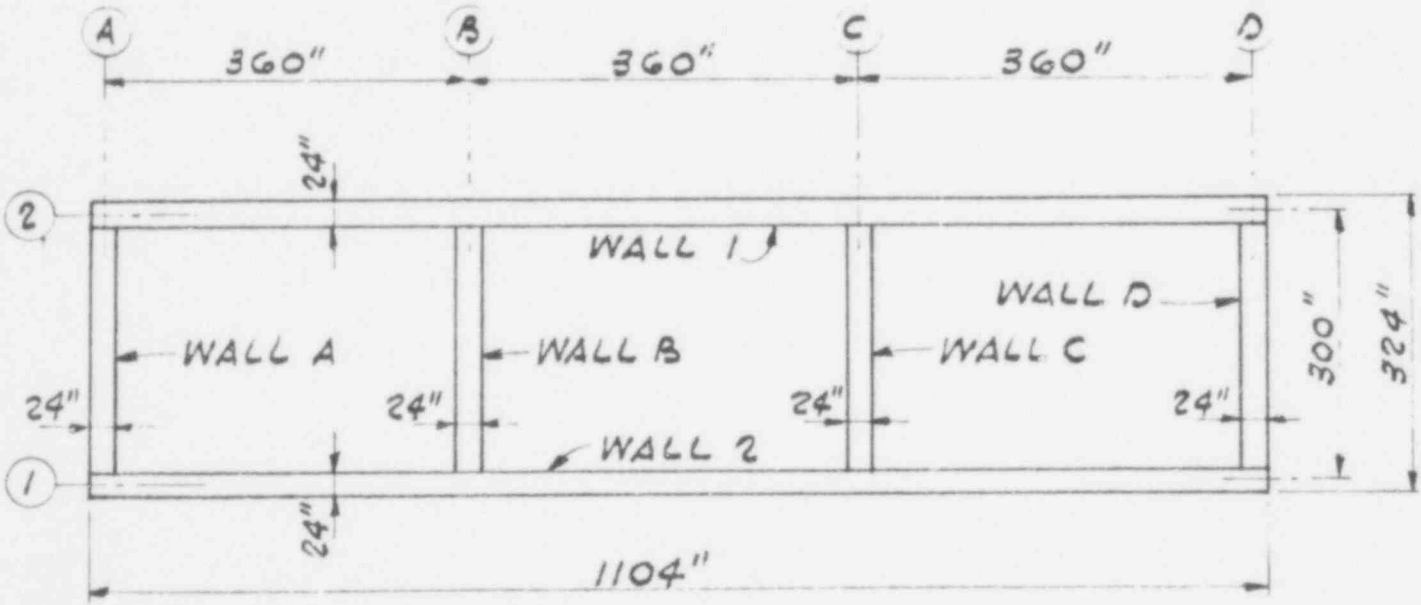

PLAN AT LEVELS 1 AND 2

DETAILS OF AUXILIARY BUILDING

528 218

NRC/NONLIN FIGURE 6.16

Building AUXILIARY BENCHMARK Direction X-LONGITUDINAL

N = 3 Earthquake 0.5g

Story Shear Model IV α = 1.0

Level, j	MODE 1 T = S_a = Γ =		MODE 2 T = S_a = Γ =		MODE 3 T = 0.086 SEC. S_a = 0.60g Γ = 3.13		DV_j (kip)	V_{y_j} (kip)	$\frac{DV_j}{V_{y_j}}$	ν_j
	F (kip)	DV_{j1} (kip)	F (kip)	DV_{j2} (kip)	F (kip)	DV_{j3} (kip)				
3					403.47	403.47	403.47	5391	0.07	
2					1078.33	1481.80	1481.80	15603	0.09	
1					789.52	2271.32	2271.32	15802	0.14	

RET ANALYSIS OF X-DIRECTION OF A HYPOTHETICAL AUXILIARY BUILDING NRC/NONLIN

FIGURE 6.17

528 219

	MODE 1	MODE 2
CYCLE 1	$T_1 = 0.086$ SEC.	$T_2 = 0.056$ SEC.
	$S_{a1} = 1.0g$	$S_{a2} = 0.7g$
	$\frac{C_b}{S_a} = 0.74$	$\frac{C_b}{S_a} = 0.10$
	$DV_1 = 3140.72^K$	$DV_2 = 297.10^K$
	$DV = (3140.72^2 + 297.10^2)^{1/2} = 3154.74^K$	
	$V_Y = 2602^K$	
	$\mu = 0.5\left(\frac{3154.74^2}{2602^2}\right) + 0.5 = 1.23$	
	$S_Y = .024"$ $S = 1.23 \times .024 = 0.030"$	
	$K' = 2602/.03 = 88143.63^{K/IN}$	
	$K = 108,935^{K/IN}$	
	$\sqrt{K/K'} = 1.11$	
CYCLE 2	$T_1 = .086 \times 1.11 = .096$ SEC.	$T_2 = 0.062$ SEC.
	$S_{a1} = 1.14$	$S_{a2} = 0.85$
	$DV_1 = 3580.42^K$	$DV_2 = 360.76^K$
	$\mu = 1.46$	
	$K' = 2602/1.46 \times 0.24 = 74257.99$	
	$\sqrt{K/K'} = 1.21$	
CYCLE 3	$T_1 = 0.104$ SEC.	$T_2 = .068$ SEC.
	$S_{a1} = 1.14g$	$S_{a2} = 0.85$
	$DV_1 = 3580.42$	$DV_2 = 360.76$
	$\mu = 1.46$	
	SOLUTION CONVERGES	
	$T_1 = 0.104$ SEC.	$T_2 = 0.068$ SEC.
	$S_{a1} = 1.14g$	$S_{a2} = 0.85g$

528 220

RET ANALYSIS OF AN AUXILIARY BUILDING
ITERATIVE ANALYSIS FOR EFFECTIVE PERIOD

NRC/NONLIN FIGURE 6.18

Building AUXILIARY BENCHMARK Direction Y-TRANSVERSE

N = 3 Earthquake 0.5g

Story Shear Model IV α = 1.0

Level, j	MODE 1 T = 0.104 SEC. S_a = 1.14g Γ = 2.84		MODE 2 T = 0.068 SEC. S_a = 0.85g Γ = 1.07		MODE 3 T = S_a = Γ =		DV_j (kip)	V_{y_j} (kip)	$\frac{DV_j}{V_{y_j}}$	μ_j
	F (kip)	DV_{j1} (kip)	F (kip)	DV_{j2} (kip)	F (kip)	DV_{j3} (kip)				
3	844.07	844.07	-107.54	-107.54			850.89	3660	0.23	-
2	1750.76	2594.83	287.47	179.93			2601.06	3484	0.75	-
1	966.80	3561.63	196.45	376.38			3581.46	2602	1.38	1.5

528 221

RET ANALYSIS OF AN AUXILIARY BUILDING

INTERSTORY DUCTILITY CALCULATION

NRC/NONLIN FIGURE 6.19

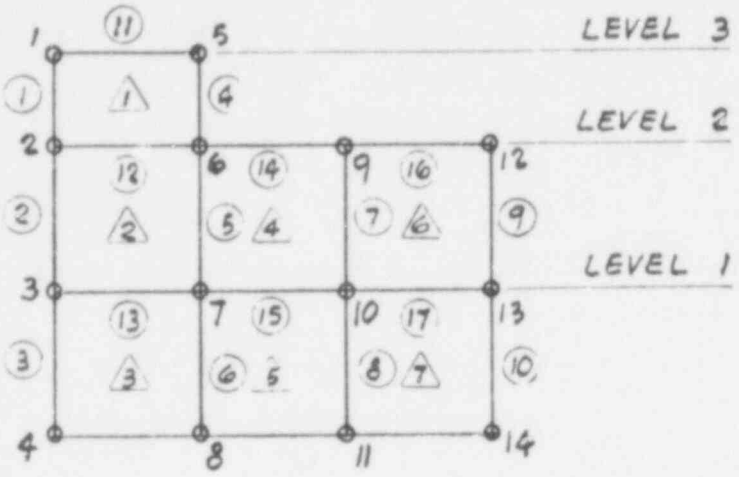

WALLS 1 & 2

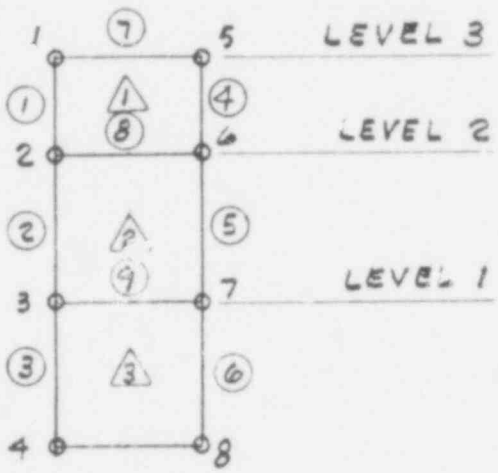

WALLS A & B

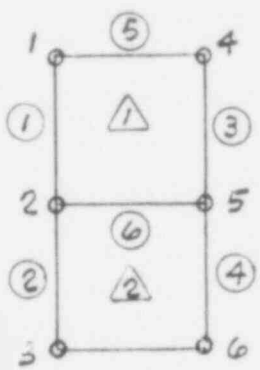

WALLS C & D

RIGOROUS ANALYSIS OF AN AUXILIARY BUILDING
MATHEMATICAL MODEL

528 222

NRC/NONLIN

FIGURE G.20

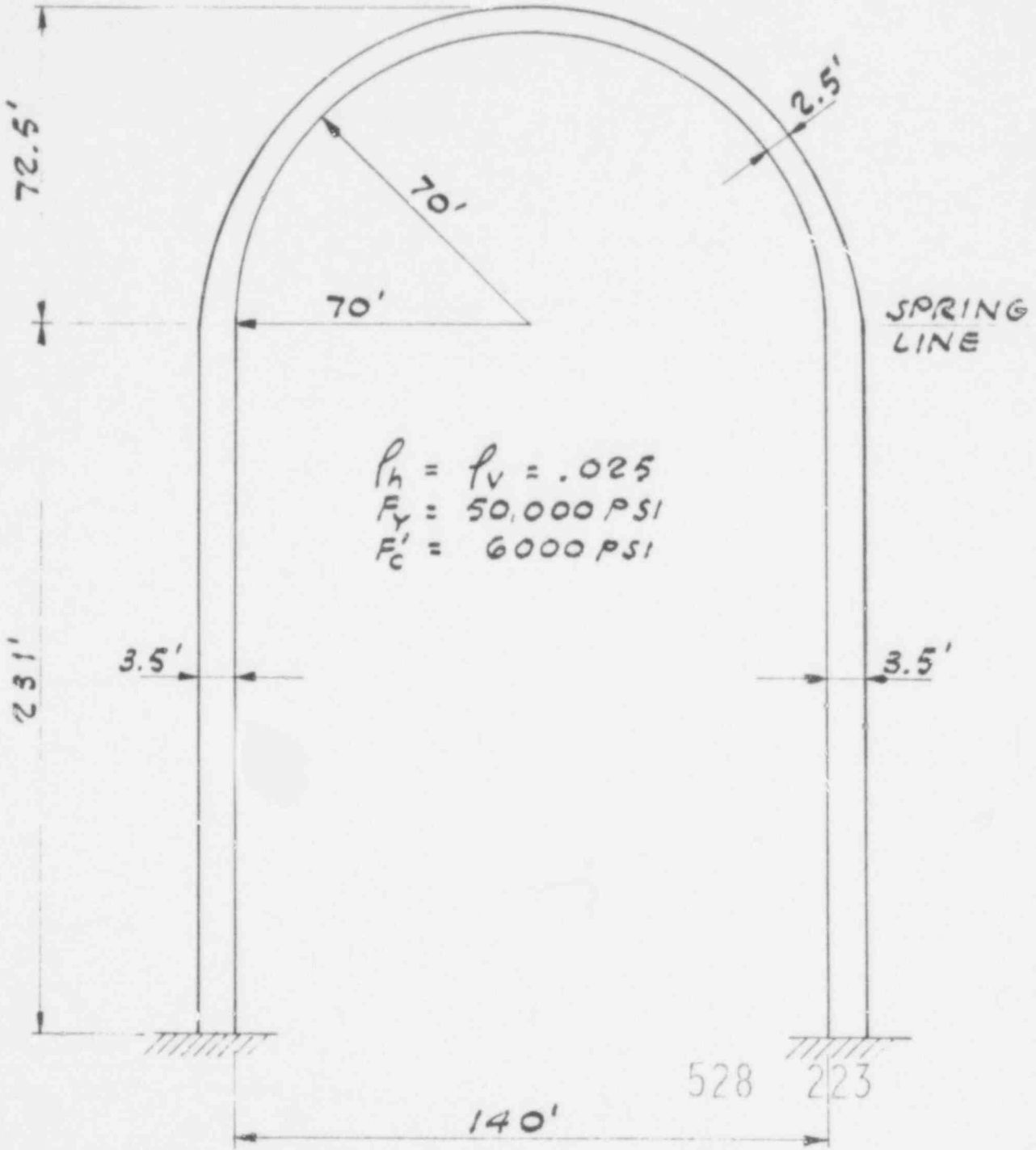

TYPICAL CONTAINMENT BUILDING

NRC/NONLIN FIGURE G.21

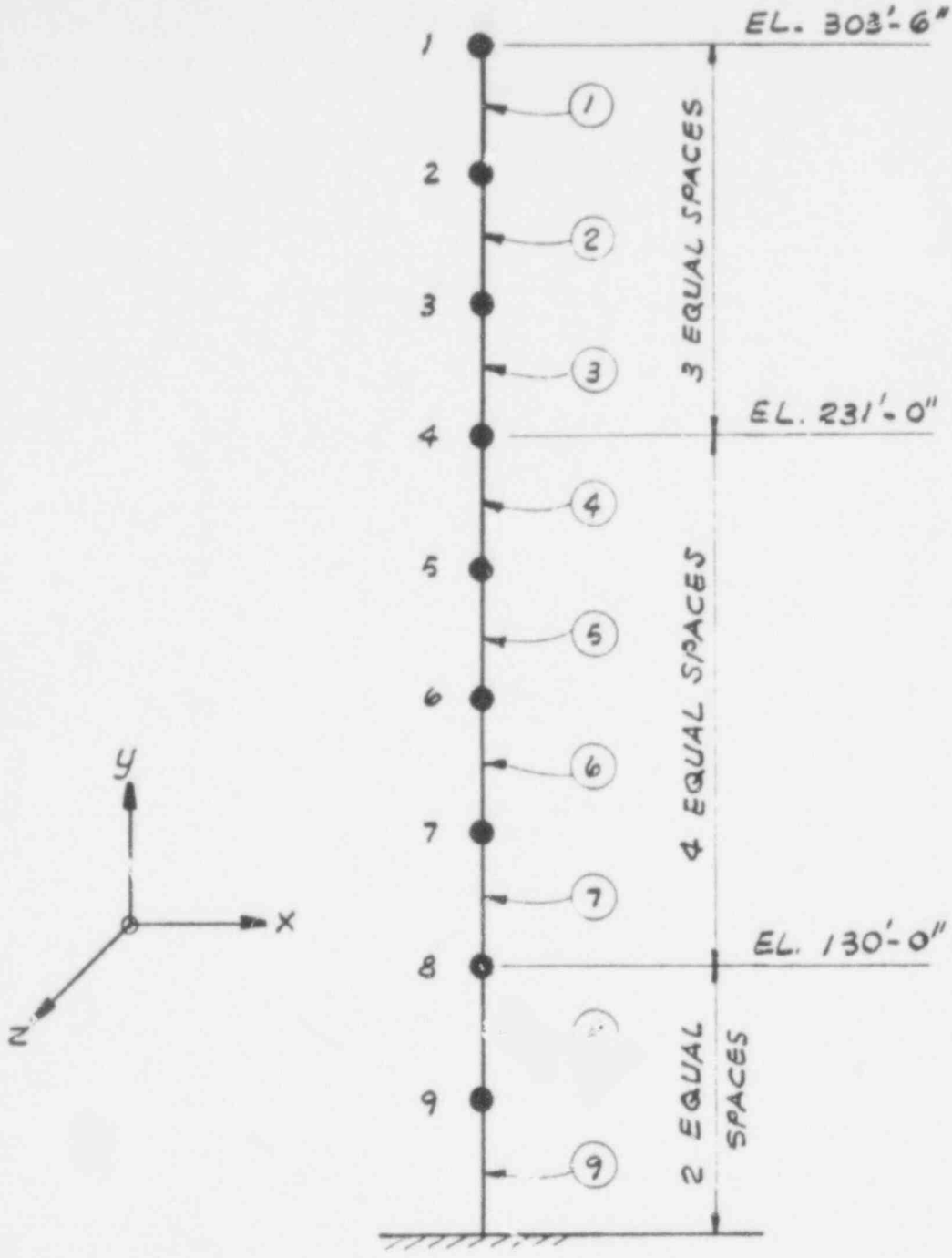

ELASTIC ANALYSIS OF CONTAINMENT BUILDINS

MATHEMATICAL MODEL

528 224

NRC/NONLIN

FIGURE 6.22

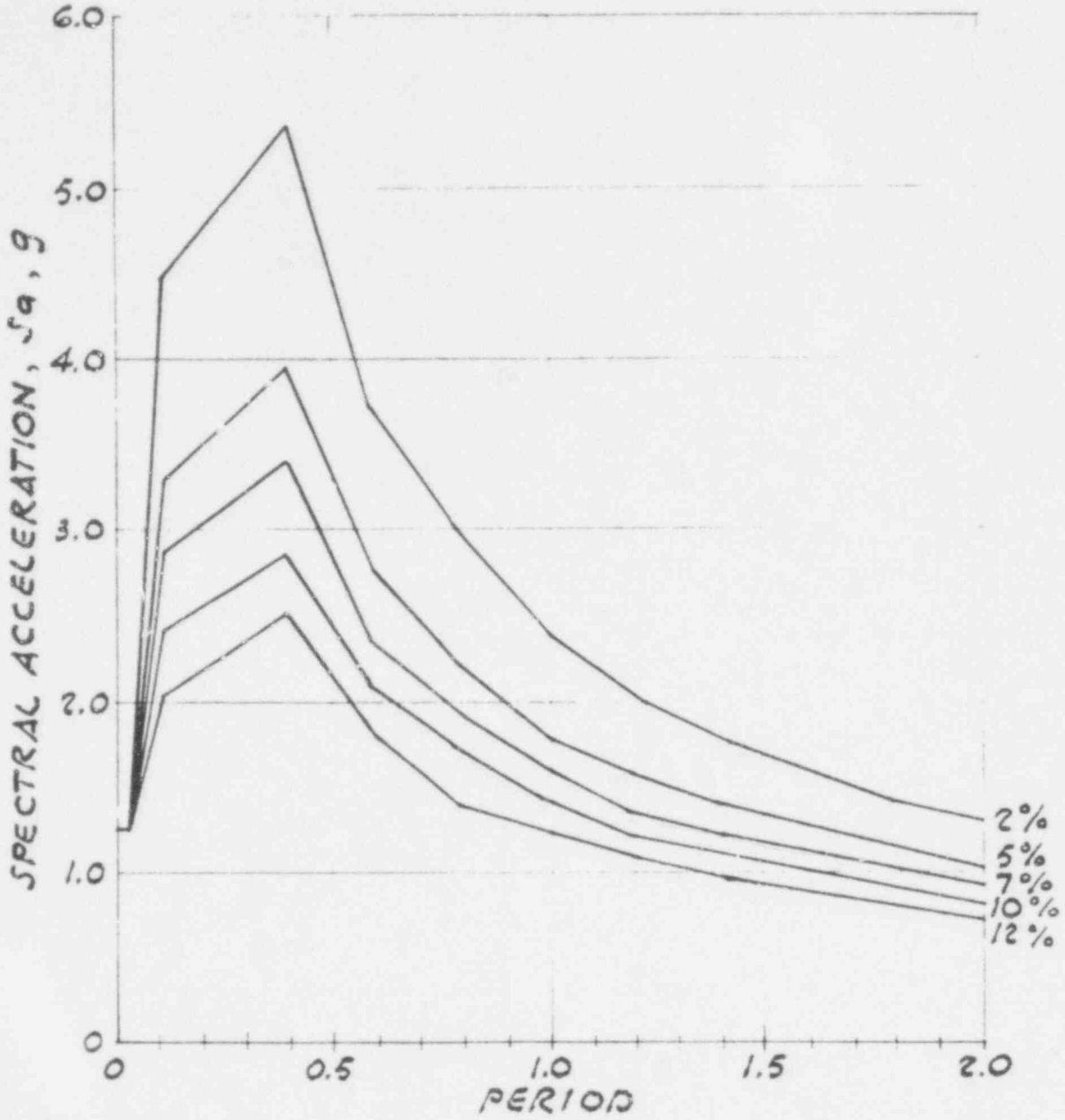

RESPONSE SPECTRA FOR ANALYSIS OF A CONTAINMENT BUILDING

528 225

NRC/NONLIN FIGURE G.23

CYCLE 1 $T_1 = 0.196$ SEC. $T_2 = 0.067$ SEC. $T_3 = 0.037$ SEC. $W = 44{,}570^K$

$S_{a1} = 3.50g$ $S_{a2} = 2.25g$ $S_{a3} = 1.40g$

$\frac{C_b}{S_{a1}} = 0.76$ $\frac{C_b}{S_{a2}} = 0.16$ $\frac{C_b}{S_{a3}} = 0.04$

$DV_1 = 118556^K$ $DV_2 = 16045^K$ $DV_3 = 2496^K$

$DV = 119663^K$ $V_Y = 87606^K$ (TABLE 6.39)

$\mu = 0.5\left(\frac{119663}{87606}\right)^2 + 0.5 = 1.43$

$\delta_Y = .0102$ (FT.) $\delta = .0103 \times 1.43 = 0.0147$ FT.

$K' = 87606/.0147 = 5{,}947{,}858$ K/FT.

$K_i = 85 [illegible] ,0^5$

$\sqrt{K_i/K'} = 1.20$

CYCLE 2 $T_1 = 0.[illegible] \times 1.2 = 0.24$ SEC. $T_2 = .067 \times 1.2 = 0.08$ SEC. $T_3 = .037 \times 1.2 = .044$ SEC.

$S_{a1} = 3.60g$ $S_{a2} = 2.60g$ $S_{a3} = 1.70g$

$DV_1 = 121944^K$ $DV_2 = 18541^K$ $DV_3 = 3030^K$

$DV = 123383^K$

$\mu = 1.47$

SOLUTION CONVERGES

$T_1 = 0.24$ SEC. $T_2 = 0.08$ SEC $T_3 = 0.044$ SEC.

$S_{a1} = 3.6g$ $S_{a_2} = 2.6g$ $S_{a_3} = 1.7g$

528 226

RET ANALYSIS OF A CONTAINMENT BUILDING
ITERATIVE PERIOD CALCULATION

NRC/NONLIN FIGURE 6.24

Building CONTAINMENT BENCHMARK Direction NA

N = 9 Earthquake 1.25g

Story Shear Model IV α = 1.0

Level, j	MODE 1 T = 0.24 SEC S_a = 3.6 g Γ = 32.39		MODE 2 T = 0.08 SEC S_a = 2.6 g Γ = -15.00		MODE 3 T = 0.044 SEC S_a = 1.7 g Γ = -7.87		DV_j (kip)	V_{y_j} (kip)	$\frac{DV_j}{V_{y_j}}$	μ_j
	F (kip)	DV_{j1} (kip)	F (kip)	DV_{j2} (kip)	F (kip)	DV_{j3} (kip)				
1	10325	10325	-3579	-3579	1051	1051	10978	62451	0.18	
2	21139	31464	-5839	-9418	1297	2348	32927	62451	0.53	
3	18773	50237	-2587	-12005	-539	1809	51683	62451	0.83	
4	19562	69799	1293	-10712	-2335	-526	70618	87606	0.81	
5	19111	88910	5412	-5300	-2447	-2973	89117	87606	1.02	1.0
6	14681	103591	7761	2461	-237	-3210	103670	87606	1.18	1.2
7	10250	113841	8025	10486	2201	-1009	114327	87606	1.31	1.4
8	5482	119323	5601	16087	2753	1744	120415	87606	1.37	1.4
9	2290	121613	2750	18837	1646	3390	123110	87600	1.41	1.5

RET ANALYSIS OF A CONTAINMENT BUILDING

INTERNODAL DUCTILITY CALCULATIONS

NRC / NONLIN

FIGURE 6.25

528 227

7. CONCLUSIONS AND RECOMMENDATIONS

7.1 Discussion

Rigorous nonlinear dynamic analysis methods are valuable tools in seismic analysis and design when combined with engineering judgment, careful detailing, and quality construction workmanship. Although the methodology applied in the solution of the equations of motion is rigorous, there are three areas in the analyses that require considerable engineering judgment and scientific development. These three areas are: (1) mathematical modeling of the mechanical behavior of structural components, (2) estimating the energy dissipation capacity of the critical regions, and (3) selecting site- and structure-specific ground motions. The analysis procedures are rigorous to the extent that these areas are representative of actual field conditions.

It is always difficult to model reinforced concrete members properly because reinforced concrete is a composite material exhibiting tensile cracking at low stress levels, bond-slip between the concrete and steel reinforcement, aggregate interlock, degrading stiffness, and spalling under cyclic loading. The models that are currently available can only reveal the overall behavior of the member (i.e., the moment-rotation relationship in case of a flexural member and the shear stress-strain relationship in case of a shear panel). Many uncertainties would still remain even if more refined mechanical models were formulated because of variations in material properties. The variation of some critical modeling parameters, such as tensile strength of concrete and modulus of elasticity, can be accounted for only in a probabilistic sense by investigating the various bounds on these parameters and their effects on the response. Until such capabilities are developed, crack propagation, spread of plasticity, concrete spalling, and crushing cannot be examined properly. However, current hysteretic models, such as the Takeda degrading-stiffness model for reinforced concrete beams, seem to be adequate to capture the overall structural response under lower levels of inelastic excursions.

An area where little work has been reported is the hysteretic behavior of

528 228

shear walls. As discussed in the Appendix C of this report, significant behavioral discrepancies were observed in low-rise and high-rise bounded or unbounded shear wall structures. The rigorous models currently available can model only bilinear constant hysteretic behavior. Additional work is needed to develop new models that will incorporate the available experimental data.

One significant point that has to be noted is that most of the nuclear power plant structures are massive, stiff structures. The bulk of the experimental data on component hysteretic behavior and the mathematical models derived therefrom are for tall, flexible structures (suitable for high-rise buildings). Additional work is needed to catalog experimental data relevant to nuclear power plant structures and to perform further tests to accumulate enough data so that accurate mathematical models encompassing the key parameters may be developed and used.

The response of a structural system after the formation of a collapse mechanism is extremely sensitive to the time variations of inertia forces. Studies have indicated that the nonlinear response of structures with short fundamental periods subjected to accelerograms with long-duration acceleration pulses would be expected to differ substantially from their elastic response. It is necessary that several accelerograms of different types of ground motion that can be expected at a site be used to account for the probabilistic nature of the seismic events.

Given the fact that hysteretic models for reinforced concrete components are still in the developmental stage, it is difficult to specify a confidence level for nonlinear responses of the structures as computed by the rigorous methods. However, the overall displacement responses of the reinforced concrete frame structures, as computed by the rigorous methods in this study, seem to be well matched with experimental data. It may be estimated, in the light of these analyses, that reliable overall displacement responses may be analytically computed for reinforced concrete frame structures subjected to the levels of inelasticity considered in the present study. Additional studies, both experimental and analytical, are needed for shear wall types of structures to determine the accuracy and the

533 227

reliability of the hysteretic models. However, it is expected that the current hysteretic models may be adequate for limited excursions in the inelastic ranges.

Additional studies aimed at developing a rigorous nonlinear dynamic analysis methodology for the containment structure subjected to seismic loading are needed. This effort might consist of three phases.

In the first phase, the containment shell may be modeled as shear beams, and a lumped-mass model may be developed. The main effort in this phase would be to develop a hysteretic model for the shear beams that would correspond to the shell behavior. Several simplifications, such as neglecting the ovaling modes, may have to be made. It would also be difficult to obtain the response of any local area of the shell. However, this phase would require minimum effort.

In the second phase, efforts may be directed at developing a nonlinear analysis algorithm for an axisymmetric structure subjected to nonaxisymmetric loading such as ground motion due to a seismic event. This will require a major software development effort and may still require quite a few broad simplifying assumptions.

In the third phase, the general three-dimensional model with three-dimensional brick or shell elements may be used. The problems here are twofold. First, no comprehensive constitutive model of concrete under triaxial cyclic loading is currently available. Secondly, the cost of a total three-dimensional analysis may be prohibitive at this point. However, with the advent of new generation computers having vector processing and pipelining capabilities, such computations may become feasible in the not-too-distant future.

Among the three phases discussed above, the first two may yield uncertain results. The first method, with its shear beam assumption of the cylindrical section, can only provide information about the overall displacement response. Accurate determination (stress, strain, cracking, etc.) at any local area may not be possible with such a method. The second phase may also

528 229

have problems in properly considering inelastic behavior of local regions on the shell surface. The third phase seems to be the most straightforward in the sense that three-dimensional elements are available for the proper modeling of the shell surface. The major problem is the computational cost, but less refined finite element meshes may be used in the beginning to make parameter studies. However, collection of experimental data and additional experimental work involving models of the containment structure are also needed for the proper calibration of the analytical work.

On the basis of comparison of the rigorous and simplified analyses of several structures and other considerations, this report concludes that the Reserve Energy Technique (RET) is a reasonably accurate yet simplified method of nonlinear seismic dynamic analysis. The method is appropriate for the prediction of maximum total inelastic displacements and ductility factors. The results of an RET analysis may be used in conjunction with the ductility criteria described in Chapter 5 for approximate evaluations of the seismic adequacy of Category I nuclear power plant structures.

The energy balance concepts of the RET appear applicable to a broad range of structural analysis problems. The accuracy of the RET is currently limited by the accuracy of various input parameters. The elastic and nonlinear idealizations used in both rigorous and simplified analyses are much simpler than the physical phenomena they represent. Considerable engineering judgment is necessary in modeling member mechanical characteristics and estimating energy dissipation capacity. Successful application of the RET requires careful considerations of these topics; otherwise, erroneous and misleading displacements and ductility factors will result. A prudent analysis with the RET would involve parameter studies to identify the sensitivity of various parameters.

The analysis of the turbine building benchmark problems demonstrated that the RET needs to be improved by adopting an analysis scheme that would allow a redistribution of member forces reflecting the changing stiffness patterns prevalant in nonlinear response. The current analysis scheme distributes member forces according to the initial relative stiffness, and this is clearly not realistic for nonlinear response. The technical

528 231

aspects of the suggested modification of the RET are quite straightforward; however, the procedural aspects may become too involved for a simplified hand analysis. Hence, development of a computer program would probably be needed. This future development of the RET should be pursued because it would substantially improve the accuracy of the method in situations involving severe inelastic action.

The various analyses that were performed as part of this work have demonstrated the reliability of the RET within the limits of applicability specified in Chapter 5. These limits could be expanded by additional studies consisting of the analysis of more benchmark structures and by parameter studies. Such studies might involve rigorous and simplified nonlinear analysis of ten or more Category I nuclear power plant structures.

Various trends indicate that the future course of structural engineering will require more explicit considerations of the nonlinear, inelastic strength and energy capacity of structures. Since rigorous nonlinear analysis seems too involved for ordinary engineering design, a quasi-nonlinear analysis method is needed. This method would probably incorporate the energy balance concepts and other aspects of the RET, and it could also utilize improved dynamic force calculation and redistribution schemes and more precise element modeling. Importantly, input for the method would consist of an elastic response spectrum. The proposed quasi-rigorous method could give results in terms of displacements, velocity, acceleration, and member forces, and it could even be extended to give floor response spectra for nonlinear response. Development of such an analysis method would be a considerable undertaking; however, it is clearly needed for a more complete yet practical accounting of the nonlinear strength of structures.

7.2 Conclusions

Main conclusions of this report are as follows:

- Compared with a rigorous nonlinear seismic analysis, the Reserve Energy Technique (RET) is a reasonably accurate yet simplified analysis method. It may be used for approximate evaluation of the

528 232

nonlinear seismic displacements of Category I structures.

- Compared with a rigorous nonlinear seismic analysis, a rigorous elastic seismic analysis is generally not sufficiently accurate although it may be acceptable in cases involving very limited inelastic response. A rigorous elastic analysis generally establishes a lower bound of inelastic displacement.

7.3 Recommendations

Recommendations of this study are as follows:

- The RET may be used in conjunction with the criteria established in Chapter 5 of this report for approximate evaluations of nonlinear seismic response of Category I nuclear power plant structures.
- The RET could be improved by a modification that would allow an approximate redistribution of shear based on the character of the inelastic response. This modification might involve iterative calculations. After each cycle of iteration, the stiffness matrix of the structure would be updated to reflect stiffness lost due to yielding. The distribution of shear for the following cycle might be based on the updated stiffness matrix.
- Additional benchmark analyses and parameter studies should be conducted to expand and more firmly establish the limits of applicability of the RET.
- Additional studies aimed at improving the mathematical models for nonlinear seismic response are needed. The appropriateness of the current models diminishes as the magnitude of inelastic response increases. Further work in this area should focus on matching measured nonlinear structural response with the results of rigorous nonlinear mathematical models. Specific areas of study should include spread of plasticity in the critical regions, stiffness deterioration under moment and curvature reversals, shearing deformations, and yielding in members subject to axial loads; the investigations should estimate the effects of these characteristics on the mechanical properties of such structure types as moment-resisting frames, braced frames, shear walls, diaphragms, and interacting shear walls and frames.
- Additional studies aimed at investigating the availability of experimental data that would be relevant to massive, stiff structures such as nuclear power plant buildings are urgently needed. On the basis of these studies, further experimental work may be

528 233

proposed that could be used to develop and check the analytical models.

- A comprehensive program of research is needed to examine the behavior of containment structures (continuous cylindrical shells with hemispherical domes at the top) in the elastic, inelastic, and ultimate ranges. A three-phase program that may be used as a basis for such research is described in section 7.1.
- Additional studies aimed at establishing the sensitivity of rigorous nonlinear analysis results to the character of the input accelerograms are needed.
- A quasi-rigorous nonlinear analysis method is needed. This analysis scheme would be a computer-based, simplified nonlinear analysis method and would allow the input dynamic disturbance to be characterized by a smooth response spectrum.

528 234

APPENDIX A

Literature Survey

528 235

CONTENTS

528 236

FIGURES

528 237

PREFACE

This appendix summarizes the results of a literature search conducted to identify the available simplified nonlinear analysis procedures, and it also identifies the available rigorous nonlinear analysis procedures (computer programs) that might be used to evaluate or verify the simplified procedures. In addition, recommendations are made regarding candidate simplified methods that were to be studied in detail and the rigorous analysis computer programs that were to be used for the detailed evaluation of the candidate simplified analysis methods.

528 238

SIMPLIFIED NONLINEAR ANALYSIS METHODS*

A review of the literature reveals that simplified methods available for performing nonlinear analyses of structures can be separated into two categories: 1) time-history analyses and 2) response spectrum analyses. The former methods generally involve the use of sophisticated models with simplification introduced only with respect to the analytical solution of the nonlinear equations of motion. The latter methods generally involve simplification of the model to that of an equivalent linear system, thus facilitating analytical simplification also because of needing to solve only linear equations of motion.

The various simplified methods currently available will be described and commented on below under the two categories of time-history analysis and response spectrum methods, respectively.

Time-History Methods

Various analytical developments have been made in recent years to reduce the substantial computational effort involved in performing nonlinear response calculations with a refined model. Two methods that might warrant consideration for this project are discussed below. These are: Modal Nonlinear Analysis and Truncated Time-Domain Analysis. Another computational expedience that has recently evolved is the explicit formulation for the solution of the governing equations of motion[1] as opposed to the previous commonly used implicit formulation. In the implicit formulation the stiffness matrix must be inverted at each time step whereas in the explicit formulation only the mass matrix is inverted. The explicit formulation therefore facilitates a significant reduction in computational work, reducing both computer time and the necessary core space.

Modal Nonlinear Analysis.[2,3] Modal nonlinear analysis is a computer-based (SA/RM) procedure that uses normal mode analysis to extend linear time-domain solutions into the nonlinear regime. It is a simplified analytical

*Names applied to the analytical methods are descriptive and are not necessarily indicative of names found in the literature.

528 239

method applicable to refined structural models. The algorithm is derived from two commonly used concepts in dynamic analysis techniques: (1) a normal mode of analysis and (2) a load-correction form of the nonlinear equation solution. These two concepts are discussed in more detail below.

The motion of a freely vibrating linear structural system can be described in the finite-element formulation by:

$$[M]\{\ddot{u}\} + [K_o]\{u\} = \{0\} \tag{1}$$

where $[M]$ and $[K_o]$ are mass and stiffness matrices, and $\{u\}$ is the displacement vector. The nontrivial solutions of Equation (1) are $\{u\} = \{\phi\}e^{i\lambda t}$, which are determined from the corresponding eigenvalue problem:

$$([M] - \lambda[K_o])\{\phi\} = \{0\} \tag{2}$$

If N is the number of linear equations in Equation (1), then, λ_i and $\{\phi_i\}$, where $i = 1...N$, determine the mode shapes and frequencies of the structural system.

The orthogonality conditions

$$\{\phi_i\}^T[M]\{\phi_j\} = 0 \qquad i \neq j$$

$$\{\phi_i\}^T[K_o]\{\phi_j\} = 0 \qquad i \neq j$$

lead to an equivalent uncoupled system of equations for the forced vibration of the structural system,

$$[\Omega]^T[M][\Omega]\{\ddot{r}\} + [\Omega]^T[K_o][\Omega]\{r\} = [\Omega]^T\{P\}$$

or,

$$[M^*]\{\ddot{r}\} + [K_o^*]\{r\} = \{P^*\} \tag{3}$$

528 240

where:

$\{P\}$ = the load vector

$[\Omega] = [\{\phi_1\}\{\phi_2\}....\{\phi_N\}]$

$\{u\} = [\Omega]\{r\}$

Solution of Equation (3) is quite straightforward and known in the literature as the mode superposition method. Often the solution is truncated at a mode number less than the total number of modes as the degree of accuracy to be achieved is satisfied.

Nonlinearity in structural systems is contributed by several sources, chief among which are material and geometric nonlinearities. Most nonlinear structural problems can be recast as an equivalent problem in which it is necessary to determine a sequence of linear solutions in order to trace the nonlinear behavior in a piecewise linear fashion. Solutions to nonlinear structural problems can be obtained from a variety of iterative, incremental, or energy search techniques.

The nonlinear equation of forced vibration of a structural system may be written as:

$$[M]\{\ddot{u}\} + ([K_o] + [K_c])\{u\} = \{P\} \tag{4}$$

where $[K_c]$ is the matrix that contains all the nonlinearities and $[K_o]$ represents a linear, reference stiffness. Equation (4) may be rewritten as:

$$[M]\{\ddot{u}\} + [K_o]\{u\} = \{P\} + \{Q\} \tag{5}$$

where, $\{Q\} = -[K_c]\{u\}$ is the correction load vector for the nonlinearities present in the structural system. Equation (5) may be transformed similarly to Equation (3):

$$[M^*]\{\ddot{r}\} + [K_o^*]\{r\} = \{P^*\} + \{Q^*\} \tag{6}$$

528 241

where $\{Q^*\} = [\Omega]^T\{Q\}$.

Equation (6) has the nonlinear term on the right side of the equation. This is known as effective-load technique and is more compatible with the normal mode of analysis because only the mass and original linear stiffness matrices are on the left side and are uncoupled because of the orthogonality conditions of the eigenvectors.

The uncoupled Equation (6) may be solved by using a central difference operator in time such as:

$$\ddot{r}^{(i)} = \frac{\dot{r}^{(i+1)} - \dot{r}^{(i)}}{\Delta t}$$

$$\dot{r}^{(i)} = \frac{r^{(i)} - r^{(i-1)}}{\Delta t} \tag{7}$$

where:

$$r^{(i)} = r(t_i)$$

The chief advantage of the modal nonlinear analysis is the economy of computation and computer storage achieved by the simple expedient of solving an uncoupled set of dynamic equations.

The modal nonlinear analysis has demonstrated good accuracy for a wide variety of nonlinear structures under both static and dynamic loads.[2,3] The technique is readily adaptable to standard linear analysis computer packages (e.g., SAP) and can be shown to be one to two orders of magnitude more efficient than corresponding refined nonlinear analyses. An added advantage can be associated with the definition of nonlinear modal contributions, which are the basis for subsequent development of simplified response spectra methods.

Truncated Time-Domain Analysis.[4,5] The use of unconditionally stable time-integration techniques provides a good potential for reducing the large number of time steps required in some wave-propagation analyses such as earthquake time-history analysis. The governing equation of interest is given by

528 242

$$[M]\{\ddot{u}\} + [c]\{\dot{u}\} + [K]\{u\} = \{P\} \quad (8)$$

An incremental form of this equation, in which the material and geometrical nonlinearities are put to the right side of the equation, has been developed. This is the effective-load technique as discussed in the section under Modal Nonlinear Analysis.

The characteristics of Equation (8) are best defined in terms of its natural frequencies and mode shapes. For a continuous system, the frequency spectrum ranges from the lowest, or fundamental, frequency up to an infinite limit point. For a discretized system, the infinite limit point does not exist; instead, a frequency exists that corresponds to the most rapidly varying mode shape. This frequency is called the cutoff frequency. If the discretized system is excited by forcing functions having frequency content above the cutoff frequency, such as might be induced in a wave-propagation problem, random spatial noise is generated in the cutoff modal response.

The above implies that a limitation is placed on the rigorousness of the time-history analysis by the structural modeling, i.e., discretization of the continuous structural system. Any frequency content in the time-history input that is greater than the cutoff frequency of the structure is not needed. These frequencies may be filtered out by the use of the fast Fourier transform (FFT) with a frequency-domain filter, e.g., the Butterworth Filter. URS/Blume maintains a library of filtered, low-frequency input ground motion time histories obtained by the application of the above method.

For the time-history analysis of such a class of problems involving lower frequencies, longer time-integration steps may be used because the high-frequency response, which is numerically damped out by the larger time steps, is of no interest. The longer time steps will result in considerable computational economy.

The truncated time-domain analysis has an advantage in being the simplest extension of currently available computer programs. The approximation can be incorporated in existing nonlinear computer programs with a minimum of programming effort.

528 243

Response Spectrum Methods

All the response spectrum based analysis techniques available fall into the (SA/SM) category. For simple structures, the analyses can be readily executed by hand calculation, but, for typical building structures it is desirable to use computers for such calculations as eigenvalues, eigenvectors, and member stresses.

The response spectrum based methods also have the common feature of implementing an equivalent linear structure model to represent the nonlinear response of the structure. Fundamentally, this must be achieved by equating the energy demand placed on the structure and the energy capacity of the structure. The survivability of a structure is then established from the ratio of demand to capacity.

Substantial research has been devoted to the subject of developing simplified methods for predicting the nonlinear response of structures because limiting conventional structures' response to maximum probable earthquake motions has been recognized as impractical. In spite of the significant research thus far conducted, there are only four simplified procedures that have evolved in the literature and in general further research is still needed. These four procedures will be referred to as: the Reserve Energy Technique, the Approximate Inelastic Response Method, the Elastoplastic Spectrum Method, the Elastic Failure Analysis Method, and the Substitute Spectrum Method, and the Substitute Structure Method.

Following are discussions of the theoretical bases and applicabilities of each of these four simplified methods of nonlinear analysis.

Reserve Energy Technique (RET). This simplified nonlinear analysis procedure was developed by Blume in the 1950s[6,7] and has been expanded in the 1970s.[8] The philosophy and some of the theoretical basics include consideration of: (a) the extreme demands of the earthquake that can cause the greatest damage or collapse; (b) the peak spectral velocity at the period of interest to compute the critical kinetic energy demands; (c) energy reconciliation between the kinetic energy and damping (heat), strain (stored), and damage (work done); (d) structural characteristics in the inelastic range

that must be used for survival; (e) any deterioration or softening from repeated cycles of loading; (f) changes from initial dynamic response properties that occur in the later stages of the earthquake when survival may be in the balance; (g) all elements of resistance and work capacity (reserve energy absorption); and (h) the procedures in analysis that sacrifice rigor for the benefit of reasonable simplicity and are reasonably conservative.

The RET compares the demands of the earthquake with the capacity of the structure. The demand is characterized by response spectra, and the capacity is characterized by the structural strength and toughness characteristics. Two response spectra are required; one represents the level of elastic response with appropriate damping and the other represents the level of inelastic response that generally has a higher equivalent damping value. The nonlinear stiffness characteristics are estimated by determining various damage threshold lateral force-displacement limits. As various nonstructural and structural elements are damaged, the stiffness characteristics are degraded, and the step-by-step incremental force-displacement diagram is developed.

The basic approach of the Reserve Energy Technique is illustrated in the following three figures. Figure 1 shows an inelastic force-displacement model that represents an idealized interstory building stiffness. By assigning values to the various parameters, brittle, elastoplastic, and bilinear softening or hardening models can be created. The ductility ratio, μ, is defined to be Δ/Δ_y, and the ultimate ductility, μ_{ult} (i.e., Δ_{ult}/Δ_y), is the value corresponding to building failure.

For displacements greater than Δ_{ult}, failure is assumed. When Δ_{ult} equals Δ_y, the model is brittle and no inelastic energy-absorbing capacity is possible. The bilinear slope ratio, ξ, which is shown graphically in Figure 1, allows simulation of the inelastic properties that many structural materials possess. When ξ equals zero, the model is said to be elastoplastic. For ξ greater than zero but less than 1, the model is a bilinear softening type. Finally, if ξ is greater than 1, a bilinear hardening model is represented.

The relationship between demand, D, capacity, C, and the bilinear parameter, ξ, with the ductility ratio, μ, is based on equating the energy absorbed by

528 245

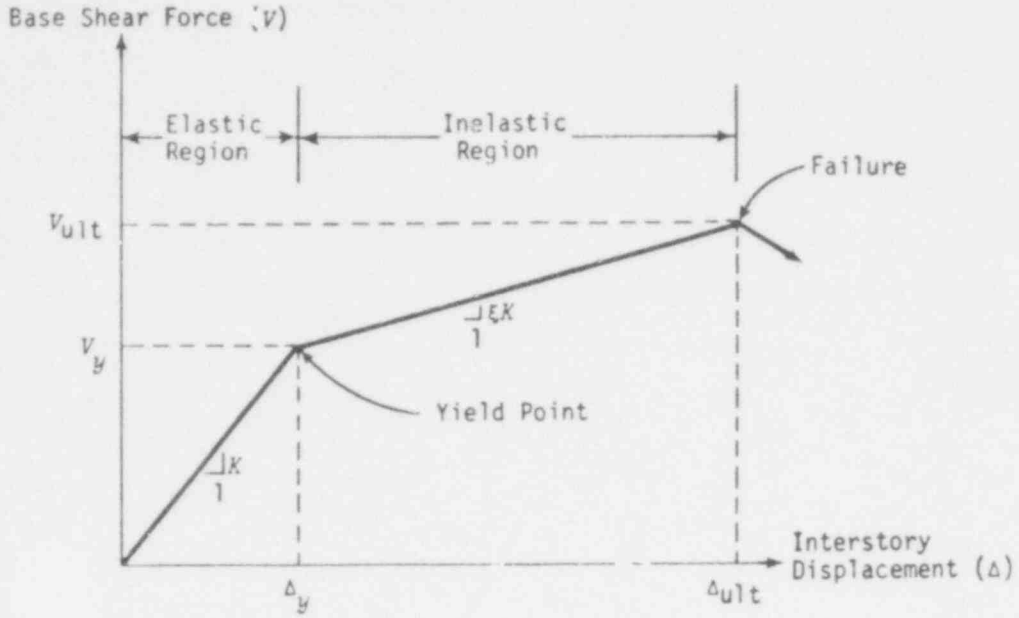

FIGURE 1 INTERSTORY INELASTIC FORCE-DISPLACEMENT MODEL

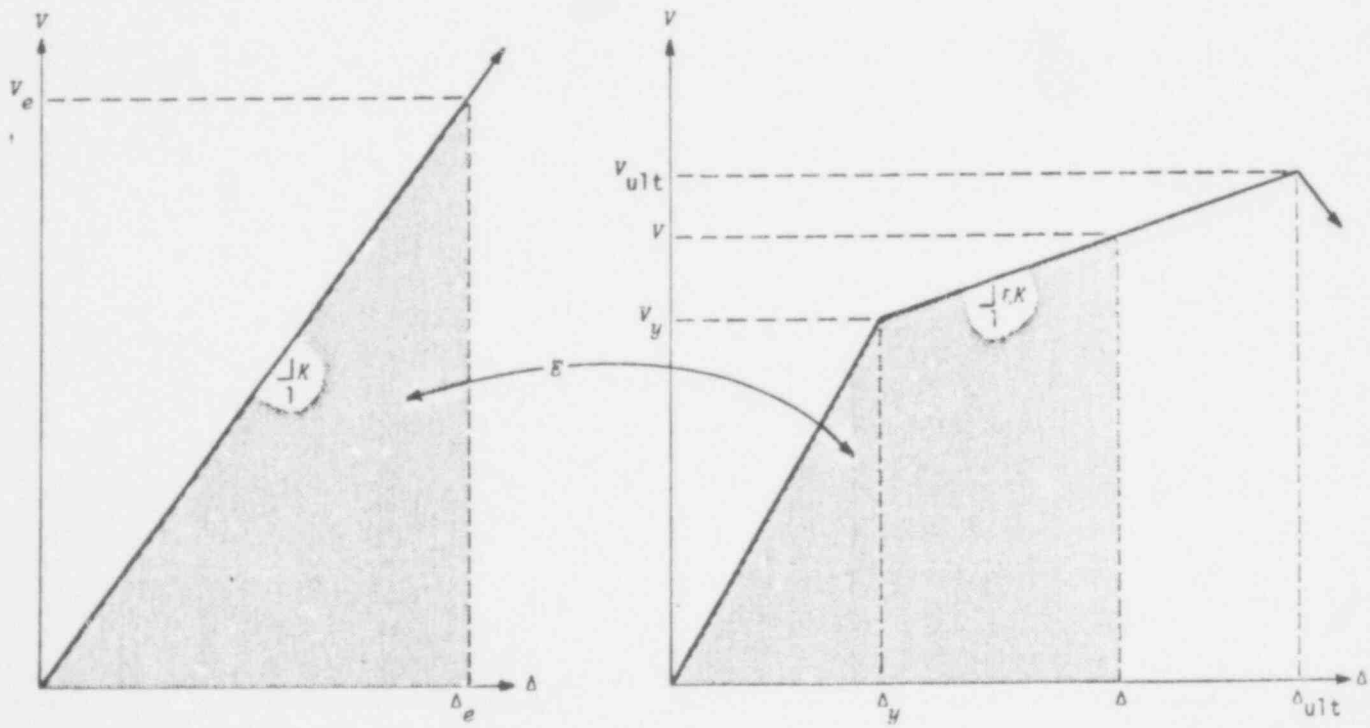

(a) Elastic Demand Model

(b) Inelastic Capacity Model

FIGURE 2 DEMAND AND CAPACITY ENERGY MODELS

528 246

the inelastic capacity model with an assumed perfectly elastic demand model. The governing assumption is that the amount of energy absorbed by the building is independent of whether the building responds elastically or inelastically. Figure 2 shows the demand and capacity models from which the relationship for ductility, μ, can be obtained. From Figure 2 the expressions for the energy, represented by the areas under the elastic and inelastic curves, are obtained as follows:

For the elastic demand model:

$$E = \frac{1}{2} \frac{V_e^2}{K} \tag{9}$$

For the inelastic capacity model:

$$E = \frac{1}{2} \frac{V_y^2}{K} + \left(\frac{V + V_y}{2} \right) \left(\Delta - \Delta_y \right)$$

but

$$V = K\Delta_y + (\Delta - \Delta_y) \xi K$$

and

$$\mu = \Delta / \Delta_y$$

hence

$$E = \frac{1}{2} \frac{V_y^2}{K} [2(\mu - 1) + (\mu - 1)^2 \xi + 1] \tag{10}$$

Equating Equations (9) and (10), the relationship for ductility, μ, is:

$$\mu = 1 - \frac{1}{\xi} + \sqrt{\frac{1}{\xi} \left[\frac{1}{\xi} + \left(\frac{V_e}{V_y} \right)^2 - 1 \right]} \tag{11}$$

528 247

Note that V_e/V_y is just D/C where demand is D and capacity is C, and both are expressed in consistent spectral response units. Finally, the relationship for ductility becomes:

$$\mu = 1 - \frac{1}{\xi} + \sqrt{\frac{1}{\xi}\left[\frac{1}{\xi} + \left(\frac{D}{C}\right)^2 - 1\right]} \qquad (12)$$

Note that for the elastoplastic case, ξ is equal to 0, and Equation (12) becomes:

$$\lim_{\xi \to 0} \mu = \frac{1}{2}\left[\left(\frac{D}{C}\right)^2 + 1\right] \qquad (13)$$

or

$$\frac{D}{C} = \sqrt{2\mu - 1} \qquad (14)$$

Figure 3 shows a hypothetical demand curve superimposed on an elastoplastic capacity curve. The example given in Figure 3 illustrates the application of the Reserve Energy Technique. Importantly, the example shows the increased story drift realized because of the inelastic response. This is important for establishing damage associated with inelastic response.

In general, the procedure is applicable to complex multimass systems and guidelines are given in Reference 7. Because of the very general formulation of the procedure, any shape capacity curve can be accommodated. It has been determined that the application of the RET would have predicted some of the serious damage in Southern California in 1971. Its application after the event seems to reproduce the effects of the 1971 San Fernando earthquake reliably on all structures investigated.[9]

Approximate Inelastic Response Method. This procedure, developed by Freeman, et al.,[10,11,12] is similar to the Reserve Energy Technique except that a graphical solution, based on the intersection of the demand response spectrum curve and the structure capacity curve, is used instead of energy calculations. The capacity of the structure is determined by performing an elastic analysis with some bilinear approximations. The demand of the ground shaking is represented by response spectra at two or more values of critical damping. Capacity and demand are reconciled by a graphical solution that accounts for changes in both the apparent response periods of vibration and percentages of critical damping.

528 248

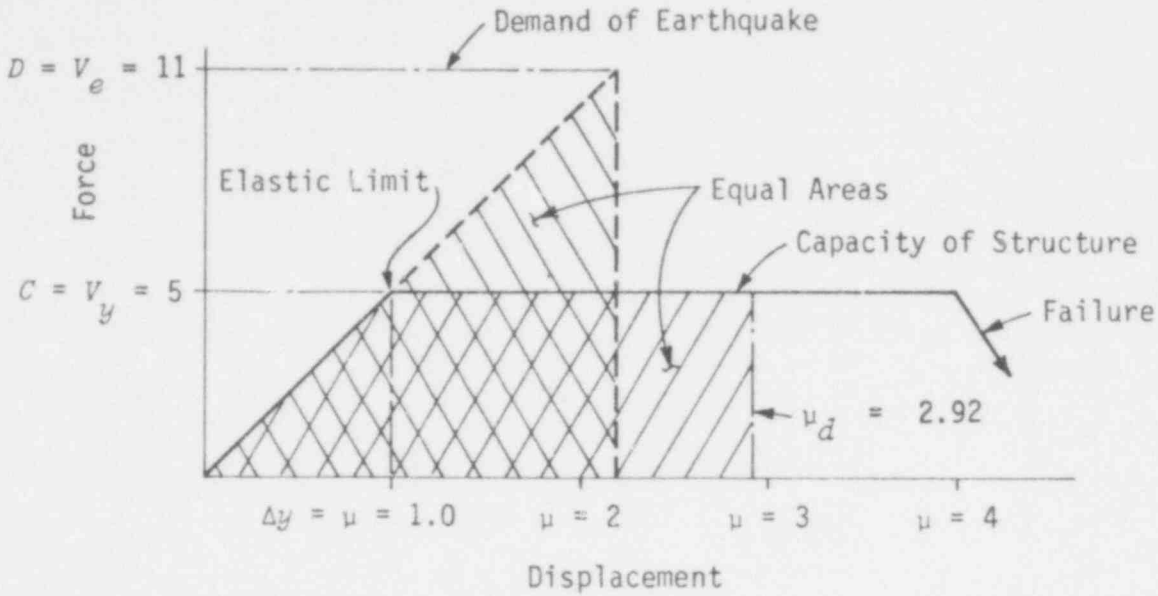

Example:

Demand of earthquake is at force level, $D = 11.0$

Elastic capacity of structure is $C = 5.0$

Idealized capacity of structure is elastic-plastic, as shown.

Energy (or work) equals areas under curves

Elastic limit displacement, Δy, represents a ductility, μ, of 1.0

The ductility demand, $\mu_d = \frac{1}{2}\left[\left(\frac{D}{C}\right)^2 + 1\right] = 2.92$

or $(D/C) = \sqrt{2\mu - 1}$

If the structure has a ductility capacity greater than 2.92, it survives the earthquake without collapse.

FIGURE 3 RESERVE ENERGY TECHNIQUE: DEMAND AND CAPACITY RECONCILIATION

528 249

The procedure requires the determination of two curves, one representing the capacity of the structure and the other representing the demand of the ground shaking, described here by spectral acceleration (S_a) and response periods of vibration (T). (Other terms, such as spectral displacements, roof displacements, and base shear coefficients, could also be used). Only the fundamental mode of vibration are explicitly considered, but the effects of the higher modes can be estimated.

The capacity characteristics of the structure are determined in much the same way as in the Reserve Energy Technique -- either by simple hand methods or by more complex computer analysis methods, depending on the complexity of the structure and the accuracy required. First, the elastic capacity threshold[13] is determined in terms of spectral acceleration, spectral displacement, and fundamental period of vibration. A mathematical model is developed that best represents the structure at this amplitude of lateral motion. Periods and participation factors are calculated. The lateral force that causes a substantial number of major members to yield is determined. The amplitude of force may be represented by a base-shear coefficient, a lateral roof displacement, or a lateral roof acceleration. These values can then be converted to spectral values by using the participation factors.

Next, the characteristics of the structure beyond the elastic range are estimated. A new mathematical model is developed; it is similar to the elastic model except that all the yielding members are assigned stiffness properties that are greatly reduced. For example, if all the girders on several or all the floors are assumed to be yielding, the moments of inertia of these girders might be reduced to 5% of the elastic values in order to approximate a bilinear effect. For this new mathematical model, a set of periods and participation factors are calculated, and the lateral force that is required to cause a more extreme failure condition is determined. This failure condition may be due to additional members yielding, members exceeding their ductility capacity, brittle failures, excessive displacements, or instability. Several intermediate thresholds may be determined depending on the conditions of the problem. Each step is represented by segmental values of period of vibration, spectral acceleration (ΔS_a), and spectral displacement (ΔS_d).

528 250

Figure 4 plots capacity spectral acceleration and spectral displacement values, that are somewhat equivalent to a force (represented by acceleration) versus displacement curve, where the slope represents the stiffness of the structure. The cumulative values of spectral accelerations (S_a) and spectral displacements (S_d) can be used to calculate an effective period of vibration (T_{eff}) for the multilinear system by using Equation (15).

$$T_{eff} = 2\pi \sqrt{\frac{S_d}{S_a\,(g)}} \qquad (15)$$

Figure 5 plots the effective period and capacity spectral acceleration values.

The demand characteristics of the ground shaking are represented by response spectra. These spectra can either be standard shapes scaled to the site, spectra developed especially for the site, or spectra obtained from recorded ground shaking. At least two values of damping are required, one representing the elastic structure, and the other representing the structure at its maximum inelastic excursions. It is assumed that effective damping varies somewhat linearly between these two conditions.

Having established the capacity characteristics and the demand characteristics, the two sets of data are plotted on the same graph; their intersection is considered to be the reconciliation between demand and capacity,[10] as shown in Figure 6, and represents the predicted maximum response of a structure for a particular earthquake. If the intersection is below the elastic capacity, no structural damage is anticipated. If the two curves do not intersect because the demand exceeds the maximum capacity of the structure, irreparable damage or collapse of the structure is anticipated. However, if the intersection is within the inelastic region of the capacity curve, the maximum response, period, damping, percentage of damage, ductility demand, and reserve capacity can be estimated. The peak spectral acceleration and period are obtained directly from the graph, and the damping is interpolated between the two damped response spectrum curves. The percent of damage is interpolated along the inelastic portion of the capacity curve (in Figure 6, $[x/y] \times 100\%$). The spectral acceleration and period are used to obtain the spectral displacement by use of Equation (15). This spectral displacement is

523 251

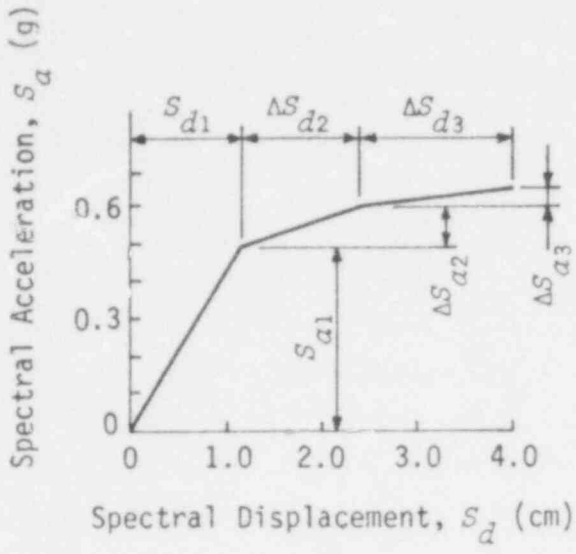

FIGURE 4 CAPACITY: SPECTRAL ACCELERATION VERSUS SPECTRAL DISPLACEMENT

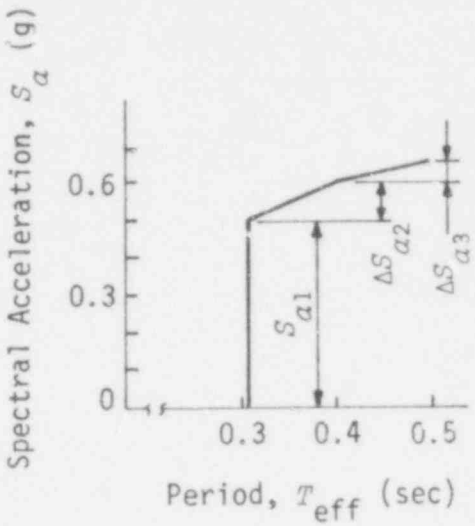

FIGURE 5 CAPACITY: SPECTRAL ACCELERATION VERSUS EFFECTIVE PERIOD

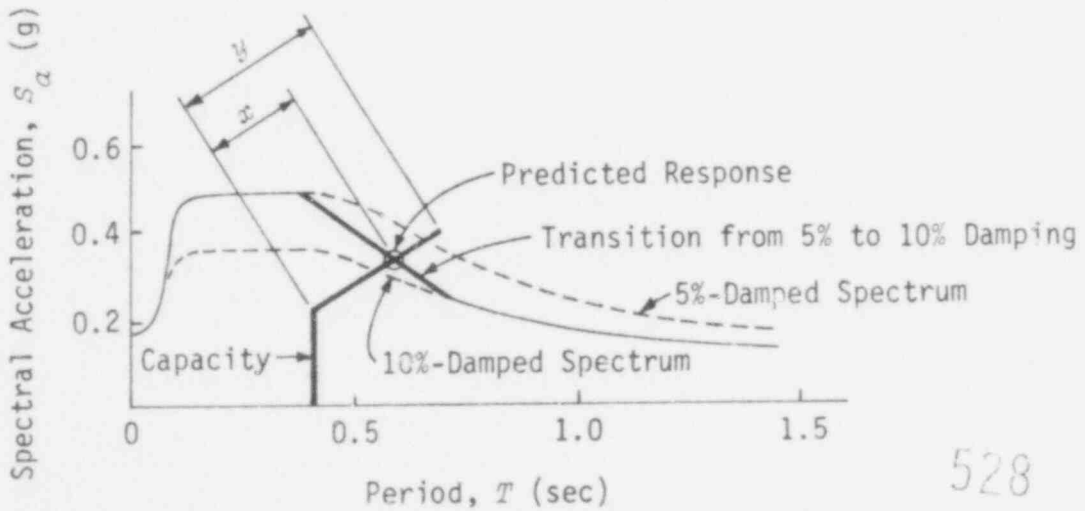

528 252

FIGURE 6 CAPACITY AND DEMAND, SPECTRAL ACCELERATION VERSUS PERIOD

compared to the elastic and maximum spectral displacements (e.g., Figure 4) to estimate ductility demands and reserve capacities.

The procedure is proposed as a reasonable approximation of inelastic response of structures to earthquake ground motion. Comparison of the results of simplified and rigorous analyses of two high-rise buildings subjected to severe ground motion during the San Fernando 1971 Earthquake[11] indicate that the procedure is reasonably reliable. The analyses conducted thus far illustrate clearly and simply that although the demand spectral acceleration for an elastic model of a structure may greatly exceed the elastic capacity, the structure can survive the earthquake motion due to the inelastic response characteristics.

Elastoplastic Spectrum Method. This procedure, initially developed by Newmark[14] and later restated by Newmark and Hall,[15] is conceptually the simplest of the simplified procedures that have been proposed. Only an elastoplastic spectrum has been presented in the literature but equivalent inelastic spectra for other materials could be developed as well.

For reference, Figure 7 is an example of typical elastic design spectra showing the ground motion amplitudes and response amplifications of acceleration, velocity, and displacement over the given frequency range for various damping values.

To use the design spectrum to approximate inelastic behavior, the following suggestions are made by the authors.[15] In the amplified displacement region of the spectra, the left-hand side, and in the amplified velocity region, at the top, the spectrum remains unchanged for total displacement, and is divided by the ductility factor to obtain yield displacement or acceleration. The upper right-hand portion sloping down at 45°, or the amplified acceleration region of the spectrum, is relocated for an elasto-plastic resistance curve, or for any other resistance curve for actual structural materials, by choosing it at a level which corresponds to the same energy absorption for the elasto-plastic curve as for an elastic curve shown for the same period of vibration. The extreme right-hand portion of the spectrum, where the response is governed by the maximum ground acceleration, remains at the same acceleration level as for the elastic case, and therefore at a corresponding

528 253

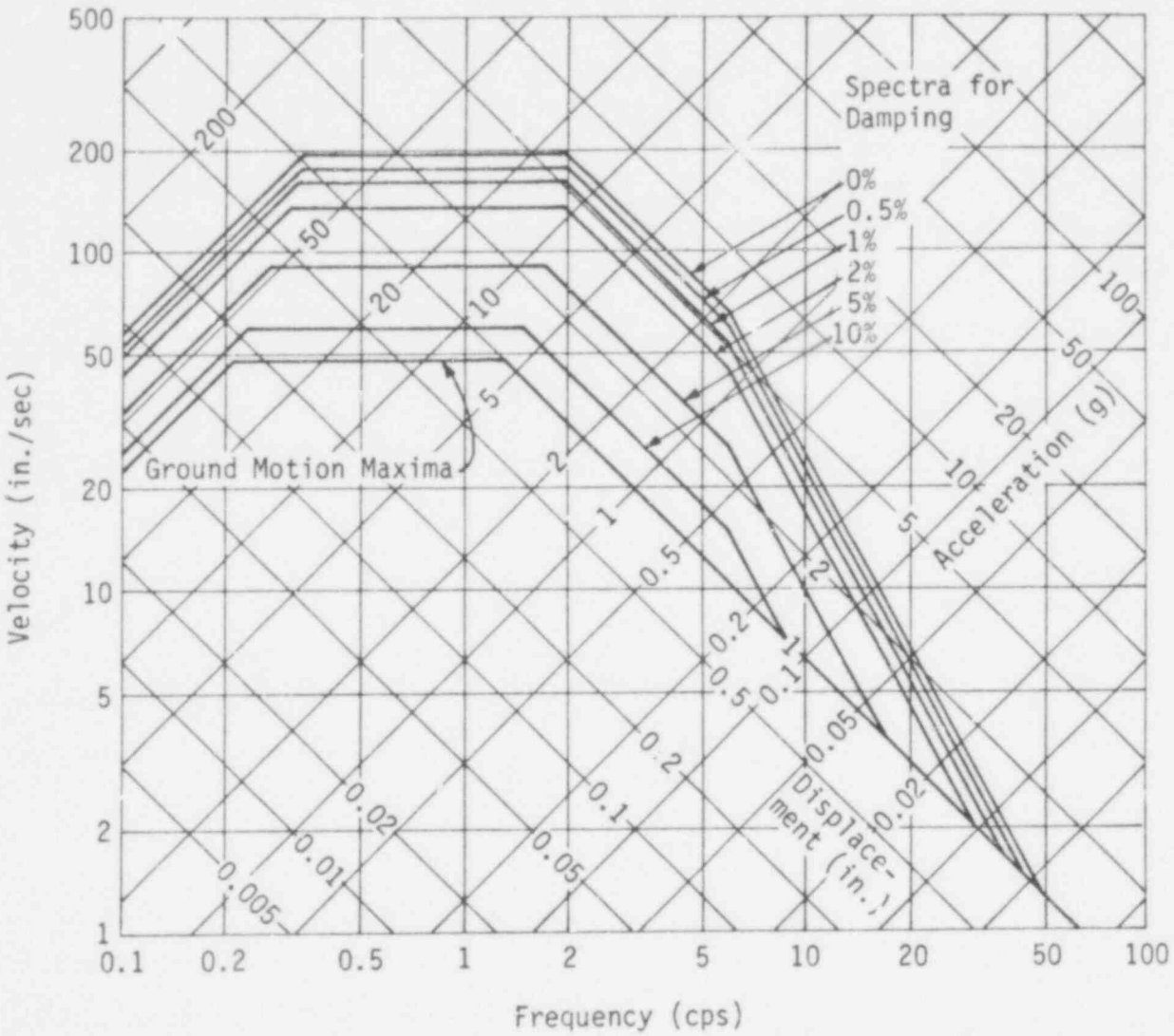

FIGURE 7 BASIC DESIGN SPECTRA NORMALIZED TO 1.0g

528 254

increased total displacement level. The frequencies at the corners are kept at the same values as in the elastic spectrum. The acceleration transition region of the response spectrum is now drawn also as a straight line transition from the newly located amplified acceleration line and the ground acceleration line, using the same frequency points of intersection as in the elastic response spectrum.

In all cases the "inelastic maximum acceleration" spectrum and the "inelastic maximum displacement" spectrum differ by the factor μ at the same frequencies. The design spectrum so obtained is shown in Figure 8, for 2% damping, for an elasto-plastic system with a ductility factor of 5. Both the maximum displacement and maximum acceleration bounds are shown, for comparison with the elastic response spectrum.

The solid line $DVAA_o$ shows the elastic response spectrum. The heavy circles at the intersections of the various branches show the frequencies which remain constant in the construction of the inelastic design spectrum.

The dashed line $D'V'A'A_o$ shows the inelastic acceleration, and the line $DVA''A''_o$ shows the inelastic displacement. These two differ by a constant factor $\mu = 5$ for the construction shown, but A and A' differ by the factor $\sqrt{2\mu - 1} = 3$, since this is the factor that corresponds to constant energy, as indicated in Reference 14.

The authors also point out that the elastoplastic or other inelastic response spectra can be used only as an approximation for multi-degree-of-freedom systems.

Although conceptually simple, application of the Elastoplastic Spectrum Method requires about as much rigor in establishing force-displacement relationships and in constructing mathematical models for calculating deformations, stresses, ductility capacities, etc., for complex multimass systems as the two methods described previously. 528 25

Substitute Structure Method. This method is based on experimental observations of the inelastic response behavior of single-degree-of-freedom structures.[16] Proposed by Shibata and Sozen,[17] the Substitute Structure Method is presented as a design (and not an analysis) procedure. However, the proce-

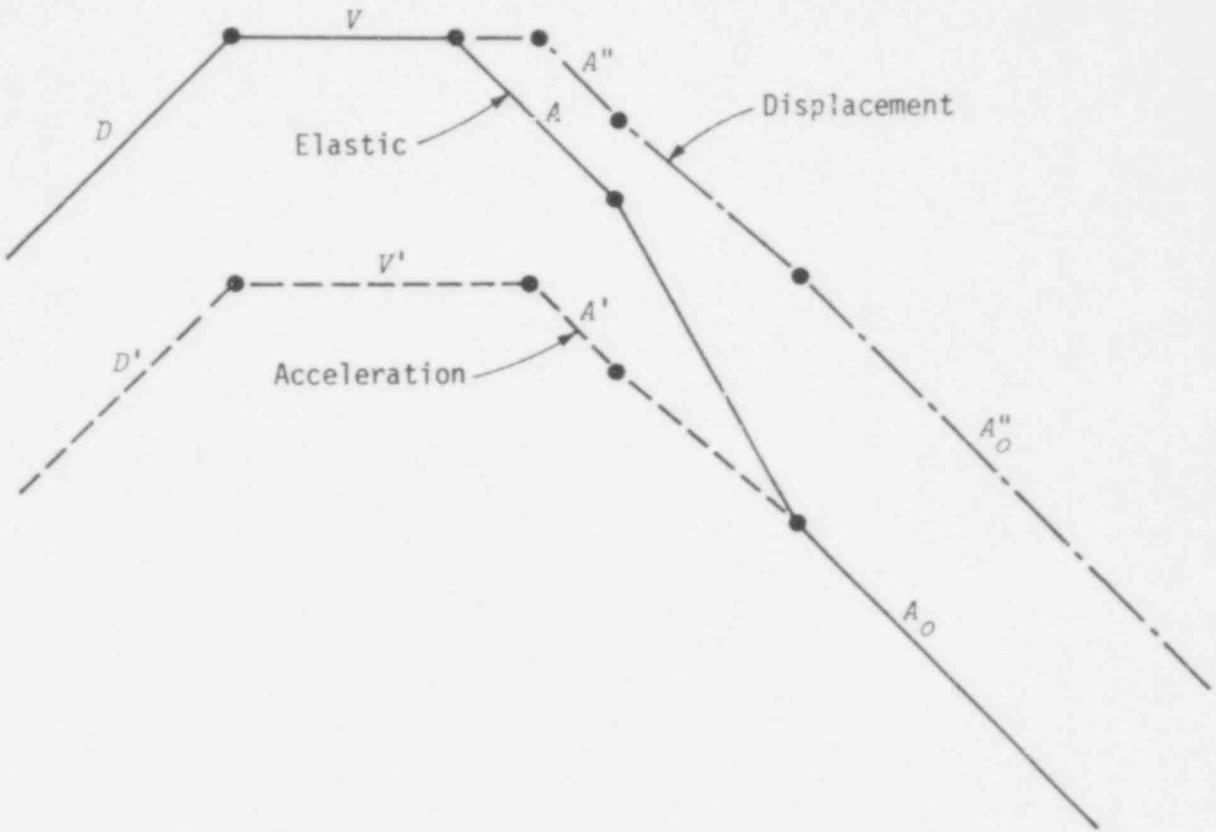

FIGURE 8 ELASTOPLASTIC DESIGN SPECTRA

528 256

dure has many aspects that are similar to the above procedures and can be used to supplement them.

The substitute-structure method is a procedure for determining the design forces, corresponding to a given type and intensity of earthquake motion represented by an elastic design spectrum, for a reinforced concrete structure. The objective of the method is to establish the minimum strengths the components of the structure must have, so that a tolerable response displacement is not likely to be exceeded.

The central and significant feature of the substitute-structure method is that it provides a simple vehicle for taking account of inelastic response of reinforced concrete in the design of multidegree-of-freedom structures. The specific advantages are: (1) Use of linear-response models for dynamic analysis; (2) choice in setting limits of tolerable response in different elements of the structure; and (3) deliberate consideration of displacements in the design process.

Main characteristics of the substitute-structure method are: (1) definition of a substitute frame, with its stiffness and damping properties related to but differing from the actual frame; and (2) calculation of design forces from a modal spectral analysis of the substitute frame using a linear-response spectrum (or from a linear-response-history analysis for a given ground motion). The operations may be divided into three steps: (1) Based on tolerable limits of inelastic response, determine the stiffnesses of the substitute-frame members; (2) calculate modal frequencies and damping factors for the substitute structure; and (3) determine design forces.

Details of the procedure for each step are described by the authors[17] as follows.

It is assumed that preliminary member sizes of the actual structure are known from gravity-load and functional requirements, precedent, or a previous trial.

Substitute Structure. The flexural stiffnesses of substitute-frame elements are related to those of actual-frame elements in accordance with

257

$$(EI)_{si} = \frac{(EI)_{ai}}{\mu_i} \tag{16}$$

in which $(EI)_{si}$ and $(EI)_{ai}$ are cross-sectional flexural stiffnesses of the element, i, in the substitute and actual frame, respectively; and μ_i is the selected tolerable "damage ratio" for element i.

Physical interpretation of the damage ratio for a particular condition, a moderately reinforced slender beam subjected to antisymmetrical end moments, is shown in Figure 9. The solid curve in Figure 9(c) represents the relationship between the applied moment, M, and the end rotation, θ, caused by flexural deformation within the span.

The term, $(EI)_a$, is calculated using the fully cracked section (linear stress-strain curves and no tensile strength for concrete). The M-θ curve, based on $(EI)_a$, corresponds approximately to a line drawn from the origin to the "yield point" of a section with compactly placed tensile reinforcement having a definite yield stress. The damage ratio, μ, sets a lower slope and implies that a rotation, approximately $\mu\theta_y$, will be attained if the effective or average stiffness of the member is changed as indicated in Equation (16). In that respect, the damage ratio, μ, is comparable to but not exactly the same as "ductility" based on the ratio of maximum to yield rotation. Quantitatively, damage and ductility ratios are identical only for elastoplastic response. It must be emphasized that a damage ratio of six requires a larger ratio of "ductility" based on curvature or strain in members with moment gradients.

Choice of tolerable damage ratios for structural elements is governed by the nature, cost, and function of the entire building as well as by the type and detailing of the elements. Recommendation of specific values was beyond the scope of the authors' presentation. To permit quantitative demonstrations, it will be assumed that the tolerable damage ratio is six based on relative story deflection of frames with rigid beams; and one for columns and six for beams of frames with flexible beams. Note that members with damage ratios exceeding one must be detailed for sustained resistance through many cycles of response to the anticipated inelastic displacement.

528 258

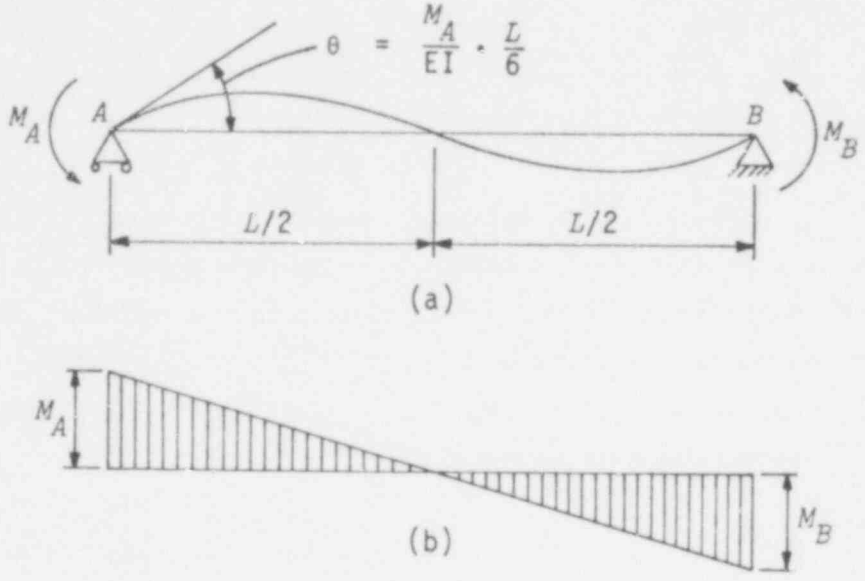

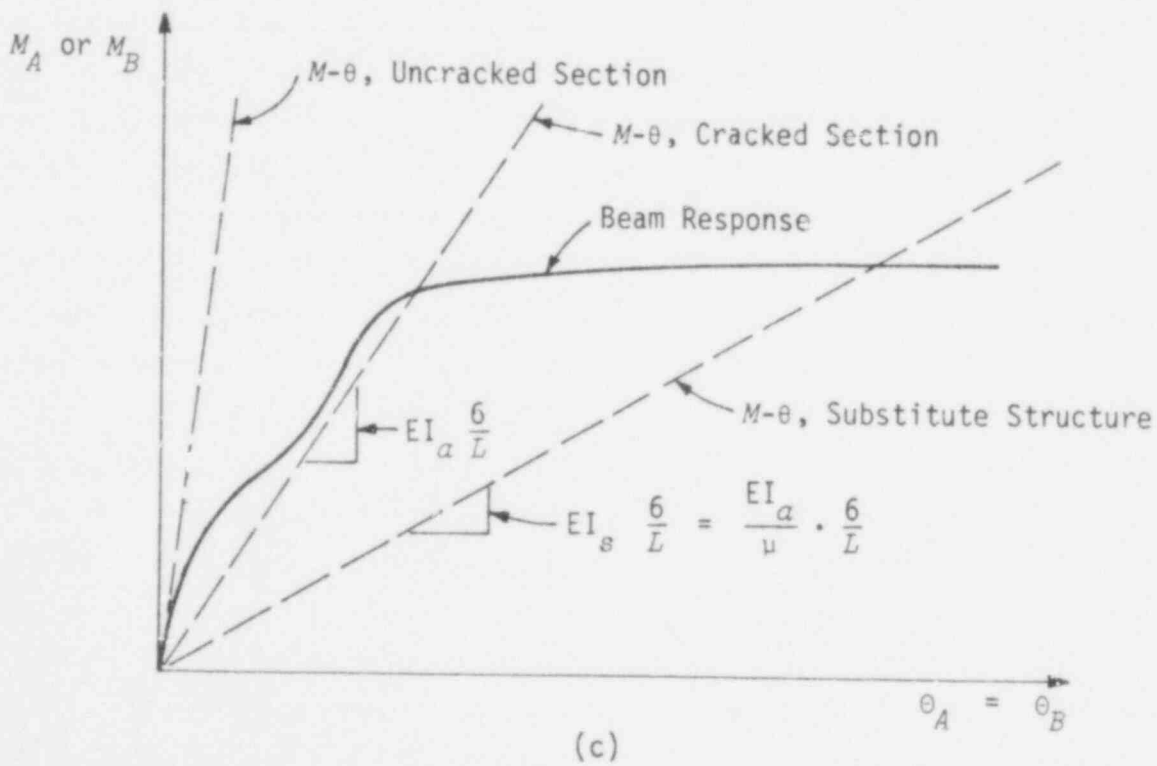

528 259

FIGURE 9 SUBSTITUTE STRUCTURE: INTERPRETATION OF DAMAGE RATIO

Modal Frequencies and Damping Factors. Periods or frequencies, mode shapes, and modal forces for the undamped substitute structure are obtained from a linear dynamic analysis.

The modal damping factors for the substitute structure are calculated as described in the following.

It was observed[16] that the maximum inelastic earthquake response of single-degree-of-freedom reinforced concrete systems could be estimated by analyzing a linear model with reduced stiffness and a substitute damping factor related to the damage ratio approximately as follows:

$$\beta_s = 0.2 \left\{1 - \left[\frac{1}{(\mu)^{1/2}}\right]\right\} + 0.02 \qquad (17)$$

in which β_s = substitute damping factor, and μ = damage ratio.

Equation (17) is based on dynamic tests of reinforced concrete elements[18] and one-story frames.[16] The form of the expression was derived[16] from a model by Jacobsen.[19] It provides a quantitative estimate of β_s (to be used with a linear-response spectrum calculated for a viscous damping factor numerically equal to β_s) to simulate the observed effect of hysteretic damping in a reinforced concrete element subjected to earthquake excitation.

If the individual elements of a frame are designed for different values of μ, individual values of β_s have to be combined to obtain a single "smeared" value for use in modal analysis. In the substitute-structure method this is done by assuming that each element contributes to the modal damping in proportion to its relative flexural strain energy associated with the mode shape:

$$\beta_m = \sum_i \frac{P_i}{\Sigma P_i} * \beta_{si} \qquad (18)$$

$$P_i = \frac{L}{6(EI)_{si}} (M_{ai}^2 + M_{bi}^2 - M_{ai}M_{bi}) \qquad (19)$$

528 260

in which β_m = smeared damping factor for mode m; L = length of frame element; $(EI)_{si}$ = assumed stiffness of substitute-frame element i; and M_{ai} and M_{bi} = moments at ends of substitute-frame element i for mode m.

An alternate method of obtaining modal damping factors for the substitute structure is provided by elements with complex stiffness[20,21]

$$k_{si} = \frac{k_{ai}}{\mu_i} [1 + 2\beta_{si} * (-1)^{1/2}] \tag{20}$$

in which k_{si} = stiffness of substitute-frame member i; k_{ai} = stiffness of actual frame member i; μ_i = tolerable damage ratio for member i; and β_{si} = substitute damping for member i from Equation (17).

Dynamic equilibrium of the entire substitute structure can then be expressed by

$$[M]\{\ddot{u}\} + ([K_1] + [K_2] * (-1)^{1/2})\{u\} = \{0\} \tag{21}$$

in which $[M]$ represents the mass matrix, $[K_1]$ and $[K_2]$ represent the real and imaginary parts of the stiffness matrix; and u refers to the displacements. Modal frequencies and damping factors are determined by solving for eigenvalues of the complex matrix.

Both methods give closely comparable answers. The method based on strain energy was recommended because of its simplicity and because of its direct relationship to the physical interpretation of the substitute structure.

Design Forces. Design forces in individual elements are based on the root-sum-square combination amplified by a factor given in terms of the base shear

$$F_i = F_{irss} * \frac{V_{rss} + V_{abs}}{2\ V_{rss}} \tag{22}$$

528 261

in which F_i = design force in element i; F_{irss} = square root of the sum of the squares (RSS) of the modal forces for member i; V_{rss} = base shear based on RSS of modal base shears; and V_{abs} = maximum value for absolute sum of any two of the modal base shears.

To reduce the risk of excessive inelastic action in the columns, the authors recommend that the design moment from Equation (21) should be amplified for columns by a factor of 1.2. This factor is, of course, of no consequence for the analysis of an existing structure but is important for design.

The Substitute Structure Method appears to be among the most highly developed of the simplified methods. The method is based on specific experimental data from single-degree-of-freedom structure tests and the multi-degree-of-freedom extension has been verified with rigorous analytical nonlinear tests using the SAKE computer program. The proposed method can be used to determine earthquake design force requirements for individual elements of a R/C structure given a design linear response spectrum and explicit decisions regarding tolerable inelastic response; with the option of different limits of inelastic response in different structure elements. As with all the simplified methods however, virtually no guidance has been provided regarding relationships between ductility and damage.

528 262

RIGOROUS NONLINEAR ANALYSIS PROCEDURES

Refined (rigorous) nonlinear computational procedures, for the dynamic analysis of various structures subjected to earthquake excitation, generally involve the step-by-step integration of the equations of motion, dividing the response history into short time increments and assuming the properties of the structure to remain constant during each increment but changing in accordance with the deformation state existing at the end of the increment. Thus the nonlinear analysis procedure is actually a sequence of linear analysis of a successively changing structure. The structures are usually discretized with a group of finite elements.

There are several nonlinear analysis programs available to industry. These may broadly be classified into two categories. The first type includes programs developed at universities under grants from different government organizations and private foundations. These programs are generally available to the public. The second type of computer programs are those developed and maintained by private companies. The well known programs--both public and private--are described below. Each of these will be categorized on the basis of underlying assumptions, limitations and applicability to the nonlinear dynamic analyses of nuclear power plant structures subjected to earthquake excitations.

General Purpose Rigorous Programs

NONSAP.[22] This is a finite-element structural analysis program for the static and dynamic response of nonlinear systems developed at the University of California, Berkeley. The system response is calculated using an incremental solution of the equation of motion with Wilson or Newmark time-integration methods. Before the time integration is carried out, the constant structure matrices, namely the linear effective stiffness matrix, linear stiffness, mass and damping matrices, whichever are applicable, and the load vectors are assembled and stored on low-speed storage. During the step-by-step solution the linear effective stiffness matrix is updated for the nonlinearities in the system. Therefore, only the nonlinearities are dealt with in the time integration and no efficiency is lost in linear analysis.

528 263

The incremental solution scheme used corresponds to a modified Newton iteration. To increase the solution efficiency, the user can specify an interval of time steps in which a new effective stiffness matrix is to be formed and an interval in which equilibrium iterations are to be carried out.

The structural system to be analyzed may be composed of a number of different finite elements. The program presently contains the following element types: (a) three-dimensional truss element, (b) two-dimensional plane stress and plane strain element, (c) two-dimensional axisymmetric shell or solid element, (d) three-dimensional solid element, (e) three-dimensional thick shell element.

The nonlinearities may be due to large displacements, large strains, and nonlinear material behavior. The material descriptions presently available are: (1) for the truss elements: (a) linear elastic, (b) nonlinear elastic; (2) for the two-dimensional elements: (a) isotropic linear elastic, (b) orthotropic linear elastic, (c) Mooney-Rivlin material, (d) elastic-plastic materials, von Mises or Drucker-Prager yield conditions, (e) variable tangent moduli model, (f) curve description model (with tension cut-off); (3) for the three-dimensional elements: (a) isotropic linear elastic, (b) curve description model.

Geomteric nonlinearities may be included for all the elements except the three-dimensional element types. The forcing function is prescribed as a load-history at any particular node.

NONSAP has quite a few limitations so far as its application to the present study is concerned. First, it does not have a facility for ground motion, i.e., acceleration time history input, which is the standard forcing function for earthquake excitations. Second, there are several limitations on the material properties available. For example, the truss element does not have a bilinear model load-deformation relationship with the consideration of buckling in compression. Also, there is no concrete-type material property with tension cut-off for the three-dimensional elements.

ADINA.[23] This program, which is basically an extension of the program *NONSAP*,

528 264

is currently in the development stage at M.I.T. and was released a few months ago. It is, however, not in the public-domain. Several material models, including creep and thermal phenomena, are being incorporated in the program. There is also a concrete material model for both two-dimensional isoparametric elements and three-dimensional solid elements. The concrete model basically uses a parabolic curve to approximate the uniaxial stress-strain curve in compression, and a straight line to approximate the stress-strain relationship in tension. The parameters required to define the stress-strain relationship are obtained from uniaxial test data.

The loading history is generally given as a force history at a node. This imposes a severe restriction on the use of the program since earthquake records are generally measured as acceleration time histories of the ground motion.

ANSR.[24] This is a general-purpose program for analysis of nonlinear structural response developed at the University of California, Berkeley. Various geometric and material nonlinear models are incorporated. At present, the following elements are available: (a) 3-dimensional truss element, (b) 2-dimensional 4- to 8-node finite element for plane stress, plane strain, and axisymmetric analysis. Nonlinearities are introduced at the element level only and may be due to large displacements, large strains, and/or nonlinear materials.

For the truss element, two alternative modes of inelastic behavior may be specified, namely (1) yielding in both tension and compression and (2) yielding in tension and elastic buckling in compression.

The two-dimensional element may have several types of material properties such as (1) isotropic linearly elastic, (2) orthotropic linearly elastic and (3) isotropic elastic-perfectly plastic with von Mises yield function.

The dynamic response is computed by stepwise time integration of the incremental equations of motion using Newmark's operator. The dynamic loading may consist of earthquake ground accelerations, time dependent nodal loads, and prescribed initial values of the nodal velocities and accelerations. The very

528 265

small element library limits its application to very simple structures only.

DRAIN 2-D.[25] This program computes the dynamic response of inelastic two-dimensional structures of arbitrary configuration subjected to earthquake-type ground motions. Independent horizontal and vertical excitation may be specified, but out-of-phase support motions cannot be considered. Static loads may be applied to the structure prior to the application of the dynamic loading, but no yielding is permitted under these loads.

The structure may be composed of elements of a variety of types, each having a different behavior pattern and yielding characteristics. Five different element types have been incorporated into this version of the program, namely, (a) truss, (b) beam-column, (c) shear (infill) plane, (d) semirigid connection, and (e) degrading stiffness reinforced concrete beams. Geometric nonlinearities may be included for the truss and beam-column elements.

The structure is idealized as a planar assemblage of discrete elements. Analysis is by the direct-stiffness method with the nodal displacements as unknowns. The dynamic response is determined by step-by-step integration, with a constant-acceleration assumption within any step. The tangent stiffness of the structure is used for each step, and linear structural behavior is assumed during the step. Viscous damping of mass-dependent and/or stiffness-dependent type may be specified.

DRAIN 2-D may be applied to any type of two-dimensional frame. Many of the factors that are frequentiy encountered in the seismic analysis of two-dimensional frames may be included in the analysis, e.g., (a) semirigid beam-column joints, (b) unsymmetrically distributed flexural strengths at the ends of beam elements, (c) axial deformations and axial load-bending moment interaction in columns, (d) compression buckling in slender diagonal braces, (e) P-Δ effect in columns, and (f) brittle failure in shear panel elements.

In general, the turbine building of a nuclear power facility consists of a combination of ductile-frame and shear-wall elements. It is possible to uncouple the responses of the building due to seismic input in the transverse or longitudinal directions and thus idealize the stucture as a two-dimensional

frame. This idealized structure can then be analyzed by DRAIN-2D, which has very elaborate constitutive relationships for ductile elements.

For example, the truss bar element, which may be used as diagonal braces, may yield in tension and yield or buckle elastically in compression. The beam-column element may have variable cross section and strength and yields through the formation of concentrated plastic hinges at its ends. Interaction between axial force and moment may be taken for cross sections of steel or reinforced concrete type.

The major assumption of the DRAIN-2D program is the constant-acceleration assumption within any time step for the step-by-step integration of the dynamic response. If vibration modes with periods that are short in comparison with the time step are present, the response computed for these modes will be grossly inaccurate with respect to variation with time but will have amplitudes of the correct order of magnitude. For vibration modes with longer periods, the response computed by the constant-acceleration method is sufficiently accurate. Greater accuracy can be expected as the integration time step is reduced.

The input to DRAIN-2D is fairly simple, and the program is not very expensive. Moreover, the program is structured in such a fashion that new elements and constitutive relationships may be incorporated without much trouble.

SAKE.[26] This special-purpose computer program was developed to analyze the inelastic behavior of a multistory, reinforced concrete frame structure subjected to an intense earthquake motion in one horizontal direction. A structure on a rigid foundation may consist of more than one regular rectangular unbraced plane frame with an arbitrary number of bays and stories.

An equivalent spring model is used in the program to stimulate the inelastic flexural deformation of a member. The analytical model recognizes stiffness changes caused by cracking of the concrete, yielding of the reinforcement, and stress reversals. Hysteresis rules for the flexural behavior of a reinforced concrete member under load reversals are adopted after Takeda.

In addition to inelastic flexural deformation, a deformation caused by bond

528 267

slip of the longitudinal reinforcement within a joint core is considered, represented by another inelastic rotational spring. Step-by-step numerical integration procedures are used to obtain the building response. Axial and shear deformations of a member are ignored. All mass at a floor level is assumed to be concentrated outside the structure and linked to the floor levels by rigid truss elements. Ground motion is considered only in one horizontal direction parallel to the plane of frames.

DRAIN-TABS.[27] This is a computer program for obtaining the inelastic earthquake response of three-dimensional buildings. This program has been developed at the University of California, Berkeley and is an extension of the program DRAIN-2D.

The building is idealized as a series of independent plane substructures interconnected by horizontal rigid diaphragms. Each substructure can be of arbitrary geometry and include structural elements of a variety of types. It is not necessary for all substructures to connect to all diaphragms, so that structures with independent diaphragms at some levels can be idealized. The analysis makes use of substructuring techniques to improve computational efficiency.

The major limitation is that the coupling of the substructures though common columns is not fully taken into account, so that the idealization is not suitable for tube-type buildings.

The program consists of a "base" program which reads and prints data for the structure and its loading, allocates storage, carries out a variety of bookkeeping operations, assembles the substructure and building stiffnesses and loadings, solves the equilibrium equations, and determines the displacement response. This base program is then combined with a library of element subroutines to produce the complete program. Subroutines for new elements can be developed independently and added to the element library with relative ease. Subroutines for truss, beam column, shear panel, semi-rigid connection, and beam elements are currently included.

The idealization selected herein for the analysis of inelastic frame buildings is essentially identical to the TABS[28] idealization. However, each individual frame is idealized as in the DRAIN-2D computer program, so that the resulting

528 268

idealization allows rather greater generality than TABS. In addition, greater freedom is allowed in the positioning of the floor diaphragms.

The structural idealizations can be summarized as follows:

(a) The building must be separated into a series of discrete plane frames, connected together by rigid horizontal diaphragms. Each frame must be in the vertical plane, but may otherwise be essentially arbitrary. The frames may be arbitrarily oriented and located in plan.

(b) Except for the common columns the only connection between frames is through the diaphragms. The diaphragms are assumed to be rigid and horizontal, but may otherwise be located arbitrarily.

(c) The displacement degrees of freedom for any frame are organized into two groups namely, (1) internal degrees of freedom and (2) connected (or external) degrees of freedom. The horizontal displacements at those joints which connect to diaphragms are kinematically related to the diaphragm displacements. These horizontal displacements are the connected degrees of freedom of the frame. All other displacements are internal degrees of freedom.

(d) Compatibility of vertical and rotational displacements at joints common to two frames is not enforced. This idealization is not suitable for structures such as framed tubes, in which there is substantial coupling through common columns.

(e) It is assumed that the axial forces in columns which are common to two different frames can be obtained by adding together the forces calculated for the two frames. This addition is carried out by the computer program and the combined force is used in assessing P-M interaction effects for common columns. For framing systems in which the computed behavior is likely to be affected little by axial deformations of the columns, this approach is believed to be a reasonable one.

The element library and material models in DRAIN-TABS are all taken from DRAIN-2D. This program seems most applicable for nonlinear analyses of shear wall-diaphragm type structures.

The auxiliary buildings of nuclear power plants are generally such structures with heavy concrete slabs at various floor elevations. These floor slabs are interconnected with numerous concrete shear walls. The usually low height-to-plan aspect ratio of such buildings indicate that under lateral

loads the predominant deformations of the walls are shear deformations. Since the predominant deformation of this type of structure under horizontal seismic loading is a horizontal shear deformation of the walls, it is possible to model the structure as a three-dimensional shear structure. At each point of interest, two in-plane translational degrees of freedom may be considered.

MARC-CDC.[29] This is a linear and nonlinear general-purpose finite element structural analysis program with heat transfer analysis capabilities. The program is developed and maintained by Marc Analysis Corporation.

MARC-CDC is a series of six separate programs of which two are mesh generations, two are postprocessor plotting programs, and the remaining two are a transient heat conduction program and the main program (i.e., stress analysis).

The main program contains some 52 elements. The nonlinear capabilities include elastic-plastic behavior with large displacements, creep analysis, and buckling phenomena. Elastic-plastic behavior is based on isotropic materials with temperature-dependent elastic properties, a von Mises yield stress criterion, and either isotropic or kinematic strain hardening. The creep analysis is based on a von Mises flow criterion and isotropic behavior described by a user-supplied equivalent creep rate law. In addition, three material models based on a hydrostatic yield dependence (Mohr-Coulomb) for soil- and rocklike materials are available. (Finite strains are included through use of a Lagrangian formulation.) The dynamic solution is obtained through integration of the equations of motion by (a) the Newmark method ($\beta = 1/4$, $\gamma = 1/2$), (b) the Houbolt method, or (c) central differences. Mode superposition is also available.

Recently (mid-1977) MARC-CDC has introduced a reinforced concrete element which is a combination of a three-dimensional 20-node brick element and a three-dimensional 20-node rebar element. This element can handle cracking at the integration points with the help of a user-supplied subroutine. However, this element has not been used very much and according to CDC (Control Data Corporation) it still needs debugging.

ANSYS.[30] This is a general-purpose analysis program that can perform static and dynamic structural analysis and heat-transfer analysis for both linear

528 270

and nonlinear problems. The program, developed by Swanson Analysis Systems, Inc., has a capacity of approximately 2500 nodes for three-dimensional problems.

The matrix-displacement method of analysis, based on finite element idealization, is employed throughout the program. The library of available finite elements numbers more than 40 for static and dynamic analyses, and 10 for heat-transfer analyses. This variety of elements gives the ANSYS program the capability of analyzing frame structures (two-dimensional frames, grids, and three-dimensional frames), piping systems, two-dimensional plane and axisymmetric solids, flat plates, three-dimensional solids, axisymmetric and three-dimensional shells and nonlinear problems including interfaces and cables.

The nonlinear capabilities include plasticity (small strain), creep (thermal- and irradiation-induced), irradiation-induced swelling, large deflection, and buckling. The dynamic capabilities include eigenvalue-eigenvector, steady-state harmonic response, and linear and nonlinear transient response. The materials may be either isotropic or anisotropic and may include nonlinear temperature dependency. This program does not have a concrete-type material with tension cut-off.

The dynamic analysis employs a consistent mass matrix and an explicit quadratic integration routine. Extensive plotting capabilities exist, including geometry, stresses, displacements, and temperatures.

Loadings on the structure may be forces, displacements, pressures, temperatures, or response spectra. Loadings may be arbitrary time functions for linear and nonlinear dynamic analyses.

Shell Rigorous Programs

528 271

In the process of literature survey, the feasibility of including containment-type structures for refined nonlinear dynamic analysis was specifically reviewed.

A typical containment structure is a continuous shell-type structure. For rigorous dynamic analysis, such structures may be modeled by generating a mesh of shell elements (representing the effects of both membrane and plate

bending effects) all around the shell surface. The computational effort required to analyze such a model is so prohibitive that alternate models were sought and it was found that an axisymmetric representation of containment shell, while retaining the rigorousness of a refined mathematical model, minimizes the computational effort by reducing the structure to a two-dimensional case and includes consideration of circumferential effects by shape functions.

Computer programs are available to do rigorous dynamic analysis of axisymmetric structures subjected to both axisymmetric (e.g., uniform pressure) and non-axisymmetric (e.g., seismic excitation) loads provided the structural system is linearly elastic. Nonlinear computational codes are also available for axisymmetric structures subjected to axisymmetric loads. But, to our knowledge, no computer code is at present available which can undertake nonlinear dynamic analysis of axisymmetric structures under non-axisymmetric loads such as seismic excitation.

The following programs were examined to evaluate their applicability in executing a nonlinear dynamic analysis of a continuous shell structure.

ASHSD2.[31] This is a computer program which applies the finite element method for the linear dynamic analysis of complex axisymmetric structures subjected to any arbitrary static or dynamic loading or base acceleration. The three-dimensional axisymmetric continuum is represented either as axisymmetric thin shell or as a solid of revolution or as a combination of both. The axisymmetric shell is discretized as a series of frustums of cones and the solid of revolution as triangular or quadrilateral toroids connected at their nodal point circles.

528 272

Hamilton's variational principle is used to derive the equations of motion for this discrete structure. This leads to a mass matrix, stiffness matrix and load vectors which are all consistent with the assumed displacement field. But to minimize computer storage and execution time a diagonal mass matrix has been assumed in writing the computer program. These equations of motion are solved numerically through the time domain either by direct integration or by mode superposition. In both cases the numerical scheme adopted is the step-by-step integration procedure. For an earthquake analysis, the response spectrum technique may be used to obtain approximate values of the maximum

response quantities if detailed time history of the response is not desired.

The program can handle five loading cases: i) dead load, ii) arbitrary static load, iii) arbitrary dynamic load, iv) horizontal and v) vertical component of earthquake acceleration record applied at the base of finite element model.

Any arbitrary loading is first expanded in terms of a cosine Fourier series (except circumferential load in sine Fourier expansion) with a finite number of terms. For each individual Fourier component the stiffness and mass matrices and the corresponding load vector are formed and the equations of motion are solved through the time domain either by direct integration or mode superposition by using a numerical step-by-step integration procedure. After solving for the response of all the Fourier terms, their contributions are summed up to obtain the total response.

This is a very versatile program and used very often in dynamic analysis of the axisymmetric structures. The limitation is that the program only analyzes linear structural systems and cannot be used for a nonlinear analysis.

SHORE.[32] This program is designed for the linear static analysis of arbitrarily loaded thin elastic shells of revolution. The meridional curve of the shell may have any quadratic shape including the case with closed end. The shell may be isotropic, or single or multi-layer orthotropic with the two principal material directions at any point coinciding with the principal directions of the middle surface. Framed structures having the form of a surface of revolution with the linear members running along the principal directions of the middle surface may also be analyzed. As a special case, flat axisymmetric plates may also be considered.

The shell is discretized by a series of curved rotational elements and, if necessary, cap elements. Discontinuous meridian curves are permissible, provided a nodal point is located at such discontinuity. Elementwise variations in thickness and material properties are admissible.

The following loading conditions can be considered: (1) Distributed pressure

528 273

loading; (2) Concentrated line loads applied at designated nodal points; (3) Gravity loads due to self weight or its fraction; (4) Thermal loads.

All loads which are not axisymmetric are required to be expanded in Fourier harmonics. The number of harmonics to be considered will depend upon the nature of loading and accuracy desired. The distributed loadings, and the temperature distribution may be allowed to vary linearly along the meridian of each element.

This program is much more limited than ASHSD2 because only static linear analyses can be done.

SAFE-CRACK. This is a computer program for the quasi-static nonlinear analysis of plane and axisymmetric reinforced or prestressed concrete structures. This program is developed by Gulf General Atomic, Incorporated (GGA). SAFE-CRACK is a GGA proprietary program. In this analysis, the specific creep of concrete as an age and temperature dependent function, concrete failure under combined stresses and transient temperature and mechanical loadings are considered. There are three types of elements--two-dimensional triangular elements, one-dimensional bar elements and membrane shell elements. Each node has two degrees of freedom--radial (horizontal) and axial (vertical) The lack of a rotational degree of freedom requires that structures or areas that undergo considerable bending be represented by a fine mesh.

This a very sophisticated program but since only static load may be applied it cannot be used for the current study.

528 274

CONCLUSIONS AND RECOMMENDATIONS

Criteria for Simplified Method of Analysis

The complete nonlinear analysis of a structure subjected to earthquake ground motion requires many steps. The two principal steps are: structure modeling and solution of the governing equations of motion (response analysis). For each of these two steps, a variety of simplifications can be interjected.

The various factors that must be considered in making nonlinear response analysis simplifications include:

1. Changes in natural period with changes in stiffness.
2. Changes in damping with response amplitude.
3. Reserve strength associated with redundancy.
4. Reserve energy associated with ductility.
5. Cyclic degradation.
6. Geometric nonlinearities.

Finally, for specific use, a simplified analysis procedure must reveal possible modes of failure and must provide some indication of the damage state at various inelastic response levels. Modes of failure include both mechanisms and buckling. The identification of damage should include evaluation for both structural and nonstructural components. The factors listed above must also be included, of course.

Simplified Nonlinear Analysis Methods

In the above section titled "Simplified Nonlinear Analysis Methods," two distinct classes of simplified analysis methods were identified, namely: time history methods and response spectrum methods. We recommend that only the response spectrum methods be considered for this study. The time history methods do not materially reduce the complexity of the problem solution and therefore offer only a marginal simplification and do not warrant further evaluation for purposes of this study.

528 275

Each of the four response spectrum methods identified has merit and should

be given more detailed review and evaluation. While much information has been given regarding the use and applicability of the various procedures, it is apparent that little information has been put forth describing necessary structure modeling requirements. Only the description accompanying the Substitute Structure Method includes modeling guidelines--but those guidelines are for design and are not in all cases directly applicable for analysis.

The explanation for the paucity of information regarding structure modeling is that the required models are extremely structure dependent. That is, each type of structure (if not each structure) requires a somewhat unique model in order to facilitate identification of the important nonlinear response, failure, and damage parameters. For this study, therefore, we recommend that hypothetical structures, representative of auxiliary building (shear wall with rigid diaphram structures) and turbine building (ductile frame and braced frame structures) Category I structures, be identified and evaluated using all four of the response spectrum methods in order to establish the specific merits and limitations of each. This process will facilitate a thorough evaluation of each of the methods and will afford detailed identification of the applicability and reliability of the methods. Based on this evaluation process, detailed procedures for a single simplified nonlinear analysis method, including modeling and response analysis, for these Category I structures will be described and recommended to the NRC for comment.

Rigorous Nonlinear Analysis Methods

In general, the turbine building of a nuclear power facility consists of a combination of ductile-frame and shear-wall elements. It is possible to uncouple the responses of the building due to seismic input in the transverse or longitudinal directions and thus idealize the structure as a two-dimensional frame.

Among the nonlinear dynamic analysis computer programs currently available, only two programs are especially suited to handle two-dimensional frame problems. These two computer programs are DRAIN-2D and SAKE. SAKE is limited to reinforced concrete frames only while DRAIN-2D may be applied to any type of two-dimensional frame. Many of the factors that are frequently

encountered in the seismic analysis of two-dimensional frames may be included in the DRAIN-2D analysis, e.g., (a) semirigid beam-column joints, (b) unsymmetrically distributed flexural strengths at the ends of beam elements, (c) axial deformations and axial load-bending moment interaction in colums, (d) compression buckling in slender diagonal braces, (3) P-Δ effect in colums, and (f) brittle failure in shear panel elements.

DRAIN-2D has very elaborate constitutive relationships for ductile elements. For example, the truss bar element, which may be used as diagonal braces, may yield in tension and yield or buckle elastically in compression. The beam-column element may have variable cross section and strength and yields through the formation of concentrated plastic hinges at its ends. Interaction between axial force and moment may be taken for cross sections of steel or reinforced concrete type materials.

The input to DRAIN-2D is fairly simple, and the program is not very expensive. Moreover, the program is structured in such a fashion that new elements and constitutive relationships may be incorporated without much trouble.

So it is concluded from the literature survey that DRAIN-2D will be used for refined (rigorous) analyses of two-dimensional braced-frame or ductile, moment-resisting frame structures.

Auxiliary buildings are generally heavy reinforced concrete shear-wall structures, with the shear walls interconnected by concrete floor diaphragms. From the literature survey, it seems that DRAIN-TABS is the candidate program most suited for the refined nonlinear analyses of such structures. In this program, the building is idealized as a series of independent plane substructures interconnected by horizontal rigid diaphragms. Each substructure can be of arbitrary geometry and include structural elements of a variety of types. The finite element library of DRAIN-TABS include truss, beam column, shear panel, semi-rigid connection and beam elements. The analysis procedure makes use of substructuring techniques to improve computational efficiency.

Shell (Containment) Structures

528 277

It may be concluded from the literature survey that no computer software is

currently available to rigorously and efficiently compute the nonlinear dynamic response of reinforced concrete containment shell-type structures subjected to earthquake excitation. Nonlinear programs exist for analyses of axisymmetric structures, but, subjected to axisymmetric static loading only. The development of a simplified method of nonlinear analysis and the rigorous evaluation of that method be considered beyond the scope of this study.

528 278

REFERENCES

1. Adeli, H., *Solution Techniques for Linear and Nonlinear Dynamics of Structures Modeled by Finite Elements*, Report No. 23, The John A. Blume Earthquake Engineering Center, Department of Civil Engineering, Stanford University, June 1976.

2. Kavanagh, K. T., "Orthogonal Modes for the Solution to Static Nonlinear Problems," *Proceedings*, ASCE Conference on Finite Element Methods in Civil Engineering, Montreal, 1972.

3. Nickell, R. E., "Nonlinear Dynamics by Mode Superposition," Paper No. 74-341, AIAA/ASME/SAE 15th Structures, Structural Dynamics, and Materials Conference, Las Vegas, April 1974.

4. Nickell, R. E., "Direct Integration Methods in Structural Dynamics," *Journal of the Engineering Mechanics Division*, ASCE, Vol. 99, No. EM2, April 1973.

5. Kanasewich, E. R., *Time Sequence Analysis in Geophysics*, The University of Alberta Press, 1973.

6. Blume, J. A., "A Reserve Energy Technique for the Earthquake Design and Rating of Structures in the Inelastic Range," *Proceedings*, Second World Conference on Earthquake Engineering, Tokyo, 1960.

7. Blume, J. A., N. M. Newmark, and L. H. Corning, *Design of Multistory Reinforced Concrete Buildings for Earthquake Motions*, Portland Cement Association, Skokie, Illinois, 1961.

8. Blume, J. A., "Elements of a Dynamic-Inelastic Design Code," *Proceedings, Fifth World Conference on Earthquake Engineering*, Rome, 1973.

9. Blume, J. A., "Analysis of Dynamic Earthquake Response," State of Art Report No. 3, Technical Committee 6, Earthquake Loading and Response, *Proceedings*, ASCE-IABSE International Conference on the Planning and Design of Tall Buildings, August 1972.

528 279

10. Freeman, S. A., J. P. Nicoletti, and J. V. Tyrell, "Evaluation of Existing Buildings for Seismic Risk -- A Case Study of Puget Sound Naval Shipyard, Bremerton, Washington," *Proceedings*, EERI National Earthquake Conference, Ann Arbor, Michigan, June 1975.

11. Freeman, S. A., "Prediction of Response of Concrete Buildings to Severe Earthquake Motion," ACI Douglas McHenry Symposium, Mexico City, October 1976.

12. Freeman, S. A., "Approximating Inelastic Response of Structures to Ground Shaking," Sixth World Conference on Earthquake Engineering, New Delhi, India, 1977.

13. URS/John A. Blume & Associates, Engineers, *Effects Prediction Guidelines for Structures Subjected to Ground Motion*, JAB-99-115, San Francisco, California, July 1975.

14. Newmark, N. M., "Current Trends in the Seismic Analysis and Design of High Rise Structures," Chapter 16 in *Earthquake Engineering*, R. L. Wiegel, Ed., Prentice-Hall, Englewood Cliffs, N.J., 1970.

15. Newmark, N. M., and W. J. Hall, "Procedures and Criteria for Earthquake Resistant Design," *Building Practices for Disaster Mitigation, Building Science Series 46*, National Bureau of Standards, Washington, D.C., February 1973.

16. Galkan, P., and M. A. Sozen, "Inelastic Response of Reinforced Concrete Structures to Earthquake Motions," *ACI Journal*, December 1974.

17. Shibata, A., and M. A. Sozen, "Substitute Structure Method for Seismic Design in Concrete," *Journal of the Structural Division*, ASCE, Vol. 102, No. ST1, 1976.

18. Takeda, T., M. A. Sozen, and N. N. Nielsen, "Reinforced Concrete Response to Simulated Earthquakes," *Journal of the Structural Division*, ASCE, Vol. 96, No. ST12, December 1970.

528 2-0

19. Jacobsen, L. S., "Damping in Composite Structures," *Proceedings*, Second World Conference on Earthquake Engineering, Tokyo, 1960.

20. Meirovitch, L., *Analytical Methods in Vibrations*, MacMillan, New York, 1967.

21. Roesset, J. M., R. V. Whitman, and R. Dobry, "Modal Analysis for Structures with Foundation Interaction," *Journal of the Structural Division*, ASCE, Vol. 99, No. ST3, March 1973.

22. Bathe, K-J., E. L. Wilson, and R. H. Iding, *NONSAP--A Structural Analysis Program for Static and Dynamic Response of Nonlinear Systems*, Report No. UC SESM74-3, Department of Civil Engineering, University of California, Berkeley, February 1974.

23. Bathe, K-J., *ADINA--A Finite Element Program for Automatic Dynamic Incremental Nonlinear Analysis*, Report 82448-1, Massachusetts Institute of Technology, May 1976.

24. Mondkar, D. P., and G. H. Powell, *ANSR-I--General Purpose Program for Analysis of Nonlinear Structural Response*, Report No. EERC 75-37, College of Engineering, University of California, Berkeley, December 1975.

25. Powell, G. H., *DRAIN-2D User's Guide*, Report No. EERC 73-22, College of Engineering, University of California, Berkeley, December 1973.

26. Otani, S., *SAKE--A Computer Program for Inelastic Response of R/C Frames to Earthquakes*, Structural Research Series No. 413, University of Illinois, Urbana, November 1974.

27. Guendelman-Israel, R., and G. H. Powell, *DRAIN-TABS, A Computer Program for Inelastic Earthquake Response of Three-Dimensional Buildings*, Report No. UCB/EERC-77/08, College of Engineering, University of California, Berkeley, March 1977.

28. Wilson, E. L., and H. Dovey, *Three-Dimensional Analysis of Building Systems--TABS*, Report No. EERC 72-8, College of Engineering, University of California, Berkeley, December 1972.

523 281

29. *MARC-CDC--General Purpose Finite Element Analysis Program, User Information Manual*, Control Data Corporation, 1976.

30. *ANSYS--Engineering Analysis System User's Manual*, Swanson Analysis Systems Inc., July 1975.

31. Ghosh, S., and E. Wilson, *Dynamic Stress Analysis of Axisymmetric Structures Under Arbitrary Loading*, Report No. EERC 69-10, College of Engineering, University of California, Berkeley, September 1975.

32. Basu, P. K., and P. L. Gould, *SHORE-II, Shell of Revolution Finite Element Program--Static Case*, Department of Civil Engineering, Washington University, March 1975.

528 282

APPENDIX B

Elements of a Dynamic-Inelastic Design Code

528 283

FIFTH WORLD CONFERENCE ON EARTHQUAKE ENGINEERING
ROME 1973

ELEMENTS OF A DYNAMIC-INELASTIC DESIGN CODE

J.A. BLUME

CALIFORNIA, U.S.A.

282

SESSION 6 C: Earthquake-Resistant Design

528 284

ELEMENTS OF A DYNAMIC-INELASTIC DESIGN CODE

by

John A. Blume[I]

SYNOPSIS

The need for a dynamic-inelastic design code that provides greater utilization of available knowledge than the current earthquake codes is discussed followed by the philosophy of such a code including the requirement for reasonable simplicity and workability. Elements of the code are presented as a supplementary section to existing static-elastic requirements. Two levels of earthquake intensity are specified. The dynamic-inelastic provisions are based upon kinetic energy reconciliation with energy stored, converted to heat, and used to do work in the inelastic range as in the reserve energy technique.

INTRODUCTION

It has become increasingly clear that static or pseudo-static seismic design codes are not adequate for the design of important, unusual or high risk structures. Even where elastic dynamic analyses are conducted using earthquake records there is a problem of what to do with the results which generally greatly exceed those from code-specified lateral forces. Rigorous inelastic modeling and analyses are complex, often costly, and the results are highly dependent upon both the elastic and inelastic model characteristics selected for analysis.

It is proposed that seismic building codes have two basic parts -- the first consisting of the most desirable procedures and requirements for a static-elastic type design such as now generally practiced, and the second be a dynamic-inelastic part which would also be required for buildings of certain types. This would in effect create a "plateau" (1) of initial resistance for the most probable earthquake demands and an ultimate-resistance control against collapse under a less probable but still possible extreme earthquake demand. This paper is concerned only with the second, dynamic-inelastic part and it is not intended to be a complete code and commentary but a presentation of key elements. Some of the material on which this code is based has been presented previously (1, 2, 3, 4, 5, 6).

A basic factor is not the dynamic analysis, whether with elastic or inelastic models, but what the real resistance values of buildings are as compared to the probable and possible demands. No analysis, per se, improves a building unless something worthwhile is done with the results of that analysis. In addition, the analysis must be based upon realistic models and conditions. The question may be raised as to which model is proper for dynamic analysis -- the one before damage or the one after damage has allowed the structural frame to act essentially alone. This code approach is that both are needed -- the first to determine the response that might lead to damage and inelasticity and the second to check the structure for survival should the strong motion continue. The

---

[I]President, John A. Blume & Associates, Engineers, 130 Jessie Street, San Francisco, California 94105

528 285

natural periods and other properties of these two models may be quite different (6, 7, 8).

There will be two extreme points of view to any dynamic-inelastic design code -- one that it is complicated and extra work for the designer, and the other that it lacks scientific rigor and is too simplified for the real problem. Obviously both can't be right, although both may have valid points. Discussion has been going on for many years while the tools have been available, and while thousands of new buildings are being constructed each year -- built to exist hopefully for 50 or more years without all the benefits of available knowledge. The Southern California hospital failures of 1971, for example, were not only predictable but preventable, but not under any then existing code. Moreover, codes rather than available knowledge seem to determine building properties. In view of these considerations the elements of a dynamic-inelastic code are presented in the following text.

BASIC REQUIREMENTS

For a dynamic-inelastic design code to be feasible and useful it must be simple, clear, and in terms and procedures with which the designer is familiar or with which he could readily become familiar. In addition, it should not depart from the good features of established practices and codes. The basic objective of such a code is to provide adequately for the effects of time and of energy which are largely lacking in existing seismic provisions. The subject is so complex that complete rigor can not be included in a code; nor is that necessary. Certain assumptions and some generalizations are therefore required. In spite of these, the code should provide for the effects of: complex realistic ground motion; damping; natural periods; changes in natural periods; mode shapes; dynamic amplification; inelastic as well as elastic properties; response of an inelastic system; force-deformation characteristics; deterioration under repeated cycles; capacity to do work; modal combinations; soil-structure interaction; energy conservation and reconciliation; all materials and elements that participate in the response; probabilistic variations in ground motion; and probabilistic variations in resistance.

Current seismic codes specify equivalent static horizontal forces from which the designer computes shears, moments, axial forces and finally stresses. However, the element of time is not included adequately and the element of energy is largely neglected. Certainly earthquake response involves time to a major degree, and the basic problem is one of mobilizing resistance to severe energy demands. The energy transmitted to the structure has to be dissipated in such manner that the structure will survive. Unless buildings are made much stronger than most codes require, this energy must be absorbed by doing work far beyond the minor amount of energy converted to heat by damping and friction and stored as elastic strain.

The Reserve Energy Technique (RET) was developed in the 1950's and presented in a series of publications (1, 2, 3) as a practical means of analysis or design in the inelastic range. It was published somewhat apologetically in view of lack of rigor and the need for more data. However, in today's state of great need for a workable dynamic design code, and in view of what has happened, it seems that RET offers a sound basis

528 286

on which to accomplish the above noted objectives. It introduces energy and the resistance of nonstructural elements as the current missing link in design procedures for earthquake resistance and it does this in such a way as to keep the analysis tractable.

PHILOSOPHY

The philosophy of RET is really quite simple and includes consideration of: (a) the extreme demands of the earthquake that can cause the greatest damage or collapse; (b) peak spectral velocity at the period of interest can be used to compute the critical kinetic energy demand; (c) there is energy reconciliation between the kinetic energy and damping (heat), strain (stored) and damage (work done); (d) some structures have characteristics in the inelastic range which must be utilized for survival and these should be evaluated and utilized; (e) any deterioration or softening from repeated cycles can be estimated; (f) changes in dynamic properties from initial response must be considered in the later stages of the earthquake when survival may be in the balance; (g) all elements of resistance and work capacity (reserve energy absorption) should be utilized in the computations as they are in the real structures; and (h) the procedures in design must sacrifice rigor for the benefit of reasonable simplicity but must be reasonably conservative.

The elements of the proposed code are presented with the full understanding that with these "key elements" there still must be extensive work done in refining numerical values, and also that local conditions vary. However, it has been found that the application of these tentative requirements would have prevented the serious damage in Southern California in 1971 and that their application after the event seems to reliably reproduce the effects of the earthquake on all of the structures investigated (6).

PROPOSED CODE ELEMENTS

DYNAMIC-INELASTIC PROVISIONS

Sec. 100. (a) General. Every building of public assembly of more than ___ persons; of public function such as hospitals, police stations, fire stations, jails; other government buildings; of community housing of more than ___ family units; for basic communications or utility purposes; of more than ___ square feet of total floor area; of height greater than ___stories or with a height to width ratio greater than ___; or as may be specifically set forth; shall be first designed as per Section 99 and then be reviewed for performance under this Section and revised as necessary to comply with or exceed the minimum requirements of both Section 99 and this Section.[II]

The provisions of this Section apply to the structure as a unit and also to all stories and parts thereof unless otherwise specifically excepted herein.

The intent of this Section is to provide for the probability that the stress levels of Section 99 may be considerably exceeded because of strong ground motion and to insure a reasonable degree of resistance against collapse under such circumstances.

[II] "Section 99" refers to an improved static-elastic code such as UBC.

528 287

(b) Definitions. The following definitions apply only to the provisions of this Section.

Damping. As used herein related only to the kinetic energy loss without damage, or further damage; assumed to be viscous.

Deterioration. The decrease or softening in stiffness, strength or both due to repeated or reversed cycles.

Elastic Response. Response computed on the basis that the structure has elastic properties regardless of the extent of response.

Inelastic Response. Response in the inelastic range between yield point and ultimate value.

Time-history. Record showing the complete plot of ground motion as a function of time.

(c) Symbols and Notations. The following symbols and notations apply only to the provisions of this Section.

b = A subscript referring to base story.

C'_j = The static story shear coefficient actually provided, using all elements of story j with Section 99 stresses; $C'_j = (\beta V_{yj})/W_j$.

C_b = The fundamental mode dynamic base shear coefficient based on S_a and a ratio from Fig. 100-4.

DV_j = The dynamic shear in story j; at base story, DV_b per Eq. 100-1

F = A force applied at the roof level of buildings over 7 stories; used solely to increase DV_j in the upper stories.

f = A factor based on mode shape; given in Fig. 100-4.

j = A subscript referring to story j, starting at the base story.

N, n = The total number of stories.

p_j = Ratio of effective energy absorption capacity in story j to the sum of same for that story plus all superimposed stories; Eq.100-3.

R_j = Reserve energy reduction factor for story j; to reduce elastic values to inelastic values; from RET.

RET = Reserve energy technique.

S_a = Spectral acceleration; g units.

T = The natural period of vibration of the fundamental mode, sec.

ult = A subscript indicating ultimate; the point on a V-Δ diagram beyond which the slope is always negative.

V_{yj} = The yield shear or yield force of story j.

V-Δ = Symbol for shear-distortion diagram of a story.

W_j = The seismic weight of the building at and above story j.

Z = Number of stories above plus the one under consideration.

α = A factor to convert elastoplastic to bilinear softening values; see Fig. 100-5.

528 288

β = The ratio of stress level at which C'_j is determined to the yield stress level; see C'_j above.

Δ_y = The yield point story distortion.

Δ_{ult} = The ultimate story distortion.

ϕ = Modal deformations as in Fig. 100-3.

μ = Ductility factor or the ratio of total story shear distortion to yield point distortion.

μ_{jI} = Ductility factor required in story j by initial earthquake.

μ_{jF} = Ductility factor required in story j by final earthquake.

μ'_{jI} = Ductility factor limitation for initial earthquake.

μ'_{jF} = Ductility factor limitation for final earthquake.

(d) Earthquake Demands.

1. The "initial" earthquake demand on the structure shall be obtained from Figure 100-1 for the appropriate seismic zone and the elastic fundamental mode period of the building. In the event that the damping in the elastic range can be shown to vary significantly from 5% of critical then adjustment factors shall be applied to S_a as set forth in Table 100-A.

2. The "final" earthquake demand on the structure shall be obtained from Figure 100-2 for the appropriate seismic zone and the fundamental mode period after the initial earthquake has occurred. In the event the damping can be shown to vary significantly from 7% of critical then adjustment factors shall be applied to S_a as set forth in Table 100-A.

3. Site Characteristics. The S_a values of (d)1 and (d)2 shall be increased as per Table 100-B for any local dominant soil or site periods greater than 0.5 sec.

4. Time-history. In lieu of response spectra, a time-history of ground motion may be used in analysis providing the time-history adequately models the specific seismic, geologic and site conditions and provided it is used (or altered as necessary and then used) to create response spectra of appropriate damping values which spectra do not significantly fall below the corresponding spectra of Figures 100-1 and 100-2 adjusted as per (d)3, at any period value. Models used with time-histories shall appropriately model the soil as well as the structure.

(e) Building Characteristics.

1. "Initial" Periods. The building periods for the initial earthquake demand shall be the elastic state fundamental periods of each horizontal direction of the building along its main axes (alternatively used) with allowance for the compliance of foundation materials. These periods shall be based upon the mass and effective stiffness of all materials and elements whether or not structural. In no case shall they exceed the period values from Section 99 without adequate demonstration of the reasons therefore.

2. "Final" Periods. The "final" periods shall be those fundamental mode periods of each horizontal direction of the building along its main axes (alternatively used) with allowance for the compliance of foundation

528 289

materials after any damage has been done by the initial earthquake. Any change in stiffness from cracking or failure of partitions, filler walls, structural walls, beams, columns, or other elements shall be taken into account as well as expected deterioration due to repeated cycles (to be assumed as 10 in number for the initial phase and also for the final phase). Each period may be assumed to change by a factor equal to the square root of the ratio of the "initial" effective stiffness to the "final" effective stiffness of the first story.

3. Mode Shapes. The fundamental mode shape shall be assumed to be the most likely idealized shape in Figure 100-3 based upon the structure's framing, walls and geometry. Should there be significant ground rocking and/or translation the "rigid" bases shown in Figure 100-3 shall be rotated and/or translated accordingly.

4. Base Shear Coefficient Ratio. The ratio of the fundamental mode dynamic base shear coefficient to spectral acceleration, C_b/S_a, shall be obtained from Figure 100-4 using the appropriate number of stories and the selected model from Figure 100-3.

5. Shear-Distortion Models. Each story, j, to be investigated shall have an appropriate idealized shear-distortion (V-Δ) model selected from Figure 100-5 to best represent the actual conditions in the story based upon static test results of materials and elements similar to those proposed. If conditions require, other V-Δ types than those shown may be used but in all cases the type selected shall be justified on the basis of reliable test results. Numerical values shall be developed to define the diagram. Should there be deterioration in the model from the "initial" earthquake, the model for the "final" earthquake shall be appropriately altered from that of the initial phase. In no case shall μ'_I and μ'_F exceed the values in Table 100-C nor any other controlling criterion such as buckling, secondary effects, overall building stability or stress combinations. The first story shall always be investigated. For buildings of over 5 stories other stories shall also be investigated so that no more than 4 typical stories fall between those investigated. In determining V_y and Δ_y the average yield value may be used in lieu of the specified (minimum) yield value.

(f) Analysis.

1. General. The analysis for both initial and final earthquakes shall be conducted as though the structure remained elastic and then those results shall be adjusted to the inelastic state by the use of the reserve energy reduction factor, R. The computed ductility excursions μ_I and μ_F must not exceed the model values μ'_I and μ'_F respectively.

2. Base Shear and Story Shears. Only the fundamental mode shall be used in the spectral analyses but the dynamic base shear shall be increased for higher mode participation as follows:

$$DV_b = \frac{C_b}{S_a}\left[1 + \frac{N-1}{100}\right] S_a W_b \qquad (100\text{-}1)$$

DV_b shall be equal to the sum of assumed horizontal forces on the building which shall be applied to the story levels (for the purpose of obtaining story shears DV_j) in proportion to the modal deformations of the model

528 290

selected from Figure 100-3 with the base rotated and/or translated as indicated for foundation compliance. DV_j shall also include additional shear from a force F applied horizontally at the roof level of all buildings over 7 stories in height for the purpose of increasing story shears for higher mode response in the upper half of the building. This force F need not be carried into the lower-half stories or to base shear, but it shall be additive in the upper stories to the forces distributed from dynamic base shear, DV_b. The force F shall be equal to 0.2 DV_b.

3. Relationships. Story j shall be checked using the following equations to see if the energy can be absorbed without the ductility excursions μ_{jI} and μ_{jF} exceeding the limiting values established for that story. If the limiting values are exceeded the story framing (and that of adjacent stories) shall be redesigned as necessary to meet these requirements.

$$R_j = \frac{\alpha \beta \sqrt{p_j}}{\sqrt{2\mu_j - 1}} = \frac{C'_j W_j}{DV_j} \qquad (100\text{-}2)$$

$$p_j = \frac{f}{\sqrt{Z}} \text{ ; but not } > 1.0 \qquad (100\text{-}3)$$

$$\mu_j = \frac{p_j \alpha^2 \beta^2}{2(R_j)^2} + \frac{1}{2} \qquad (100\text{-}4)$$

or,

$$\mu_j = \frac{p_j \alpha^2 (DV_j)^2}{2(V_{yj})^2} + \frac{1}{2} \qquad (100\text{-}5)$$

The above relationships apply to the initial and the final earthquakes with the appropriate values of DV_j obtained under paragraph (f)2 with the appropriate values of S_a and C_b. The coefficient α may also vary between the two earthquakes if the model changes from damage or deterioration. Using subscripts, the requirements for all stories in each direction are:

$$\mu_{jI} \leq \mu'_{jI} \qquad (100\text{-}6)$$

and,

$$\mu_{jF} \leq \mu'_{jF} \qquad (100\text{-}7)$$

In no story shall the sum of the ratios of μ_{jF}/μ'_{jF} for the transverse and longitudinal directions exceed 1.6.

(g) Redesign. If design changes are made for any reason including the results of analysis under this Section, they shall be done so as to meet (or exceed) all minimum requirements of Section 99, and the design as finally developed must also meet (or exceed) all minimum requirements of this Section.

(h) Connections. All joints and connections shall be capable of resisting the stresses and strains caused by the ductility excursions of the dynamic-inelastic analyses under this Section.

528 291

(i) Stability. The overall stability of the building shall be adequate under all the extreme story ductilities μ_{jF} assumed to exist simultaneously or in any other combination.

(j) Safety Factor. The intent of this Section as outlined in 100(a) is expected to be met in general by this Section. However, there are by necessity some averaged values and some assumptions included, some of which may involve minor conservatism and some none. On the whole, no planned safety factors for the given earthquake spectra have been provided. If and as such may be desired -- and this is recommended -- the values of μ_{jF} should be less than the maximum values allowed by the story models.

CONCLUSION

The tables and figures for the dynamic-inelastic "code" need considerable work to be completed, and the code itself should be considered a draft until these are completed and the whole document is reconciled. In addition, a commentary with examples would be essential. Although more research is needed in such matters as the effective mass of a building and the effective energy absorption on various stories simultaneously, the interim assumptions are generally conservative and the code is possible today. It is also simple to use. It would greatly improve the survival characteristics of proposed buildings and it would reveal existing buildings of high risk.

REFERENCES

(1) Blume, John A., "Structural Dynamics in Earthquake Resistant Design", Transactions, ASCE, 125:1088-1139, 1960.

(2) Blume, John A., "A Reserve Energy Technique for the Design and Rating of Structures in the Inelastic Range", Proceedings, 2WCEE, Japan, 1960.

(3) Blume, John A., N. M. Newmark and Leo H. Corning, Appendix B, "Design of Multistory Reinforced Concrete Buildings for Earthquake Motions", Portland Cement Association, Skokie, Illinois, 1961.

(4) Blume, John A., "The Motion and Damping of Buildings Relative to Seismic Response Spectra", BSSA, 60:1:231-259, February 1970.

(5) Blume, John A., and Robert E. Monroe, "The Spectral Matrix Method of Predicting Damage from Ground Motion", report JAB-99-81, UC-35 to the USAEC, Nevada Operations Office, September 1971, National Technical Information Service, Springfield, VA 22151.

(6) Blume, John A., "Analysis of Dynamic Earthquake Response", State of Art Report No. 3, Technical Committee 6, Earthquake Loading and Response, Proceedings, ASCE-IABSE International Conference on the Planning and Design of Tall Buildings, August 1972.

(7) "The San Fernando Earthquake of February 9, 1971", Section on Building Analysis, EERI/NOAA, in publication.

(8) Freeman, Sigmund A., "Comparisons of Results of Dynamic Seismic Analyses of Two Identical Structures Located on Two Different Sites, Based on Site Seismograms from the San Fernando Earthquake", Proceedings, 41st Annual Convention SEAOC, October 6, 1972.

523 292

TABLE 100-A would provide (a) factors to change from 5% damped S_a values at various period bands to other damping values such as 2, 3, 4, 6, 7 and 8%; and (b) similar factors except to change from 7% to 4, 5, 6, 8, 9 or 10% damping.

TABLE 100-B would provide data for adjusting the response spectra beyond the 0.5 sec period for dominant site periods associated with deep soil layers over rock. (Shorter site periods would be covered statistically in Figures 100-1 and 100-2.)

TABLE 100-C would provide ductility factor limitations, for the "initial" earthquake and for the "final" earthquake, based on the material and the type of stress, as for example shear in concrete, bar tension in ductile concrete, steel in compression, etc.

FIGURE 100-1 would be a smoothed plot of 5% damped S_a spectra versus period T for the median conditions (50% probability of exceedance) in each region. Each seismic zone would have its own spectral curve, based upon intensive studies of actual earthquake records.

FIGURE 100-2 would be like Figure 100-1 except it would be for 7% damping and be for only 16% probability of exceedance in a 100-year period.

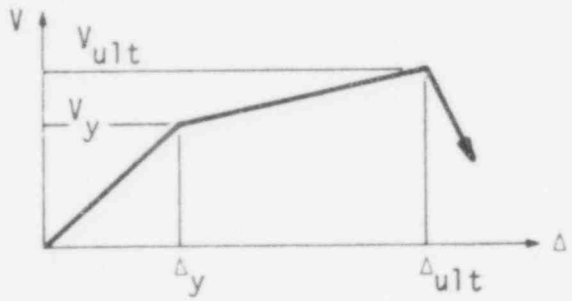

Model	Δ_{ult}/Δ_y	V_{ult}/V_y	α
I	1	1	1
II	2	1	1
III	.	1	1
IV	6	1	1
V	4	1.5	0.90
VI	6	1.5	0.90
VII	8	1.5	0.90
VIII	4	2	0.83
IX	6	2	0.83
X	8	2	0.83
XI	11	1	1
XII	11	2	0 83

FIG. 100-5 Inelastic Story Shear Models

528 293

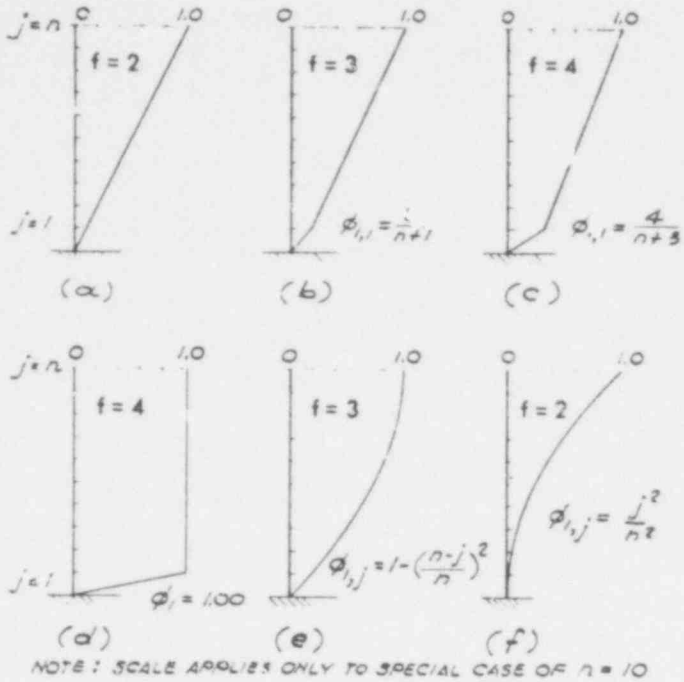

FIG. 100-3 Idealized fundamental mode shapes.

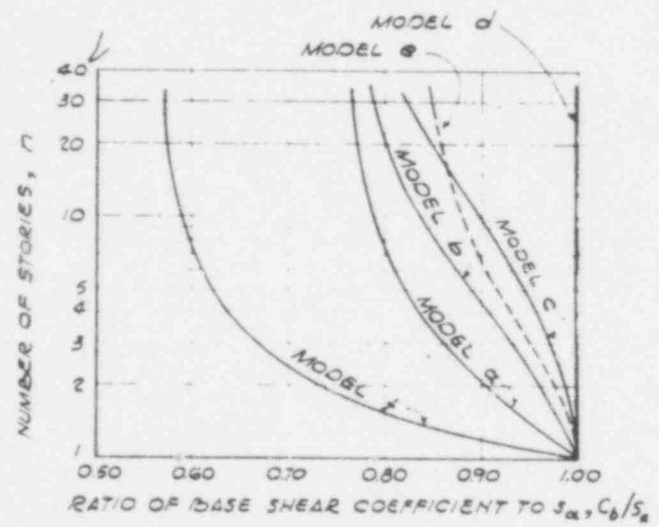

FIG. 100-4 Fundamental mode base shear ratios for models with uniform story heights and masses.

528 294

APPENDIX C

Modeling the Nonlinear Response Characteristics of Low-Rise Reinforced Concrete Shear Walls

528 295

MODELING THE NONLINEAR RESPONSE CHARACTERISTICS OF LOW-RISE REINFORCED CONCRETE SHEAR WALLS

Introduction

Part of the NRC/NONLIN project is the development of a mathematical model to represent the significant features of the nonlinear response of low-rise reinforced concrete shear walls. The most recent low-rise concrete wall test data were collected and compared to two mathematical models. As a result of this study, it was concluded that the models presented in Figures 1 and 2 will be used in the NRC/NONLIN project. The advantages of these models are that they are based on existing reinforced concrete technology, are easy to apply, and match fairly well with test data. The disadvantages of these models are that they seem to underestimate shear resistance and that simplified analyses with these models may lead to the conclusion that low-rise walls are capable of very limited inelastic behavior.

Data Collection

As compared to other aspects of reinforced concrete technology, relatively little experimental research has been conducted on the dynamic response of low-rise reinforced concrete walls. Pioneering work in this field was done at Stanford[1,2,3,4,5], MIT[6,7], and in Japan[8,9,10,11,12]. These investigations have been recently supplemented with tests by the PCA[13], and additional tests in Japan[14,15]. All the above mentioned tests have been conducted on infill panels which are surrounded by reinforced concrete edgemembers. Tests on isolated shear walls without edgemembers have been conducted at the University of Canterbury, New Zealand[16].

This investigation of the nonlinear response characteristics of low-rise reinforced concrete shear walls draws information from the early tests at Stanford, the recent Japanese data, the PCA tests, and the New Zealand tests.

528 296

These test results were studied to determine the way in which parameter variations affect the ductility of low-rise walls. Most of the data considered in this study demonstrated a reduction in load capacity after the ultimate load -- i.e., there is no yield plateau or ductility by the conventional meaning of that term. Ductility is qualitatively defined as the absence of a rapid decrease in load capacity after the ultimate load has been reached. The more ductile panels were judged to be those which lose their load capacity at a slower rate as compared to others.

Tests at Stanford

These test specimens consisted of 1-story reinforced concrete panels enclosed by reinforced concrete edgemembers. The panels were reinforced in both directions with various amounts of reinforcing steel, and the size and steel content of the edgemembers were also varied.

The Stanford test data indicated a trend of reduced ductility as edgemember reinforcing is increased. This is similar to reinforced concrete beam behavior in that under-reinforced beams demonstrate more ductile failure as compared to over-reinforced beams.

The data also demonstrated that the amount of panel reinforcement influences the ultimate strength but has relatively little effect on ductility.

Recent Japanese Tests

The recent Japanese test panels demonstrated load-deflection characteristics which were similar to those obtained from the Stanford tests. The shapes of these curves appeared to be independent of the amount of panel reinforcement and the panel thickness. This lack of dependence on the amount of panel steel was also noted in the Stanford tests. The Japanese tests only recorded one data point after the ultimate load; therefore, these tests are of limited value in determining post-ultimate load behavior.

528 297

PCA Tests

The PCA has conducted numerous low-rise wall tests on specimens having large, highly reinforced edgemembers. The variables considered in the PCA

tests were steel in the edgemembers, horizontal wall reinforcing, and vertical wall reinforcing.

Most results for specimens with varying amounts of edgemember reinforcement were consistent with observations from the Stanford data. However, one specimen did not follow the general trend.

The influence of horizontal wall reinforcement was studied in the PCA tests. The results showed that the absence of horizontal steel has only a moderate effect on the ultimate strength and ductility of the specimens.

The influence of vertical wall reinforcement was also considered. The data indicated a decrease in ultimate strength and an increase in ductility as the vertical wall reinforcement is decreased. This is analogous to the behavior of under-reinforced concrete beams.

The PCA tests included specimens with different aspect ratios (i.e., the ratio of height to length); however, no consistent trend of ductility with aspect ratio was noted.

New Zealand Tests

Tests conducted at the University of Canterbury, New Zealand, considered small-scale walls without edgemembers. These results indicated considerably greater ductility potential then obtained in other investigations. The only major difference between the New Zealand tests and those conducted at Stanford, in Japan, and by the PCA is that the New Zealand test specimens lacked edgemembers. This suggests that walls without edgemembers may have a greater ductility potential than walls with edgemembers. Tests by the PCA on high-rise walls seem to substantiate this observation.[17]

It is possible that the different load-deflection curves observed from tests with and without edgemembers is related to the fact that panels with edgemembers have a much greater shear load capacity than similar panels without edgemembers. At the ultimate load, both the panel and

528 298

and edgemember are probably very highly stressed. A brittle failure of the edgemembers would suddenly increase the stress in the panel well above its ultimate shear capacity. This might damage the panel and thereby account for the sudden reduction of load capacity after the ultimate load is reached. In contrast, a panel without edgemembers may never be subjected to stresses in excess of its ultimate shear capacity.

The New Zealand tests demonstrate the ductile behavior of walls that are not stressed beyond their ultimate capacity.

Conclusions Regarding Ductility Potential

Four sets of test data have been studied to determine the ductility potential of low-rise walls and the effect of various parameters on ductility. There are five conclusions which may be drawn from this study:

1. All the low-rise walls with edgemembers studied demonstrate a loss of load capacity after the ultimate load is reached -- i.e., there is no yield plateau. Limited tests on low-rise walls without edgemembers indicate substantial ductile behavior.

2. The ultimate strength is decreased and the apparent ductility is increased by reducing the vertical wall reinforcing steel and vertical edgemember reinforcing steel.

3. Strength and ductility are only moderately affected by the amount of horizontal wall steel.

4. Changes in the aspect ratio caused great changes in ductility; however, there is not a consistent trend in the data presented.

5. Walls with edgemembers are less ductile than walls without edgemembers.

528 299

Strength Evaluation

The data from the Japanese tests[14] and the recent PCA tests[13] were combined with additional data from earlier PCA tests[18] to evaluate the adequacy

of current ACI code shear strength prediction equations.[19] A comparison of measured and computed results is shown in Table 1. It appears that the ultimate strengths calculated by the ACI code consistently underestimate the Japanese measured results. However, it should be kept in mind that the Japanese tested small-scale panels (47 in. x 19 in. x 1.6 in.) The possible influence of scale effects has not been considered in this analysis, and this may significantly influence the results. The two sets of test results obtained from the PCA compare favorably with the ACI strength prediction. One noteworthy exception is for PCA specimen B4-3, which shows a ratio of measured to computed strength of 4.7. B4-3 had no horizontal reinforcing steel, and this greatly reduced the calculated strength but only slightly reduced the measured strength. Excluding B4-3, the mean ratio of measured to computed strength for the two sets of PCA data is 1.3. The standard deviation is 0.29, and the coefficient of variation is 22%.

Based on the comparison shown in Table 1, it is concluded that the shear strength prediction equation given by ACI 316-71[17] is appropriate for use in this study (NRC/NONLIN). The comparison shows that the ACI prediction may be expected to underestimate strength by about 30% on the average. Although this may appear to be an unreasonably large factor of safety for this evaluation of ultimate nonlinear performance of shear walls, any increase beyond the ACI calculated strength would involve an unacceptably high risk of overestimating available strength.

528 300

Load-Deflection Models

The goal of this section is to develop mathematical models that are capable of predicting load deflection characteristics of low-rise walls from basic information such as material properties, dimension, and reinforcing ratios.

These models are intended to be used with four simplified nonlinear analysis methods. A constraint is that the model must be relatively uncomplicated and simple to apply.

Data from the Japanese and PCA tests were compared to a strut model developed by Klingner and Bertero.[20] This model consists of an elastic loading curve

$$S = \frac{AE}{L}\delta$$

and a strength envelope curve

$$S = A f'_c (e^{-\gamma\delta})$$

where:

- S = axial force in an equivalent strut
- δ = axial deformation of an equivalent strut
- A = area of an equivalent strut
- L = length of an equivalent strut
- f'_c = compressive strength
- E = Young's modulus
- γ = a parameter to model strength degradation after the ultimate load is reached.

The Klingner-Bertero strut model was compared to various measured data. The parameter γ controls the exponential decay of the strength envelope, and this parameter is varied between 2 and 6 to match the measured data. Logic suggests that γ is correlated with the amount of reinforcing steel in the panel, but at the present time the available data is not adequate to firmly establish this correlation. From the comparisons made with the available data, it seems that $\gamma = 3$ matches well in most cases.

Recommended Mathematical Model for Low-Rise Shear Walls

The strut model developed by Klingner and Bertero seems to be a reasonable model for shear walls with edgemembers. The modifications shown in Figure 1 are introduced to limit the model to the ultimate shear strengths defined by the ACI code. These modifications are necessary because the basic Klingner-Bertero model tended to overestimate the ultimate shear stress and fell far below the measured data at large displacement. For walls without edgemembers, the elasto-plastic model shown in Figure 2 has been adopted. The limiting stress is V_u as computed by the ACI, and the slope of the elastic curve is the shear modulus.

528 301

REFERENCES

1. Williams, H. A., and J. R. Benjamin, *Investigation of Shear Walls, Part 3 - Experimental and Mathematical Studies of the Behavior of Plain and Reinforced Concrete Walled Bents Under Static Shear Loading*, Department of Civil Engineering, Stanford University, July 1953.

2. Benjamin, J. R., and H. A. Williams, *Investigation of Shear Walls, Part 6 - Continued Experimental and Mathematical Studies of Reinforced Concrete Walled Bents Under Static Shear Loading*, Department of Civil Engineering, Stanford University, August 1954.

3. Benjamin, J. R., and H. A. Williams, *Investigation of Shear Walls, Part 9 - Continued Experimental and Mathematical Studies of Reinforced Concrete Walled Bents Under Static Shear Loading*, Department of Civil Engineering, Stanford University, September 1955.

4. Benjamin, J. R., and H. A. Williams, *Investigation of Shear Walls, Part 12 - Studies of Reinforced Concrete Shear Walls Assemblies*, Department of Civil Engineering, Stanford University, December 1956.

5. Stivers, R. H., J. R. Benjamin, and H. A. Williams, *Investigation of Shear Walls, Part 8 - Stresses and Deflections in Reinforced Concrete Shear Walls Containing Rectangular Openings*, Department of Civil Engineering, Stanford University, August 1954.

6. Antebi, J., S. Utku, and R. J. Hansen, *The Response of Shear Walls to Dynamic Loads*, Department of Civil and Sanitary Engineering, Massachusetts Institute of Technology, Cambridge, August 1960.

7. Galletly, G. D., *Behavior of Reinforced Concrete Shear Walls Under Static Load*, Department of Civil and Sanitary Engineering, Massachusetts Institute of Technology, Cambridge, August 1952.

528 302

8. Naito, T., "Theory of Earthquake Resistant Frame Structures", *Proceedings, Institute of Japan Architects,* January 1921, pp. 487-510.

9. Sano, T., and T. Taniguchi, *"Earthquake Resistant Design"* Iwanami Publishing Co., Ltd., Tokyo, 1934.

10. Tanabashi, R., "Experimental Investigation of the Decrease of Shear Resistance by the Opening in Wall," *Convention Proceedings, Institute of Japan Architects,* April 1934, pp. 320-327.

11. Ban, S , "Distribution of Seismic Resistance Between Wall and Frame Due to the Theory of Elasticity," *Transactions, Institute of Japan Architects,* No. 4, February 1937, pp. 16-25.

12. Tsuboi, Y., "Shear Deformation of Seismic Wall - Stress Analysis of Seismic Wall," *Transactions, Architectural Institute of Japan,* March 1953, pp. 53-59.

13. Barda, F., J. Hanson, and W. Corley, "Shear Strength of Low-Rise Walls with Boundary Elements," *Reinforced Concrete Structures in Seismic Zones,* ACI Publication SP-42, American Concrete Institute, Detroit, 1974.

14. Yamada, M., H. Kawamura, and K. Katagihara, "Reinforced Concrete Shear Walls Without Openings; Test and Analysis," *Shear in Reinforced Concrete,* Vol. 2, ACI Publication SP-42, American Concrete Institute, Detroit, 1974.

15. Yamada, M., H. Kawamura, and K. Katagihara, "Reinforced Concrete Shear Walls With Openings; Test and Analysis," *Shear in Reinforced Concrete,* Vol. 2, ACI Publication SP-42, American Concrete Institute, Detroit, 1974.

16. Beekhuis, W. J., "An Experimental Study of Squat Shear Walls," Master of Engineering Report, Department of Civil Engineering, University of Canturbury, Christchurch (New Zealand), 1971.

528 303

17. Cardenas, A. E., and D. D. Magura, "Strength of High-Rise Shear Walls - Rectangular Cross Sections," *Response of Multistory Concrete Structures to Lateral Forces*, ACI Publication SP-36, American Concrete Institute, Detroit, 1973, pp. 119-150.

18. Cardenas, A. E., J. M. Hanson, W. G. Corley, and E. Hogenstat, "Design Provisions for Shear Walls," *ACI Journal*, American Concrete Institute, Detroit, March 1973.

19. *Building Code Requirements for Reinforced Concrete*, (ACI 3/8/71), American Concrete Institute, Detroit, 1971.

20. Klingner, R. E., and V. V. Bertero, *Infilled Frames in Earthquake-Resistant Construction*, EERC 76-32, Earthquake Engineering Research Center, University of California, Berkeley, December 1976.

528 304

TABLE 1

A COMPARISON OF MEASURED AND COMPUTED

ULTIMATE SHEAR STRENGTHS

Source of Data		Measured V_{ULT}(kip)	Computed V_{ULT}(kip)	Ratio
Japan[14]	ρ_w = 0 (t = 40)	56	20	2.8
	ρ_w = .0031 (t = 40)	83	30	2.8
	ρ_w = .0063 (t = 40)	82	40	2.1
	ρ_w = .0126 (t = 40)	98	60	1.6
	ρ_w = .008 (t = 30)	61	33	1.9
	ρ_w = .0063 (t = 20)	47	20	2.4
	ρ_w = .0126 (t = 20)	49	29	1.7
PCA[13]	B1-1	274	156	1.8
	B2-1	220	150	1.5
	B3-2	249	164	1.5
	B4-3	229	49	4.7*
	B5-4	155	167	0.9
	B6-4	197	156	1.3
	B7-5	256	160	1.6
	B8-5	199	156	1.3
PCA[16]	SW-7	117	73	1.6
	SW-8	128	80	1.6
	SW-9	153	143	1.07
	SW-10	69	53	1.3
	SW-11	137	154	0.89
	SW-12	148	157	0.44
	SW-13	142	142	1.00

528 305

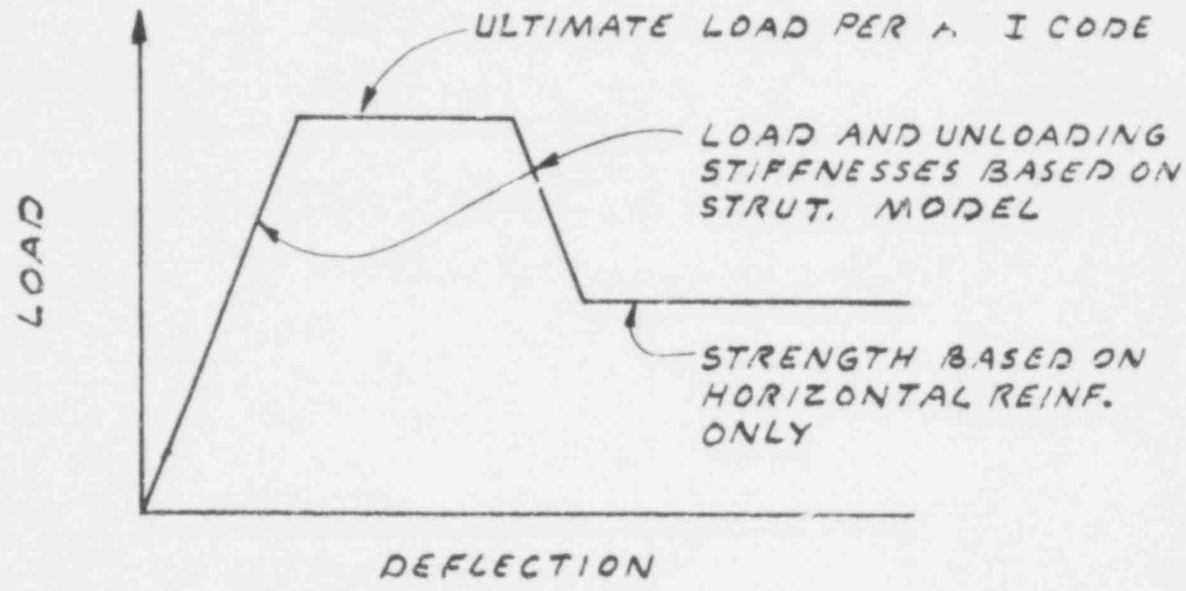

WITH EDGEMEMBERS

528 306

ASSUMED LOAD BEHAVIOR
OF REINFORCED CONCRETE SHEAR WALLS

NRC/NONLIN FIGURE 1

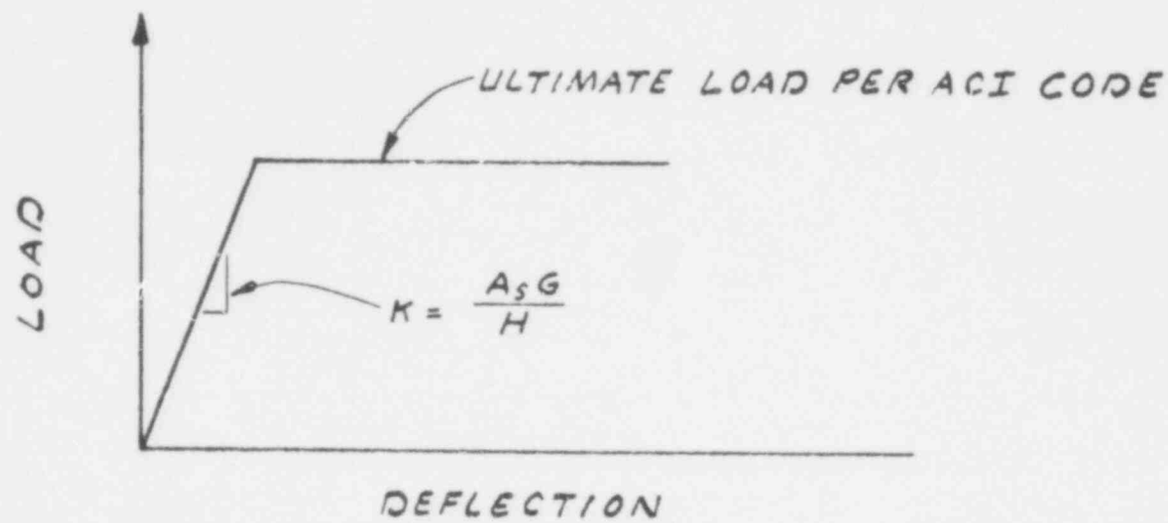

WITHOUT EDGEMEMBERS

528 307

ASSUMED LOAD BEHAVIOR
OF REINFORCED CONCRETE SHEAR WALLS

NRC/NONLIN FIGURE 2

NRC FORM 335 (7-77)

U.S. NUCLEAR REGULATORY COMMISSION

BIBLIOGRAPHIC DATA SHEET

1. REPORT NUMBER *(Assigned by DDC)*: NUREG/CR-0948

4. TITLE AND SUBTITLE *(Add Volume No., if appropriate)*: "NONLINEAR STRUCTURAL DYNAMIC ANALYSIS PROCEDURES FOR CATEGORY I STRUCTURES"

2. *(Leave blank)*

3. RECIPIENT'S ACCESSION NO.

7. AUTHOR(S): URS/JOHN A. BLUME & ASSOCIATES, ENGINEERS

5. DATE REPORT COMPLETED: MONTH: September; YEAR: 1978

9. PERFORMING ORGANIZATION NAME AND MAILING ADDRESS *(Include Zip Code)*:
URS/John A. Blume & Associates, Engineers
130 Jessie Street
San Francisco, CA 94105

DATE REPORT ISSUED: MONTH: July; YEAR: 1979

6. *(Leave blank)*

8. *(Leave blank)*

12. SPONSORING ORGANIZATION NAME AND MAILING ADDRESS *(Include Zip Code)*:
U. S. Nuclear Regulatory Commission
Office of Nuclear Reactor Regulation
Division of Systems Safety
Washington, DC 20555

10. PROJECT/TASK/WORK UNIT NO.: NA

11. CONTRACT NO.: NRC-03-77-173

13. TYPE OF REPORT: Technical

PERIOD COVERED *(Inclusive dates)*: September 1977 to September 1978

15. SUPPLEMENTARY NOTES

14. *(Leave blank)*

16. ABSTRACT *(200 words or less)*

This report presents the results of studies conducted to identify and recommend a simplified dynamic analysis procedure applicable for performing nonlinear analyses of Category I nuclear power plant structures. For the recommended simplified procedures, the theoretical background, mathematical formulation, analytical solution, verification of reliability, and interpretation of results were established. In addition, studies were conducted to compare the results of conventional linear analysis with nonlinear analyses to establish the relative merits of the two approaches.

528 308

17. KEY WORDS AND DOCUMENT ANALYSIS

17a. DESCRIPTORS

17b. IDENTIFIERS/OPEN-ENDED TERMS

18. AVAILABILITY STATEMENT

19. SECURITY CLASS *(This report)*: Unclassified

21. NO. OF PAGES

20. SECURITY CLASS *(This page)*: Unclassified

22. PRICE: $

UNITED STATES
NUCLEAR REGULATORY COMMISSION
WASHINGTON, D. C. 20555

OFFICIAL BUSINESS
PENALTY FOR PRIVATE USE, $300

POSTAGE AND FEES PAID
U.S. NUCLEAR REGULATORY
COMMISSION

528 309